Site-Specific Soil Parameters
Westinghouse Former Fuel Cycle Facility D&D Project

Prepared for:

Westinghouse Electric Company
Hematite Facility
Festus, Missouri 63028

September 15, 2003

LEGGETTE, BRASHEARS AND GRAHAM, INC.
Professional Ground-Water and Environmental Services
4850 Lemay Ferry Road, Suite 205
St. Louis, Missouri 63129
(314) 845-0535

Site-Specific Soil Parameters
Westinghouse Former Fuel Cycle Facility D&D Project

Approved by:
J. Kevin Powers
Principal

Prepared for:

Westinghouse Electric Company
Hematite Facility
Festus, Missouri 63028

Prepared by:

LEGGETTE, BRASHEARS & GRAHAM, INC.
Professional Ground-Water & Environmental Services

John L. Bognar, R.G.
Senior Associate
Missouri Registered Geologist

September 15, 2003

REUSE OF DOCUMENTS
This document has been developed for a specific application and not for general use; therefore, it may not be used or copied without the written approval of Leggette, Brashears & Graham, Inc. Unapproved use is at the sole responsibility of the unauthorized user.

Copyright©, Leggette, Brashears & Graham, Inc. 2003
4850 Lemay Ferry Road, Suite 205, St. Louis, MO 63129 (314) 845-0535 Fax (314) 845-3573

TABLE OF CONTENTS

RESRAD Parameter Table for ^{99}Tc 1
Reference Footnotes for ^{99}Tc 2
RESRAD Parameter Table for ^{235}U 5
Reference Footnotes for ^{235}U 6
RESRAD Parameter Table for ^{228}Ac 10
Reference Footnotes for ^{228}Ac 11
RESRAD Parameter Table for ^{212}Bi 15
Reference Footnotes for ^{212}Bi 16
RESRAD Parameter Table for ^{212}Pb 20
Reference Footnotes for ^{212}Pb 21
RESRAD Parameter Table for ^{208}Tl 25
Reference Footnotes for ^{208}Tl 26
RESRAD Parameter Table for ^{234}U 30
Reference Footnotes for ^{234}U 31
RESRAD Parameter Table for ^{238}U 35
Reference Footnotes for ^{238}U 36
RESRAD Parameter Table for ^{237}Np 40
Reference Footnotes for ^{237}Np 41
RESRAD Parameter Table for ^{239}Pu 44
Reference Footnotes for ^{239}Pu 45
RESRAD Parameter Table for ^{232}Th 48
Reference Footnotes for ^{232}Th 49
RESRAD Parameter Table for ^{228}Ra 53
Reference Footnotes for ^{228}Ra 54
RESRAD Parameter Table for ^{228}Th 58
Reference Footnotes for ^{228}Th 59
RESRAD Parameter Table for ^{224}Ra 63
Reference Footnotes for ^{224}Ra 64

LIST OF FIGURES
(at end of report)

Figure

1 Ground-Water Flow Direction and Gradient, and Length of Contaminated Zone Parallel to the Aquifer Flow in the DSCC

2 Area of Contaminated Zone ^{99}Tc

3 Watershed Area

4 Area of Contaminated Zone ^{235}U, ^{234}U, ^{238}U, ^{228}Ac, ^{212}Bi, ^{212}Pb, ^{208}Tl, ^{237}Np, ^{239}Pu, ^{232}Th, ^{228}Ra, ^{228}Th, ^{224}Ra

LIST OF APPENDICES
(at end of report)

Appendix

A Ground-Water Concentration Supporting Documentation

B Supporting Documentation for ^{99}Tc Area of Contamination Zone

C RESRAD Default Value Table

D Total Porosity, Dry Density and Hydraulic Conductivity Calculations and Supporting Documentation

E Field Capacity Calculation

F Representative Values of Soil-Specific Exponential b Parameter

G Well Pump Intake Calculations and Supporting Documentation

H Well Pumping Rate Calculation and Supporting Documentation

Site-Specific Soil Parameters
Westinghouse Former Fuel Cycle Facility D&&D Project

RESRAD Parameter Table for ^{99}Tc

Parameter	Recommended Value	RESRAD Code Designation	Units	Uncertainty Range			Probabilistic Function	Reference
				Low Value	High Value	Number of Samples		
Groundwater Concentration	179	W(i)	pCi/L	24.9	1590	7	Lognormal	1
Area of Contaminated Zone	6432	AREA	m^2	5146	7718	NA	Normal	2
Thickness of Contaminated Zone	2	THICKO	m	1.00E-10	11.74	NA	Bounded Lognormal	3
Length Parallel to Aquifer	291	LCZPAQ	m	233	349	NA	Bounded Normal	4
Density of Contaminated Zone	1.69	DENSCZ	g/cm^3	1.39	2.11	28	Normal	5
Contaminated Zone Erosion Rate	0.00005	VCZ	m/yr	0.00004	0.00006	NA	Bounded Normal	6
Contaminated Zone Total Porosity	0.45	TPCZ	0.xx	0.41	0.483	13	Normal	7
Contaminated Zone Field Capacity	0.17	FCCZ	0.xx	0.01	0.2	NA	Bounded Normal	8
Contaminated Zone Hydraulic Conductivity	14.56	HCCZ	m/yr	1.38E-03	1.45E+02	13	Lognormal	9
Contaminated Zone b Parameter	10.40	BCZ	unitless	4.05	11.4	NA	Lognormal	10
Watershed Area	998939	WAREA	m^2	988950	1008928	NA	Bounded Normal	11
Density of Saturated Zone	1.69	DENSAQ	g/cm^3	1.39	2.11	28	Normal	5
Saturated Zone Total Porosity	0.45	TPSZ	0.xx	0.41	0.483	13	Normal	7
Saturated Zone Effective Porosity	0.29	EPSZ	0.xx	0.281	0.425	NA	Normal	12
Saturated Zone Field Capacity	0.17	FCSZ	0.xx	0.01	0.2	NA	Bounded Normal	8
Saturated Zone Hydraulic Conductivity	169.58	HCSZ	m/yr	1.56E+01	8.51E+01	12	Lognormal	13
Saturated Zone Hydraulic Gradient	0.015	HGWT	unitless	0.013	0.018	NA	Bounded Lognormal	14
Saturated Zone b Parameter	10.40	BSZ	unitless	4.05	11.4	NA	Lognormal	10
Water Table Drop Rate	0.00	VWT	m/yr	NA	NA	NA	None Recommended	15
Well Pump Intake Depth	9.41	DWIBWT	m	5.4	11.7	10	Bounded Normal	16
Well Pumping Rate	562	UW	m^3/yr	450	674	NA	Bounded Normal	17

REFERENCE FOOTNOTES for ^{99}Tc

1 ^{99}Tc ground-water concentration data were taken from piezometer GWE-6, which was sampled by Gateway Environmental and analyzed by ABB in September 1996. This information was referenced in Table 3-3, *"Investigation to Determine the Source of ^{99}TC in Groundwater Monitoring Wells 17 and 17B."* Figure 1 shows the former location of GWE-6 and Appendix A contains a copy of Table 3-3. The low and high values of the uncertainty range correspond to concentrations from WS-14 and GWE-4, respectively.

2 ^{99}Tc data does not exist for soil. Therefore, LBG assumes the contaminated zone is based on operations where ^{99}Tc may have been stored or disposed. This includes the former ring storage area and the evaporation ponds, located immediately south of the existing structures. This assumption is based on information provided on page 15 of the *"Remedial Investigation/Feasibility Study (RI/FS) Work Plan, Revision 0,"* dated May 9, 2003. Figure 2 shows the Area of Contamination boundary for ^{99}Tc and Appendix B contains a copy of page 15. The low and high uncertainty range values are not expected to be more than 20 percent above or below the recommended value.

3 Due to a lack of soil data for ^{99}Tc, the RESRAD default value was chosen, based on Table 1.3 of *"Data Collection Handbook to Support Modeling Impacts of Radioactive Material in Soil,"* April 1993. Appendix C contains a copy of Table 1.3. The low value of the uncertainty range is based on the lower bounds value in Table 1.3. The high value of the uncertainty range is the maximum depth of the overburden.

4 Figure 1 shows the ground-water flow direction and gradient, and length of contaminated zone. The source of Figure 1 is from *"Hydrogeologic Investigation and Ground-Water, Soil and Stream Characterization"* performed by LBG in March 1999. The low and high uncertainty range values for the Length Parallel to Aquifer are not expected to be more than 20 percent above or below the recommended value.

5 Taken from an average of dry density calculations from work performed by Fitch, University of Missouri – Rolla, 1998, presented in *"Fourth Sampling Event Report in Conjunction with the Hydrogeologic Investigation and Ground-Water, Soil and Stream Characterization"*, prepared by LBG in November 1999, and Shannon and Wilson (Appendix B of *"Hydrogeologic Investigation and Ground-Water, Soil and Stream Characterization"* performed by LBG in March 1999). Appendix D includes a table with these values showing how the value was derived. It also includes a copy of the reference data. The low and high values for the uncertainty range are associated with the lowest and highest values from the data set.

6 Jefferson County does not have a published soil survey which typically provide values for erosion rates. Therefore, the default value (0.001 m/yr) provided in Table 1.3 of *"Data Collection Handbook to Support Modeling Impacts of Radioactive Material in Soil,"* April 1993, was used as a starting point. Since approximately 95 percent of the area of contamination is covered with impervious material, the default value was multiplied by .05 to

give a value of 0.00005 m/yr. The low and high uncertainty range values are not expected to be more than 20 percent above or below the recommended value.

7 From Shannon and Wilson, (Appendix B of "*Hydrogeologic Investigation and Ground-Water, Soil and Stream Characterization*" performed by LBG in March 1999). Appendix D includes a table with these values showing how the value was derived. It also includes a copy of the reference data. The low and high values for the uncertainty range are associated with the lowest and highest values from the data set.

8 Derived using Formula 4.4 on page 28 of "*Data Collection Handbook to Support Modeling Impacts of Radioactive Material in Soil*," April 1993. The value for total porosity was taken from the average of Shannon and Wilson data (0.446; see footnote 7 above) and the value for effective porosity was based on a default value for silty clay in Table 3.3-1 of "*Development of Probabilistic RESRAD 6.0 and RESRAD-Build 3.0 Computer Codes*," November 2000. A copy of page 28, the completed formula, and Table 3.3-1 are provided in Appendix E. The low value of the uncertainty range cannot be zero (thus 0.01 was chosen), and the high value is derived by using the highest total porosity and effective porosity values in the calculation.

9 Shannon and Wilson (Appendix B of "*Hydrogeologic Investigation and Ground-Water, Soil and Stream Characterization*" prepared by LBG in March 1999) performed permeability tests on numerous soil samples. The average vertical permeability (hydraulic conductivity; K) for each sample was determined by averaging the last three permeability readings (telephone communication with Mr. Chris Groves, Vice-President, Shannon and Wilson on August 13, 2003). Once averages were calculated for each sample, an average of the entire data set was determined. The vertical hydraulic conductivity test data and a table developed to show the average K per sample, and the average K for the data set are provided in Appendix D. The low and high values for the uncertainty range are associated with the lowest and highest values from the data set.

10 Based on the default value for silty clay provided in Table 13.1, in "*Data Collection Handbook to Support Modeling Impacts of Radioactive Material in Soil*," April 1993. A copy of Table 13.1 is provided in Appendix F. The low and high values for the uncertainty range are associated with the lowest and highest values in Table 13.1.

11 The areal extent of the Watershed Area is defined on Figure 3. The low and high uncertainty range values are not expected to be more than 1 percent above or below the recommended value.

12 The effective porosity value is based on a default value for silty clay in Table 3.3-1 of "*Development of Probabilistic RESRAD 6.0 and RESRAD-Build 3.0 Computer Codes*," November 2000. A copy of Table 3.3-1 is provided in Appendix E. The low and high values for the uncertainty range are associated with the lowest and highest values in Table 3.3-1.

13 The average horizontal hydraulic conductivity value was calculated using an average of the

values for NSSSC and DSCC as determined in Table 2 of "*Hydrogeologic Investigation and Ground-Water, Soil and Stream Characterization*" performed by LBG in March 1999). Appendix D includes a table with these values showing how the value was derived. It also includes a copy of the reference data. The low and high values for the uncertainty range are associated with the lowest and highest values from the data set.

14 Figure 1 shows the ground-water flow direction and gradient, and length of contaminated zone. Source of Figure 1 is from "*Hydrogeologic Investigation and Ground-Water, Soil and Stream Characterization*" performed by LBG in March 1999. The low and high values of the uncertainty range correspond to the lowest and highest gradient values from the LBG quarterly sampling reports.

15 Because the overburden aquifer is not used as a source of drinking water or for irrigation purposes, no net loss of ground water is expected to occur. Therefore, the value for the Water Table Drop Rate is zero. Low and high values of the uncertainty range are not applicable.

16 The Pump Intake Depth would be near the bottom of the DSCC, which would be approximately two feet above bedrock at the Site. The bottom of the screen depth of all DSCC wells was averaged and two feet was subtracted from that value. Table 5 from the RI/FS work plan was used to estimated the bottom of the wells, a copy of which is included in Appendix G. A table showing how the average was derived is also provided. The low and high values for the uncertainty range are associated with the lowest and highest values in Table 5.

17 Table 3.10-1 of "*Development of Probabilistic RESRAD 6.0 and RESRAD-Build 3.0 Computer Codes*," November 2000 provides a basis for determining the well pumping rate. The example scenario assumes a household of 4 adults, each requiring 225 liters of water per day. Agricultural parcels in this part of Missouri are typically not irrigated, so pumping rates for irrigation have not been provided. Water consumption for livestock is included in this parameter. Based on "*Principles of Controlled Grazing*," prepared by David W. Pratt in 1993, 2 head of cattle per acre on remote ranges or non-irrigated pasture is common. If the entire contaminated zone (1.59 acres) were used for pastureland, approximately 4 head of cattle would require drinking water needs. The example scenario assumes each head of cattle will require 160 liters of water per day. A calculation provided in Appendix H shows annual well pumping rate required for this scenario. A copy of Table 3.10-1 and pertinent information from "*Principles of Controlled Grazing*" are also provided. The low and high uncertainty range values are not expected to be more than 20 percent above or below the recommended

Site-Specific Soil Parameters
Westinghouse Former Fuel Cycle Facility D&&D Project

RESRAD Parameter Table for ^{235}U

Parameter	Recommended Value	RESRAD Code Designation	Units	Uncertainty Range			Probabilistic Function	Reference
				Low Value	High Value	Number of Samples		
Groundwater Concentration	13.4	W(i)	pCi/L	0	60.6	12	Lognormal	1
Area of Contaminated Zone	77458	AREA	m^2	61966	92950	NA	Normal	2
Thickness of Contaminated Zone	2	THICKO	m	1.00E-10	11.74	NA	Bounded Lognormal	3
Length Parallel to Aquifer	291	LCZPAQ	m	233	349	NA	Bounded Normal	4
Density of Contaminated Zone	1.69	DENSCZ	g/cm^3	1.39	2.11	28	Normal	5
Contaminated Zone Erosion Rate	0.0003	VCZ	m/yr	0.00024	0.00036	NA	Bounded Normal	6
Contaminated Zone Total Porosity	0.45	TPCZ	0.xx	0.41	0.483	13	Normal	7
Contaminated Zone Field Capacity	0.17	FCCZ	0.xx	0.01	0.2	NA	Bounded Normal	8
Contaminated Zone Hydraulic Conductivity	14.56	HCCZ	m/yr	1.38E-03	1.45E+02	13	Lognormal	9
Contaminated Zone b Parameter	10.40	BCZ	unitless	4.05	11.4	NA	Lognormal	10
Watershed Area	998939	WAREA	m^2	988950	1008928	NA	Bounded Normal	11
Density of Saturated Zone	1.69	DENSAQ	g/cm^3	1.39	2.11	28	Normal	5
Saturated Zone Total Porosity	0.45	TPSZ	0.xx	0.41	0.483	13	Normal	7
Saturated Zone Effective Porosity	0.29	EPSZ	0.xx	0.281	0.425	NA	Normal	12
Saturated Zone Field Capacity	0.17	FCSZ	0.xx	0.01	0.2	NA	Bounded Normal	8
Saturated Zone Hydraulic Conductivity	169.58	HCSZ	m/yr	1.56E+01	8.51E+01	12	Lognormal	13
Saturated Zone Hydraulic Gradient	0.015	HGWT	unitless	0.013	0.018	NA	Bounded Lognormal	14
Saturated Zone b Parameter	10.40	BSZ	unitless	4.05	11.4	NA	Lognormal	10
Water Table Drop Rate	0.00	VWT	m/yr	NA	NA	NA	None Recommended	15
Well Pump Intake Depth	9.41	DWIBWT	m	5.4	11.7	10	Bounded Normal	16
Well Pumping Rate	913	UW	m^3/yr	730	1096	NA	Bounded Normal	17

REFERENCE FOOTNOTES for ^{235}U

1 ^{235}U ground-water concentration data was taken from piezometer MW-32, which was sampled by Leggette, Brashears & Graham, Inc. in August 1999. This information was referenced in Table 7, *"Fourth Sampling Event Report in Conjunction with the Hydrogeologic Investigation and Ground-Water, Soil and Stream Characterization"*, prepared by LBG in November 1999. Figure 1 shows the location of MW-32 and Appendix A contains a copy of Table 7. The low value of the uncertainty range corresponds to the numerous non-detections during the four quarterly sampling events, and the high value corresponds to concentrations from WS-27 (November 1998).

2 Only sparse ^{235}U data exists for soil. LBG assumes the Area of Contaminated Zone is where operations involving ^{235}U occurred. Therefore, the Area of Contamination is defined by the following: Missouri State Highway P to the northwest, the Northeast Site Creek to the northeast, the fenceline to the southeast, and the Site Pond/Creek to the southwest. The northern limits include the Health Physics building and Red Room Roof Burial area, which are in close proximity to the highway. The eastern limits include the burial area, which is located between the plant and the Northeast Site Creek. The south fence line is just northwest of the railway easement. The western limits of extend to the Site Pond/Creek to encompass the location of the cistern/burn pit and red room roof burial area. Figure 4 shows the Area of Contamination for ^{235}U. The low and high uncertainty range values are not expected to be more than 20 percent above or below the recommended value.

3 Due to a sparse amount of soil data for ^{235}U, the RESRAD default value was chosen, based on Table 1.3 of *"Data Collection Handbook to Support Modeling Impacts of Radioactive Material in Soil,"* April 1993. Appendix C contains a copy of Table 1.3. The low value of the uncertainty range is based on the lower bounds value in Table 1.3. The high value of the uncertainty range is the maximum depth of the overburden.

4 Figure 1 shows the ground-water flow direction and gradient, and length of contaminated zone. The source of Figure 1 is from *"Hydrogeologic Investigation and Ground-Water, Soil and Stream Characterization"* performed by LBG in March 1999. The low and high uncertainty range values for the Length Parallel to Aquifer are not expected to be more than 20 percent above or below the recommended value.

5 Taken from an average of dry density calculations from work performed by Fitch, University of Missouri – Rolla, 1998, presented in *"Fourth Sampling Event Report in Conjunction with the Hydrogeologic Investigation and Ground-Water, Soil and Stream Characterization"*, prepared by LBG in November 1999, and Shannon and Wilson (Appendix B of *"Hydrogeologic Investigation and Ground-Water, Soil and Stream Characterization"* performed by LBG in March 1999). Appendix D includes a table with these values showing how the value was derived. It also includes a copy of the reference data. The low and high values for the uncertainty range are associated with the lowest and highest values from the data

set.

6 Jefferson County does not have a published soil survey which typically provide values for erosion rates. Therefore, the default value (0.001 m/yr) provided in Table 1.3 of "*Data Collection Handbook to Support Modeling Impacts of Radioactive Material in Soil*," April 1993, was used as a starting point. Since approximately 70 percent of the area of contamination is covered with impervious material, the default value was multiplied by .30 to give a value of 0.0003 m/yr. The low and high uncertainty range values are not expected to be more than 20 percent above or below the recommended value.

7 From Shannon and Wilson, (Appendix B of "*Hydrogeologic Investigation and Ground-Water, Soil and Stream Characterization*" performed by LBG in March 1999). Appendix D includes a table with these values showing how the value was derived. It also includes a copy of the reference data. The low and high values for the uncertainty range are associated with the lowest and highest values from the data set.

8 Derived using Formula 4.4 on page 28 of "*Data Collection Handbook to Support Modeling Impacts of Radioactive Material in Soil*," April 1993. The value for total porosity was taken from the average of Shannon and Wilson data (0.446; see footnote 7 above) and the value for effective porosity was based on a default value for silty clay in Table 3.3-1 of "*Development of Probabilistic RESRAD 6.0 and RESRAD-Build 3.0 Computer Codes*," November 2000. A copy of page 28, the completed formula, and Table 3.3-1 are provided in Appendix E. The low value of the uncertainty range cannot be zero (thus 0.01 was chosen), and the high value is derived by using the highest total porosity and effective porosity values in the calculation.

9 Shannon and Wilson (Appendix B of "*Hydrogeologic Investigation and Ground-Water, Soil and Stream Characterization*" prepared by LBG in March 1999) performed permeability tests on numerous soil samples. The average vertical permeability (hydraulic conductivity; K) for each sample was determined by averaging the last three permeability readings (telephone communication with Mr. Chris Groves, Vice-President, Shannon and Wilson on August 13, 2003). Once averages were calculated for each sample, an average of the entire data set was determined. The vertical hydraulic conductivity test data and a table developed to show the average K per sample, and the average K for the data set are provided in Appendix D. The low and high values for the uncertainty range are associated with the lowest and highest values from the data set.

10 Based on the default value for silty clay provided in Table 13.1, in "*Data Collection Handbook to Support Modeling Impacts of Radioactive Material in Soil*," April 1993. A copy of Table 13.1 is provided in Appendix F. The low and high values for the uncertainty range are associated with the lowest and highest values in Table 13.1.

11 The areal extent of the Watershed Area is defined on Figure 3. The low and high uncertainty range values are not expected to be more than 1 percent above or below the recommended

value.

12 The effective porosity value is based on a default value for silty clay in Table 3.3-1 of "*Development of Probabilistic RESRAD 6.0 and RESRAD-Build 3.0 Computer Codes*," November 2000. A copy of Table 3.3-1 is provided in Appendix E. The low and high values for the uncertainty range are associated with the lowest and highest values in Table 3.3-1.

13 The average horizontal hydraulic conductivity value was calculated using an average of the values for near-surface silt, silty-clay (NSSSC) and deep silty-clay, clay (DSCC) as determined in Table 2 of "*Hydrogeologic Investigation and Ground-Water, Soil and Stream Characterization*" performed by LBG in March 1999). Appendix D includes a table with these values showing how the value was derived. It also includes a copy of the reference data. The low and high values for the uncertainty range are associated with the lowest and highest values from the data set.

14 Figure 1 shows the ground-water flow direction and gradient, and length of contaminated zone. Source of Figure 1 is from "*Hydrogeologic Investigation and Ground-Water, Soil and Stream Characterization*" performed by LBG in March 1999. The low and high values of the uncertainty range correspond to the lowest and highest gradient values from the LBG quarterly sampling reports.

15 Because the overburden aquifer is not used as a source of drinking water or for irrigation purposes, no net loss of ground water is expected to occur. Therefore, the value for the Water Table Drop Rate is zero. Low and high values of the uncertainty range are not applicable.

16 The Pump Intake Depth would be near the bottom of the DSCC, which would be approximately two feet above bedrock at the Site. The bottom of the screen depth of all DSSC wells was averaged and two feet was subtracted from that value. Table 5 from the RI/FS work plan was used to estimated the bottom of the wells, a copy of which is included in Appendix G. A table showing how the average was derived is also provided. The low and high values for the uncertainty range are associated with the lowest and highest values in Table 5.

17 Table 3.10-1 of "*Development of Probabilistic RESRAD 6.0 and RESRAD-Build 3.0 Computer Codes*," November 2000 provides a basis for determining the well pumping rate. The example scenario assumes a household of 4 adults, each requiring 225 liters of water per day. Agricultural parcels in this part of Missouri are typically not irrigated, so pumping rates for irrigation have not been provided. Water consumption for livestock is included in this parameter. Based on "*Principles of Controlled Grazing*," prepared by David W. Pratt in 1993, 2 head of cattle per acre on remote ranges or non-irrigated pasture is common. If the entire contaminated zone (19.14 acres) were used for pastureland, approximately 10 head of cattle would require drinking water needs. The example scenario assumes each head of cattle will require 160 liters of Water per day. A calculation provided in Appendix H shows annual well pumping rate required for this scenario. A copy of Table 3.10-1 and pertinent information

from "*Principles of Controlled Grazing*" are also provided. The low and high uncertainty range values are not expected to be more than 20 percent above or below the recommended value.

Site-Specific Soil Parameters
Westinghouse Former Fuel Cycle Facility D&&D Project

RESRAD Parameter Table for ^{228}Ac

Parameter	Recommended Value	RESRAD Code Designation	Units	Uncertainty Range			Probabilistic Function	Reference
				Low Value	High Value	Number of Samples		
Groundwater Concentration	29.3	W(i)	pCi/L	0	41.8	12	Lognormal	1
Area of Contaminated Zone	77458	AREA	m^2	61966	92950	NA	Normal	2
Thickness of Contaminated Zone	2	THICKO	m	1.00E-10	11.74	NA	Bounded Lognormal	3
Length Parallel to Aquifer	291	LCZPAQ	m	233	349	NA	Bounded Normal	4
Density of Contaminated Zone	1.69	DENSCZ	g/cm^3	1.39	2.11	28	Normal	5
Contaminated Zone Erosion Rate	0.0003	VCZ	m/yr	0.00024	0.00036	NA	Bounded Normal	6
Contaminated Zone Total Porosity	0.45	TPCZ	0.xx	0.41	0.483	13	Normal	7
Contaminated Zone Field Capacity	0.17	FCCZ	0.xx	0.01	0.2	NA	Bounded Normal	8
Contaminated Zone Hydraulic Conductivity	14.56	HCCZ	m/yr	1.38E-03	1.45E+02	13	Lognormal	9
Contaminated Zone b Parameter	10.40	BCZ	unitless	4.05	11.4	NA	Lognormal	10
Watershed Area	998939	WAREA	m^2	988950	1008928	NA	Bounded Normal	11
Density of Saturated Zone	1.69	DENSAQ	g/cm^3	1.39	2.11	28	Normal	5
Saturated Zone Total Porosity	0.45	TPSZ	0.xx	0.41	0.483	13	Normal	7
Saturated Zone Effective Porosity	0.29	EPSZ	0.xx	0.281	0.425	NA	Normal	12
Saturated Zone Field Capacity	0.17	FCSZ	0.xx	0.01	0.2	NA	Bounded Normal	8
Saturated Zone Hydraulic Conductivity	169.58	HCSZ	m/yr	1.56E+01	8.51E+01	12	Lognormal	13
Saturated Zone Hydraulic Gradient	0.015	HGWT	unitless	0.013	0.018	NA	Bounded Lognormal	14
Saturated Zone b Parameter	10.40	BSZ	unitless	4.05	11.4	NA	Lognormal	10
Water Table Drop Rate	0.00	VWT	m/yr	NA	NA	NA	None Recommended	15
Well Pump Intake Depth	9.41	DWIBWT	m	5.4	11.7	10	Bounded Normal	16
Well Pumping Rate	913	UW	m^3/yr	730	1096	NA	Bounded Normal	17

REFERENCE FOOTNOTES for ^{228}Ac

1 ^{228}Ac ground-water concentration data was taken from piezometer MW-32, which was sampled by Leggette, Brashears & Graham, Inc. in May 1999. This information was referenced in Table 7, *"Fourth Sampling Event Report in Conjunction with the Hydrogeologic Investigation and Ground-Water, Soil and Stream Characterization"*, prepared by LBG in November 1999. Figure 1 shows the location of MW-32 and Appendix A contains a copy of Table 7. The low value of the uncertainty range corresponds to the numerous non-detections during the four quarterly sampling events, and the high value corresponds to concentrations from WS-27 (August 1999).

2 Only sparse ^{228}Ac data exists for soil. LBG assumes the Area of Contaminated Zone is where operations involving radioactive materials occurred. Therefore, the Area of Contamination is defined by the following: Missouri State Highway P to the northwest, the Northeast Site Creek to the northeast, the fenceline to the southeast, and the Site Pond/Creek to the southwest. The northern limits include the Health Physics building and Red Room Roof Burial area, which are in close proximity to the highway. The eastern limits include the burial area, which is located between the plant and the Northeast Site Creek. The south fence line is just northwest of the railway easement. The western limits of extend to the Site Pond/Creek to encompass the location of the cistern/burn pit and red room roof burial area. Figure 4 shows the Area of Contamination for ^{228}Ac. The low and high uncertainty range values are not expected to be more than 20 percent above or below the recommended value.

3 Due to a sparse amount of soil data for ^{228}Ac, the RESRAD default value was chosen, based on Table 1.3 of *"Data Collection Handbook to Support Modeling Impacts of Radioactive Material in Soil,"* April 1993. Appendix C contains a copy of Table 1.3. The low value of the uncertainty range is based on the lower bounds value in Table 1.3. The high value of the uncertainty range is the maximum depth of the overburden.

4 Figure 1 shows the ground-water flow direction and gradient, and length of contaminated zone. The source of Figure 1 is from *"Hydrogeologic Investigation and Ground-Water, Soil and Stream Characterization"* performed by LBG in March 1999. The low and high uncertainty range values for the Length Parallel to Aquifer are not expected to be more than 20 percent above or below the recommended value.

5 Taken from an average of dry density calculations from work performed by Fitch, University of Missouri – Rolla, 1998, presented in *"Fourth Sampling Event Report in Conjunction with the Hydrogeologic Investigation and Ground-Water, Soil and Stream Characterization"*, prepared by LBG in November 1999, and Shannon and Wilson (Appendix B of *"Hydrogeologic Investigation and Ground-Water, Soil and Stream Characterization"* performed by LBG in March 1999). Appendix D includes a table with these values showing how the value was derived. It also includes a copy of the reference data. The low and high values for the uncertainty range are associated with the lowest and highest values from the data set.

6 Jefferson County does not have a published soil survey which typically provide values for erosion rates. Therefore, the default value (0.001 m/yr) provided in Table 1.3 of "*Data Collection Handbook to Support Modeling Impacts of Radioactive Material in Soil*," April 1993, was used as a starting point. Since approximately 70 percent of the area of contamination is covered with impervious material, the default value was multiplied by .30 to give a value of 0.0003 m/yr. The low and high uncertainty range values are not expected to be more than 20 percent above or below the recommended value.

7 From Shannon and Wilson, (Appendix B of "*Hydrogeologic Investigation and Ground-Water, Soil and Stream Characterization*" performed by LBG in March 1999). Appendix D includes a table with these values showing how the value was derived. It also includes a copy of the reference data. The low and high values for the uncertainty range are associated with the lowest and highest values from the data set.

8 Derived using Formula 4.4 on page 28 of "*Data Collection Handbook to Support Modeling Impacts of Radioactive Material in Soil*," April 1993. The value for total porosity was taken from the average of Shannon and Wilson data (0.446; see footnote 7 above) and the value for effective porosity was based on a default value for silty clay in Table 3.3-1 of "*Development of Probabilistic RESRAD 6.0 and RESRAD-Build 3.0 Computer Codes*," November 2000. A copy of page 28, the completed formula, and Table 3.3-1 are provided in Appendix E. The low value of the uncertainty range cannot be zero (thus 0.01 was chosen), and the high value is derived by using the highest total porosity and effective porosity values in the calculation.

9 Shannon and Wilson (Appendix B of "*Hydrogeologic Investigation and Ground-Water, Soil and Stream Characterization*" prepared by LBG in March 1999) performed permeability tests on numerous soil samples. The average vertical permeability (hydraulic conductivity; K) for each sample was determined by averaging the last three permeability readings (telephone communication with Mr. Chris Groves, Vice-President, Shannon and Wilson on August 13, 2003). Once averages were calculated for each sample, an average of the entire data set was determined. The vertical hydraulic conductivity test data and a table developed to show the average K per sample, and the average K for the data set are provided in Appendix D. The low and high values for the uncertainty range are associated with the lowest and highest values from the data set.

10 Based on the default value for silty clay provided in Table 13.1, in "*Data Collection Handbook to Support Modeling Impacts of Radioactive Material in Soil*," April 1993. A copy of Table 13.1 is provided in Appendix F. The low and high values for the uncertainty range are associated with the lowest and highest values in Table 13.1.

11 The areal extent of the Watershed Area is defined on Figure 3. The low and high uncertainty range values are not expected to be more than 1 percent above or below the recommended value.

12 The effective porosity value is based on a default value for silty clay in Table 3.3-1 of *"Development of Probabilistic RESRAD 6.0 and RESRAD-Build 3.0 Computer Codes,"* November 2000. A copy of Table 3.3-1 is provided in Appendix E. The low and high values for the uncertainty range are associated with the lowest and highest values in Table 3.3-1.

13 The average horizontal hydraulic conductivity value was calculated using an average of the values for near-surface silt, silty-clay (NSSSC) and deep silty-clay, clay (DSCC) as determined in Table 2 of *"Hydrogeologic Investigation and Ground-Water, Soil and Stream Characterization"* performed by LBG in March 1999). Appendix D includes a table with these values showing how the value was derived. It also includes a copy of the reference data. The low and high values for the uncertainty range are associated with the lowest and highest values from the data set.

14 Figure 1 shows the ground-water flow direction and gradient, and length of contaminated zone. Source of Figure 1 is from *"Hydrogeologic Investigation and Ground-Water, Soil and Stream Characterization"* performed by LBG in March 1999. The low and high values of the uncertainty range correspond to the lowest and highest gradient values from the LBG quarterly sampling reports.

15 Because the overburden aquifer is not used as a source of drinking water or for irrigation purposes, no net loss of ground water is expected to occur. Therefore, the value for the Water Table Drop Rate is zero. Low and high values of the uncertainty range are not applicable.

16 The Pump Intake Depth would be near the bottom of the DSCC, which would be approximately two feet above bedrock at the Site. The bottom of the screen depth of all DSSC wells was averaged and two feet was subtracted from that value. Table 5 from the RI/FS work plan was used to estimated the bottom of the wells, a copy of which is included in Appendix G. A table showing how the average was derived is also provided. The low and high values for the uncertainty range are associated with the lowest and highest values in Table 5.

17 Table 3.10-1 of *"Development of Probabilistic RESRAD 6.0 and RESRAD-Build 3.0 Computer Codes,"* November 2000 provides a basis for determining the well pumping rate. The example scenario assumes a household of 4 adults, each requiring 225 liters of water per day. Agricultural parcels in this part of Missouri are typically not irrigated, so pumping rates for irrigation have not been provided. Water consumption for livestock is included in this parameter. Based on *"Principles of Controlled Grazing,"* prepared by David W. Pratt in 1993, 2 head of cattle per acre on remote ranges or non-irrigated pasture is common. If the entire contaminated zone (19.14 acres) were used for pastureland, approximately 10 head of cattle would require drinking water needs. The example scenario assumes each head of cattle will require 160 liters of Water per day. A calculation provided in Appendix H shows annual well pumping rate required for this scenario. A copy of Table 3.10-1 and pertinent information

from "*Principles of*

Controlled Grazing" are also provided. The low and high uncertainty range values are not expected to be more than 20 percent above or below the recommended value.

Site-Specific Soil Parameters
Westinghouse Former Fuel Cycle Facility D&&D Project

RESRAD Parameter Table for ^{212}Bi

Parameter	Recommended Value	RESRAD Code Designation	Units	Uncertainty Range			Probabilistic Function	Reference
				Low Value	High Value	Number of Samples		
Groundwater Concentration	1.49	W(i)	pCi/L	0	1.49	12	Lognormal	1
Area of Contaminated Zone	77458	AREA	m^2	61966	92950	NA	Normal	2
Thickness of Contaminated Zone	2	THICKO	m	1.00E-10	11.74	NA	Bounded Lognormal	3
Length Parallel to Aquifer	291	LCZPAQ	m	233	349	NA	Bounded Normal	4
Density of Contaminated Zone	1.69	DENSCZ	g/cm^3	1.39	2.11	28	Normal	5
Contaminated Zone Erosion Rate	0.0003	VCZ	m/yr	0.00024	0.00036	NA	Bounded Normal	6
Contaminated Zone Total Porosity	0.45	TPCZ	0.xx	0.41	0.483	13	Normal	7
Contaminated Zone Field Capacity	0.17	FCCZ	0.xx	0.01	0.2	NA	Bounded Normal	8
Contaminated Zone Hydraulic Conductivity	14.56	HCCZ	m/yr	1.38E-03	1.45E+02	13	Lognormal	9
Contaminated Zone b Parameter	10.40	BCZ	unitless	4.05	11.4	NA	Lognormal	10
Watershed Area	998939	WAREA	m^2	988950	1008928	NA	Bounded Normal	11
Density of Saturated Zone	1.69	DENSAQ	g/cm^3	1.39	2.11	28	Normal	5
Saturated Zone Total Porosity	0.45	TPSZ	0.xx	0.41	0.483	13	Normal	7
Saturated Zone Effective Porosity	0.29	EPSZ	0.xx	0.281	0.425	NA	Normal	12
Saturated Zone Field Capacity	0.17	FCSZ	0.xx	0.01	0.2	NA	Bounded Normal	8
Saturated Zone Hydraulic Conductivity	169.58	HCSZ	m/yr	1.56E+01	8.51E+01	12	Lognormal	13
Saturated Zone Hydraulic Gradient	0.015	HGWT	unitless	0.013	0.018	NA	Bounded Lognormal	14
Saturated Zone b Parameter	10.40	BSZ	unitless	4.05	11.4	NA	Lognormal	10
Water Table Drop Rate	0.00	VWT	m/yr	NA	NA	NA	None Recommended	15
Well Pump Intake Depth	9.41	DWIBWT	m	5.4	11.7	10	Bounded Normal	16
Well Pumping Rate	913	UW	m^3/yr	730	1096	NA	Bounded Normal	17

REFERENCE FOOTNOTES for ^{212}Bi

1 ^{212}Bi ground-water concentration data was taken from piezometer MW-23, which was sampled by Leggette, Brashears & Graham, Inc. in May 1999. This information was referenced in Table 7, *"Fourth Sampling Event Report in Conjunction with the Hydrogeologic Investigation and Ground-Water, Soil and Stream Characterization"*, prepared by LBG in November 1999. Figure 1 shows the location of MW-23 and Appendix A contains a copy of Table 7. The low value of the uncertainty range corresponds to the numerous non-detections during the four quarterly sampling events, and the high value corresponds to the recommended value (1.49; May 1999).

2 Only sparse ^{212}Bi data exists for soil. LBG assumes the Area of Contaminated Zone is where operations involving radioactive materials occurred. Therefore, the Area of Contamination is defined by the following: Missouri State Highway P to the northwest, the Northeast Site Creek to the northeast, the fenceline to the southeast, and the Site Pond/Creek to the southwest. The northern limits include the Health Physics building and Red Room Roof Burial area, which are in close proximity to the highway. The eastern limits include the burial area, which is located between the plant and the Northeast Site Creek. The south fence line is just northwest of the railway easement. The western limits of extend to the Site Pond/Creek to encompass the location of the cistern/burn pit and red room roof burial area. Figure 4 shows the Area of Contamination for ^{212}Bi. The low and high uncertainty range values are not expected to be more than 20 percent above or below the recommended value.

3 Due to a sparse amount of soil data for ^{212}Bi, the RESRAD default value was chosen, based on Table 1.3 of *"Data Collection Handbook to Support Modeling Impacts of Radioactive Material in Soil,"* April 1993. Appendix C contains a copy of Table 1.3. The low value of the uncertainty range is based on the lower bounds value in Table 1.3. The high value of the uncertainty range is the maximum depth of the overburden.

4 Figure 1 shows the ground-water flow direction and gradient, and length of contaminated zone. The source of Figure 1 is from *"Hydrogeologic Investigation and Ground-Water, Soil and Stream Characterization"* performed by LBG in March 1999. The low and high uncertainty range values for the Length Parallel to Aquifer are not expected to be more than 20 percent above or below the recommended value.

5 Taken from an average of dry density calculations from work performed by Fitch, University of Missouri – Rolla, 1998, presented in *"Fourth Sampling Event Report in Conjunction with the Hydrogeologic Investigation and Ground-Water, Soil and Stream Characterization"*, prepared by LBG in November 1999, and Shannon and Wilson (Appendix B of *"Hydrogeologic Investigation and Ground-Water, Soil and Stream Characterization"* performed by LBG in March 1999). Appendix D includes a table with these values showing how the value was derived. It also includes a copy of the reference data. The low and high values for the uncertainty range are associated with the lowest and highest values from the data set.

6 Jefferson County does not have a published soil survey which typically provide values for erosion rates. Therefore, the default value (0.001 m/yr) provided in Table 1.3 of "*Data Collection Handbook to Support Modeling Impacts of Radioactive Material in Soil*," April 1993, was used as a starting point. Since approximately 70 percent of the area of contamination is covered with impervious material, the default value was multiplied by .30 to give a value of 0.0003 m/yr. The low and high uncertainty range values are not expected to be more than 20 percent above or below the recommended value.

7 From Shannon and Wilson, (Appendix B of "*Hydrogeologic Investigation and Ground-Water, Soil and Stream Characterization*" performed by LBG in March 1999). Appendix D includes a table with these values showing how the value was derived. It also includes a copy of the reference data. The low and high values for the uncertainty range are associated with the lowest and highest values from the data set.

8 Derived using Formula 4.4 on page 28 of "*Data Collection Handbook to Support Modeling Impacts of Radioactive Material in Soil*," April 1993. The value for total porosity was taken from the average of Shannon and Wilson data (0.446; see footnote 7 above) and the value for effective porosity was based on a default value for silty clay in Table 3.3-1 of "*Development of Probabilistic RESRAD 6.0 and RESRAD-Build 3.0 Computer Codes*," November 2000. A copy of page 28, the completed formula, and Table 3.3-1 are provided in Appendix E. The low value of the uncertainty range cannot be zero (thus 0.01 was chosen), and the high value is derived by using the highest total porosity and effective porosity values in the calculation.

9 Shannon and Wilson (Appendix B of "*Hydrogeologic Investigation and Ground-Water, Soil and Stream Characterization*" prepared by LBG in March 1999) performed permeability tests on numerous soil samples. The average vertical permeability (hydraulic conductivity; K) for each sample was determined by averaging the last three permeability readings (telephone communication with Mr. Chris Groves, Vice-President, Shannon and Wilson on August 13, 2003). Once averages were calculated for each sample, an average of the entire data set was determined. The vertical hydraulic conductivity test data and a table developed to show the average K per sample, and the average K for the data set are provided in Appendix D. The low and high values for the uncertainty range are associated with the lowest and highest values from the data set.

10 Based on the default value for silty clay provided in Table 13.1, in "*Data Collection Handbook to Support Modeling Impacts of Radioactive Material in Soil*," April 1993. A copy of Table 13.1 is provided in Appendix F. The low and high values for the uncertainty range are associated with the lowest and highest values in Table 13.1.

11 The areal extent of the Watershed Area is defined on Figure 3. The low and high uncertainty range values are not expected to be more than 1 percent above or below the recommended value.

12 The effective porosity value is based on a default value for silty clay in Table 3.3-1 of "*Development of Probabilistic RESRAD 6.0 and RESRAD-Build 3.0 Computer Codes*," November 2000. A copy of Table 3.3-1 is provided in Appendix E. The low and high values for the uncertainty range are associated with the lowest and highest values in Table 3.3-1.

13 The average horizontal hydraulic conductivity value was calculated using an average of the values for near-surface silt, silty-clay (NSSSC) and deep silty-clay, clay (DSCC) as determined in Table 2 of "*Hydrogeologic Investigation and Ground-Water, Soil and Stream Characterization*" performed by LBG in March 1999). Appendix D includes a table with these values showing how the value was derived. It also includes a copy of the reference data. The low and high values for the uncertainty range are associated with the lowest and highest values from the data set.

14 Figure 1 shows the ground-water flow direction and gradient, and length of contaminated zone. Source of Figure 1 is from "*Hydrogeologic Investigation and Ground-Water, Soil and Stream Characterization*" performed by LBG in March 1999. The low and high values of the uncertainty range correspond to the lowest and highest gradient values from the LBG quarterly sampling reports.

15 Because the overburden aquifer is not used as a source of drinking water or for irrigation purposes, no net loss of ground water is expected to occur. Therefore, the value for the Water Table Drop Rate is zero. Low and high values of the uncertainty range are not applicable.

16 The Pump Intake Depth would be near the bottom of the DSCC, which would be approximately two feet above bedrock at the Site. The bottom of the screen depth of all DSSC wells was averaged and two feet was subtracted from that value. Table 5 from the RI/FS work plan was used to estimated the bottom of the wells, a copy of which is included in Appendix G. A table showing how the average was derived is also provided. The low and high values for the uncertainty range are associated with the lowest and highest values in Table 5.

17 Table 3.10-1 of "*Development of Probabilistic RESRAD 6.0 and RESRAD-Build 3.0 Computer Codes*," November 2000 provides a basis for determining the well pumping rate. The example scenario assumes a household of 4 adults, each requiring 225 liters of water per day. Agricultural parcels in this part of Missouri are typically not irrigated, so pumping rates for irrigation have not been provided. Water consumption for livestock is included in this parameter. Based on "*Principles of Controlled Grazing*," prepared by David W. Pratt in 1993, 2 head of cattle per acre on remote ranges or non-irrigated pasture is common. If the entire contaminated zone (19.14 acres) were used for pastureland, approximately 10 head of cattle would require drinking water needs. The example scenario assumes each head of cattle will require 160 liters of Water per day. A calculation provided in Appendix H shows annual well pumping rate required for this scenario. A copy of Table 3.10-1 and pertinent information

from "*Principles of*

Controlled Grazing" are also provided. The low and high uncertainty range values are not expected to be more than 20 percent above or below the recommended value.

Site-Specific Soil Parameters
Westinghouse Former Fuel Cycle Facility D&&D Project

RESRAD Parameter Table for ^{212}Pb

Parameter	Recommended Value	RESRAD Code Designation	Units	Uncertainty Range			Probabilistic Function	Reference
				Low Value	High Value	Number of Samples		
Groundwater Concentration	31.8	W(i)	pCi/L	0	78.4	12	Lognormal	1
Area of Contaminated Zone	77458	AREA	m^2	61966	92950	NA	Normal	2
Thickness of Contaminated Zone	2	THICKO	m	1.00E-10	11.74	NA	Bounded Lognormal	3
Length Parallel to Aquifer	291	LCZPAQ	m	233	349	NA	Bounded Normal	4
Density of Contaminated Zone	1.69	DENSCZ	g/cm^3	1.39	2.11	28	Normal	5
Contaminated Zone Erosion Rate	0.0003	VCZ	m/yr	0.00024	0.00036	NA	Bounded Normal	6
Contaminated Zone Total Porosity	0.45	TPCZ	0.xx	0.41	0.483	13	Normal	7
Contaminated Zone Field Capacity	0.17	FCCZ	0.xx	0.01	0.2	NA	Bounded Normal	8
Contaminated Zone Hydraulic Conductivity	14.56	HCCZ	m/yr	1.38E-03	1.45E+02	13	Lognormal	9
Contaminated Zone b Parameter	10.40	BCZ	unitless	4.05	11.4	NA	Lognormal	10
Watershed Area	998939	WAREA	m^2	988950	1008928	NA	Bounded Normal	11
Density of Saturated Zone	1.69	DENSAQ	g/cm^3	1.39	2.11	28	Normal	5
Saturated Zone Total Porosity	0.45	TPSZ	0.xx	0.41	0.483	13	Normal	7
Saturated Zone Effective Porosity	0.29	EPSZ	0.xx	0.281	0.425	NA	Normal	12
Saturated Zone Field Capacity	0.17	FCSZ	0.xx	0.01	0.2	NA	Bounded Normal	8
Saturated Zone Hydraulic Conductivity	169.58	HCSZ	m/yr	1.56E+01	8.51E+01	12	Lognormal	13
Saturated Zone Hydraulic Gradient	0.015	HGWT	unitless	0.013	0.018	NA	Bounded Lognormal	14
Saturated Zone b Parameter	10.40	BSZ	unitless	4.05	11.4	NA	Lognormal	10
Water Table Drop Rate	0.00	VWT	m/yr	NA	NA	NA	None Recommended	15
Well Pump Intake Depth	9.41	DWIBWT	m	5.4	11.7	10	Bounded Normal	16
Well Pumping Rate	913	UW	m^3/yr	730	1096	NA	Bounded Normal	17

REFERENCE FOOTNOTES for ^{212}Pb

1 ^{212}Pb ground-water concentration data was taken from piezometer MW-32, which was sampled by Leggette, Brashears & Graham, Inc. in February 1999. This information was referenced in Table 7, *"Fourth Sampling Event Report in Conjunction with the Hydrogeologic Investigation and Ground-Water, Soil and Stream Characterization"*, prepared by LBG in November 1999. Figure 1 shows the location of MW-32 and Appendix A contains a copy of Table 7. The low value of the uncertainty range corresponds to the numerous non-detections during the four quarterly sampling events, and the high value corresponds to concentrations from WS-23 (February 1999).

2 Only sparse ^{212}Pb data exists for soil. LBG assumes the Area of Contaminated Zone is where operations involving radioactive materials occurred. Therefore, the Area of Contamination is defined by the following: Missouri State Highway P to the northwest, the Northeast Site Creek to the northeast, the fenceline to the southeast, and the Site Pond/Creek to the southwest. The northern limits include the Health Physics building and Red Room Roof Burial area, which are in close proximity to the highway. The eastern limits include the burial area, which is located between the plant and the Northeast Site Creek. The south fence line is just northwest of the railway easement. The western limits of extend to the Site Pond/Creek to encompass the location of the cistern/burn pit and red room roof burial area. Figure 4 shows the Area of Contamination for ^{212}Pb. The low and high uncertainty range values are not expected to be more than 20 percent above or below the recommended value.

3 Due to a sparse amount of soil data for ^{212}Pb, the RESRAD default value was chosen, based on Table 1.3 of *"Data Collection Handbook to Support Modeling Impacts of Radioactive Material in Soil,"* April 1993. Appendix C contains a copy of Table 1.3. The low value of the uncertainty range is based on the lower bounds value in Table 1.3. The high value of the uncertainty range is the maximum depth of the overburden.

4 Figure 1 shows the ground-water flow direction and gradient, and length of contaminated zone. The source of Figure 1 is from *"Hydrogeologic Investigation and Ground-Water, Soil and Stream Characterization"* performed by LBG in March 1999. The low and high uncertainty range values for the Length Parallel to Aquifer are not expected to be more than 20 percent above or below the recommended value.

5 Taken from an average of dry density calculations from work performed by Fitch, University of Missouri – Rolla, 1998, presented in *"Fourth Sampling Event Report in Conjunction with the Hydrogeologic Investigation and Ground-Water, Soil and Stream Characterization"*, prepared by LBG in November 1999, and Shannon and Wilson (Appendix B of *"Hydrogeologic Investigation and Ground-Water, Soil and Stream Characterization"* performed by LBG in March 1999). Appendix D includes a table with these values showing how the value was derived. It also includes a copy of the reference data. The low and high values for the uncertainty range are associated with the lowest and highest values from the data set.

6 Jefferson County does not have a published soil survey which typically provide values for erosion rates. Therefore, the default value (0.001 m/yr) provided in Table 1.3 of "*Data Collection Handbook to Support Modeling Impacts of Radioactive Material in Soil*," April 1993, was used as a starting point. Since approximately 70 percent of the area of contamination is covered with impervious material, the default value was multiplied by .30 to give a value of 0.0003 m/yr. The low and high uncertainty range values are not expected to be more than 20 percent above or below the recommended value.

7 From Shannon and Wilson, (Appendix B of "*Hydrogeologic Investigation and Ground-Water, Soil and Stream Characterization*" performed by LBG in March 1999). Appendix D includes a table with these values showing how the value was derived. It also includes a copy of the reference data. The low and high values for the uncertainty range are associated with the lowest and highest values from the data set.

8 Derived using Formula 4.4 on page 28 of "*Data Collection Handbook to Support Modeling Impacts of Radioactive Material in Soil*," April 1993. The value for total porosity was taken from the average of Shannon and Wilson data (0.446; see footnote 7 above) and the value for effective porosity was based on a default value for silty clay in Table 3.3-1 of "*Development of Probabilistic RESRAD 6.0 and RESRAD-Build 3.0 Computer Codes*," November 2000. A copy of page 28, the completed formula, and Table 3.3-1 are provided in Appendix E. The low value of the uncertainty range cannot be zero (thus 0.01 was chosen), and the high value is derived by using the highest total porosity and effective porosity values in the calculation.

9 Shannon and Wilson (Appendix B of "*Hydrogeologic Investigation and Ground-Water, Soil and Stream Characterization*" prepared by LBG in March 1999) performed permeability tests on numerous soil samples. The average vertical permeability (hydraulic conductivity; K) for each sample was determined by averaging the last three permeability readings (telephone communication with Mr. Chris Groves, Vice-President, Shannon and Wilson on August 13, 2003). Once averages were calculated for each sample, an average of the entire data set was determined. The vertical hydraulic conductivity test data and a table developed to show the average K per sample, and the average K for the data set are provided in Appendix D. The low and high values for the uncertainty range are associated with the lowest and highest values from the data set.

10 Based on the default value for silty clay provided in Table 13.1, in "*Data Collection Handbook to Support Modeling Impacts of Radioactive Material in Soil*," April 1993. A copy of Table 13.1 is provided in Appendix F. The low and high values for the uncertainty range are associated with the lowest and highest values in Table 13.1.

11 The areal extent of the Watershed Area is defined on Figure 3. The low and high uncertainty range values are not expected to be more than 1 percent above or below the recommended value.

12 The effective porosity value is based on a default value for silty clay in Table 3.3-1 of "*Development of Probabilistic RESRAD 6.0 and RESRAD-Build 3.0 Computer Codes*," November 2000. A copy of Table 3.3-1 is provided in Appendix E. The low and high values for the uncertainty range are associated with the lowest and highest values in Table 3.3-1.

13 The average horizontal hydraulic conductivity value was calculated using an average of the values for near-surface silt, silty-clay (NSSSC) and deep silty-clay, clay (DSCC) as determined in Table 2 of "*Hydrogeologic Investigation and Ground-Water, Soil and Stream Characterization*" performed by LBG in March 1999). Appendix D includes a table with these values showing how the value was derived. It also includes a copy of the reference data. The low and high values for the uncertainty range are associated with the lowest and highest values from the data set.

14 Figure 1 shows the ground-water flow direction and gradient, and length of contaminated zone. Source of Figure 1 is from "*Hydrogeologic Investigation and Ground-Water, Soil and Stream Characterization*" performed by LBG in March 1999. The low and high values of the uncertainty range correspond to the lowest and highest gradient values from the LBG quarterly sampling reports.

15 Because the overburden aquifer is not used as a source of drinking water or for irrigation purposes, no net loss of ground water is expected to occur. Therefore, the value for the Water Table Drop Rate is zero. Low and high values of the uncertainty range are not applicable.

16 The Pump Intake Depth would be near the bottom of the DSCC, which would be approximately two feet above bedrock at the Site. The bottom of the screen depth of all DSSC wells was averaged and two feet was subtracted from that value. Table 5 from the RI/FS work plan was used to estimated the bottom of the wells, a copy of which is included in Appendix G. A table showing how the average was derived is also provided. The low and high values for the uncertainty range are associated with the lowest and highest values in Table 5.

17 Table 3.10-1 of "*Development of Probabilistic RESRAD 6.0 and RESRAD-Build 3.0 Computer Codes*," November 2000 provides a basis for determining the well pumping rate. The example scenario assumes a household of 4 adults, each requiring 225 liters of water per day. Agricultural parcels in this part of Missouri are typically not irrigated, so pumping rates for irrigation have not been provided. Water consumption for livestock is included in this parameter. Based on "*Principles of Controlled Grazing*," prepared by David W. Pratt in 1993, 2 head of cattle per acre on remote ranges or non-irrigated pasture is common. If the entire contaminated zone (19.14 acres) were used for pastureland, approximately 10 head of cattle would require drinking water needs. The example scenario assumes each head of cattle will require 160 liters of Water per day. A calculation provided in Appendix H shows annual well pumping rate required for this scenario. A copy of Table 3.10-1 and pertinent information

from "*Principles of*

Controlled Grazing" are also provided. The low and high uncertainty range values are not expected to be more than 20 percent above or below the recommended value.

Site-Specific Soil Parameters
Westinghouse Former Fuel Cycle Facility D&&D Project

RESRAD Parameter Table for ^{208}Tl

Parameter	Recommended Value	RESRAD Code Designation	Units	Uncertainty Range			Probabilistic Function	Reference
				Low Value	High Value	Number of Samples		
Groundwater Concentration	8.3	W(i)	pCi/L	0	12.3	12	Lognormal	1
Area of Contaminated Zone	77458	AREA	m^2	61966	92950	NA	Normal	2
Thickness of Contaminated Zone	2	THICKO	m	1.00E-10	11.74	NA	Bounded Lognormal	3
Length Parallel to Aquifer	291	LCZPAQ	m	233	349	NA	Bounded Normal	4
Density of Contaminated Zone	1.69	DENSCZ	g/cm^3	1.39	2.11	28	Normal	5
Contaminated Zone Erosion Rate	0.0003	VCZ	m/yr	0.00024	0.00036	NA	Bounded Normal	6
Contaminated Zone Total Porosity	0.45	TPCZ	0.xx	0.41	0.483	13	Normal	7
Contaminated Zone Field Capacity	0.17	FCCZ	0.xx	0.01	0.2	NA	Bounded Normal	8
Contaminated Zone Hydraulic Conductivity	14.56	HCCZ	m/yr	1.38E-03	1.45E+02	13	Lognormal	9
Contaminated Zone b Parameter	10.40	BCZ	unitless	4.05	11.4	NA	Lognormal	10
Watershed Area	998939	WAREA	m^2	988950	1008928	NA	Bounded Normal	11
Density of Saturated Zone	1.69	DENSAQ	g/cm^3	1.39	2.11	28	Normal	5
Saturated Zone Total Porosity	0.45	TPSZ	0.xx	0.41	0.483	13	Normal	7
Saturated Zone Effective Porosity	0.29	EPSZ	0.xx	0.281	0.425	NA	Normal	12
Saturated Zone Field Capacity	0.17	FCSZ	0.xx	0.01	0.2	NA	Bounded Normal	8
Saturated Zone Hydraulic Conductivity	169.58	HCSZ	m/yr	1.56E+01	8.51E+01	12	Lognormal	13
Saturated Zone Hydraulic Gradient	0.015	HGWT	unitless	0.013	0.018	NA	Bounded Lognormal	14
Saturated Zone b Parameter	10.40	BSZ	unitless	4.05	11.4	NA	Lognormal	10
Water Table Drop Rate	0.00	VWT	m/yr	NA	NA	NA	None Recommended	15
Well Pump Intake Depth	9.41	DWIBWT	m	5.4	11.7	10	Bounded Normal	16
Well Pumping Rate	913	UW	m^3/yr	730	1096	NA	Bounded Normal	17

REFERENCE FOOTNOTES for ^{208}Tl

1 ^{208}Tl ground-water concentration data was taken from piezometer MW-17B, which was sampled by Leggette, Brashears & Graham, Inc. in February 1999. This information was referenced in Table 7, *"Fourth Sampling Event Report in Conjunction with the Hydrogeologic Investigation and Ground-Water, Soil and Stream Characterization"*, prepared by LBG in November 1999. Figure 1 shows the location of MW-17B and Appendix A contains a copy of Table 7. The low value of the uncertainty range corresponds to the numerous non-detections during the four quarterly sampling events, and the high value corresponds to concentrations from WS-22 (August 1999).

2 Only sparse ^{208}Tl data exists for soil. LBG assumes the Area of Contaminated Zone is where operations involving radioactive materials occurred. Therefore, the Area of Contamination is defined by the following: Missouri State Highway P to the northwest, the Northeast Site Creek to the northeast, the fenceline to the southeast, and the Site Pond/Creek to the southwest. The northern limits include the Health Physics building and Red Room Roof Burial area, which are in close proximity to the highway. The eastern limits include the burial area, which is located between the plant and the Northeast Site Creek. The south fence line is just northwest of the railway easement. The western limits of extend to the Site Pond/Creek to encompass the location of the cistern/burn pit and red room roof burial area. Figure 4 shows the Area of Contamination for ^{208}Tl. The low and high uncertainty range values are not expected to be more than 20 percent above or below the recommended value.

3 Due to a sparse amount of soil data for ^{208}Tl, the RESRAD default value was chosen, based on Table 1.3 of *"Data Collection Handbook to Support Modeling Impacts of Radioactive Material in Soil,"* April 1993. Appendix C contains a copy of Table 1.3. The low value of the uncertainty range is based on the lower bounds value in Table 1.3. The high value of the uncertainty range is the maximum depth of the overburden.

4 Figure 1 shows the ground-water flow direction and gradient, and length of contaminated zone. The source of Figure 1 is from *"Hydrogeologic Investigation and Ground-Water, Soil and Stream Characterization"* performed by LBG in March 1999. The low and high uncertainty range values for the Length Parallel to Aquifer are not expected to be more than 20 percent above or below the recommended value.

5 Taken from an average of dry density calculations from work performed by Fitch, University of Missouri – Rolla, 1998, presented in *"Fourth Sampling Event Report in Conjunction with the Hydrogeologic Investigation and Ground-Water, Soil and Stream Characterization"*, prepared by LBG in November 1999, and Shannon and Wilson (Appendix B of *"Hydrogeologic Investigation and Ground-Water, Soil and Stream Characterization"* performed by LBG in March 1999). Appendix D includes a table with these values showing how the value was derived. It also includes a copy of the reference data. The low and high values for the uncertainty range are associated with the lowest and highest values from the data set.

6 Jefferson County does not have a published soil survey which typically provide values for erosion rates. Therefore, the default value (0.001 m/yr) provided in Table 1.3 of "*Data Collection Handbook to Support Modeling Impacts of Radioactive Material in Soil*," April 1993, was used as a starting point. Since approximately 70 percent of the area of contamination is covered with impervious material, the default value was multiplied by .30 to give a value of 0.0003 m/yr. The low and high uncertainty range values are not expected to be more than 20 percent above or below the recommended value.

7 From Shannon and Wilson, (Appendix B of "*Hydrogeologic Investigation and Ground-Water, Soil and Stream Characterization*" performed by LBG in March 1999). Appendix D includes a table with these values showing how the value was derived. It also includes a copy of the reference data. The low and high values for the uncertainty range are associated with the lowest and highest values from the data set.

8 Derived using Formula 4.4 on page 28 of "*Data Collection Handbook to Support Modeling Impacts of Radioactive Material in Soil*," April 1993. The value for total porosity was taken from the average of Shannon and Wilson data (0.446; see footnote 7 above) and the value for effective porosity was based on a default value for silty clay in Table 3.3-1 of "*Development of Probabilistic RESRAD 6.0 and RESRAD-Build 3.0 Computer Codes*," November 2000. A copy of page 28, the completed formula, and Table 3.3-1 are provided in Appendix E. The low value of the uncertainty range cannot be zero (thus 0.01 was chosen), and the high value is derived by using the highest total porosity and effective porosity values in the calculation.

9 Shannon and Wilson (Appendix B of "*Hydrogeologic Investigation and Ground-Water, Soil and Stream Characterization*" prepared by LBG in March 1999) performed permeability tests on numerous soil samples. The average vertical permeability (hydraulic conductivity; K) for each sample was determined by averaging the last three permeability readings (telephone communication with Mr. Chris Groves, Vice-President, Shannon and Wilson on August 13, 2003). Once averages were calculated for each sample, an average of the entire data set was determined. The vertical hydraulic conductivity test data and a table developed to show the average K per sample, and the average K for the data set are provided in Appendix D. The low and high values for the uncertainty range are associated with the lowest and highest values from the data set.

10 Based on the default value for silty clay provided in Table 13.1, in "*Data Collection Handbook to Support Modeling Impacts of Radioactive Material in Soil*," April 1993. A copy of Table 13.1 is provided in Appendix F. The low and high values for the uncertainty range are associated with the lowest and highest values in Table 13.1.

11 The areal extent of the Watershed Area is defined on Figure 3. The low and high uncertainty range values are not expected to be more than 1 percent above or below the recommended value.

12 The effective porosity value is based on a default value for silty clay in Table 3.3-1 of "*Development of Probabilistic RESRAD 6.0 and RESRAD-Build 3.0 Computer Codes*," November 2000. A copy of Table 3.3-1 is provided in Appendix E. The low and high values for the uncertainty range are associated with the lowest and highest values in Table 3.3-1.

13 The average horizontal hydraulic conductivity value was calculated using an average of the values for near-surface silt, silty-clay (NSSSC) and deep silty-clay, clay (DSCC) as determined in Table 2 of "*Hydrogeologic Investigation and Ground-Water, Soil and Stream Characterization*" performed by LBG in March 1999). Appendix D includes a table with these values showing how the value was derived. It also includes a copy of the reference data. The low and high values for the uncertainty range are associated with the lowest and highest values from the data set.

14 Figure 1 shows the ground-water flow direction and gradient, and length of contaminated zone. Source of Figure 1 is from "*Hydrogeologic Investigation and Ground-Water, Soil and Stream Characterization*" performed by LBG in March 1999. The low and high values of the uncertainty range correspond to the lowest and highest gradient values from the LBG quarterly sampling reports.

15 Because the overburden aquifer is not used as a source of drinking water or for irrigation purposes, no net loss of ground water is expected to occur. Therefore, the value for the Water Table Drop Rate is zero. Low and high values of the uncertainty range are not applicable.

16 The Pump Intake Depth would be near the bottom of the DSCC, which would be approximately two feet above bedrock at the Site. The bottom of the screen depth of all DSSC wells was averaged and two feet was subtracted from that value. Table 5 from the RI/FS work plan was used to estimated the bottom of the wells, a copy of which is included in Appendix G. A table showing how the average was derived is also provided. The low and high values for the uncertainty range are associated with the lowest and highest values in Table 5.

17 Table 3.10-1 of "*Development of Probabilistic RESRAD 6.0 and RESRAD-Build 3.0 Computer Codes*," November 2000 provides a basis for determining the well pumping rate. The example scenario assumes a household of 4 adults, each requiring 225 liters of water per day. Agricultural parcels in this part of Missouri are typically not irrigated, so pumping rates for irrigation have not been provided. Water consumption for livestock is included in this parameter. Based on "*Principles of Controlled Grazing*," prepared by David W. Pratt in 1993, 2 head of cattle per acre on remote ranges or non-irrigated pasture is common. If the entire contaminated zone (19.14 acres) were used for pastureland, approximately 10 head of cattle would require drinking water needs. The example scenario assumes each head of cattle will require 160 liters of Water per day. A calculation provided in Appendix H shows annual well pumping rate required for this scenario. A copy of Table 3.10-1 and pertinent information

from "*Principles of*

Controlled Grazing" are also provided. The low and high uncertainty range values are not expected to be more than 20 percent above or below the recommended value.

Site-Specific Soil Parameters
Westinghouse Former Fuel Cycle Facility D&&D Project

RESRAD Parameter Table for ^{234}U

Parameter	Recommended Value	RESRAD Code Designation	Units	Uncertainty Range			Probabilistic Function	Reference
				Low Value	High Value	Number of Samples		
Groundwater Concentration	213	W(i)	pCi/L	0	238	12	Lognormal	1
Area of Contaminated Zone	77458	AREA	m^2	61966	92950	NA	Normal	2
Thickness of Contaminated Zone	2	THICKO	m	1.00E-10	11.74	NA	Bounded Lognormal	3
Length Parallel to Aquifer	291	LCZPAQ	m	233	349	NA	Bounded Normal	4
Density of Contaminated Zone	1.69	DENSCZ	g/cm^3	1.39	2.11	28	Normal	5
Contaminated Zone Erosion Rate	0.0003	VCZ	m/yr	0.00024	0.00036	NA	Bounded Normal	6
Contaminated Zone Total Porosity	0.45	TPCZ	0.xx	0.41	0.483	13	Normal	7
Contaminated Zone Field Capacity	0.17	FCCZ	0.xx	0.01	0.2	NA	Bounded Normal	8
Contaminated Zone Hydraulic Conductivity	14.56	HCCZ	m/yr	1.38E-03	1.45E+02	13	Lognormal	9
Contaminated Zone b Parameter	10.40	BCZ	unitless	4.05	11.4	NA	Lognormal	10
Watershed Area	998939	WAREA	m^2	988950	1008928	NA	Bounded Normal	11
Density of Saturated Zone	1.69	DENSAQ	g/cm^3	1.39	2.11	28	Normal	5
Saturated Zone Total Porosity	0.45	TPSZ	0.xx	0.41	0.483	13	Normal	7
Saturated Zone Effective Porosity	0.29	EPSZ	0.xx	0.281	0.425	NA	Normal	12
Saturated Zone Field Capacity	0.17	FCSZ	0.xx	0.01	0.2	NA	Bounded Normal	8
Saturated Zone Hydraulic Conductivity	169.58	HCSZ	m/yr	1.56E+01	8.51E+01	12	Lognormal	13
Saturated Zone Hydraulic Gradient	0.015	HGWT	unitless	0.013	0.018	NA	Bounded Lognormal	14
Saturated Zone b Parameter	10.40	BSZ	unitless	4.05	11.4	NA	Lognormal	10
Water Table Drop Rate	0.00	VWT	m/yr	NA	NA	NA	None Recommended	15
Well Pump Intake Depth	9.41	DWIBWT	m	5.4	11.7	10	Bounded Normal	16
Well Pumping Rate	913	UW	m^3/yr	730	1096	NA	Bounded Normal	17

REFERENCE FOOTNOTES for ^{234}U

1 ^{234}U ground-water concentration data does not exist. However ^{234}Th (a Parent isotope of ^{234}U) ground-water data does exist. If we assume that ^{234}U is in 100% equilibrium with ^{234}Th we can use the same data. ^{234}Th data was taken from piezometer MW-32, which was sampled by Leggette, Brashears & Graham, Inc. in August 1999. This information was referenced in Table 7, *"Fourth Sampling Event Report in Conjunction with the Hydrogeologic Investigation and Ground-Water, Soil and Stream Characterization"*, prepared by LBG in November 1999. Figure 1 shows the location of MW-32 and Appendix A contains a copy of Table 7. The low value of the uncertainty range corresponds to the numerous non-detections during the four quarterly sampling events, and the high value corresponds to concentrations from WS-27 (February 1999).

2 Only sparse ^{234}U data exists for soil. LBG assumes the Area of Contaminated Zone is where operations involving ^{234}U occurred. Therefore, the Area of Contamination is defined by the following: Missouri State Highway P to the northwest, the Northeast Site Creek to the northeast, the fenceline to the southeast, and the Site Pond/Creek to the southwest. The northern limits include the Health Physics building and Red Room Roof Burial area, which are in close proximity to the highway. The eastern limits include the burial area, which is located between the plant and the Northeast Site Creek. The south fence line is just northwest of the railway easement. The western limits of extend to the Site Pond/Creek to encompass the location of the cistern/burn pit and red room roof burial area. Figure 4 shows the Area of Contamination for ^{234}U. The low and high uncertainty range values are not expected to be more than 20 percent above or below the recommended value.

3 Due to a sparse amount of soil data for ^{234}U, the RESRAD default value was chosen, based on Table 1.3 of *"Data Collection Handbook to Support Modeling Impacts of Radioactive Material in Soil,"* April 1993. Appendix C contains a copy of Table 1.3. The low value of the uncertainty range is based on the lower bounds value in Table 1.3. The high value of the uncertainty range is the maximum depth of the overburden.

4 Figure 1 shows the ground-water flow direction and gradient, and length of contaminated zone. The source of Figure 1 is from *"Hydrogeologic Investigation and Ground-Water, Soil and Stream Characterization"* performed by LBG in March 1999. The low and high uncertainty range values for the Length Parallel to Aquifer are not expected to be more than 20 percent above or below the recommended value.

5 Taken from an average of dry density calculations from work performed by Fitch, University of Missouri – Rolla, 1998, presented in *"Fourth Sampling Event Report in Conjunction with the Hydrogeologic Investigation and Ground-Water, Soil and Stream Characterization"*, prepared by LBG in November 1999, and Shannon and Wilson (Appendix B of *"Hydrogeologic Investigation and Ground-Water, Soil and Stream Characterization"* performed by LBG in March 1999). Appendix D includes a table with these values showing how the value was derived. It also includes a copy of the reference

data. The low and high values for the uncertainty range are associated with the lowest and highest values from the data set.

6 Jefferson County does not have a published soil survey which typically provide values for erosion rates. Therefore, the default value (0.001 m/yr) provided in Table 1.3 of "*Data Collection Handbook to Support Modeling Impacts of Radioactive Material in Soil*," April 1993, was used as a starting point. Since approximately 70 percent of the area of contamination is covered with impervious material, the default value was multiplied by .30 to give a value of 0.0003 m/yr. The low and high uncertainty range values are not expected to be more than 20 percent above or below the recommended value.

7 From Shannon and Wilson, (Appendix B of "*Hydrogeologic Investigation and Ground-Water, Soil and Stream Characterization*" performed by LBG in March 1999). Appendix D includes a table with these values showing how the value was derived. It also includes a copy of the reference data. The low and high values for the uncertainty range are associated with the lowest and highest values from the data set.

8 Derived using Formula 4.4 on page 28 of "*Data Collection Handbook to Support Modeling Impacts of Radioactive Material in Soil*," April 1993. The value for total porosity was taken from the average of Shannon and Wilson data (0.446; see footnote 7 above) and the value for effective porosity was based on a default value for silty clay in Table 3.3-1 of "*Development of Probabilistic RESRAD 6.0 and RESRAD-Build 3.0 Computer Codes*," November 2000. A copy of page 28, the completed formula, and Table 3.3-1 are provided in Appendix E. The low value of the uncertainty range cannot be zero (thus 0.01 was chosen), and the high value is derived by using the highest total porosity and effective porosity values in the calculation.

9 Shannon and Wilson (Appendix B of "*Hydrogeologic Investigation and Ground-Water, Soil and Stream Characterization*" prepared by LBG in March 1999) performed permeability tests on numerous soil samples. The average vertical permeability (hydraulic conductivity; K) for each sample was determined by averaging the last three permeability readings (telephone communication with Mr. Chris Groves, Vice-President, Shannon and Wilson on August 13, 2003). Once averages were calculated for each sample, an average of the entire data set was determined. The vertical hydraulic conductivity test data and a table developed to show the average K per sample, and the average K for the data set are provided in Appendix D. The low and high values for the uncertainty range are associated with the lowest and highest values from the data set.

10 Based on the default value for silty clay provided in Table 13.1, in "*Data Collection Handbook to Support Modeling Impacts of Radioactive Material in Soil*," April 1993. A copy of Table 13.1 is provided in Appendix F. The low and high values for the uncertainty range are associated with the lowest and highest values in Table 13.1.

11 The areal extent of the Watershed Area is defined on Figure 3. The low and high uncertainty range values are not expected to be more than 1 percent above or below the recommended value.

12 The effective porosity value is based on a default value for silty clay in Table 3.3-1 of "*Development of Probabilistic RESRAD 6.0 and RESRAD-Build 3.0 Computer Codes*," November 2000. A copy of Table 3.3-1 is provided in Appendix E. The low and high values for the uncertainty range are associated with the lowest and highest values in Table 3.3-1.

13 The average horizontal hydraulic conductivity value was calculated using an average of the values for near-surface silt, silty-clay (NSSSC) and deep silty-clay, clay (DSCC) as determined in Table 2 of "*Hydrogeologic Investigation and Ground-Water, Soil and Stream Characterization*" performed by LBG in March 1999). Appendix D includes a table with these values showing how the value was derived. It also includes a copy of the reference data. The low and high values for the uncertainty range are associated with the lowest and highest values from the data set.

14 Figure 1 shows the ground-water flow direction and gradient, and length of contaminated zone. Source of Figure 1 is from "*Hydrogeologic Investigation and Ground-Water, Soil and Stream Characterization*" performed by LBG in March 1999. The low and high values of the uncertainty range correspond to the lowest and highest gradient values from the LBG quarterly sampling reports.

15 Because the overburden aquifer is not used as a source of drinking water or for irrigation purposes, no net loss of ground water is expected to occur. Therefore, the value for the Water Table Drop Rate is zero. Low and high values of the uncertainty range are not applicable.

16 The Pump Intake Depth would be near the bottom of the DSCC, which would be approximately two feet above bedrock at the Site. The bottom of the screen depth of all DSSC wells was averaged and two feet was subtracted from that value. Table 5 from the RI/FS work plan was used to estimated the bottom of the wells, a copy of which is included in Appendix G. A table showing how the average was derived is also provided. The low and high values for the uncertainty range are associated with the lowest and highest values in Table 5.

17 Table 3.10-1 of "*Development of Probabilistic RESRAD 6.0 and RESRAD-Build 3.0 Computer Codes*," November 2000 provides a basis for determining the well pumping rate. The example scenario assumes a household of 4 adults, each requiring 225 liters of water per day. Agricultural parcels in this part of Missouri are typically not irrigated, so pumping rates for irrigation have not been provided. Water consumption for livestock is included in this parameter. Based on "*Principles of Controlled Grazing*," prepared by David W. Pratt in 1993, 2 head of cattle per acre on remote ranges or non-irrigated pasture is common. If the entire contaminated zone (19.14 acres) were used for pastureland, approximately 10 head of cattle would require drinking water needs. The example scenario assumes each head of cattle

will require 160 liters of Water per day. A calculation provided in Appendix H shows annual well pumping rate required for this scenario. A copy of Table 3.10-1 and pertinent information from "*Principles of*

Controlled Grazing" are also provided. The low and high uncertainty range values are not expected to be more than 20 percent above or below the recommended value.

RESRAD Parameter Table for ^{238}U

Parameter	Recommended Value	RESRAD Code Designation	Units	Uncertainty Range			Probabilistic Function	Reference
				Low Value	High Value	Number of Samples		
Groundwater Concentration	213	W(i)	pCi/L	0	238	12	Lognormal	1
Area of Contaminated Zone	77458	AREA	m^2	61966	92950	NA	Normal	2
Thickness of Contaminated Zone	2	THICKO	m	1.00E-10	11.74	NA	Bounded Lognormal	3
Length Parallel to Aquifer	291	LCZPAQ	m	233	349	NA	Bounded Normal	4
Density of Contaminated Zone	1.69	DENSCZ	g/cm^3	1.39	2.11	28	Normal	5
Contaminated Zone Erosion Rate	0.0003	VCZ	m/yr	0.00024	0.00036	NA	Bounded Normal	6
Contaminated Zone Total Porosity	0.45	TPCZ	0.xx	0.41	0.483	13	Normal	7
Contaminated Zone Field Capacity	0.17	FCCZ	0.xx	0.01	0.2	NA	Bounded Normal	8
Contaminated Zone Hydraulic Conductivity	14.56	HCCZ	m/yr	1.38E-03	1.45E+02	13	Lognormal	9
Contaminated Zone b Parameter	10.40	BCZ	unitless	4.05	11.4	NA	Lognormal	10
Watershed Area	998939	WAREA	m^2	988950	1008928	NA	Bounded Normal	11
Density of Saturated Zone	1.69	DENSAQ	g/cm^3	1.39	2.11	28	Normal	5
Saturated Zone Total Porosity	0.45	TPSZ	0.xx	0.41	0.483	13	Normal	7
Saturated Zone Effective Porosity	0.29	EPSZ	0.xx	0.281	0.425	NA	Normal	12
Saturated Zone Field Capacity	0.17	FCSZ	0.xx	0.01	0.2	NA	Bounded Normal	8
Saturated Zone Hydraulic Conductivity	169.58	HCSZ	m/yr	1.56E+01	8.51E+01	12	Lognormal	13
Saturated Zone Hydraulic Gradient	0.015	HGWT	unitless	0.013	0.018	NA	Bounded Lognormal	14
Saturated Zone b Parameter	10.40	BSZ	unitless	4.05	11.4	NA	Lognormal	10
Water Table Drop Rate	0.00	VWT	m/yr	NA	NA	NA	None Recommended	15
Well Pump Intake Depth	9.41	DWIBWT	m	5.4	11.7	10	Bounded Normal	16
Well Pumping Rate	913	UW	m^3/yr	730	1096	NA	Bounded Normal	17

REFERENCE FOOTNOTES for ^{238}U

1 ^{238}U ground-water concentration data does not exist. However ^{234}Th (a daughter of ^{238}U) ground-water data does exist. If we assume that ^{238}U is in 100% equilibrium with ^{234}Th, we can use the same data. ^{234}Th data was taken from piezometer MW-32, which was sampled by Leggette, Brashears & Graham, Inc. in August 1999. This information was referenced in Table 7, *"Fourth Sampling Event Report in Conjunction with the Hydrogeologic Investigation and Ground-Water, Soil and Stream Characterization"*, prepared by LBG in November 1999. Figure 1 shows the location of MW-32 and Appendix A contains a copy of Table 7. The low value of the uncertainty range corresponds to the numerous non-detections during the four quarterly sampling events, and the high value corresponds to concentrations from WS-27 (February 1999).

2 Only sparse ^{238}U data exists for soil. LBG assumes the Area of Contaminated Zone is where operations involving ^{238}U occurred. Therefore, the Area of Contamination is defined by the following: Missouri State Highway P to the northwest, the Northeast Site Creek to the northeast, the fenceline to the southeast, and the Site Pond/Creek to the southwest. The northern limits include the Health Physics building and Red Room Roof Burial area, which are in close proximity to the highway. The eastern limits include the burial area, which is located between the plant and the Northeast Site Creek. The south fence line is just northwest of the railway easement. The western limits of extend to the Site Pond/Creek to encompass the location of the cistern/burn pit and red room roof burial area. Figure 4 shows the Area of Contamination for ^{238}U. The low and high uncertainty range values are not expected to be more than 20 percent above or below the recommended value.

3 Due to a sparse amount of soil data for ^{238}U, the RESRAD default value was chosen, based on Table 1.3 of *"Data Collection Handbook to Support Modeling Impacts of Radioactive Material in Soil,"* April 1993. Appendix C contains a copy of Table 1.3. The low value of the uncertainty range is based on the lower bounds value in Table 1.3. The high value of the uncertainty range is the maximum depth of the overburden.

4 Figure 1 shows the ground-water flow direction and gradient, and length of contaminated zone. The source of Figure 1 is from *"Hydrogeologic Investigation and Ground-Water, Soil and Stream Characterization"* performed by LBG in March 1999. The low and high uncertainty range values for the Length Parallel to Aquifer are not expected to be more than 20 percent above or below the recommended value.

5 Taken from an average of dry density calculations from work performed by Fitch, University of Missouri – Rolla, 1998, presented in *"Fourth Sampling Event Report in Conjunction with the Hydrogeologic Investigation and Ground-Water, Soil and Stream Characterization"*, prepared by LBG in November 1999, and Shannon and Wilson (Appendix B of *"Hydrogeologic Investigation and Ground-Water, Soil and Stream Characterization"* performed by LBG in March 1999). Appendix D includes a table with these values showing

how the value was derived. It also includes a copy of the reference

data. The low and high values for the uncertainty range are associated with the lowest and highest values from the data set.

6 Jefferson County does not have a published soil survey which typically provide values for erosion rates. Therefore, the default value (0.001 m/yr) provided in Table 1.3 of "*Data Collection Handbook to Support Modeling Impacts of Radioactive Material in Soil*," April 1993, was used as a starting point. Since approximately 70 percent of the area of contamination is covered with impervious material, the default value was multiplied by .30 to give a value of 0.0003 m/yr. The low and high uncertainty range values are not expected to be more than 20 percent above or below the recommended value.

7 From Shannon and Wilson, (Appendix B of "*Hydrogeologic Investigation and Ground-Water, Soil and Stream Characterization*" performed by LBG in March 1999). Appendix D includes a table with these values showing how the value was derived. It also includes a copy of the reference data. The low and high values for the uncertainty range are associated with the lowest and highest values from the data set.

8 Derived using Formula 4.4 on page 28 of "*Data Collection Handbook to Support Modeling Impacts of Radioactive Material in Soil*," April 1993. The value for total porosity was taken from the average of Shannon and Wilson data (0.446; see footnote 7 above) and the value for effective porosity was based on a default value for silty clay in Table 3.3-1 of "*Development of Probabilistic RESRAD 6.0 and RESRAD-Build 3.0 Computer Codes*," November 2000. A copy of page 28, the completed formula, and Table 3.3-1 are provided in Appendix E. The low value of the uncertainty range cannot be zero (thus 0.01 was chosen), and the high value is derived by using the highest total porosity and effective porosity values in the calculation.

9 Shannon and Wilson (Appendix B of "*Hydrogeologic Investigation and Ground-Water, Soil and Stream Characterization*" prepared by LBG in March 1999) performed permeability tests on numerous soil samples. The average vertical permeability (hydraulic conductivity; K) for each sample was determined by averaging the last three permeability readings (telephone communication with Mr. Chris Groves, Vice-President, Shannon and Wilson on August 13, 2003). Once averages were calculated for each sample, an average of the entire data set was determined. The vertical hydraulic conductivity test data and a table developed to show the average K per sample, and the average K for the data set are provided in Appendix D. The low and high values for the uncertainty range are associated with the lowest and highest values from the data set.

10 Based on the default value for silty clay provided in Table 13.1, in "*Data Collection Handbook to Support Modeling Impacts of Radioactive Material in Soil*," April 1993. A copy of Table 13.1 is provided in Appendix F. The low and high values for the uncertainty

range are associated with the lowest and highest values in Table 13.1.

11 The areal extent of the Watershed Area is defined on Figure 3. The low and high uncertainty range values are not expected to be more than 1 percent above or below the recommended value.

12 The effective porosity value is based on a default value for silty clay in Table 3.3-1 of "*Development of Probabilistic RESRAD 6.0 and RESRAD-Build 3.0 Computer Codes*," November 2000. A copy of Table 3.3-1 is provided in Appendix E. The low and high values for the uncertainty range are associated with the lowest and highest values in Table 3.3-1.

13 The average horizontal hydraulic conductivity value was calculated using an average of the values for near-surface silt, silty-clay (NSSSC) and deep silty-clay, clay (DSCC) as determined in Table 2 of "*Hydrogeologic Investigation and Ground-Water, Soil and Stream Characterization*" performed by LBG in March 1999). Appendix D includes a table with these values showing how the value was derived. It also includes a copy of the reference data. The low and high values for the uncertainty range are associated with the lowest and highest values from the data set.

14 Figure 1 shows the ground-water flow direction and gradient, and length of contaminated zone. Source of Figure 1 is from "*Hydrogeologic Investigation and Ground-Water, Soil and Stream Characterization*" performed by LBG in March 1999. The low and high values of the uncertainty range correspond to the lowest and highest gradient values from the LBG quarterly sampling reports.

15 Because the overburden aquifer is not used as a source of drinking water or for irrigation purposes, no net loss of ground water is expected to occur. Therefore, the value for the Water Table Drop Rate is zero. Low and high values of the uncertainty range are not applicable.

16 The Pump Intake Depth would be near the bottom of the DSCC, which would be approximately two feet above bedrock at the Site. The bottom of the screen depth of all DSSC wells was averaged and two feet was subtracted from that value. Table 5 from the RI/FS work plan was used to estimated the bottom of the wells, a copy of which is included in Appendix G. A table showing how the average was derived is also provided. The low and high values for the uncertainty range are associated with the lowest and highest values in Table 5.

17 Table 3.10-1 of "*Development of Probabilistic RESRAD 6.0 and RESRAD-Build 3.0 Computer Codes*," November 2000 provides a basis for determining the well pumping rate. The example scenario assumes a household of 4 adults, each requiring 225 liters of water per day. Agricultural parcels in this part of Missouri are typically not irrigated, so pumping rates for irrigation have not been provided. Water consumption for livestock is included in this parameter. Based on "*Principles of Controlled Grazing*," prepared by David W. Pratt in 1993, 2 head of cattle per acre on remote ranges or non-irrigated pasture is common. If the

entire contaminated zone (19.14 acres) were used for pastureland, approximately 10 head of cattle would require drinking water needs. The example scenario assumes each head of cattle will require 160 liters of Water per day. A calculation provided in Appendix H shows annual well pumping rate required for this scenario. A copy of Table 3.10-1 and pertinent information from "*Principles of Controlled Grazing*" are also provided. The low and high uncertainty range values are not expected to be more than 20 percent above or below the recommended value.

Site-Specific Soil Parameters
Westinghouse Former Fuel Cycle Facility D&&D Project

RESRAD Parameter Table for ^{237}Np

Parameter	Recommended Value	RESRAD Code Designation	Units	Uncertainty Range			Probabilistic Function	Reference
				Low Value	High Value	Number of Samples		
Groundwater Concentration	0	W(i)	pCi/L	0	1.00E+20	NA	Lognormal	1
Area of Contaminated Zone	77458	AREA	m^2	61966	92950	NA	Normal	2
Thickness of Contaminated Zone	2	THICKO	m	1.00E-10	11.74	NA	Bounded Lognormal	3
Length Parallel to Aquifer	291	LCZPAQ	m	233	349	NA	Bounded Normal	4
Density of Contaminated Zone	1.69	DENSCZ	g/cm^3	1.39	2.11	28	Normal	5
Contaminated Zone Erosion Rate	0.0003	VCZ	m/yr	0.00024	0.00036	NA	Bounded Normal	6
Contaminated Zone Total Porosity	0.45	TPCZ	0.xx	0.41	0.483	13	Normal	7
Contaminated Zone Field Capacity	0.17	FCCZ	0.xx	0.01	0.2	NA	Bounded Normal	8
Contaminated Zone Hydraulic Conductivity	14.56	HCCZ	m/yr	1.38E-03	1.45E+02	13	Lognormal	9
Contaminated Zone b Parameter	10.40	BCZ	unitless	4.05	11.4	NA	Lognormal	10
Watershed Area	998939	WAREA	m^2	988950	1008928	NA	Bounded Normal	11
Density of Saturated Zone	1.69	DENSAQ	g/cm^3	1.39	2.11	28	Normal	5
Saturated Zone Total Porosity	0.45	TPSZ	0.xx	0.41	0.483	13	Normal	7
Saturated Zone Effective Porosity	0.29	EPSZ	0.xx	0.281	0.425	NA	Normal	12
Saturated Zone Field Capacity	0.17	FCSZ	0.xx	0.01	0.2	NA	Bounded Normal	8
Saturated Zone Hydraulic Conductivity	169.58	HCSZ	m/yr	1.56E+01	8.51E+01	12	Lognormal	13
Saturated Zone Hydraulic Gradient	0.015	HGWT	unitless	0.013	0.018	NA	Bounded Lognormal	14
Saturated Zone b Parameter	10.40	BSZ	unitless	4.05	11.4	NA	Lognormal	10
Water Table Drop Rate	0.00	VWT	m/yr	NA	NA	NA	None Recommended	15
Well Pump Intake Depth	9.41	DWIBWT	m	5.4	11.7	10	Bounded Normal	16
Well Pumping Rate	913	UW	m^3/yr	730	1096	NA	Bounded Normal	17

REFERENCE FOOTNOTES for ^{237}Np

1 ^{237}Np ground-water data does not exist, and it is not in a decay series where known concentrations can be used in equilibrium. Therefore, the RESRAD default value (0 pci/L) will be used. Low and high values will also correspond to default values.

2 No ^{237}Np data exists for soil. LBG assumes the Area of Contaminated Zone is where operations involving U occurred. Therefore, the Area of Contamination is defined by the following: Missouri State Highway P to the northwest, the Northeast Site Creek to the northeast, the fenceline to the southeast, and the Site Pond/Creek to the southwest. The northern limits include the Health Physics building and Red Room Roof Burial area, which are in close proximity to the highway. The eastern limits include the burial area, which is located between the plant and the Northeast Site Creek. The south fence line is just northwest of the railway easement. The western limits of extend to the Site Pond/Creek to encompass the location of the cistern/burn pit and red room roof burial area. Figure 4 shows the Area of Contamination for ^{237}Np. The low and high uncertainty range values are not expected to be more than 20 percent above or below the recommended value.

3 Since no soil data exists for ^{237}Np, the RESRAD default value was chosen, based on Table 1.3 of "*Data Collection Handbook to Support Modeling Impacts of Radioactive Material in Soil*," April 1993. Appendix C contains a copy of Table 1.3. The low value of the uncertainty range is based on the lower bounds value in Table 1.3. The high value of the uncertainty range is the maximum depth of the overburden.

4 Figure 1 shows the ground-water flow direction and gradient, and length of contaminated zone. The source of Figure 1 is from "*Hydrogeologic Investigation and Ground-Water, Soil and Stream Characterization*" performed by LBG in March 1999. The low and high uncertainty range values for the Length Parallel to Aquifer are not expected to be more than 20 percent above or below the recommended value.

5 Taken from an average of dry density calculations from work performed by Fitch, University of Missouri – Rolla, 1998, presented in "*Fourth Sampling Event Report in Conjunction with the Hydrogeologic Investigation and Ground-Water, Soil and Stream Characterization*", prepared by LBG in November 1999, and Shannon and Wilson (Appendix B of "*Hydrogeologic Investigation and Ground-Water, Soil and Stream Characterization*" performed by LBG in March 1999). Appendix D includes a table with these values showing how the value was derived. It also includes a copy of the reference data. The low and high values for the uncertainty range are associated with the lowest and highest values from the data set.

6 Jefferson County does not have a published soil survey which typically provide values for erosion rates. Therefore, the default value (0.001 m/yr) provided in Table 1.3 of "*Data Collection Handbook to Support Modeling Impacts of Radioactive Material in Soil*," April

1993, was used as a starting point. Since approximately 70 percent of the area of contamination is covered with impervious material, the default value was multiplied by .30 to give a value of 0.0003 m/yr. The low and high uncertainty range values are not expected to be more than 20 percent above or below the recommended value.

7 From Shannon and Wilson, (Appendix B of "*Hydrogeologic Investigation and Ground-Water, Soil and Stream Characterization*" performed by LBG in March 1999). Appendix D includes a table with these values showing how the value was derived. It also includes a copy of the reference data. The low and high values for the uncertainty range are associated with the lowest and highest values from the data set.

8 Derived using Formula 4.4 on page 28 of "*Data Collection Handbook to Support Modeling Impacts of Radioactive Material in Soil*," April 1993. The value for total porosity was taken from the average of Shannon and Wilson data (0.446; see footnote 7 above) and the value for effective porosity was based on a default value for silty clay in Table 3.3-1 of "*Development of Probabilistic RESRAD 6.0 and RESRAD-Build 3.0 Computer Codes*," November 2000. A copy of page 28, the completed formula, and Table 3.3-1 are provided in Appendix E. The low value of the uncertainty range cannot be zero (thus 0.01 was chosen), and the high value is derived by using the highest total porosity and effective porosity values in the calculation.

9 Shannon and Wilson (Appendix B of "*Hydrogeologic Investigation and Ground-Water, Soil and Stream Characterization*" prepared by LBG in March 1999) performed permeability tests on numerous soil samples. The average vertical permeability (hydraulic conductivity; K) for each sample was determined by averaging the last three permeability readings (telephone communication with Mr. Chris Groves, Vice-President, Shannon and Wilson on August 13, 2003). Once averages were calculated for each sample, an average of the entire data set was determined. The vertical hydraulic conductivity test data and a table developed to show the average K per sample, and the average K for the data set are provided in Appendix D. The low and high values for the uncertainty range are associated with the lowest and highest values from the data set.

10 Based on the default value for silty clay provided in Table 13.1, in "*Data Collection Handbook to Support Modeling Impacts of Radioactive Material in Soil*," April 1993. A copy of Table 13.1 is provided in Appendix F. The low and high values for the uncertainty range are associated with the lowest and highest values in Table 13.1.

11 The areal extent of the Watershed Area is defined on Figure 3. The low and high uncertainty range values are not expected to be more than 1 percent above or below the recommended value.

12 The effective porosity value is based on a default value for silty clay in Table 3.3-1 of "*Development of Probabilistic RESRAD 6.0 and RESRAD-Build 3.0 Computer Codes*,"

November 2000. A copy of Table 3.3-1 is provided in Appendix E. The low and high values for the uncertainty range are associated with the lowest and highest values in Table 3.3-1.

13 The average horizontal hydraulic conductivity value was calculated using an average of the values for near-surface silt, silty-clay (NSSSC) and deep silty-clay, clay (DSCC) as determined in Table 2 of "*Hydrogeologic Investigation and Ground-Water, Soil and Stream Characterization*" performed by LBG in March 1999). Appendix D includes a table with these values showing how the value was derived. It also includes a copy of the reference data. The low and high values for the uncertainty range are associated with the lowest and highest values from the data set.

14 Figure 1 shows the ground-water flow direction and gradient, and length of contaminated zone. Source of Figure 1 is from "*Hydrogeologic Investigation and Ground-Water, Soil and Stream Characterization*" performed by LBG in March 1999. The low and high values of the uncertainty range correspond to the lowest and highest gradient values from the LBG quarterly sampling reports.

15 Because the overburden aquifer is not used as a source of drinking water or for irrigation purposes, no net loss of ground water is expected to occur. Therefore, the value for the Water Table Drop Rate is zero. Low and high values of the uncertainty range are not applicable.

16 The Pump Intake Depth would be near the bottom of the DSCC, which would be approximately two feet above bedrock at the Site. The bottom of the screen depth of all DSSC wells was averaged and two feet was subtracted from that value. Table 5 from the RI/FS work plan was used to estimated the bottom of the wells, a copy of which is included in Appendix G. A table showing how the average was derived is also provided. The low and high values for the uncertainty range are associated with the lowest and highest values in Table 5.

17 Table 3.10-1 of "*Development of Probabilistic RESRAD 6.0 and RESRAD-Build 3.0 Computer Codes*," November 2000 provides a basis for determining the well pumping rate. The example scenario assumes a household of 4 adults, each requiring 225 liters of water per day. Agricultural parcels in this part of Missouri are typically not irrigated, so pumping rates for irrigation have not been provided. Water consumption for livestock is included in this parameter. Based on "*Principles of Controlled Grazing*," prepared by David W. Pratt in 1993, 2 head of cattle per acre on remote ranges or non-irrigated pasture is common. If the entire contaminated zone (19.14 acres) were used for pastureland, approximately 10 head of cattle would require drinking water needs. The example scenario assumes each head of cattle will require 160 liters of Water per day. A calculation provided in Appendix H shows annual well pumping rate required for this scenario. A copy of Table 3.10-1 and pertinent information from "*Principles of Controlled Grazing*" are also provided. The low and high uncertainty range values are not expected to be more than 20 percent above or below the recommended value.

Site-Specific Soil Parameters
Westinghouse Former Fuel Cycle Facility D&&D Project

RESRAD Parameter Table for ^{239}Pu

Parameter	Recommended Value	RESRAD Code Designation	Units	Uncertainty Range			Probabilistic Function	Reference
				Low Value	High Value	Number of Samples		
Groundwater Concentration	0	W(i)	pCi/L	0	1.00E+20	NA	Lognormal	1
Area of Contaminated Zone	77458	AREA	m^2	61966	92950	NA	Normal	2
Thickness of Contaminated Zone	2	THICKO	m	1.00E-10	11.74	NA	Bounded Lognormal	3
Length Parallel to Aquifer	291	LCZPAQ	m	233	349	NA	Bounded Normal	4
Density of Contaminated Zone	1.69	DENSCZ	g/cm^3	1.39	2.11	28	Normal	5
Contaminated Zone Erosion Rate	0.0003	VCZ	m/yr	0.00024	0.00036	NA	Bounded Normal	6
Contaminated Zone Total Porosity	0.45	TPCZ	0.xx	0.41	0.483	13	Normal	7
Contaminated Zone Field Capacity	0.17	FCCZ	0.xx	0.01	0.2	NA	Bounded Normal	8
Contaminated Zone Hydraulic Conductivity	14.56	HCCZ	m/yr	1.38E-03	1.45E+02	13	Lognormal	9
Contaminated Zone b Parameter	10.40	BCZ	unitless	4.05	11.4	NA	Lognormal	10
Watershed Area	998939	WAREA	m^2	988950	1008928	NA	Bounded Normal	11
Density of Saturated Zone	1.69	DENSAQ	g/cm^3	1.39	2.11	28	Normal	5
Saturated Zone Total Porosity	0.45	TPSZ	0.xx	0.41	0.483	13	Normal	7
Saturated Zone Effective Porosity	0.29	EPSZ	0.xx	0.281	0.425	NA	Normal	12
Saturated Zone Field Capacity	0.17	FCSZ	0.xx	0.01	0.2	NA	Bounded Normal	8
Saturated Zone Hydraulic Conductivity	169.58	HCSZ	m/yr	1.56E+01	8.51E+01	12	Lognormal	13
Saturated Zone Hydraulic Gradient	0.015	HGWT	unitless	0.013	0.018	NA	Bounded Lognormal	14
Saturated Zone b Parameter	10.40	BSZ	unitless	4.05	11.4	NA	Lognormal	10
Water Table Drop Rate	0.00	VWT	m/yr	NA	NA	NA	None Recommended	15
Well Pump Intake Depth	9.41	DWIBWT	m	5.4	11.7	10	Bounded Normal	16
Well Pumping Rate	913	UW	m^3/yr	730	1096	NA	Bounded Normal	17

REFERENCE FOOTNOTES for ^{239}Pu

1 ^{239}Pu ground-water data does not exist, and it is not in a decay series where known concentrations can be used in equilibrium. Therefore, the RESRAD default value (0 pci/L) will be used. Low and high values will also correspond to default values.

2 No ^{239}Pu data exists for soil. LBG assumes the Area of Contaminated Zone is where operations involving U occurred. Therefore, the Area of Contamination is defined by the following: Missouri State Highway P to the northwest, the Northeast Site Creek to the northeast, the fenceline to the southeast, and the Site Pond/Creek to the southwest. The northern limits include the Health Physics building and Red Room Roof Burial area, which are in close proximity to the highway. The eastern limits include the burial area, which is located between the plant and the Northeast Site Creek. The south fence line is just northwest of the railway easement. The western limits of extend to the Site Pond/Creek to encompass the location of the cistern/burn pit and red room roof burial area. Figure 4 shows the Area of Contamination for ^{239}Pu. The low and high uncertainty range values are not expected to be more than 20 percent above or below the recommended value.

3 Since no soil data exists for ^{239}Pu, the RESRAD default value was chosen, based on Table 1.3 of "*Data Collection Handbook to Support Modeling Impacts of Radioactive Material in Soil*," April 1993. Appendix C contains a copy of Table 1.3. The low value of the uncertainty range is based on the lower bounds value in Table 1.3. The high value of the uncertainty range is the maximum depth of the overburden.

4 Figure 1 shows the ground-water flow direction and gradient, and length of contaminated zone. The source of Figure 1 is from "*Hydrogeologic Investigation and Ground-Water, Soil and Stream Characterization*" performed by LBG in March 1999. The low and high uncertainty range values for the Length Parallel to Aquifer are not expected to be more than 20 percent above or below the recommended value.

5 Taken from an average of dry density calculations from work performed by Fitch, University of Missouri – Rolla, 1998, presented in "*Fourth Sampling Event Report in Conjunction with the Hydrogeologic Investigation and Ground-Water, Soil and Stream Characterization*", prepared by LBG in November 1999, and Shannon and Wilson (Appendix B of "*Hydrogeologic Investigation and Ground-Water, Soil and Stream Characterization*" performed by LBG in March 1999). Appendix D includes a table with these values showing how the value was derived. It also includes a copy of the reference data. The low and high values for the uncertainty range are associated with the lowest and highest values from the data set.

6 Jefferson County does not have a published soil survey which typically provide values for erosion rates. Therefore, the default value (0.001 m/yr) provided in Table 1.3 of "*Data*

Collection Handbook to Support Modeling Impacts of Radioactive Material in Soil," April 1993, was used as a starting point. Since approximately 70 percent of the area of contamination is covered with impervious material, the default value was multiplied by .30 to give a value of 0.0003 m/yr. The low and high uncertainty range values are not expected to be more than 20 percent above or below the recommended value.

7 From Shannon and Wilson, (Appendix B of "*Hydrogeologic Investigation and Ground-Water, Soil and Stream Characterization*" performed by LBG in March 1999). Appendix D includes a table with these values showing how the value was derived. It also includes a copy of the reference data. The low and high values for the uncertainty range are associated with the lowest and highest values from the data set.

8 Derived using Formula 4.4 on page 28 of "*Data Collection Handbook to Support Modeling Impacts of Radioactive Material in Soil,*" April 1993. The value for total porosity was taken from the average of Shannon and Wilson data (0.446; see footnote 7 above) and the value for effective porosity was based on a default value for silty clay in Table 3.3-1 of "*Development of Probabilistic RESRAD 6.0 and RESRAD-Build 3.0 Computer Codes,*" November 2000. A copy of page 28, the completed formula, and Table 3.3-1 are provided in Appendix E. The low value of the uncertainty range cannot be zero (thus 0.01 was chosen), and the high value is derived by using the highest total porosity and effective porosity values in the calculation.

9 Shannon and Wilson (Appendix B of "*Hydrogeologic Investigation and Ground-Water, Soil and Stream Characterization*" prepared by LBG in March 1999) performed permeability tests on numerous soil samples. The average vertical permeability (hydraulic conductivity; K) for each sample was determined by averaging the last three permeability readings (telephone communication with Mr. Chris Groves, Vice-President, Shannon and Wilson on August 13, 2003). Once averages were calculated for each sample, an average of the entire data set was determined. The vertical hydraulic conductivity test data and a table developed to show the average K per sample, and the average K for the data set are provided in Appendix D. The low and high values for the uncertainty range are associated with the lowest and highest values from the data set.

10 Based on the default value for silty clay provided in Table 13.1, in "*Data Collection Handbook to Support Modeling Impacts of Radioactive Material in Soil,*" April 1993. A copy of Table 13.1 is provided in Appendix F. The low and high values for the uncertainty range are associated with the lowest and highest values in Table 13.1.

11 The areal extent of the Watershed Area is defined on Figure 3. The low and high uncertainty range values are not expected to be more than 1 percent above or below the recommended value.

12 The effective porosity value is based on a default value for silty clay in Table 3.3-1 of "*Development of Probabilistic RESRAD 6.0 and RESRAD-Build 3.0 Computer Codes*," November 2000. A copy of Table 3.3-1 is provided in Appendix E. The low and high values for the uncertainty range are associated with the lowest and highest values in Table 3.3-1.

13 The average horizontal hydraulic conductivity value was calculated using an average of the values for near-surface silt, silty-clay (NSSSC) and deep silty-clay, clay (DSCC) as determined in Table 2 of "*Hydrogeologic Investigation and Ground-Water, Soil and Stream Characterization*" performed by LBG in March 1999). Appendix D includes a table with these values showing how the value was derived. It also includes a copy of the reference data. The low and high values for the uncertainty range are associated with the lowest and highest values from the data set.

14 Figure 1 shows the ground-water flow direction and gradient, and length of contaminated zone. Source of Figure 1 is from "*Hydrogeologic Investigation and Ground-Water, Soil and Stream Characterization*" performed by LBG in March 1999. The low and high values of the uncertainty range correspond to the lowest and highest gradient values from the LBG quarterly sampling reports.

15 Because the overburden aquifer is not used as a source of drinking water or for irrigation purposes, no net loss of ground water is expected to occur. Therefore, the value for the Water Table Drop Rate is zero. Low and high values of the uncertainty range are not applicable.

16 The Pump Intake Depth would be near the bottom of the DSCC, which would be approximately two feet above bedrock at the Site. The bottom of the screen depth of all DSSC wells was averaged and two feet was subtracted from that value. Table 5 from the RI/FS work plan was used to estimated the bottom of the wells, a copy of which is included in Appendix G. A table showing how the average was derived is also provided. The low and high values for the uncertainty range are associated with the lowest and highest values in Table 5.

17 Table 3.10-1 of "*Development of Probabilistic RESRAD 6.0 and RESRAD-Build 3.0 Computer Codes*," November 2000 provides a basis for determining the well pumping rate. The example scenario assumes a household of 4 adults, each requiring 225 liters of water per day. Agricultural parcels in this part of Missouri are typically not irrigated, so pumping rates for irrigation have not been provided. Water consumption for livestock is included in this parameter. Based on "*Principles of Controlled Grazing*," prepared by David W. Pratt in 1993, 2 head of cattle per acre on remote ranges or non-irrigated pasture is common. If the entire contaminated zone (19.14 acres) were used for pastureland, approximately 10 head of cattle would require drinking water needs. The example scenario assumes each head of cattle will require 160 liters of Water per day. A calculation provided in Appendix H shows annual well pumping rate required for this scenario. A copy of Table 3.10-1 and pertinent information from "*Principles of Controlled Grazing*" are also provided. The low and high uncertainty

range values are not expected to be more than 20 percent above or below the recommended value.

Site-Specific Soil Parameters
Westinghouse Former Fuel Cycle Facility D&&D Project

RESRAD Parameter Table for ^{232}Th

Parameter	Recommended Value	RESRAD Code Designation	Units	Uncertainty Range			Probabilistic Function	Reference
				Low Value	High Value	Number of Samples		
Groundwater Concentration	29.3	W(i)	pCi/L	0	41.8	12	Lognormal	1
Area of Contaminated Zone	77458	AREA	m^2	61966	92950	NA	Normal	2
Thickness of Contaminated Zone	2	THICKO	m	1.00E-10	11.74	NA	Bounded Lognormal	3
Length Parallel to Aquifer	291	LCZPAQ	m	233	349	NA	Bounded Normal	4
Density of Contaminated Zone	1.69	DENSCZ	g/cm^3	1.39	2.11	28	Normal	5
Contaminated Zone Erosion Rate	0.0003	VCZ	m/yr	0.00024	0.00036	NA	Bounded Normal	6
Contaminated Zone Total Porosity	0.45	TPCZ	0.xx	0.41	0.483	13	Normal	7
Contaminated Zone Field Capacity	0.17	FCCZ	0.xx	0.01	0.2	NA	Bounded Normal	8
Contaminated Zone Hydraulic Conductivity	14.56	HCCZ	m/yr	1.38E-03	1.45E+02	13	Lognormal	9
Contaminated Zone b Parameter	10.40	BCZ	unitless	4.05	11.4	NA	Lognormal	10
Watershed Area	998939	WAREA	m^2	988950	1008928	NA	Bounded Normal	11
Density of Saturated Zone	1.69	DENSAQ	g/cm^3	1.39	2.11	28	Normal	5
Saturated Zone Total Porosity	0.45	TPSZ	0.xx	0.41	0.483	13	Normal	7
Saturated Zone Effective Porosity	0.29	EPSZ	0.xx	0.281	0.425	NA	Normal	12
Saturated Zone Field Capacity	0.17	FCSZ	0.xx	0.01	0.2	NA	Bounded Normal	8
Saturated Zone Hydraulic Conductivity	169.58	HCSZ	m/yr	1.56E+01	8.51E+01	12	Lognormal	13
Saturated Zone Hydraulic Gradient	0.015	HGWT	unitless	0.013	0.018	NA	Bounded Lognormal	14
Saturated Zone b Parameter	10.40	BSZ	unitless	4.05	11.4	NA	Lognormal	10
Water Table Drop Rate	0.00	VWT	m/yr	NA	NA	NA	None Recommended	15
Well Pump Intake Depth	9.41	DWIBWT	m	5.4	11.7	10	Bounded Normal	16
Well Pumping Rate	913	UW	m^3/yr	730	1096	NA	Bounded Normal	17

REFERENCE FOOTNOTES for ^{232}Th

1 ^{232}Th ground-water concentration data does not exist. However ^{228}Ac (a daughter of ^{232}Th) ground-water data does exist. If we assume that ^{232}Th is in 100% equilibrium with ^{228}Ac, we can use the same data. ^{228}Ac data was taken from piezometer MW-32, which was sampled by Leggette, Brashears & Graham, Inc. in May 1999. This information was referenced in Table 7, "*Fourth Sampling Event Report in Conjunction with the Hydrogeologic Investigation and Ground-Water, Soil and Stream Characterization*", prepared by LBG in November 1999. Figure 1 shows the location of MW-32 and Appendix A contains a copy of Table 7. The low value of the uncertainty range corresponds to the numerous non-detections during the four quarterly sampling events, and the high value corresponds to concentrations from WS-27 (August 1999).

2 Only sparse ^{232}Th data exists for soil. LBG assumes the Area of Contaminated Zone is where operations involving ^{232}Th occurred. Therefore, the Area of Contamination is defined by the following: Missouri State Highway P to the northwest, the Northeast Site Creek to the northeast, the fenceline to the southeast, and the Site Pond/Creek to the southwest. The northern limits include the Health Physics building and Red Room Roof Burial area, which are in close proximity to the highway. The eastern limits include the burial area, which is located between the plant and the Northeast Site Creek. The south fence line is just northwest of the railway easement. The western limits of extend to the Site Pond/Creek to encompass the location of the cistern/burn pit and red room roof burial area. Figure 4 shows the Area of Contamination for ^{232}Th. The low and high uncertainty range values are not expected to be more than 20 percent above or below the recommended value.

3 Due to a sparse amount of soil data for ^{235}U, the RESRAD default value was chosen, based on Table 1.3 of "*Data Collection Handbook to Support Modeling Impacts of Radioactive Material in Soil*," April 1993. Appendix C contains a copy of Table 1.3. The low value of the uncertainty range is based on the lower bounds value in Table 1.3. The high value of the uncertainty range is the maximum depth of the overburden.

4 Figure 1 shows the ground-water flow direction and gradient, and length of contaminated zone. The source of Figure 1 is from "*Hydrogeologic Investigation and Ground-Water, Soil and Stream Characterization*" performed by LBG in March 1999. The low and high uncertainty range values for the Length Parallel to Aquifer are not expected to be more than 20 percent above or below the recommended value.

5 Taken from an average of dry density calculations from work performed by Fitch, University of Missouri – Rolla, 1998, presented in "*Fourth Sampling Event Report in Conjunction with the Hydrogeologic Investigation and Ground-Water, Soil and Stream Characterization*", prepared by LBG in November 1999, and Shannon and Wilson (Appendix B of "*Hydrogeologic Investigation and Ground-Water, Soil and Stream Characterization*" performed by LBG in March 1999). Appendix D includes a table with these values showing how the value was derived. It also includes a copy of the reference

data. The low and high values for the uncertainty range are associated with the lowest and highest values from the data set.

6 Jefferson County does not have a published soil survey which typically provide values for erosion rates. Therefore, the default value (0.001 m/yr) provided in Table 1.3 of "*Data Collection Handbook to Support Modeling Impacts of Radioactive Material in Soil*," April 1993, was used as a starting point. Since approximately 70 percent of the area of contamination is covered with impervious material, the default value was multiplied by .30 to give a value of 0.0003 m/yr. The low and high uncertainty range values are not expected to be more than 20 percent above or below the recommended value.

7 From Shannon and Wilson, (Appendix B of "*Hydrogeologic Investigation and Ground-Water, Soil and Stream Characterization*" performed by LBG in March 1999). Appendix D includes a table with these values showing how the value was derived. It also includes a copy of the reference data. The low and high values for the uncertainty range are associated with the lowest and highest values from the data set.

8 Derived using Formula 4.4 on page 28 of "*Data Collection Handbook to Support Modeling Impacts of Radioactive Material in Soil*," April 1993. The value for total porosity was taken from the average of Shannon and Wilson data (0.446; see footnote 7 above) and the value for effective porosity was based on a default value for silty clay in Table 3.3-1 of "*Development of Probabilistic RESRAD 6.0 and RESRAD-Build 3.0 Computer Codes*," November 2000. A copy of page 28, the completed formula, and Table 3.3-1 are provided in Appendix E. The low value of the uncertainty range cannot be zero (thus 0.01 was chosen), and the high value is derived by using the highest total porosity and effective porosity values in the calculation.

9 Shannon and Wilson (Appendix B of "*Hydrogeologic Investigation and Ground-Water, Soil and Stream Characterization*" prepared by LBG in March 1999) performed permeability tests on numerous soil samples. The average vertical permeability (hydraulic conductivity; K) for each sample was determined by averaging the last three permeability readings (telephone communication with Mr. Chris Groves, Vice-President, Shannon and Wilson on August 13, 2003). Once averages were calculated for each sample, an average of the entire data set was determined. The vertical hydraulic conductivity test data and a table developed to show the average K per sample, and the average K for the data set are provided in Appendix D. The low and high values for the uncertainty range are associated with the lowest and highest values from the data set.

10 Based on the default value for silty clay provided in Table 13.1, in "*Data Collection Handbook to Support Modeling Impacts of Radioactive Material in Soil*," April 1993. A copy of Table 13.1 is provided in Appendix F. The low and high values for the uncertainty range are associated with the lowest and highest values in Table 13.1.

11 The areal extent of the Watershed Area is defined on Figure 3. The low and high uncertainty range values are not expected to be more than 1 percent above or below the recommended value.

12 The effective porosity value is based on a default value for silty clay in Table 3.3-1 of "*Development of Probabilistic RESRAD 6.0 and RESRAD-Build 3.0 Computer Codes*," November 2000. A copy of Table 3.3-1 is provided in Appendix E. The low and high values for the uncertainty range are associated with the lowest and highest values in Table 3.3-1.

13 The average horizontal hydraulic conductivity value was calculated using an average of the values for near-surface silt, silty-clay (NSSSC) and deep silty-clay, clay (DSCC) as determined in Table 2 of "*Hydrogeologic Investigation and Ground-Water, Soil and Stream Characterization*" performed by LBG in March 1999). Appendix D includes a table with these values showing how the value was derived. It also includes a copy of the reference data. The low and high values for the uncertainty range are associated with the lowest and highest values from the data set.

14 Figure 1 shows the ground-water flow direction and gradient, and length of contaminated zone. Source of Figure 1 is from "*Hydrogeologic Investigation and Ground-Water, Soil and Stream Characterization*" performed by LBG in March 1999. The low and high values of the uncertainty range correspond to the lowest and highest gradient values from the LBG quarterly sampling reports.

15 Because the overburden aquifer is not used as a source of drinking water or for irrigation purposes, no net loss of ground water is expected to occur. Therefore, the value for the Water Table Drop Rate is zero. Low and high values of the uncertainty range are not applicable.

16 The Pump Intake Depth would be near the bottom of the DSCC, which would be approximately two feet above bedrock at the Site. The bottom of the screen depth of all DSSC wells was averaged and two feet was subtracted from that value. Table 5 from the RI/FS work plan was used to estimated the bottom of the wells, a copy of which is included in Appendix G. A table showing how the average was derived is also provided. The low and high values for the uncertainty range are associated with the lowest and highest values in Table 5.

17 Table 3.10-1 of "*Development of Probabilistic RESRAD 6.0 and RESRAD-Build 3.0 Computer Codes*," November 2000 provides a basis for determining the well pumping rate. The example scenario assumes a household of 4 adults, each requiring 225 liters of water per day. Agricultural parcels in this part of Missouri are typically not irrigated, so pumping rates for irrigation have not been provided. Water consumption for livestock is included in this parameter. Based on "*Principles of Controlled Grazing*," prepared by David W. Pratt in 1993, 2 head of cattle per acre on remote ranges or non-irrigated pasture is common. If the entire contaminated zone (19.14 acres) were used for pastureland, approximately 10 head of cattle would require drinking water needs. The example scenario assumes each head of cattle

will require 160 liters of Water per day. A calculation provided in Appendix H shows annual well pumping rate required for this scenario. A copy of Table 3.10-1 and pertinent information from "*Principles of*

Controlled Grazing" are also provided. The low and high uncertainty range values are not expected to be more than 20 percent above or below the recommended value.

Site-Specific Soil Parameters
Westinghouse Former Fuel Cycle Facility D&&D Project

RESRAD Parameter Table for ^{228}Ra

Parameter	Recommended Value	RESRAD Code Designation	Units	Uncertainty Range			Probabilistic Function	Reference
				Low Value	High Value	Number of Samples		
Groundwater Concentration	29.3	W(i)	pCi/L	0	41.8	12	Lognormal	1
Area of Contaminated Zone	77458	AREA	m^2	61966	92950	NA	Normal	2
Thickness of Contaminated Zone	2	THICKO	m	1.00E-10	11.74	NA	Bounded Lognormal	3
Length Parallel to Aquifer	291	LCZPAQ	m	233	349	NA	Bounded Normal	4
Density of Contaminated Zone	1.69	DENSCZ	g/cm^3	1.39	2.11	28	Normal	5
Contaminated Zone Erosion Rate	0.0003	VCZ	m/yr	0.00024	0.00036	NA	Bounded Normal	6
Contaminated Zone Total Porosity	0.45	TPCZ	0.xx	0.41	0.483	13	Normal	7
Contaminated Zone Field Capacity	0.17	FCCZ	0.xx	0.01	0.2	NA	Bounded Normal	8
Contaminated Zone Hydraulic Conductivity	14.56	HCCZ	m/yr	1.38E-03	1.45E+02	13	Lognormal	9
Contaminated Zone b Parameter	10.40	BCZ	unitless	4.05	11.4	NA	Lognormal	10
Watershed Area	998939	WAREA	m^2	988950	1008928	NA	Bounded Normal	11
Density of Saturated Zone	1.69	DENSAQ	g/cm^3	1.39	2.11	28	Normal	5
Saturated Zone Total Porosity	0.45	TPSZ	0.xx	0.41	0.483	13	Normal	7
Saturated Zone Effective Porosity	0.29	EPSZ	0.xx	0.281	0.425	NA	Normal	12
Saturated Zone Field Capacity	0.17	FCSZ	0.xx	0.01	0.2	NA	Bounded Normal	8
Saturated Zone Hydraulic Conductivity	169.58	HCSZ	m/yr	1.56E+01	8.51E+01	12	Lognormal	13
Saturated Zone Hydraulic Gradient	0.015	HGWT	unitless	0.013	0.018	NA	Bounded Lognormal	14
Saturated Zone b Parameter	10.40	BSZ	unitless	4.05	11.4	NA	Lognormal	10
Water Table Drop Rate	0.00	VWT	m/yr	NA	NA	NA	None Recommended	15
Well Pump Intake Depth	9.41	DWIBWT	m	5.4	11.7	10	Bounded Normal	16
Well Pumping Rate	913	UW	m^3/yr	730	1096	NA	Bounded Normal	17

REFERENCE FOOTNOTES for ^{228}Ra

1 ^{228}Ra ground-water concentration data does not exist. However ^{228}Ac (a daughter of ^{228}Ra) ground-water data does exist. If we assume that ^{228}Ra is in 100% equilibrium with ^{228}Ac, we can use the same data. ^{228}Ac data was taken from piezometer MW-32, which was sampled by Leggette, Brashears & Graham, Inc. in May 1999. This information was referenced in Table 7, *"Fourth Sampling Event Report in Conjunction with the Hydrogeologic Investigation and Ground-Water, Soil and Stream Characterization"*, prepared by LBG in November 1999. Figure 1 shows the location of MW-32 and Appendix A contains a copy of Table 7. The low value of the uncertainty range corresponds to the numerous non-detections during the four quarterly sampling events, and the high value corresponds to concentrations from WS-27 (August 1999).

2 Only sparse ^{228}Ra data exists for soil. LBG assumes the Area of Contaminated Zone is where operations involving ^{228}Ra occurred. Therefore, the Area of Contamination is defined by the following: Missouri State Highway P to the northwest, the Northeast Site Creek to the northeast, the fenceline to the southeast, and the Site Pond/Creek to the southwest. The northern limits include the Health Physics building and Red Room Roof Burial area, which are in close proximity to the highway. The eastern limits include the burial area, which is located between the plant and the Northeast Site Creek. The south fence line is just northwest of the railway easement. The western limits of extend to the Site Pond/Creek to encompass the location of the cistern/burn pit and red room roof burial area. Figure 4 shows the Area of Contamination for ^{228}Ra. The low and high uncertainty range values are not expected to be more than 20 percent above or below the recommended value.

3 Due to a sparse amount of soil data for ^{235}U, the RESRAD default value was chosen, based on Table 1.3 of *"Data Collection Handbook to Support Modeling Impacts of Radioactive Material in Soil,"* April 1993. Appendix C contains a copy of Table 1.3. The low value of the uncertainty range is based on the lower bounds value in Table 1.3. The high value of the uncertainty range is the maximum depth of the overburden.

4 Figure 1 shows the ground-water flow direction and gradient, and length of contaminated zone. The source of Figure 1 is from *"Hydrogeologic Investigation and Ground-Water, Soil and Stream Characterization"* performed by LBG in March 1999. The low and high uncertainty range values for the Length Parallel to Aquifer are not expected to be more than 20 percent above or below the recommended value.

5 Taken from an average of dry density calculations from work performed by Fitch, University of Missouri – Rolla, 1998, presented in *"Fourth Sampling Event Report in Conjunction with the Hydrogeologic Investigation and Ground-Water, Soil and Stream Characterization"*, prepared by LBG in November 1999, and Shannon and Wilson (Appendix B of *"Hydrogeologic Investigation and Ground-Water, Soil and Stream Characterization"* performed by LBG in March 1999). Appendix D includes a table with these values showing how the value was derived. It also includes a copy of the reference

data. The low and high values for the uncertainty range are associated with the lowest and highest values from the data set.

6 Jefferson County does not have a published soil survey which typically provide values for erosion rates. Therefore, the default value (0.001 m/yr) provided in Table 1.3 of "*Data Collection Handbook to Support Modeling Impacts of Radioactive Material in Soil*," April 1993, was used as a starting point. Since approximately 70 percent of the area of contamination is covered with impervious material, the default value was multiplied by .30 to give a value of 0.0003 m/yr. The low and high uncertainty range values are not expected to be more than 20 percent above or below the recommended value.

7 From Shannon and Wilson, (Appendix B of "*Hydrogeologic Investigation and Ground-Water, Soil and Stream Characterization*" performed by LBG in March 1999). Appendix D includes a table with these values showing how the value was derived. It also includes a copy of the reference data. The low and high values for the uncertainty range are associated with the lowest and highest values from the data set.

8 Derived using Formula 4.4 on page 28 of "*Data Collection Handbook to Support Modeling Impacts of Radioactive Material in Soil*," April 1993. The value for total porosity was taken from the average of Shannon and Wilson data (0.446; see footnote 7 above) and the value for effective porosity was based on a default value for silty clay in Table 3.3-1 of "*Development of Probabilistic RESRAD 6.0 and RESRAD-Build 3.0 Computer Codes*," November 2000. A copy of page 28, the completed formula, and Table 3.3-1 are provided in Appendix E. The low value of the uncertainty range cannot be zero (thus 0.01 was chosen), and the high value is derived by using the highest total porosity and effective porosity values in the calculation.

9 Shannon and Wilson (Appendix B of "*Hydrogeologic Investigation and Ground-Water, Soil and Stream Characterization*" prepared by LBG in March 1999) performed permeability tests on numerous soil samples. The average vertical permeability (hydraulic conductivity; K) for each sample was determined by averaging the last three permeability readings (telephone communication with Mr. Chris Groves, Vice-President, Shannon and Wilson on August 13, 2003). Once averages were calculated for each sample, an average of the entire data set was determined. The vertical hydraulic conductivity test data and a table developed to show the average K per sample, and the average K for the data set are provided in Appendix D. The low and high values for the uncertainty range are associated with the lowest and highest values from the data set.

10 Based on the default value for silty clay provided in Table 13.1, in "*Data Collection Handbook to Support Modeling Impacts of Radioactive Material in Soil*," April 1993. A copy of Table 13.1 is provided in Appendix F. The low and high values for the uncertainty range are associated with the lowest and highest values in Table 13.1.

11 The areal extent of the Watershed Area is defined on Figure 3. The low and high uncertainty range values are not expected to be more than 1 percent above or below the recommended value.

12 The effective porosity value is based on a default value for silty clay in Table 3.3-1 of "*Development of Probabilistic RESRAD 6.0 and RESRAD-Build 3.0 Computer Codes*," November 2000. A copy of Table 3.3-1 is provided in Appendix E. The low and high values for the uncertainty range are associated with the lowest and highest values in Table 3.3-1.

13 The average horizontal hydraulic conductivity value was calculated using an average of the values for near-surface silt, silty-clay (NSSSC) and deep silty-clay, clay (DSCC) as determined in Table 2 of "*Hydrogeologic Investigation and Ground-Water, Soil and Stream Characterization*" performed by LBG in March 1999). Appendix D includes a table with these values showing how the value was derived. It also includes a copy of the reference data. The low and high values for the uncertainty range are associated with the lowest and highest values from the data set.

14 Figure 1 shows the ground-water flow direction and gradient, and length of contaminated zone. Source of Figure 1 is from "*Hydrogeologic Investigation and Ground-Water, Soil and Stream Characterization*" performed by LBG in March 1999. The low and high values of the uncertainty range correspond to the lowest and highest gradient values from the LBG quarterly sampling reports.

15 Because the overburden aquifer is not used as a source of drinking water or for irrigation purposes, no net loss of ground water is expected to occur. Therefore, the value for the Water Table Drop Rate is zero. Low and high values of the uncertainty range are not applicable.

16 The Pump Intake Depth would be near the bottom of the DSCC, which would be approximately two feet above bedrock at the Site. The bottom of the screen depth of all DSSC wells was averaged and two feet was subtracted from that value. Table 5 from the RI/FS work plan was used to estimated the bottom of the wells, a copy of which is included in Appendix G. A table showing how the average was derived is also provided. The low and high values for the uncertainty range are associated with the lowest and highest values in Table 5.

17 Table 3.10-1 of "*Development of Probabilistic RESRAD 6.0 and RESRAD-Build 3.0 Computer Codes*," November 2000 provides a basis for determining the well pumping rate. The example scenario assumes a household of 4 adults, each requiring 225 liters of water per day. Agricultural parcels in this part of Missouri are typically not irrigated, so pumping rates for irrigation have not been provided. Water consumption for livestock is included in this parameter. Based on "*Principles of Controlled Grazing*," prepared by David W. Pratt in 1993, 2 head of cattle per acre on remote ranges or non-irrigated pasture is common. If the

entire contaminated zone (19.14 acres) were used for pastureland, approximately 10 head of cattle would require drinking water needs. The

example scenario assumes each head of cattle will require 160 liters of Water per day. A calculation provided in Appendix H shows annual well pumping rate required for this scenario. A copy of Table 3.10-1 and pertinent information from "*Principles of Controlled Grazing*" are also provided. The low and high uncertainty range values are not expected to be more than 20 percent above or below the recommended value.

Site-Specific Soil Parameters
Westinghouse Former Fuel Cycle Facility D&&D Project

RESRAD Parameter Table for ^{228}Th

Parameter	Recommended Value	RESRAD Code Designation	Units	Uncertainty Range			Probabilistic Function	Reference
				Low Value	High Value	Number of Samples		
Groundwater Concentration	29.3	W(i)	pCi/L	0	41.8	12	Lognormal	1
Area of Contaminated Zone	77458	AREA	m^2	61966	92950	NA	Normal	2
Thickness of Contaminated Zone	2	THICKO	m	1.00E-10	11.74	NA	Bounded Lognormal	3
Length Parallel to Aquifer	291	LCZPAQ	m	233	349	NA	Bounded Normal	4
Density of Contaminated Zone	1.69	DENSCZ	g/cm^3	1.39	2.11	28	Normal	5
Contaminated Zone Erosion Rate	0.0003	VCZ	m/yr	0.00024	0.00036	NA	Bounded Normal	6
Contaminated Zone Total Porosity	0.45	TPCZ	0.xx	0.41	0.483	13	Normal	7
Contaminated Zone Field Capacity	0.17	FCCZ	0.xx	0.01	0.2	NA	Bounded Normal	8
Contaminated Zone Hydraulic Conductivity	14.56	HCCZ	m/yr	1.38E-03	1.45E+02	13	Lognormal	9
Contaminated Zone b Parameter	10.40	BCZ	unitless	4.05	11.4	NA	Lognormal	10
Watershed Area	998939	WAREA	m^2	988950	1008928	NA	Bounded Normal	11
Density of Saturated Zone	1.69	DENSAQ	g/cm^3	1.39	2.11	28	Normal	5
Saturated Zone Total Porosity	0.45	TPSZ	0.xx	0.41	0.483	13	Normal	7
Saturated Zone Effective Porosity	0.29	EPSZ	0.xx	0.281	0.425	NA	Normal	12
Saturated Zone Field Capacity	0.17	FCSZ	0.xx	0.01	0.2	NA	Bounded Normal	8
Saturated Zone Hydraulic Conductivity	169.58	HCSZ	m/yr	1.56E+01	8.51E+01	12	Lognormal	13
Saturated Zone Hydraulic Gradient	0.015	HGWT	unitless	0.013	0.018	NA	Bounded Lognormal	14
Saturated Zone b Parameter	10.40	BSZ	unitless	4.05	11.4	NA	Lognormal	10
Water Table Drop Rate	0.00	VWT	m/yr	NA	NA	NA	None Recommended	15
Well Pump Intake Depth	9.41	DWIBWT	m	5.4	11.7	10	Bounded Normal	16
Well Pumping Rate	913	UW	m^3/yr	730	1096	NA	Bounded Normal	17

REFERENCE FOOTNOTES for ^{228}Th

1 ^{228}Th ground-water concentration data does not exist. However ^{228}Ac (a parent of ^{228}Th) ground-water data does exist. If we assume that ^{228}Th is in 100% equilibrium with ^{228}Ac, we can use the same data. ^{228}Ac data was taken from piezometer MW-32, which was sampled by Leggette, Brashears & Graham, Inc. in May 1999. This information was referenced in Table 7, "*Fourth Sampling Event Report in Conjunction with the Hydrogeologic Investigation and Ground-Water, Soil and Stream Characterization*", prepared by LBG in November 1999. Figure 1 shows the location of MW-32 and Appendix A contains a copy of Table 7. The low value of the uncertainty range corresponds to the numerous non-detections during the four quarterly sampling events, and the high value corresponds to concentrations from WS-27 (August 1999).

2 Only sparse ^{228}Th data exists for soil. LBG assumes the Area of Contaminated Zone is where operations involving ^{228}Th occurred. Therefore, the Area of Contamination is defined by the following: Missouri State Highway P to the northwest, the Northeast Site Creek to the northeast, the fenceline to the southeast, and the Site Pond/Creek to the southwest. The northern limits include the Health Physics building and Red Room Roof Burial area, which are in close proximity to the highway. The eastern limits include the burial area, which is located between the plant and the Northeast Site Creek. The south fence line is just northwest of the railway easement. The western limits of extend to the Site Pond/Creek to encompass the location of the cistern/burn pit and red room roof burial area. Figure 4 shows the Area of Contamination for ^{228}Th. The low and high uncertainty range values are not expected to be more than 20 percent above or below the recommended value.

3 Due to a sparse amount of soil data for ^{235}U, the RESRAD default value was chosen, based on Table 1.3 of "*Data Collection Handbook to Support Modeling Impacts of Radioactive Material in Soil*," April 1993. Appendix C contains a copy of Table 1.3. The low value of the uncertainty range is based on the lower bounds value in Table 1.3. The high value of the uncertainty range is the maximum depth of the overburden.

4 Figure 1 shows the ground-water flow direction and gradient, and length of contaminated zone. The source of Figure 1 is from "*Hydrogeologic Investigation and Ground-Water, Soil and Stream Characterization*" performed by LBG in March 1999. The low and high uncertainty range values for the Length Parallel to Aquifer are not expected to be more than 20 percent above or below the recommended value.

5 Taken from an average of dry density calculations from work performed by Fitch, University of Missouri – Rolla, 1998, presented in "*Fourth Sampling Event Report in Conjunction with the Hydrogeologic Investigation and Ground-Water, Soil and Stream Characterization*", prepared by LBG in November 1999, and Shannon and Wilson (Appendix B of "*Hydrogeologic Investigation and Ground-Water, Soil and Stream Characterization*" performed by LBG in March 1999). Appendix D includes a table with these values showing how the value was derived. It also includes a copy of the reference

data. The low and high values for the uncertainty range are associated with the lowest and highest values from the data set.

6 Jefferson County does not have a published soil survey which typically provide values for erosion rates. Therefore, the default value (0.001 m/yr) provided in Table 1.3 of "*Data Collection Handbook to Support Modeling Impacts of Radioactive Material in Soil*," April 1993, was used as a starting point. Since approximately 70 percent of the area of contamination is covered with impervious material, the default value was multiplied by .30 to give a value of 0.0003 m/yr. The low and high uncertainty range values are not expected to be more than 20 percent above or below the recommended value.

7 From Shannon and Wilson, (Appendix B of "*Hydrogeologic Investigation and Ground-Water, Soil and Stream Characterization*" performed by LBG in March 1999). Appendix D includes a table with these values showing how the value was derived. It also includes a copy of the reference data. The low and high values for the uncertainty range are associated with the lowest and highest values from the data set.

8 Derived using Formula 4.4 on page 28 of "*Data Collection Handbook to Support Modeling Impacts of Radioactive Material in Soil*," April 1993. The value for total porosity was taken from the average of Shannon and Wilson data (0.446; see footnote 7 above) and the value for effective porosity was based on a default value for silty clay in Table 3.3-1 of "*Development of Probabilistic RESRAD 6.0 and RESRAD-Build 3.0 Computer Codes*," November 2000. A copy of page 28, the completed formula, and Table 3.3-1 are provided in Appendix E. The low value of the uncertainty range cannot be zero (thus 0.01 was chosen), and the high value is derived by using the highest total porosity and effective porosity values in the calculation.

9 Shannon and Wilson (Appendix B of "*Hydrogeologic Investigation and Ground-Water, Soil and Stream Characterization*" prepared by LBG in March 1999) performed permeability tests on numerous soil samples. The average vertical permeability (hydraulic conductivity; K) for each sample was determined by averaging the last three permeability readings (telephone communication with Mr. Chris Groves, Vice-President, Shannon and Wilson on August 13, 2003). Once averages were calculated for each sample, an average of the entire data set was determined. The vertical hydraulic conductivity test data and a table developed to show the average K per sample, and the average K for the data set are provided in Appendix D. The low and high values for the uncertainty range are associated with the lowest and highest values from the data set.

10 Based on the default value for silty clay provided in Table 13.1, in "*Data Collection Handbook to Support Modeling Impacts of Radioactive Material in Soil*," April 1993. A copy of Table 13.1 is provided in Appendix F. The low and high values for the uncertainty range are associated with the lowest and highest values in Table 13.1.

11 The areal extent of the Watershed Area is defined on Figure 3. The low and high uncertainty range values are not expected to be more than 1 percent above or below the recommended value.

12 The effective porosity value is based on a default value for silty clay in Table 3.3-1 of "*Development of Probabilistic RESRAD 6.0 and RESRAD-Build 3.0 Computer Codes*," November 2000. A copy of Table 3.3-1 is provided in Appendix E. The low and high values for the uncertainty range are associated with the lowest and highest values in Table 3.3-1.

13 The average horizontal hydraulic conductivity value was calculated using an average of the values for near-surface silt, silty-clay (NSSSC) and deep silty-clay, clay (DSCC) as determined in Table 2 of "*Hydrogeologic Investigation and Ground-Water, Soil and Stream Characterization*" performed by LBG in March 1999). Appendix D includes a table with these values showing how the value was derived. It also includes a copy of the reference data. The low and high values for the uncertainty range are associated with the lowest and highest values from the data set.

14 Figure 1 shows the ground-water flow direction and gradient, and length of contaminated zone. Source of Figure 1 is from "*Hydrogeologic Investigation and Ground-Water, Soil and Stream Characterization*" performed by LBG in March 1999. The low and high values of the uncertainty range correspond to the lowest and highest gradient values from the LBG quarterly sampling reports.

15 Because the overburden aquifer is not used as a source of drinking water or for irrigation purposes, no net loss of ground water is expected to occur. Therefore, the value for the Water Table Drop Rate is zero. Low and high values of the uncertainty range are not applicable.

16 The Pump Intake Depth would be near the bottom of the DSCC, which would be approximately two feet above bedrock at the Site. The bottom of the screen depth of all DSSC wells was averaged and two feet was subtracted from that value. Table 5 from the RI/FS work plan was used to estimated the bottom of the wells, a copy of which is included in Appendix G. A table showing how the average was derived is also provided. The low and high values for the uncertainty range are associated with the lowest and highest values in Table 5.

17 Table 3.10-1 of "*Development of Probabilistic RESRAD 6.0 and RESRAD-Build 3.0 Computer Codes*," November 2000 provides a basis for determining the well pumping rate. The example scenario assumes a household of 4 adults, each requiring 225 liters of water per day. Agricultural parcels in this part of Missouri are typically not irrigated, so pumping rates for irrigation have not been provided. Water consumption for livestock is included in this parameter. Based on "*Principles of Controlled Grazing*," prepared by David W. Pratt in 1993, 2 head of cattle per acre on remote ranges or non-irrigated pasture is common. If the

entire contaminated zone (19.14 acres) were used for pastureland, approximately 10 head of cattle would require drinking water needs. The

example scenario assumes each head of cattle will require 160 liters of Water per day. A calculation provided in Appendix H shows annual well pumping rate required for this scenario. A copy of Table 3.10-1 and pertinent information from "*Principles of Controlled Grazing*" are also provided. The low and high uncertainty range values are not expected to be more than 20 percent above or below the recommended value.

Site-Specific Soil Parameters
Westinghouse Former Fuel Cycle Facility D&&D Project

RESRAD Parameter Table for ^{224}Ra

Parameter	Recommended Value	RESRAD Code Designation	Units	Uncertainty Range			Probabilistic Function	Reference
				Low Value	High Value	Number of Samples		
Groundwater Concentration	29.3	W(i)	pCi/L	0	41.8	12	Lognormal	1
Area of Contaminated Zone	77458	AREA	m^2	61966	92950	NA	Normal	2
Thickness of Contaminated Zone	2	THICKO	m	1.00E-10	11.74	NA	Bounded Lognormal	3
Length Parallel to Aquifer	291	LCZPAQ	m	233	349	NA	Bounded Normal	4
Density of Contaminated Zone	1.69	DENSCZ	g/cm^3	1.39	2.11	28	Normal	5
Contaminated Zone Erosion Rate	0.0003	VCZ	m/yr	0.00024	0.00036	NA	Bounded Normal	6
Contaminated Zone Total Porosity	0.45	TPCZ	0.xx	0.41	0.483	13	Normal	7
Contaminated Zone Field Capacity	0.17	FCCZ	0.xx	0.01	0.2	NA	Bounded Normal	8
Contaminated Zone Hydraulic Conductivity	14.56	HCCZ	m/yr	1.38E-03	1.45E+02	13	Lognormal	9
Contaminated Zone b Parameter	10.40	BCZ	unitless	4.05	11.4	NA	Lognormal	10
Watershed Area	998939	WAREA	m^2	988950	1008928	NA	Bounded Normal	11
Density of Saturated Zone	1.69	DENSAQ	g/cm^3	1.39	2.11	28	Normal	5
Saturated Zone Total Porosity	0.45	TPSZ	0.xx	0.41	0.483	13	Normal	7
Saturated Zone Effective Porosity	0.29	EPSZ	0.xx	0.281	0.425	NA	Normal	12
Saturated Zone Field Capacity	0.17	FCSZ	0.xx	0.01	0.2	NA	Bounded Normal	8
Saturated Zone Hydraulic Conductivity	169.58	HCSZ	m/yr	1.56E+01	8.51E+01	12	Lognormal	13
Saturated Zone Hydraulic Gradient	0.015	HGWT	unitless	0.013	0.018	NA	Bounded Lognormal	14
Saturated Zone b Parameter	10.40	BSZ	unitless	4.05	11.4	NA	Lognormal	10
Water Table Drop Rate	0.00	VWT	m/yr	NA	NA	NA	None Recommended	15
Well Pump Intake Depth	9.41	DWIBWT	m	5.4	11.7	10	Bounded Normal	16
Well Pumping Rate	913	UW	m^3/yr	730	1096	NA	Bounded Normal	17

REFERENCE FOOTNOTES for ^{224}Ra

1 ^{224}Ra ground-water concentration data does not exist. However ^{228}Ac (a parent of ^{224}Ra) ground-water data does exist. If we assume that ^{224}Ra is in 100% equilibrium with ^{228}Ac, we can use the same data. ^{228}Ac data was taken from piezometer MW-32, which was sampled by Leggette, Brashears & Graham, Inc. in May 1999. This information was referenced in Table 7, "*Fourth Sampling Event Report in Conjunction with the Hydrogeologic Investigation and Ground-Water, Soil and Stream Characterization*", prepared by LBG in November 1999. Figure 1 shows the location of MW-32 and Appendix A contains a copy of Table 7. The low value of the uncertainty range corresponds to the numerous non-detections during the four quarterly sampling events, and the high value corresponds to concentrations from WS-27 (August 1999).

2 Only sparse ^{224}Ra data exists for soil. LBG assumes the Area of Contaminated Zone is where operations involving ^{224}Ra occurred. Therefore, the Area of Contamination is defined by the following: Missouri State Highway P to the northwest, the Northeast Site Creek to the northeast, the fenceline to the southeast, and the Site Pond/Creek to the southwest. The northern limits include the Health Physics building and Red Room Roof Burial area, which are in close proximity to the highway. The eastern limits include the burial area, which is located between the plant and the Northeast Site Creek. The south fence line is just northwest of the railway easement. The western limits of extend to the Site Pond/Creek to encompass the location of the cistern/burn pit and red room roof burial area. Figure 4 shows the Area of Contamination for ^{224}Ra. The low and high uncertainty range values are not expected to be more than 20 percent above or below the recommended value.

3 Due to a sparse amount of soil data for ^{235}U, the RESRAD default value was chosen, based on Table 1.3 of "*Data Collection Handbook to Support Modeling Impacts of Radioactive Material in Soil*," April 1993. Appendix C contains a copy of Table 1.3. The low value of the uncertainty range is based on the lower bounds value in Table 1.3. The high value of the uncertainty range is the maximum depth of the overburden.

4 Figure 1 shows the ground-water flow direction and gradient, and length of contaminated zone. The source of Figure 1 is from "*Hydrogeologic Investigation and Ground-Water, Soil and Stream Characterization*" performed by LBG in March 1999. The low and high uncertainty range values for the Length Parallel to Aquifer are not expected to be more than 20 percent above or below the recommended value.

5 Taken from an average of dry density calculations from work performed by Fitch, University of Missouri – Rolla, 1998, presented in "*Fourth Sampling Event Report in Conjunction with the Hydrogeologic Investigation and Ground-Water, Soil and Stream Characterization*", prepared by LBG in November 1999, and Shannon and Wilson (Appendix B of "*Hydrogeologic Investigation and Ground-Water, Soil and Stream Characterization*" performed by LBG in March 1999). Appendix D includes a table with these values showing how the value was derived. It also includes a copy of the reference

data. The low and high values for the uncertainty range are associated with the lowest and highest values from the data set.

6 Jefferson County does not have a published soil survey which typically provide values for erosion rates. Therefore, the default value (0.001 m/yr) provided in Table 1.3 of "*Data Collection Handbook to Support Modeling Impacts of Radioactive Material in Soil*," April 1993, was used as a starting point. Since approximately 70 percent of the area of contamination is covered with impervious material, the default value was multiplied by .30 to give a value of 0.0003 m/yr. The low and high uncertainty range values are not expected to be more than 20 percent above or below the recommended value.

7 From Shannon and Wilson, (Appendix B of "*Hydrogeologic Investigation and Ground-Water, Soil and Stream Characterization*" performed by LBG in March 1999). Appendix D includes a table with these values showing how the value was derived. It also includes a copy of the reference data. The low and high values for the uncertainty range are associated with the lowest and highest values from the data set.

8 Derived using Formula 4.4 on page 28 of "*Data Collection Handbook to Support Modeling Impacts of Radioactive Material in Soil*," April 1993. The value for total porosity was taken from the average of Shannon and Wilson data (0.446; see footnote 7 above) and the value for effective porosity was based on a default value for silty clay in Table 3.3-1 of "*Development of Probabilistic RESRAD 6.0 and RESRAD-Build 3.0 Computer Codes*," November 2000. A copy of page 28, the completed formula, and Table 3.3-1 are provided in Appendix E. The low value of the uncertainty range cannot be zero (thus 0.01 was chosen), and the high value is derived by using the highest total porosity and effective porosity values in the calculation.

9 Shannon and Wilson (Appendix B of "*Hydrogeologic Investigation and Ground-Water, Soil and Stream Characterization*" prepared by LBG in March 1999) performed permeability tests on numerous soil samples. The average vertical permeability (hydraulic conductivity; K) for each sample was determined by averaging the last three permeability readings (telephone communication with Mr. Chris Groves, Vice-President, Shannon and Wilson on August 13, 2003). Once averages were calculated for each sample, an average of the entire data set was determined. The vertical hydraulic conductivity test data and a table developed to show the average K per sample, and the average K for the data set are provided in Appendix D. The low and high values for the uncertainty range are associated with the lowest and highest values from the data set.

10 Based on the default value for silty clay provided in Table 13.1, in "*Data Collection Handbook to Support Modeling Impacts of Radioactive Material in Soil*," April 1993. A copy of Table 13.1 is provided in Appendix F. The low and high values for the uncertainty range are associated with the lowest and highest values in Table 13.1.

11 The areal extent of the Watershed Area is defined on Figure 3. The low and high uncertainty range values are not expected to be more than 1 percent above or below the recommended value.

12 The effective porosity value is based on a default value for silty clay in Table 3.3-1 of "*Development of Probabilistic RESRAD 6.0 and RESRAD-Build 3.0 Computer Codes*," November 2000. A copy of Table 3.3-1 is provided in Appendix E. The low and high values for the uncertainty range are associated with the lowest and highest values in Table 3.3-1.

13 The average horizontal hydraulic conductivity value was calculated using an average of the values for near-surface silt, silty-clay (NSSSC) and deep silty-clay, clay (DSCC) as determined in Table 2 of "*Hydrogeologic Investigation and Ground-Water, Soil and Stream Characterization*" performed by LBG in March 1999). Appendix D includes a table with these values showing how the value was derived. It also includes a copy of the reference data. The low and high values for the uncertainty range are associated with the lowest and highest values from the data set.

14 Figure 1 shows the ground-water flow direction and gradient, and length of contaminated zone. Source of Figure 1 is from "*Hydrogeologic Investigation and Ground-Water, Soil and Stream Characterization*" performed by LBG in March 1999. The low and high values of the uncertainty range correspond to the lowest and highest gradient values from the LBG quarterly sampling reports.

15 Because the overburden aquifer is not used as a source of drinking water or for irrigation purposes, no net loss of ground water is expected to occur. Therefore, the value for the Water Table Drop Rate is zero. Low and high values of the uncertainty range are not applicable.

16 The Pump Intake Depth would be near the bottom of the DSCC, which would be approximately two feet above bedrock at the Site. The bottom of the screen depth of all DSSC wells was averaged and two feet was subtracted from that value. Table 5 from the RI/FS work plan was used to estimated the bottom of the wells, a copy of which is included in Appendix G. A table showing how the average was derived is also provided. The low and high values for the uncertainty range are associated with the lowest and highest values in Table 5.

17 Table 3.10-1 of "*Development of Probabilistic RESRAD 6.0 and RESRAD-Build 3.0 Computer Codes*," November 2000 provides a basis for determining the well pumping rate. The example scenario assumes a household of 4 adults, each requiring 225 liters of water per day. Agricultural parcels in this part of Missouri are typically not irrigated, so pumping rates for irrigation have not been provided. Water consumption for livestock is included in this parameter. Based on "*Principles of Controlled Grazing*," prepared by David W. Pratt in

1993, 2 head of cattle per acre on remote ranges or non-irrigated pasture is common. If the entire contaminated zone (19.14 acres) were used for pastureland, approximately 10 head of cattle would require drinking water needs. The

example scenario assumes each head of cattle will require 160 liters of Water per day. A calculation provided in Appendix H shows annual well pumping rate required for this scenario. A copy of Table 3.10-1 and pertinent information from "*Principles of Controlled Grazing*" are also provided. The low and high uncertainty range values are not expected to be more than 20 percent above or below the recommended value.

FIGURES

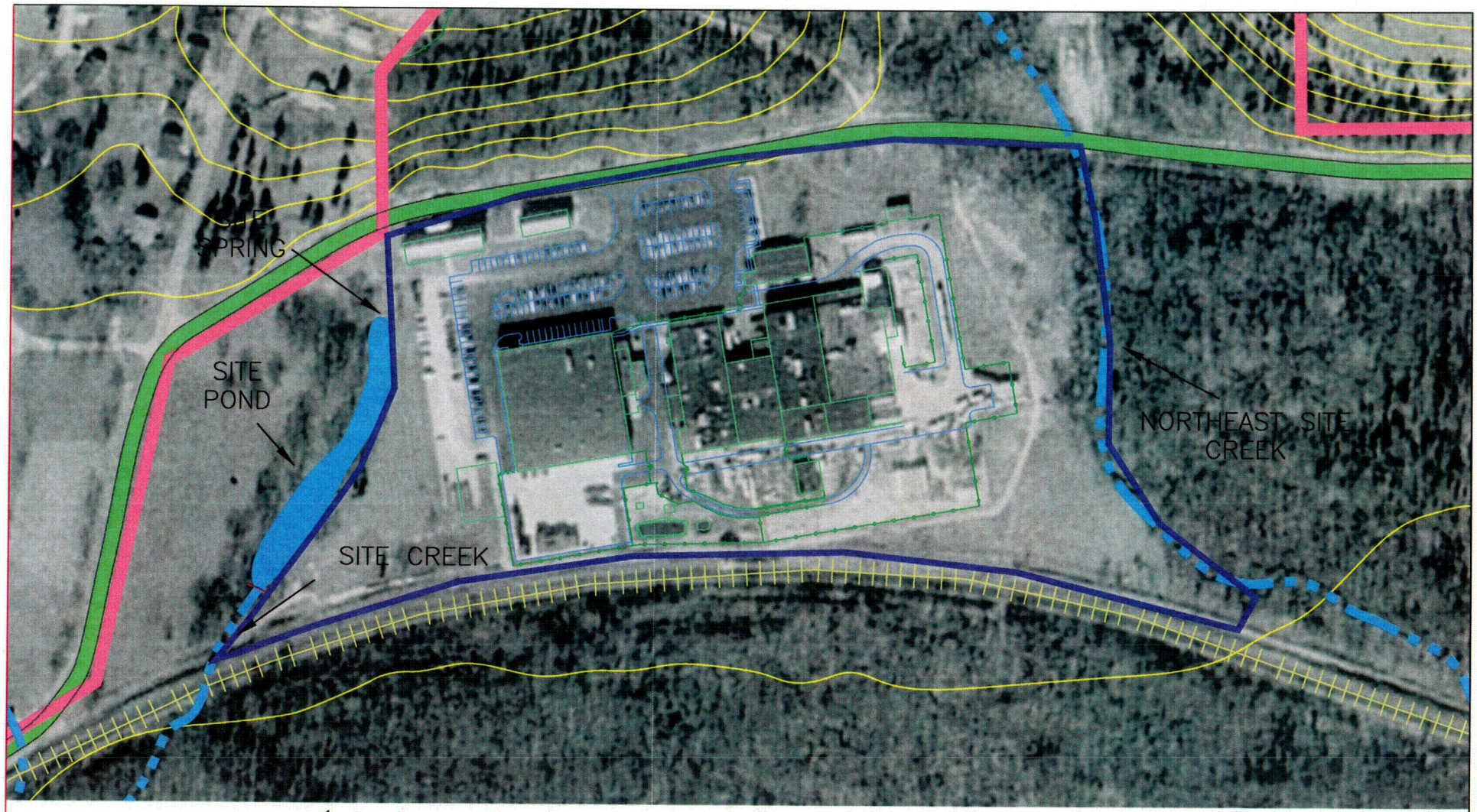

APPROXIMATE PROPERTY BOUNDARY
PERENNIAL STREAM
INTERMITTENT STREAM
10-FOOT CONTOUR LINE
FENCE LINE
AREA OF CONTAMINATED ZONE

N

0 150
FEET

SOURCES:
DIGITAL ORTHOPHOTO: USGS, MARCH 1998
DIGITAL ELEVATION MODEL: USGS, JANUARY, 1964
BORING LOCATIONS: BURDINE, 1998-1999
PROPERTY BOUNDARY: ZAHNER & ASSOC., MAY, 2000

DATE	REVISED

Prepared By:
LEGGETTE, BRASHEARS & GRAHAM, INC.
Professional Ground-Water and
Environmental Engineering Services
4850 Lemay Ferry Road, Suite 205
St. Louis, MO 63129
(314) 845-0535

WESTINGHOUSE ELECTRIC COMPANY
HEMATITE, MISSOURI FACILITY
HEMATITE, MISSOURI

AREA OF CONTAMINATED ZONE -- U-235, Ac-228, Bi-212, Pb-212, Tl-208

FILE: Area of Contaminated Zone -- U-235.dwg | DATE: AUGUST 2003 | FIGURE: 4

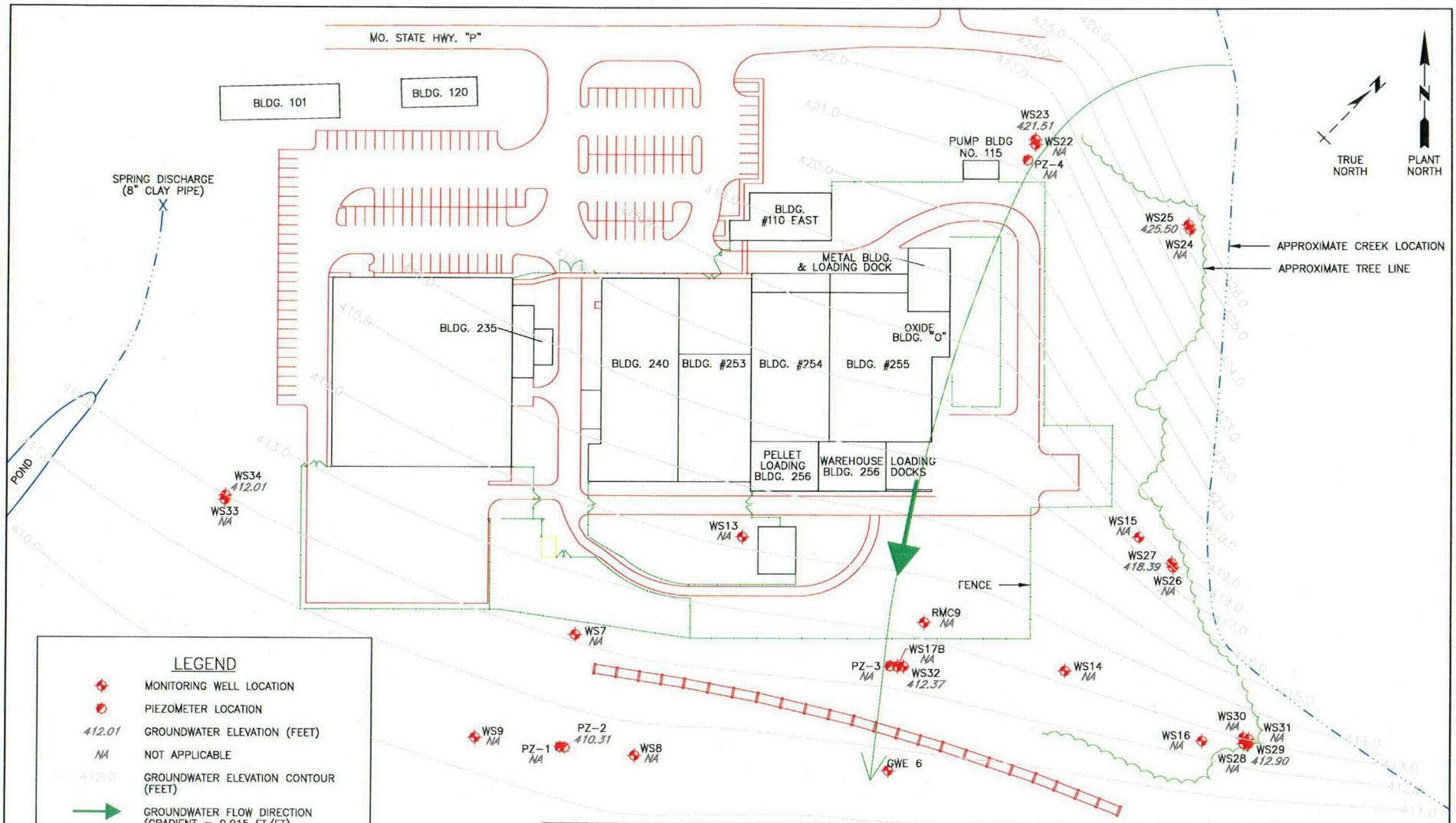

SOURCE: FOURTH SAMPLING EVENT REPORT IN CONJUNCTION WITH THE HYDROGEOLOGIC AND GROUNDWATER, SOIL AND STREAM CHARACTERIZATION, LBG, NOVEMBER 1999

DATE	REVISED

Prepared By:
LEGGETTE, BRASHEARS & GRAHAM, INC.
Professional Ground-Water and Environmental Services
4850 Lemay Ferry Road, Suite 205
St. Louis, MO 63129
(314) 845-0535

WESTINGHOUSE ELECTRIC COMPANY
MISSOURI STATE ROUTE P
HEMATITE, MISSOURI

GROUND-WATER FLOW DIRECTION AND GRADIENT, AND LENGTH OF CONTAMINATED ZONE PARALLEL TO THE AQUIFER FLOW IN THE DSCC

FILE: RESRAO contam zone parallel to aquifer flow.dwg | DATE: AUGUST 2003 | FIGURE: 1

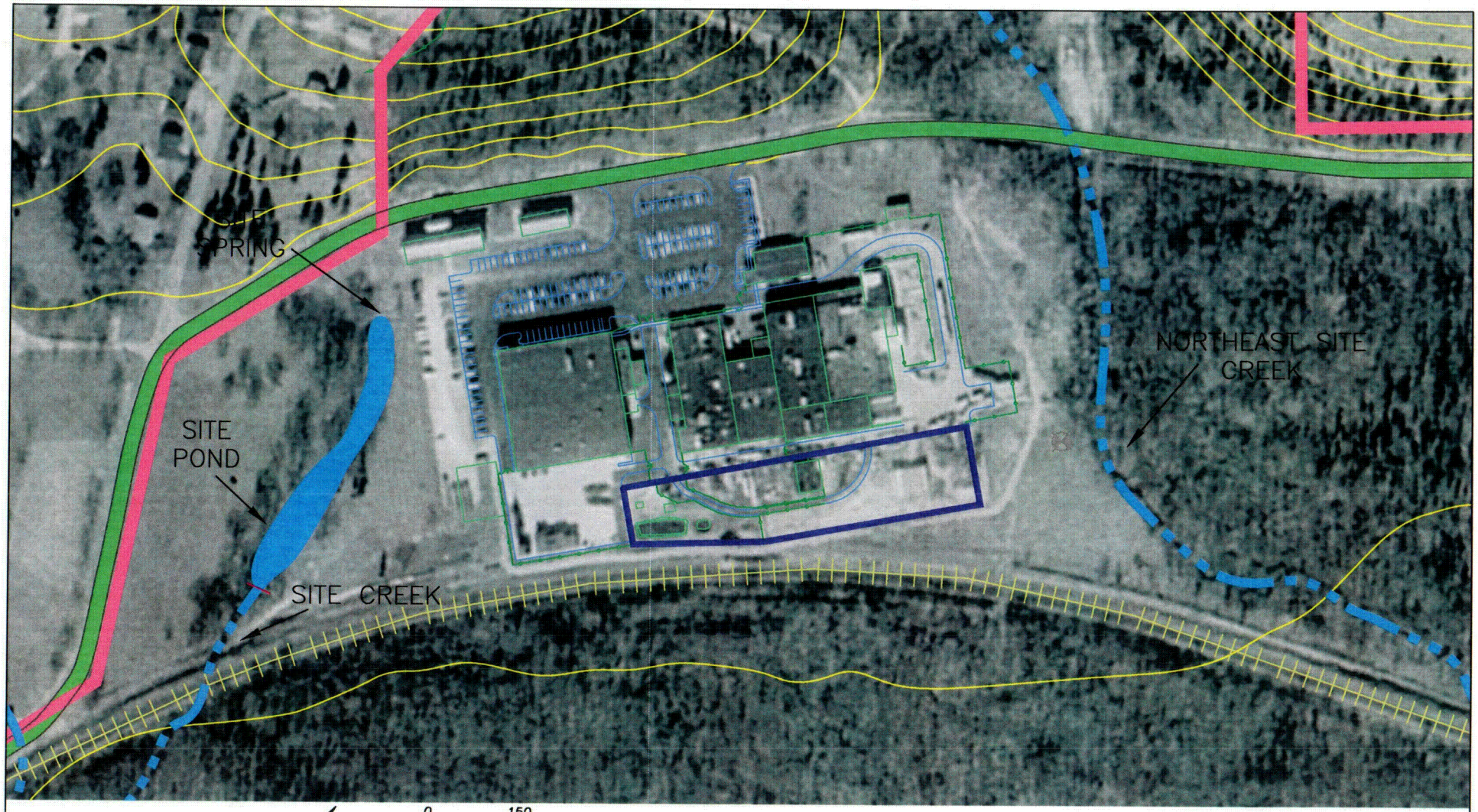

APPROXIMATE PROPERTY BOUNDARY
PERENNIAL STREAM
INTERMITTENT STREAM
10-FOOT CONTOUR LINE
FENCE LINE
AREA OF CONTAMINATED ZONE

0 150
FEET

SOURCES:
DIGITAL ORTHOPHOTO: USGS, MARCH 1996
DIGITAL ELEVATION MODEL: USGS, JANUARY, 1964
BORING LOCATIONS: BURDINE, 1998-1999
PROPERTY BOUNDARY: ZAHNER & ASSOC., MAY, 2000

DATE	REVISED

Prepared By:
LEGGETTE, BRASHEARS & GRAHAM, INC.
Professional Ground-Water and
Environmental Engineering Services
4850 Lemay Ferry Road, Suite 205
St. Louis, MO 63129
(314) 845-0535

WESTINGHOUSE ELECTRIC COMPANY
HEMATITE, MISSOURI FACILITY
HEMATITE, MISSOURI

AREA OF CONTAMINATED ZONE -- TC-99

FILE: Area of Contaminated Zone -- TC-99.dwg | DATE: AUGUST 2003 | FIGURE: 2

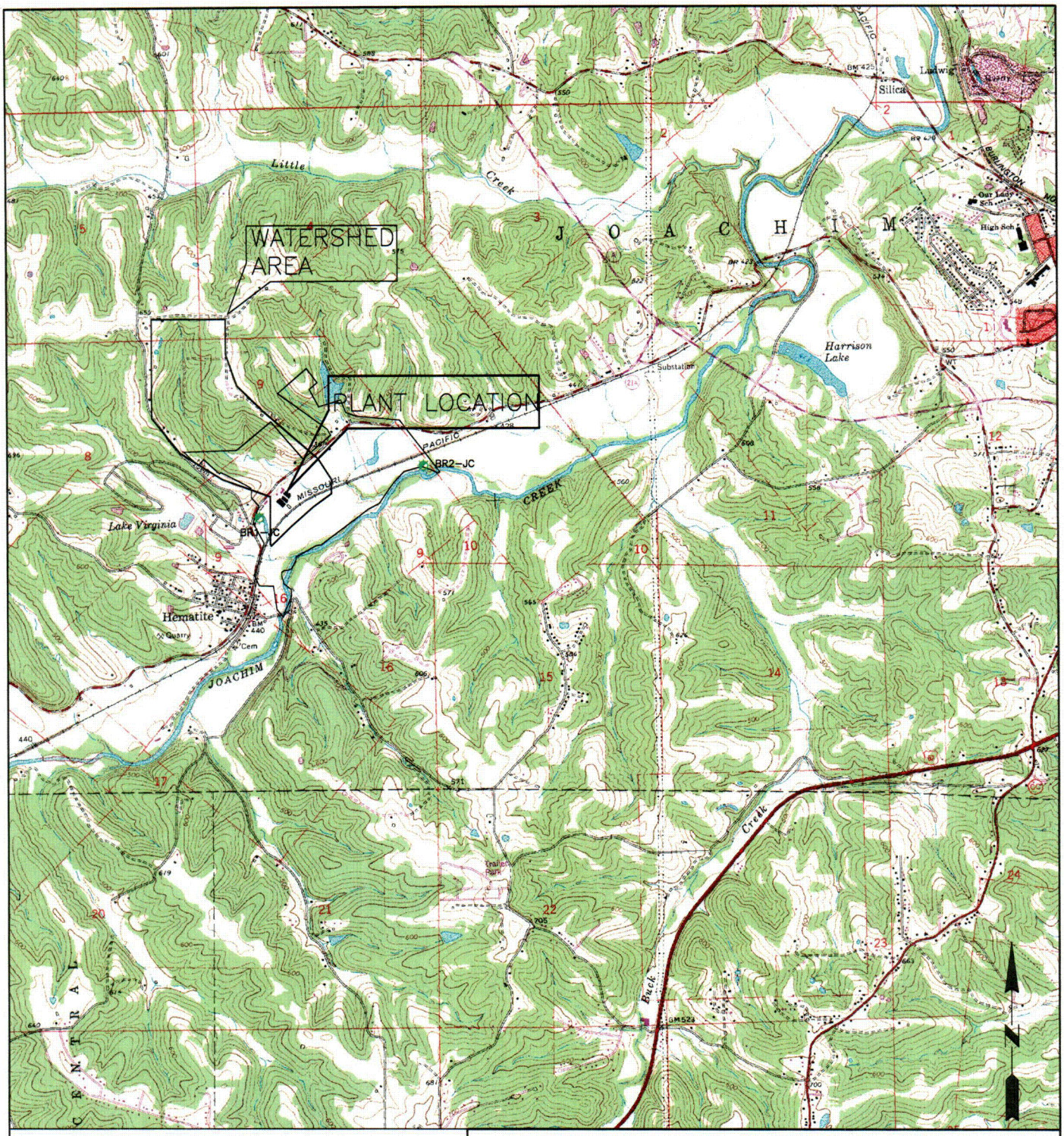

0 3281

SCALE IN FEET

SOURCE:
U.S.G.S. TOPOGRAPHIC MAP
FESTUS, MISSOURI
7.5 MINUTE QUADRANGLE

WESTINGHOUSE ELECTRIC COMPANY

HEMATITE, MISSOURI FACILITY
HEMATITE, MISSOURI

WATERSHED AREA

DATE	REVISED

Prepared By:

LEGGETTE, BRASHEARS & GRAHAM, INC.
Professional Ground-Water and
Environmental Engineering Services
4850 Lemay Ferry Road, Suite 205
St. Louis, MO 63129
(314) 845-0535

FILE:	WATERSHED AREA.dwg	DATE:	AUGUST 2003	FIGURE:	3

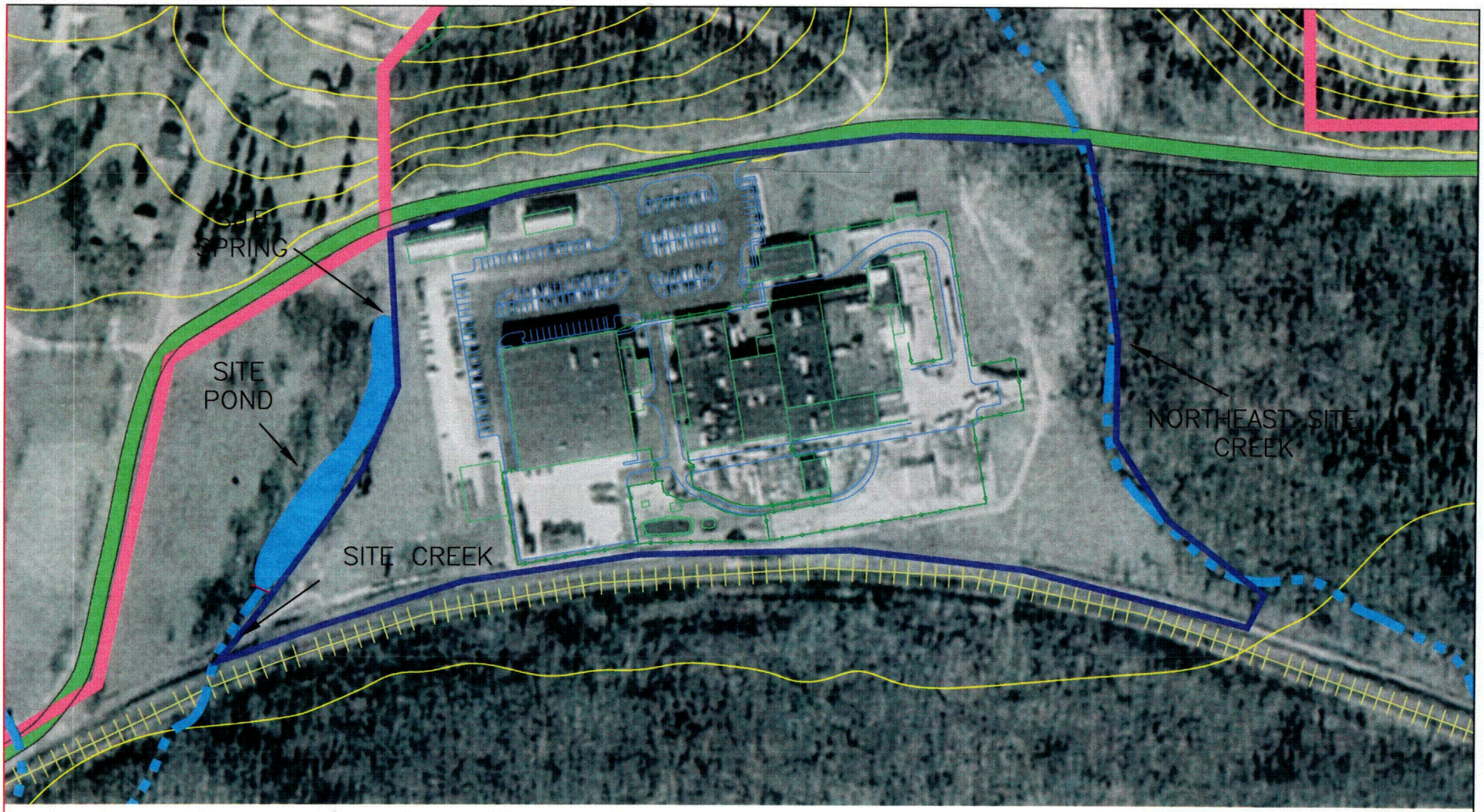

APPROXIMATE PROPERTY BOUNDARY
PERENNIAL STREAM
INTERMITTENT STREAM
10-FOOT CONTOUR LINE
FENCE LINE
AREA OF CONTAMINATED ZONE

N

0 150
FEET

SOURCES:
DIGITAL ORTHOPHOTO: USGS, MARCH 1996
DIGITAL ELEVATION MODEL: USGS, JANUARY, 1964
BORING LOCATIONS: BURDINE, 1995-1999
PROPERTY BOUNDARY: ZAHNER & ASSOC., MAY, 2000

DATE	REVISED

Prepared By:
LEGGETTE, BRASHEARS & GRAHAM, INC.
Professional Ground-Water and
Environmental Engineering Services
4850 Lemay Ferry Road, Suite 205
St. Louis, MO 63129
(314) 845-0535

WESTINGHOUSE ELECTRIC COMPANY
HEMATITE, MISSOURI FACILITY
HEMATITE, MISSOURI

AREA OF CONTAMINATED ZONE -- U-235, Ac-228, Bi-212, Pb-212, Tl-208

FILE: Area of Contaminated Zone -- U-235.dwg | DATE: AUGUST 2003 | FIGURE: 4

APPENDICES

APPENDIX A

Ground-Water Concentration Supporting Documentation

TABLE 3-3
^{99}Tc Concentration (pCi/L) in Selected Groundwater Monitoring Wells
CE COMBUSTION ENGINEERING
HEMATITE, MISSOURI

Groundwater Monitoring Well Identity	^{99}Tc Concentration (pCi/L) Aug.27, 1996
WS-14	24.9
GWE-2	260
GWE-3	142
GWE-4	1590
GWE-5	874
GWE-6	179
GWE-8	317

TABLE 7
COMBUSTION ENGINEERING
MISSOURI STATE ROUTE P
HEMATITE, MISSOURI

FILTERED GAMMA RADIOACTIVE GROUND-WATER AND STREAM SURFACE WATER ANALYTICAL DATA
USEPA METHODS 900.0 AND 901.1M
PICOCURIES PER LITER (pCi/L)

WELL	DATE	K-40 Potassium		Tl-208 Thallium		Pb-212 Lead		Bi-212 Bismuth		Bi-214 Bismuth		Pb-214 Lead		Radium-226*		Ac-228 Actinium		Th-234** Thorium		U-235 Uranium	
		CONCENTRATION	MDL	CONCENTRATION	MDL	CONCENTRATION	MDL	CONCENTRATION	MDL	CONCENTRATION	MDL	CONCENTRATION	MDL	CONCENTRATION	MDL	CONCENTRATION	MDL	CONCENTRATION	MDL	CONCENTRATION	MDL
SW-1	Nov-98	BDL	83.6	BDL	7.9	BDL	12.8			BDL	14.5	ND	ND			BDL	26.4	BDL	91.7	BDL	9.3
(Surface Water)	Feb-99	BDL	173	BDL	12.6	BDL	18.8	BDL	83.6	BDL	24.9	BDL	21.5	BDL	24.9	BDL	43.2	BDL	101.0	BDL	54
	May-99	BDL	137	BDL	11.1	BDL	21.1	BDL	66.5	BDL	19.8	BDL	16.7	BDL	152	BDL	35.3	BDL	101	BDL	9.23
	Aug-99	BDL	156	BDL	19.9	BDL	18.7	BDL	73.4	BDL	26	BDL	23.4	BDL	201	BDL	36.9	BDL	192	BDL	12.2
SW-2	Nov-98	BDL	62.8	BDL	6.3	BDL	15.6			BDL	11.6	BDL	14.3			BDL	20.8	BDL	105.0	BDL	10.0
(Surface Water)	Feb-99	BDL	92	BDL	7.0	BDL	10.1	BDL	45.7	BDL	13.4	BDL	14.7	BDL	13.4	BDL	21.3	BDL	78.5	BDL	31.9
	May-99	BDL	103	BDL	6.90	BDL	14.3	BDL	55.2	BDL	15.0	BDL	12.0	128 +/- 37.1	104	BDL	25.3	BDL	134	17.7 +/- 7.41	9.87
	Aug-99	BDL	159	BDL	10.20	22.9 +/- 3.97	12.8	BDL	59	BDL	19.2	BDL	22.7	BDL	168	BDL	29.9	BDL	120	BDL	7.10
SW-3	Nov-98	BDL	6.1	BDL	6.1	BDL	13.0			3.8 +/- 11.3	10.4	BDL	13.3			BDL	18.2	BDL	9.0	58 +/- 75	76.0
(Surface Water)	Feb-99	BDL	69	BDL	5.1	BDL	7.6	BDL	36.9	BDL	10.2	BDL	11.0	BDL	10.2	BDL	17.2	BDL	86.4	BDL	29.0
	May-99	277 +/- 44.0	98.4	BDL	13.5	25.6 +/- 10.8	21.1	23.3 +/- 118	16.4	BDL	23.4	BDL	23.2	165 +/- 25.3	142	BDL	43.5	BDL	129	BDL	12.8
	Aug-99	182 +/- 46.8	128	BDL	14.6	BDL	32.8	BDL	46.4	BDL	71.6	BDL	61	428 +/- 111	350	BDL	69.2	379 +/- 43.3	153	26.0 +/- 6.77	21.3
SW-4	Nov-98	BDL	4.6	BDL	4.0	BDL	10.2			BDL	8.0	ND	ND			BDL	14.4	8.1 +/- 5.0	7.3	104 +/- 53.6	80.4
(Surface Water)	Feb-99	BDL	124	BDL	8.9	BDL	13.4	BDL	56.7	BDL	16.2	BDL	15.1	BDL	16.2	BDL	28.9	BDL	70.2	BDL	35.0
	May-99	BDL	96.7	BDL	6.24	BDL	9.72	BDL	57.0	BDL	15.4	BDL	16.1	189 +/- 45.7	120	BDL	27.4	BDL	160	BDL	10.5
	Aug-99	130 +/- 35.1	100	BDL	7.88	16.9 +/- 4.09	16.2	BDL	61.8	BDL	37.9	13.1 +/- 2.40	12.4	BDL	163	22.4 +/- 3.57	16.1	BDL	93	BDL	9.91
SW-5	May-99	BDL	93.3	BDL	8.94	12.1 +/- 4.39	13.9	BDL	57.6	18.0 +/- 5.46	18.4	BDL	14.5	200 +/- 41.0	94.3	14.8 +/- 10.1	22.4	BDL	147	BDL	9.49
(BD of SW-3)	Aug-99	BDL	207.0	BDL	28.50	BDL	27.6	BDL	46.4	BDL	22.1	BDL	35.8	50.3 +/- 145	483.0	BDL	65.1	BDL	192	BDL	29.40
WS17B	Nov-98	NA	NA	NA	NA	NA	NA	NA	NA	NA	NA	NA	NA	NA	NA	NA	NA	NA	NA	NA	NA
(NSSSC)	Feb-99	153 +/- 18.5	50.1	8.3 +/- 0.8	4.4	BDL	10.2	BDL	42.8	22.4 +/- 3.3	10.6	12.0 +/- 3.2	10.3	18.1 +/- 3.6	12.8	23.9 +/- 5.7	19.8	BDL	73.0	BDL	31.9
	May-99	279 +/- 43.4	94.3	BDL	11.9	BDL	22.7	BDL	16.4	BDL	21.0	BDL	23.3	BDL	158	BDL	33.9	BDL	119	BDL	13.5
	Aug-99	BDL	164	BDL	15.8	BDL	29.3	BDL	81.9	59.2 +/- 6.84	25.8	72.2 +/- 7.78	24.1	BDL	403	BDL	40.5	BDL	189	BDL	24.5
WS22	Nov-98	BDL	56.3	BDL	7.1	BDL	8.9			BDL	7.9	BDL	9.9			BDL	16.1	BDL	91.0	BDL	12.2
(NSSSC)	Feb-99	85.8 +/- 22.5	85.0	BDL	5.3	11.0 +/- 1.4	80.6	BDL	41.2	9.2 +/- 2.4	7.5	7.4 +/- 2.3	7.2	BDL	10.8	BDL	17.9	180 +/- 32.9	101	BDL	30.8
	May-99	BDL	75.1	BDL	5.70	BDL	7.63	BDL	39.4	25.8 +/- 4.33	14.9	28.0 +/- 3.52	12.6	151 +/- 31.9	78.5	BDL	21.2	BDL	120	14.4 +/- 4.69	8.67
	Aug-99	BDL	160	12.3 +/- 2.72	8.19	BDL	17.4	BDL	32.4	40.9 +/- 5.85	19.8	26.8 +/- 4.03	17.1	BDL	199	30.4 +/- 7.43	26.5	BDL	88.9	BDL	12.1
WS23	Nov-98	BDL	87.1	BDL	8.7	BDL	21.0			BDL	14.2	ND	ND			BDL	28.4	8.8 +/- 10.9	17.6	36.1 +/- 105	173.0
(DSCC)	Feb-99	BDL	160	BDL	17.1	78.4 +/- 83.7	13.4	BDL	55.4	BDL	32.9	BDL	27.9	23.0 +/- 4.6	15.8	BDL	48.0	BDL	232	BDL	34.7
	May-99	BDL	120	BDL	6.92	27.9 +/- 3.34	18.2	1.49 +/- 66.4	8.22	43.6 +/- 5.82	18.8	36.1 +/- 5.26	21.7	BDL	232	BDL	32.1	BDL	91.6	BDL	16.8
	Aug-99	BDL	266	BDL	18.3	36.5 +/- 4.77	31.2	BDL	30.2	44.1 +/- 11.9	41.5	BDL	37.4	BDL	453	BDL	64.4	199 +/- 48.2	186	BDL	27.5
WS24	Nov-98	BDL	52.6	BDL	6.0	8.3 +/- 12.0	12.2			2.6 +/- 12.0	12.4	4.4 +/- 12.0	12.7			BDL	21.6	3.9 +/- 9.4	12.2	22.3 +/- 95.5	126.0
(NSSSC)	Feb-99	140 +/- 17.7	44.4	10.3 +/- 1.6	4.7	40.2 +/- 3.7	10.1	BDL	42.8	16.7 +/- 3.3	10.0	13.4 +/- 1.5	9.0	13.5 +/- 3.0	12.2	24.9 +/- 2.5	13.3	BDL	70.2	BDL	31.6
	May-99	BDL	90.8	BDL	10.0	BDL	12.9	BDL	47.7	BDL	12.3	BDL	11.6	BDL	213	BDL	23.1	BDL	118	BDL	12.0
	Aug-99	140 +/- 33.0	87.0	BDL	9.7	32.0 +/- 4.03	16.6	BDL	66.8	BDL	32.8	BDL	23.1	BDL	160	28.7 +/- 3.98	18.9	BDL	134	BDL	9.8
WS25	Nov-98	BDL	69.6	BDL	6.7	BDL	15.5			BDL	12.8	BDL	15.0			BDL	20.3	BDL	111	BDL	12.7
(DSCC)	Feb-99	58.7 +/- 17.2	50.2	2.9 +/- 1.8	5.9	5.9 +/- 2.2	75.7	BDL	39.5	8.6 +/- 2.8	8.8	5.0 +/- 1.2	6.4	BDL	10.4	10.8 +/- 3.5	13.8	179.0 +/- 33.1	94.5	BDL	29.2
	May-99	BDL	157	BDL	10.1	BDL	24.2	BDL +/- 69.0	16.4	69.9 +/- 25.3	25.5	BDL	29.3	BDL	177	BDL	38.5	BDL	102	BDL	14.3
	Aug-99	BDL	172	BDL	10.8	BDL	28.8	BDL	75	BDL	30.0	BDL	22.9	BDL	241	BDL	34.7	BDL	200	BDL	14.7
WS26	Nov-98	Dry	Dry	Dry	Dry	Dry	Dry			Dry	Dry	Dry	Dry			Dry	Dry	Dry	Dry	Dry	Dry
	Feb-99	174.0 +/- 26.7	61.6	9.0 +/- 1.8	5.3	BDL	97.7	BDL	45.4	11.2 +/- 2.9	9.9	1.1 +/- 4.8	16.0	14.7 +/- 3.0	11.7	23.6 +/- 3.6	13.3	BDL	84.1	BDL	31.2
	May-99	BDL	145	BDL	9.45	BDL	21.9	BDL	16.4	14.9 +/- 16.3	21.0	BDL	22.1	BDL	197	BDL	39.3	BDL	131	BDL	15.2
	Aug-99	BDL	286	BDL	15.0	BDL	31.5	BDL	30.2	BDL	29.4	BDL	36.9	BDL	501	BDL	36.2	BDL	191	BDL	30.5
WS27	Nov-98	BDL	44.7	BDL	3.6	BDL	12.8			BDL	7.3	ND	ND			BDL	14.3	6.6 +/- 5.5	8.6	60.6 +/- 52.8	84.3
(DSCC)	Feb-99	84.1 +/- 17.8	46.2	BDL	5.0	BDL	76.7	BDL	37.5	BDL	12.5	BDL	12.5	BDL	10.7	BDL	17.1	238.0 +/- 24.1	71.6	BDL	29.4
	May-99	BDL	159	BDL	8.48	BDL	27.4	BDL	16.4	BDL	18.5	BDL	30.6	BDL	237	BDL	44.9	BDL	142	4.10 +/- 18.8	17.2
	Aug-99	128 +/- 32.0	89.6	9.50 +/- 1.41	6.57	BDL	20.2	BDL	166	BDL	36.1	BDL	22.5	BDL	194	41.8 +/- 6.27	18.3	BDL	125	BDL	11.8

BDL=BELOW DETECTION LIMIT
ND=NOT DETECTED
NA=NOT ANALYZED
BD=BLIND DUPLICATE
SD=SPIKE DUPLICATE INCLUDING ALPHA CONCENTRATION OF 9×10^{-6} pCi/L AND BETA CONCENTRATION OF 1×10^{-4} pCi/L
*=RADIUM 226 REPORTED VALUE HAS NOT BEEN CORRECTED FOR POSSIBLE U-235 INTERFERENCES
**=Th-234 RESULTS MAY NOT BE RELIABLE SINCE THEY WERE RUN ON A "P-TYPE" DETECTOR

LEGGETTE, BRASHEARS & GRAHAM, INC.

TABLE 7
COMBUSTION ENGINEERING
MISSOURI STATE ROUTE P
HEMATITE, MISSOURI

FILTERED GAMMA RADIOACTIVE GROUND-WATER AND STREAM SURFACE WATER ANALYTICAL DATA
USEPA METHODS 900.0 AND 901.1M
PICOCURIES PER LITER (pCi/L)

WELL	DATE	K-40 Potassium		Tl-208 Thallium		Pb-212 Lead		Bi-212 Bismuth		Bi-214 Bismuth		Pb-214 Lead		Radium-226*		Ac-228 Actinium		Th-234** Thorium		U-235 Uranium	
		CONCENTRATION	MDL	CONCENTRATION	MDL	CONCENTRATION	MDL	CONCENTRATION	MDL	CONCENTRATION	MDL	CONCENTRATION	MDL	CONCENTRATION	MDL	CONCENTRATION	MDL	CONCENTRATION	MDL	CONCENTRATION	MDL
WS28	Nov-98	BDL	65.8	BDL	6.2	BDL	13.5			BDL	10.9	BDL	9.2			BDL	20.3	BDL	110.0	BDL	11.0
(NSSSC)	Feb-99	BDL	151.0	BDL	16.4	BDL	13.1	BDL	58.1	BDL	33.3	BDL	24.9	BDL	15.7	BDL	51.4	BDL	224.0	BDL	34.9
	May-99	BDL	161	6.91 +/- 2.22	8.19	BDL	24.7	BDL +/- 22.6	16.4	BDL	19.1	BDL	27.1	BDL	234	BDL	38.7	BDL	106	BDL +/- 5.11	17.1
	Aug-99	BDL	183	BDL	12.0	BDL	13.6	BDL	16.5	26.0 +/- 6.05	18.1	BDL	17.7	BDL	262	BDL	38.2	BDL	179	BDL	15.9
WS29	Nov-98	BDL	88.1	BDL	7.7	BDL	16.8			BDL	14.8	ND				BDL	27.6	BDL	89.6	BDL	10.1
(DSCC)	Feb-99	BDL	155.0	BDL	15.7	56.4 +/- 17.3	13.1	BDL	56.4	BDL	33.3	BDL	25.5	BDL	15.9	BDL	48.0	BDL	222.0	BDL	34.8
	May-99	BDL	121	BDL	12.2	BDL	19.5	BDL	62.2	BDL	20.8	12.2 +/- 2.26	11.6	BDL	111	BDL	34.3	BDL	105	BDL	6.72
	Aug-99	BDL	129	BDL	7.33	BDL	11.1	BDL	50.0	BDL	17.5	BDL	22.4	BDL	140	BDL	22.9	BDL	107	BDL	8.53
WS30	Nov-98	BDL	100.0	BDL	8.4	BDL	9.6			BDL	16.3	BDL	13.4			BDL	30.0	BDL	99	BDL	9.8
(Bed)	Feb-99	162.0 +/- 25.9	61.5	9.4 +/- 1.0	4.1	BDL	99.5	BDL	44.0	14.2 +/- 3.3	11.5	10.2 +/- 1.6	8.0	BDL	12.1	24.1 +/- 4.4	16.2	BDL	34.1	BDL	31.4
	May-99	96.8 +/- 40.3	127	BDL	11.4	9.83 +/- 8.27	16.0	BDL	79.2	BDL	22.2	15.6 +/- 2.44	15.8	BDL	179	BDL	33.3	BDL	108	BDL	10.9
	Aug-99	BDL	178	BDL	7.33	BDL	20.9	BDL	78.1	20.0 +/- 5.48	17.6	BDL	22.3	BDL	278	BDL	22.4	BDL	238	BDL	16.9
WS31	Nov-98	BDL	59.9	BDL	6.7	BDL	14.6			BDL	12.5	BDL	15.0			BDL	20.7	BDL	96.1	BDL	11.3
(Bed)	Feb-99	65.9 +/- 16.6	46.1	BDL	3.7	BDL	75.2	BDL	38.5	BDL	12.4	BDL	9.3	BDL	10.8	BDL	14.8	185.0 +/- 34.5	92.8	BDL	30.1
	May-99	BDL	146	BDL	10.7	27.6 +/- 4.71	22.4	BDL	16.4	BDL	19.1	BDL	22.9	145 +/- 32.0	102	BDL	38.8	BDL	108	BDL	11.3
	Aug-99	150 +/- 22.2	63.8	12.5 +/- 1.32	6.57	17.2 +/- 3.74	11.7	BDL	65.9	BDL	37.2	BDL	22.6	BDL	74.8	BDL	28	BDL	105	BDL	4.54
WS32	Nov-98	BDL	107.0	ND	ND	BDL	14.7			BDL	16.3	ND				BDL	33.4	BDL	98.2	BDL	10.4
(DSCC)	Feb-99	BDL	154.0	BDL	15.6	31.8 +/- 13.6	13.1	BDL	57.1	BDL	32.6	BDL	24.0	24.6 +/- 14.9	15.4	BDL	53.3	BDL	222.0	BDL	35.0
	May-99	BDL	142	BDL	12.9	BDL	16.2	BDL	89.5	BDL	21.5	7.25 +/- 5.56	8.60	BDL	188	29.3 +/- 10.7	33.0	BDL	108	10.9 +/- 3.66	11.4
	Aug-99	BDL	78.9	BDL	9.89	BDL	14.1	BDL	80.1	BDL	48.9	BDL	34.80	BDL	208	BDL	35.1	213 +/- 42.5	137	13.4 +/- 3.97	12.6
WS33	Nov-98	BDL	68.1	BDL	6.4	BDL	14.2			BDL	12.6	BDL	17.7			BDL	20.4	BDL	97.0	BDL	10.2
(NSSSC)	Feb-99	124.0 +/- 16.5	52.0	BDL	9.3	BDL	10.1	BDL	46.7	12.8 +/- 3.7	11.7	BDL	12.1	BDL	12.3	27.9 +/- 3.3	14.3	BDL	77.5	BDL	31.6
	May-99	BDL	164	BDL	9.47	BDL	20.9	BDL	16.4	BDL	20.9	BDL	23.3	BDL	216	BDL	39.2	BDL	121	BDL	16.2
	Aug-99	BDL	202	BDL	14.4	BDL	19.4	BDL	16.5	19.0 +/- 5.67	18.2	BDL	18.5	BDL	312	BDL	36.7	BDL	156	BDL	19.0
WS34	Nov-98	BDL	99.2	ND	ND	BDL	14.1			BDL	15.3	ND				BDL	34.0	BDL	98.0	BDL	10.9
(DSCC)	Feb-99	113.0 +/- 19.1	43.5	BDL	3.5	BDL	77.2	BDL	39.1	BDL	10.6	BDL	12.5	BDL	10.6	BDL	12.0	178.0 +/- 31.7	87.3	BDL	29.5
	May-99	BDL	125	BDL	6.74	BDL	10.2	BDL	56.2	BDL	17.5	BDL	12.5	266 +/- 62.9	166	BDL	27.8	BDL	155	BDL	12.6
	Aug-99	BDL	262	BDL	22.9	BDL	32.4	BDL	21.4	BDL	43.1	BDL	43.5	BDL	417	BDL	94.2	BDL	175	BDL	25.4
WS35	May-99	BDL	108	BDL	7.57	BDL	11.0	BDL	53.2	BDL	15.2	BDL	15.2	155 +/- 47.9	139	BDL	25.9	BDL	188	BDL	11.3
(BD of WS31)	Aug-99	159 +/- 16.8	75.0	8.85 +/- 2.14	6.32	29.0 +/- 3.87	15.9	BDL	62.9	BDL	36.8	BDL	22.1	BDL	176	28.9 +/- 6.94	25.9	155 +/- 48.1	149	BDL	10.7
WS36	May-99	BDL	94.3	BDL	9.00	BDL	12.5	BDL	53.2	BDL	21.4	BDL	15.5	220 +/- 37.1	99.5	BDL	24.5	BDL	124	BDL	9.68
(Deionized Water)	Aug-99	BDL	126	BDL	7.03	BDL	11.6	BDL	51.3	BDL	13.9	42.3 +/- 4.17	12.6	BDL	346	BDL	23.7	BDL	155	BDL	21.1
WS37 SO	May-99	437 +/- 52.8	83.5	BDL	12.1	BDL	25.8	20.6 +/- 22.3	18.4	BDL	26.8	BDL	23.3	2390 +/- 171	262	BDL	43.1	193 +/- 29.4	129	140 +/- 9.63	18.5
	Aug-99	BDL	150	BDL	10.4	34.3 +/- 5.00	16.2	BDL	61.8	BDL	18.7	BDL	22.9	BDL	178	BDL	31.3	BDL	109	BDL	10.8
WS38	May-99	91.7 +/- 41.9	133	BDL	11.0	BDL	17.9	BDL	71.9	31.8 +/- 20.1	22.0	21.7 +/- 2.87	16.3	358 +/- 58.4	146	26.3 +/- 9.97	33.0	BDL	118	21.9 +/- 3.50	8.87
(BD of WS17B)	Aug-99	BDL	91.8	BDL	7.57	BDL	11.2	BDL	37.8	BDL	13.9	40.7 +/- 4.32	12.9	BDL	113	BDL	24.1	BDL	91.6	BDL	6.87

BDL=BELOW DETECTION LIMIT
ND=NOT DETECTED
NA=NOT ANALYZED
BD=BLIND DUPLICATE
SO=SPIKE DUPLICATE INCLUDING ALPHA CONCENTRATION OF 8×10^{-4} pCi/L AND BETA CONCENTRATION OF 1×10^{-4} pCi/L
*=RADIUM-226 REPORTED VALUE HAS NOT BEEN CORRECTED FOR POSSIBLE U-235 INTERFERENCES
**=Th-234 RESULTS MAY NOT BE RELIABLE SINCE THEY WERE RUN ON A "P-TYPE" DETECTOR

LEGGETTE, BRASHEARS & GRAHAM, INC.

APPENDIX B

Supporting Documentation for ^{99}Tc Area of Contamination Zone

detectable levels above background in the northwest corner of the burial site. RMC determined that these levels were due to sources on-site (most likely UF_6 storage area) at that time rather than buried material. RMC concluded that little or no thorium was present near the ground surface. Results of surface soil sampling revealed low level surface contamination. RMC concluded that the surface contamination may have resulted from burial activities or from past effluent (i.e., stack) releases. Results of subsurface soil sampling showed the highest U-234 activity in the Burial Pits to be approximately 400 pCi/g, and the highest U-234 level estimated for surface soil at approximately 47 pCi/g. These levels were based on an estimated U-234/U-238 activity ratio of about 10 to 1.

2.6.2 Investigation to Determine the Source of Technetium-99 in Groundwater Monitoring Wells WS-17 and WS-17B, September 1996

Gateway Environmental Associates, Inc., conducted an investigation to determine the source of Technetium-99 (^{99}Tc) in monitoring wells WS-17 and WS-17B. (Gateway, 1996a) The investigation was conducted to answer concerns expressed by the NRC regarding the source of ^{99}Tc. Gateway Environmental Associates concluded that the ^{99}Tc may have entered the ground-water system within the former ring storage area and traveled down gradient toward the monitoring wells in question. Historical ^{99}Tc and TCE waste disposal practices at the evaporation ponds, may have been a source for contamination in WS17/17B because a nearby gas pipeline may have created a connection between the evaporation ponds and WS17/17B.

^{99}Tc is a low energy beta emitting byproduct of the nuclear fission of Uranium-235 and has a half-life of 213,000 years. ^{99}Tc has appeared as a contaminant in the fuel cycle from the United States Enrichment Company (USEC) facilities. The ^{99}Tc contaminant was present in commercial UF_6 as a result of US government recycling and re-enrichment activities at the gaseous diffusion plants.

One pathway to the evaporation ponds was through the cylinder wash operations. On site UF_6 cylinder washing was performed intermittently over the operating years of the facility. UF_6 cylinder heels preferentially contain the less volatile compounds including ^{99}Tc. The wash solution removed the technetium that was subsequently

APPENDIX C

RESRAD Default Value Table

TABLE 1.3 Default Values, Lower Bounds, and Upper Bounds for RESRAD Input Parameters

Parameter	Unit	Default Value	Lower[a] Bound	Upper[a] Bound
Soil bulk density				
Cover material	g/cm³	1.5	0	100
Contaminated zone	g/cm³	1.5	0	100
Unsaturated zone	g/cm³	1.5	0	100
Saturated zone	g/cm³	1.5	0	100
Building foundation material	g/cm³	2.4	0	100
Total porosity				
Cover material	-	.4	0	1
Contaminated zone	-	.4	0	1
Unsaturated zone	-	.4	0	
Saturated zone	-	.4	0	1
Building foundation material	-	.1	0	1
Effective porosity				
Contaminated zone		.2	0	
Saturated zone		.2	0	
Unsaturated zone		.2	0	
Hydraulic conductivity				
Contaminated zone	m/yr	10	0	1×10^{10}
Unsaturated zone	m/yr	10	0	1×10^{10}
Saturated zone	m/yr	100	0	1×10^{10}
Volumetric water content				
Cover material		0.05	0	
Building foundation material		0.03	0	
Effective radon diffusion coefficient				
Cover material	m²/s	2×10^{-6}	c	
Contaminated zone	m²/s	2×10^{-6}	c	1
Building foundation material	m²/s	3×10^{-7}	c	
Radon emanation coefficient (Rn-222/Rn-220)		0.25/0.15	0.01	1
Precipitation rate	m/yr		0	10
Runoff coefficient		0.2	0	
Irrigation rate	m/yr	0.2	0	10
Evapotranspiration coefficient		0.5	0	0.999
Soil-specific *b* parameter				
Contaminated zone		5.3	0	15
Unsaturated zone		5.3	0	15
Saturated zone		5.3	0	15
Erosion rate				

Cover material	m/yr	0.001	0	5
Contaminated zone	m/yr	0.001	0	5
Hydraulic gradient	-	0.02	0	10
Length of contaminated zone parallel to the aquifer flow	m	100	0	∞

TABLE 1.3 (Cont.)

Parameter	Unit	Default Value	Lower[a] Bound	Upper[a] Bound
Watershed area for nearby stream or pond	m^2	1×10^6	0	
Water table drop rate	m/yr	0.001	0	5
Well-pump intake depth	m	10	0	1,000
Radon vertical dimension of mixing	m	2	0	1,000
Average annual wind speed	m/s	2	0	100
Average building air exchange rate	1/h	0.5	0	1,000
Building room height	m	2.5	0	100
Building indoor area factor		0	0	100
Thickness of uncontaminated unsaturated zone	m	4	0	10,000
Building foundation thickness	m	0.15	0	10
Foundation depth below ground surface	m	1	0	100
Fraction of time spent indoors on-site		0.5	0	1
Fraction of time spent outdoors on-site		0.25	0	1
Area of contaminated zone	m^2	10,000	0	∞
Cover depth	m	0	0	100
Distribution coefficients	cm^3/g	d	0	1×10^{10}
Fractions of annular areas within contaminated area		0	0	1
Radionuclide concentration in groundwater	pCi/L	0	0	1×10^{20}
Leach rate	1/yr	0	0	1×10^{10}
Livestock fodder intake				
Meat	kg/d	68	0	300
Milk	kg/d	55	0	300
Mass loading for inhalation	g/m^3	2×10^{-4}	0	2
Milk consumption rate	L/yr	92	0	1,000

Shielding factor for inhalation		0.4	0	1
Depth of roots		0.9		100
Soil ingestion rate	g/yr	36.5		10,000

TABLE 1.3 (Cont.)

Parameter	Unit	Default Value	Lower[a] Bound	Upper[a] Bound
Thickness of contaminated zone	m	2	1×10^{10}	
Radiation dose limit	mrem/yr	30	0.01	
Dilution length for airborne dust	m	3	0	
Seafood consumption rate				
Fish	kg/yr	5.4	0	1,000
Other seafood	kg/yr	0.9	0	100
Fruit, vegetable, and grain consumption rates	kg/yr	160	0	
Inhalation rate	m^3/yr	8,400	0	
Leafy vegetable consumption rate	kg/yr	14	0	100
Livestock water intake rate				
Meat	L/d	50	0	500
Milk	L/d	160	0	500
Meat and poultry consumption rate	kg/yr	63	0	300
Shielding factor for external gamma		0.7	0	1
Elapsed time of waste placement	yr	0	0	1,000
Shape factor, external gamma		1	0[c]	
Initial concentrations of principal radionuclide	pCi/g	d	0	1×10^{20}
Drinking water intake rate	L/yr	510	0	1,000
Fraction of drinking water from site		1	0	1
Fraction of aquatic food from site		0.5	0	
Mass loading for foliar deposition	g/m^3	1×10^{-4}	0	1
Depth of soil mixing layer	m	0.15	0	1
Fraction from groundwater				
Drinking water	-	1	0	1
Livestock water	-	1	0	1
Irrigation water	-	1	0	1

[a] The lower and upper bound values represent the lower and upper limit of an input parameter that can be used in RESRAD. For some secondary (derived) parameters (e.g., leach rate), the upper and lower bounds are derived from other primary (basic) parameters

(e.g., thickness of contaminated zone).

A hyphen indicates that the parameter is dimensionless.

A negative value for this parameter serves as a flag in RESRAD. See the section in the handbook on the particular parameter for details.

The default value is radionuclide dependent.

2 SOIL DENSITY

2.1 DEFINITION

Density, as applied to any kind of homogeneous monophasic material of mass M and volume V, is expressed as the ratio of M to V. Under specified conditions, this definition leads to unique values that represent a well-defined property of the material. For heterogeneous and multiphasic materials, however, such as porous media, application of this definition can lead to different results, depending on the exact way the mass and volume of the system are defined.

Soil is a typical heterogeneous multiphasic porous system which, in its general form, contains three natural phases: (1) the solid phase or the soil matrix (formed by mineral particles and solid organic materials); (2) the liquid phase, which is often represented by water and which could more properly be called the soil solution; and (3) the gaseous phase, which contains air and other gases. In this three-phase soil system, the concept of average density can be used to define the following densities: (1) density of solids or soil particle density, ρ_s; (2) bulk or dry density, ρ_b; and (3) total or wet density, ρ_t.

The masses and volumes associated with the three soil phases must be defined before the definitions of the different densities that characterize the soil system can be formalized. Thus, consider a representative elementary volume (REV) of soil that satisfies the following criteria (Bear 1972; Marsily 1986):

1. A sufficiently large volume of soil containing a large number of pores, such that the concept of mean global properties is applicable, and

2. A sufficiently small volume of soil so that the variation of any parameter of the soil from one part of the domain to another can be approximated by continuous functions.

Within a REV, the masses of the phases composing the soil can be defined as follows:

M_s = the mass of solids,

M_l = the mass of liquids,

M_g = the mass of gases (negligible compared with the masses of the solid and liquid phases), and

M_t = $M_s + M_l$ = the total mass.

APPENDIX D

Total Porosity, Dry Density and Hydraulic Conductivity Calculations and Supporting Documentation

TOTAL POROSITY **CALCULATIONS**

Shannon and Wilson Data	
MW or Piez	**Total Porosity**
PZ2	0.467
WS22	0.447
WS23	0.452
WS24	0.41
WS25	0.418
WS26	0.476
WS27	0.461
WS28	0.464
WS29	0.483
WS32	0.41
WS32	0.482
WS33	0.415
WS34	0.408

Shannon and Wilson Data from Appendix B of "Hydrogeologic Investigation and Ground-Water, Soil and Stream Characterization," prepared by LBG in March 1999.

DRY DENSITY CALCULATIONS

TABLE 10/Fitch Data		Shannon and Wilson Data		
MW or Piez	Density g/cm3	MW or Piez	Density pcf	Density g/cm3
PZ2	2.05	PZ2	90.1	1.44
PZ2	1.71	WS22	96.3	1.54
WS23	1.85	WS23	90.6	1.45
WS23	1.74	WS24	98.3	1.57
WS25	2.04	WS25	99.1	1.59
WS25	1.77	WS26	90.3	1.45
WS25	1.81	WS27	88.2	1.41
WS27	1.9	WS28	90.6	1.45
WS27	1.43	WS29	87	1.39
WS29	2.11	WS32	96.1	1.54
WS29	1.86	WS32	88.3	1.41
WS32	1.92	WS33	96.4	1.54
WS32	2.01	WS34	99.7	1.6
WS34	1.86			
WS34	1.85			
AVERAGE OF ALL DATA				1.69

Table 10/Fitch data from "Fourth Sampling Event Report in Conjuction with the Hydrogeologic Investigation and Ground-Water, Soil and Stream Characterization," prepared by LBG in November 1999.

Shannon and Wilson Data from Appendix B of "Hydrogeologic Investigation and Ground-Water, Soil and Stream Characterization," prepared by LBG in March 1999.

HYDRAULIC CONDUCTIVITY CALCULATIONS

HORIZONTAL HYDRAULIC CONDUCTIVITY TABLE 2/LBG DATA		
MW or Piez	K (cm/sec)	K (m/yr)
WS-22	2.63E-04	8.29E+01
WS-24	6.94E-05	2.19E+01
WS-28	4.95E-05	1.56E+01
WS-33	2.05E-04	6.46E+01
PZ-1	6.62E-05	2.09E+01
WS-23	6.76E-04	2.13E+02
WS-25	3.26E-04	1.03E+02
WS-27	6.13E-04	1.93E+02
WS-29	8.27E-04	2.61E+02
WS-32	2.70E-03	8.51E+02
WS-34	3.84E-04	1.21E+02
PZ-2	2.76E-04	8.70E+01
AVERAGE		169.58

VERTICAL HYDRAULIC CONDUCTIVITY Shannon and Wilson Data			
MW or Piez	K (cm/sec)	Avg K (cm/sec)	K (m/yr)
PZ-2	3.60E-07	3.67E-07	1.16E-01
	3.60E-07		
	3.80E-07		
WS-22	4.50E-09	4.37E-09	1.38E-03
	4.40E-09		
	4.20E-09		
WS-23	2.90E-05	2.77E-05	8.72E+00
	2.60E-05		
	2.80E-05		
WS-24	2.40E-06	2.50E-06	7.88E-01
	2.40E-06		
	2.70E-06		
WS-25	4.90E-08	4.97E-08	1.57E-02
	4.80E-08		
	5.20E-08		
WS-26	5.30E-06	5.23E-06	1.65E+00
	5.20E-06		
	5.20E-06		
WS-27	4.60E-04	4.60E-04	1.45E+02
	4.70E-04		
	4.50E-04		
WS-28	6.50E-05	6.47E-05	2.04E+01
	6.30E-05		
	6.60E-05		
WS-29	1.80E-07	1.90E-07	5.99E-02
	2.00E-07		
	1.90E-07		
WS-32	1.90E-05	1.93E-05	6.10E+00
	2.00E-05		
	1.90E-05		
WS-32	2.00E-05	2.03E-05	6.41E+00
	2.00E-05		
	2.10E-05		
WS-33	1.70E-08	1.83E-08	5.78E-03
	2.00E-08		
	1.80E-08		
WS-34	1.70E-08	1.83E-08	5.78E-03
	1.90E-08		
	1.90E-08		
AVERAGE			14.56

Table 2/LBG data from "*Hydrogeologic Investigation and Ground-Water, Soil and Stream Characterization*" prepared by LBG in March 1999.

Shannon and Wilson Data from Appendix B of "*Hydrogeologic Investigation and Ground-Water, Soil and Stream Characterization*," prepared by LBG in March 1999. The permeability (K) for each sample was derived by averaging the last three readings from the test (verbal communication with Chris Groves - Vice-President, Shannon & Wilson, August 13, 2003). Vertical permeability (K) determined according to ASTM 5084-90.

TRIAXIAL PERMEABILITY DATA SHEET

SHANNON & WILSON, INC.

ject Combustion Engineering Test. by KDM-10/19/98

Job No. E-1039-01 Boring PZ-2 Sample 25.0-27.0 Checked by KWH - 12/7/98

Description Dark grey fat CLAY, with some Fe stains, occa f & c gravels, rare sm roots

Depth Permeant tap water Test Method ASTM 5084-90

Permeameter No. 8 Standpipe Vol (cc/cm) Inflow: 1.297 Outflow: 1.294

	Before Test	After Test		Before Test	After Test
Sample Diameter (in)	2.869	2.875	Tare No.	K1	82
Sample Length (in)	2.752	2.762	Tare Wt. (g)	2.63	83.62
Sample Area (cm^2)	41.71	41.88	Wet Soil + Tare (g)	98.32	633.61
Sample Volume (CC)	291.54	293.83	Dry Soil + Tare (g)	75.87	501.19
Sample Wt. (g)	549.92	549.99	Water Content (%)	30.7	31.7
Wet Density (pcf)	117.7	116.8	Porosity	0.467	
Dry Density (pcf)	90.1	88.7	Pore Volume (CC)	136.23	

Effective Consolidation (psi) 5 min 6 max

Degree of Saturation 95

Specific Gravity 2.71

Read Time Y hr min	Pcell psi	Pin psi	Pout psi	Readings (cm) hin	hout	Inflow PV	Outflow PV	Storage PV	Total PV	i	K cm/s
1 9 42	50	45	44	64.20	64.20	—	—	—	—	10.1	—
1 11 4	50	45	44	63.55	64.85	-0.01	0.01	0.00	0.01	9.9	4.1E-07
1 12 34	50	45	44	62.80	65.45	-0.01	0.01	0.00	0.01	9.7	4.0E-07
1 13 23	50	45	44	62.45	65.80	0.00	0.00	0.00	0.02	9.6	3.8E-07
1 15 11	50	45	44	61.65	66.50	-0.01	0.01	0.00	0.02	9.4	3.8E-07
1 16 24	50	45	44	61.15	67.00	0.00	0.00	0.00	0.03	9.2	3.8E-07
1 16 43	50	45	44	61.00	67.10	0.00	0.00	0.00	0.03	9.2	3.7E-07
2 9 55	50	45	44	60.80	67.00					9.2	
2 12 34	50	45	44	59.70	68.05	-0.01	0.01	0.00	0.04	8.9	3.9E-07
2 13 57	50	45	44	59.20	68.55	0.00	0.00	0.00	0.04	8.7	3.5E-07
2 16 35	50	45	44	58.20	69.55	-0.01	0.01	0.00	0.05	8.4	3.8E-07
2 18 27	50	45	44	57.55	70.10	-0.01	0.01	0.00	0.06	8.3	3.3E-07
3 8 13	50	45	44	53.05	74.40	-0.04	0.04	0.00	0.10	7.0	3.6E-07
3 9 37	50	45	44	52.60	74.75	0.00	0.00	0.00	0.10	6.9	3.5E-07
3 11 1	50	45	44	52.20	75.15	0.00	0.00	0.00	0.10	6.8	3.6E-07
3 14 25	50	45	44	51.25	76.10	-0.01	0.01	0.00	0.11	6.5	3.6E-07
3 17 53	50	45	44	50.15	76.95	-0.01	0.01	0.00	0.12	6.2	3.8E-07

TRIAXIAL PERMEABILITY DATA SHEET

SHANNON & WILSON, INC.

ect Combustion Engineering — Test. by KDM-10/29/98

Job No. E-1039-01 — Boring WS-22 — Sample 16.0-18.0 — Checked by [illegible] - 12/7/98

Description Brown & grey fat CLAY, with some Fe stains, some sm Fe nodules, occa decomposed roots

Depth — Permeant tap water — Test Method ASTM 5084-90

Permeameter No. 16 — Standpipe Vol (cc/cm) Inflow: 1.312 Outflow: 1.308

	Before Test	After Test		Before Test	After Test
Sample Diameter (in)	2.850	2.886	Tare No.	K2	109
Sample Length (in)	2.316	2.349	Tare Wt. (g)	2.63	84.34
Sample Area (cm^2)	41.16	42.20	Wet Soil + Tare (g)	79.99	570.13
Sample Volume (CC)	242.11	251.81	Dry Soil + Tare (g)	62.91	459.02
Sample Wt. (g)	479.39	485.79	Water Content (%)	28.3	29.7
Wet Density (pcf)	123.6	120.4	Porosity	0.447	
Dry Density (pcf)	96.3	92.8	Pore Volume (CC)	108.23	
Effective Consolidation (psi)	5 min	6 max	Degree of Saturation	95	
			Specific Gravity	2.79	

Read Time			Pcell	Pin	Pout	Readings (cm)		Inflow	Outflow	Storage	Total	i	K
	hr	min	psi	psi	psi	hin	hout	PV	PV	PV	PV		cm/s
1	12	55	50	45	44	64.40	65.40	—	—	—	—	11.8	—
2	8	13	50	45	44	64.00	65.50	0.00	0.00	0.00	0.00	11.7	9.8E-09
2	15	3	50	45	44	63.95	65.55		0.00	0.00	0.00	11.7	5.5E-09
2	15	4	50	45	43	63.95	65.55					23.6	
3	9	43	50	45	43	63.55	65.80	0.00	0.00	0.00	0.00	23.5	6.5E-09
4	8	31	50	45	43	63.10	66.00	-0.01	0.00	0.00	0.01	23.4	5.4E-09
5	8	13	50	45	43	62.70	66.20	0.00	0.00	0.00	0.01	23.3	4.8E-09
5	17	56	50	45	43	62.60	66.30	0.00	0.00	0.00	0.01	23.3	3.9E-09
6	12	6	50	45	43	62.30	66.40	0.00	0.00	0.00	0.01	23.2	4.2E-09
6	12	7	50	45	43	60.70	60.05					24.0	
9	8	45	50	45	43	59.95	60.65	-0.01	0.01	0.00	0.02	23.8	3.6E-09
10	8	30	50	45	43	59.60	60.80	0.00	0.00	0.00	0.02	23.7	3.9E-09
11	8	15	50	45	43	59.30	61.00	0.00	0.00	0.00	0.02	23.6	3.9E-09
12	17	40	50	45	43	58.90	61.35	0.00	0.00	0.00	0.03	23.5	4.2E-09
13	16	45	50	45	43	58.60	61.60	0.00	0.00	0.00	0.03	23.4	4.5E-09
14	10	6	50	45	43	58.35	61.75	0.00	0.00	0.00	0.03	23.3	4.4E-09
1	9	59	50	45	43	57.30	62.30	-0.01	0.01	0.00	0.04	23.1	4.2E-09

TRIAXIAL PERMEABILITY DATA SHEET

SHANNON & WILSON, INC.

ject Combustion Engineering — Test. by KDM-10/28/98

Job No. E-1039-01 — Boring WS-23 — Sample 26.5-28.5 — Checked by KWB - 12/7/98

Description Dark grey fat CLAY, with occa sm roots & root holes, some worm burrows, sl blocky

Depth — Permeant tap water — Test Method ASTM 5084-90

Permeameter No. 7 — Standpipe Vol (cc/cm) Inflow: 1.304 Outflow: 1.288

	Before Test	After Test		Before Test	After Test
Sample Diameter (in)	2.872	2.870	Tare No.	K3	78
Sample Length (in)	2.508	2.510	Tare Wt. (g)	2.63	83.16
Sample Area (cm^2)	41.80	41.74	Wet Soil + Tare (g)	94.29	589.43
Sample Volume (CC)	266.25	266.09	Dry Soil + Tare (g)	73.14	469.60
Sample Wt. (g)	502.58	506.27	Water Content (%)	30.0	31.0
Wet Density (pcf)	117.8	118.7	Porosity	0.452	
Dry Density (pcf)	90.6	90.6	Pore Volume (CC)	120.36	
Effective Consolidation (psi)	5 min	6 max	Degree of Saturation	100	
			Specific Gravity	2.65	

Read Time y hr min	Pcell psi	Pin psi	Pout psi	Readings (cm) hin	hout	Inflow PV	Outflow PV	Storage PV	Total PV	i	K cm/s
1 15	50	45	44	61.85	63.10	—	—	—	—	10.8	—
1 15 1	50	45	44	61.20	63.90	-0.01	0.01	0.00	0.01	10.6	3.5E-05
1 15 2	50	45	44	60.60	64.45	-0.01	0.01	0.00	0.01	10.4	2.8E-05
1 15 3	50	45	44	60.10	64.95	-0.01	0.01	0.00	0.02	10.3	2.5E-05
1 15 4	50	45	44	59.70	65.35	0.00	0.00	0.00	0.02	10.2	2.0E-05
1 15 6	50	45	44	59.00	66.00	-0.01	0.01	0.00	0.03	9.9	1.7E-05
1 15 8	50	45	44	58.35	66.65	-0.01	0.01	0.00	0.04	9.7	1.7E-05
1 15 10	50	45	44	57.75	67.25	-0.01	0.01	0.00	0.04	9.5	1.6E-05
3 8	50	45	44	57.45	65.85					9.7	
3 8 1	50	45	44	56.20	67.20	-0.01	0.01	0.00	0.06	9.3	7.1E-05
3 8 2	50	45	44	55.25	68.15	-0.01	0.01	0.00	0.07	9.0	5.4E-05
3 8 3	50	45	44	54.40	69.00	-0.01	0.01	0.00	0.08	8.7	4.9E-05
3 8 4	50	45	44	53.60	69.80	-0.01	0.01	0.00	0.09	8.5	4.8E-05
3 8 6	50	45	44	52.35	71.05	-0.01	0.01	0.00	0.10	8.1	3.9E-05
3 8 9	50	45	44	50.65	72.75	-0.02	0.02	0.00	0.12	7.6	3.7E-05
3 8 11	50	45	44	49.75	73.65	-0.01	0.01	0.00	0.13	7.3	3.1E-05
3 8 13	50	45	44	48.95	74.45	-0.01	0.01	0.00	0.14	7.0	2.9E-05

TRIAXIAL PERMEABILITY DATA SHEET

SHANNON & WILSON, INC.

ect Combustion Engineering Test. by KDM-10/28/98

Job No. E-1039-01 Boring WS-23 Sample 26.5-28.5 Checked by KWH 12/7/98

Description Dark grey fat CLAY, with occa sm roots & root holes, some worm burrows, sl blocky

Depth Permeant tap water Test Method ASTM 5084-90

Permeameter No. 7 Standpipe Vol (cc/cm) Inflow: 1.304 Outflow: 1.288

3 8 15	50	45	44	48.15	75.25	-0.01	0.01	0.00	0.15	6.8	3.0E-05
3 8 17	50	45	44	47.45	75.95	-0.01	0.01	0.00	0.15	6.6	2.7E-05
3 8 19	50	45	44	46.80	76.60	-0.01	0.01	0.00	0.16	6.4	2.6E-05
3 8 21	50	45	44	46.20	77.20	-0.01	0.01	0.00	0.17	6.2	2.5E-05
6 9 2	50	45	44	44.50	61.60					8.4	
6 9 4	50	45	44	43.55	62.55	-0.01	0.01	0.00	0.18	8.1	3.0E-05
6 9 6	50	45	44	42.70	63.40	-0.01	0.01	0.00	0.19	7.8	2.8E-05
6 9 7	50	45	44	54.80	63.80					9.6	
6 9 16	50	45	44	50.30	68.30	-0.05	0.05	0.00	0.23	8.2	2.9E-05
6 9 17	50	45	44	50.30	62.00					9.2	
6 9 22	50	45	44	47.80	64.40	-0.03	0.03	0.00	0.26	8.4	2.9E-05
9 25	50	45	44	46.60	65.65	-0.01	0.01	0.00	0.27	8.1	2.6E-05
6 9 28	50	45	44	45.30	66.90	-0.01	0.01	0.00	0.29	7.6	2.8E-05

TRIAXIAL PERMEABILITY DATA SHEET

SHANNON & WILSON, INC.

ject Combustion Engineering — Test. by KDM-10/15/98

Job No. E-1039-01 — Boring WS-24 — Sample 16.0-18.0 — Checked by CWH -12/7/98

Description Brown lean CLAY, with numerous Fe stains, some sm Fe nodules, occa sm roots, sl blocky

Depth — Permeant tap water — Test Method ASTM 5084-90

Permeameter No. 17 — Standpipe Vol (cc/cm) Inflow: 1.298 Outflow: 1.293

	Before Test	After Test		Before Test	After Test
Sample Diameter (in)	2.871	2.859	Tare No.	K4	96
Sample Length (in)	2.212	2.224	Tare Wt. (g)	2.63	83.29
Sample Area (cm^2)	41.77	41.42	Wet Soil + Tare (g)	88.57	546.78
Sample Volume (CC)	234.66	233.97	Dry Soil + Tare (g)	70.80	452.15
Sample Wt. (g)	465.96	463.49	Water Content (%)	26.1	25.7
Wet Density (pcf)	123.9	123.6	Porosity	0.410	
Dry Density (pcf)	98.3	98.4	Pore Volume (CC)	96.23	

Effective Consolidation (psi) 5 min — 6 max

Degree of Saturation 99

Specific Gravity 2.67

Read Time y hr min	Pcell psi	Pin psi	Pout psi	Readings (cm) hin	hout	Inflow PV	Outflow PV	Storage PV	Total PV	i	K cm/s
1 12	50	45	44	64.80	66.20	—	—	—	—	12.3	—
1 12 15	50	45	44	63.80	67.20	-0.01	0.01	0.00	0.01	11.9	2.9E-06
1 12 41	50	45	44	62.40	68.60	-0.02	0.02	0.00	0.03	11.4	2.4E-06
1 13 3	50	45	44	61.25	69.75	-0.02	0.02	0.00	0.05	11.0	2.4E-06
1 13 19	50	45	44	60.50	70.50	-0.01	0.01	0.00	0.06	10.7	2.2E-06
1 13 51	50	45	44	59.00	72.00	-0.02	0.02	0.00	0.08	10.2	2.3E-06
1 14 12	50	45	44	58.10	72.90	-0.01	0.01	0.00	0.09	9.9	2.2E-06
1 14 40	50	45	44	56.90	74.05	-0.02	0.02	0.00	0.11	9.5	2.2E-06
1 15 15	50	45	44	55.50	75.50	-0.02	0.02	0.00	0.12	9.0	2.3E-06
1 15 34	50	45	44	54.75	76.25	-0.01	0.01	0.00	0.14	8.7	2.3E-06
1 15 46	50	45	44	54.30	76.70	-0.01	0.01	0.00	0.14	8.5	2.3E-06
1 16 5	50	45	44	53.60	77.40	-0.01	0.01	0.00	0.15	8.3	2.3E-06
1 16 28	50	45	44	52.80	78.20	-0.01	0.01	0.00	0.16	8.0	2.2E-06
1 17 6	50	45	44	51.40	79.60	-0.02	0.02	0.00	0.18	7.5	2.5E-06
3 8 34	50	45	44	50.85	79.40					7.4	
3 8 55	50	45	44	50.20	80.20	-0.01	0.01	0.00	0.19	7.2	2.4E-06
3 9 17	50	45	44	49.45	80.90	-0.01	0.01	0.00	0.20	6.9	2.4E-06

TRIAXIAL PERMEABILITY DATA SHEET

SHANNON & WILSON, INC.

ect Combustion Engineering Test. by KDM-10/15/98

Job No. E-1039-01 Boring WS-24 Sample 16.0-18.0 Checked by KWH - 12/7/98

Description Brown lean CLAY, with numerous Fe stains, some sm Fe nodules, occa sm roots, sl blocky

Depth Permeant tap water Test Method ASTM 5084-90

Permeameter No. 17 Standpipe Vol (cc/cm) Inflow: 1.298 Outflow: 1.293

3 11 45	50	45	44	45.30	85.05	-0.06	0.06	0.00	0.26	5.4	2.4E-06
3 13 55	50	45	44	42.05	88.30	-0.04	0.04	0.00	0.30	4.3	2.7E-06

TRIAXIAL PERMEABILITY DATA SHEET

SHANNON & WILSON, INC.

ject Combustion Engineering Test. by KMH/KDM-11/2/98

Job No. E-1039-01 Boring WS-25 Sample 30.0-31.5 Checked by KMH-12/7/98

Description Dark grey fat CLAY, with some c sands, occa f gravels, rare sm roots

Depth _____ Permeant tap water Test Method ASTM 5084-90

Permeameter No. 8 Standpipe Vol (cc/cm) Inflow: 1.297 Outflow: 1.294

	Before Test	After Test		Before Test	After Test
Sample Diameter (in)	2.880	2.884	Tare No.	AB1	95
Sample Length (in)	2.366	2.365	Tare Wt. (g)	2.63	84.26
Sample Area (cm^2)	42.03	42.15	Wet Soil + Tare (g)	67.67	587.10
Sample Volume (CC)	252.58	253.17	Dry Soil + Tare (g)	54.65	485.10
Sample Wt. (g)	501.38	502.84	Water Content (%)	25.0	25.4
Wet Density (pcf)	123.9	123.9	Porosity	0.418	
Dry Density (pcf)	99.1	98.8	Pore Volume (CC)	105.68	

Effective Consolidation (psi) 5 min 6 max

Degree of Saturation 96

Specific Gravity 2.73

Read Time y hr min	Pcell psi	Pin psi	Pout psi	Readings (cm) hin	hout	Inflow PV	Outflow PV	Storage PV	Total PV	i	K cm/s
1 8 13	50	45	44	68.85	71.30	—	—	—	—	11.3	—
1 17 40	50	45	44	68.15	71.90	-0.01	0.01	0.00	0.01	11.1	5.3E-08
2 8 55	50	45	44	67.15	72.80	-0.01	0.01	0.00	0.02	10.8	4.9E-08
2 16 44	50	45	44	66.65	73.25	-0.01	0.01	0.00	0.02	10.6	4.9E-08
3 10 12	50	45	44	65.50	74.30	-0.01	0.01	0.00	0.04	10.2	5.2E-08
5 7 49	50	45	44	62.90	76.80	-0.03	0.03	0.00	0.07	9.4	4.9E-08
6 7 50	50	45	44	61.60	78.20	-0.02	0.02	0.00	0.08	8.9	5.3E-08
7 10 12	50	45	44	60.30	79.70	-0.02	0.02	0.00	0.10	8.5	5.2E-08
8 8 42	50	45	44	59.15	75.25					9.0	
8 15 21	50	45	44	58.80	75.60	0.00	0.00	0.00	0.11	8.9	5.0E-08
9 9 25	50	45	44	57.90	76.50	-0.01	0.01	0.00	0.12	8.6	4.9E-08
10 10 15	50	45	44	56.75	77.70	-0.01	0.01	0.00	0.13	8.2	4.8E-08
12 11 24	50	45	44	54.40	80.00	-0.03	0.03	0.00	0.16	7.4	5.2E-08

TRIAXIAL PERMEABILITY DATA SHEET

SHANNON & WILSON, INC.

ject Combustion Engineering — Test. by KMH-11/19/98

Job No. E-1039-01 — Boring WS-26 — Sample 13.0-15.0 — Checked by KMH - 12/7/98

Description Grey fat CLAY, with some Fe stains, some sm Fe nodules, weathered shells, slickensides

Depth — Permeant tap water — Test Method ASTM 5084-90

Permeameter No. 5 — Standpipe Vol (cc/cm) Inflow: 1.280 Outflow: 1.281

	Before Test	After Test		Before Test	After Test
Sample Diameter (in)	2.875	2.879	Tare No.	K5	100
Sample Length (in)	2.538	2.558	Tare Wt. (g)	2.63	86.14
Sample Area (cm^2)	41.88	42.00	Wet Soil + Tare (g)	83.24	604.41
Sample Volume (CC)	270.00	272.88	Dry Soil + Tare (g)	64.42	478.21
Sample Wt. (g)	509.68	518.27	Water Content (%)	30.5	32.2
Wet Density (pcf)	117.8	118.5	Porosity	0.476	
Dry Density (pcf)	90.3	89.7	Pore Volume (CC)	128.44	
			Degree of Saturation		96
Effective Consolidation (psi)	5 min	6 max	Specific Gravity	2.76	

Read Time hr	min	Pcell psi	Pin psi	Pout psi	Readings (cm) hin	hout	Inflow PV	Outflow PV	Storage PV	Total PV	i	K cm/s
1	13 25	50	45	44	63.25	66.35	—	—	—	—	10.4	—
1	13 43	50	45	44	58.05	71.45	-0.05	0.05	0.00	0.05	8.8	1.5E-05
2	9	50	45	44	58.00	58.20					10.9	
2	9 5	50	45	44	56.90	59.20	-0.01	0.01	0.00	0.06	10.6	1.0E-05
2	9 10	50	45	44	56.00	60.10	-0.01	0.01	0.00	0.07	10.3	8.8E-06
2	9 20	50	45	44	54.40	61.60	-0.02	0.01	0.00	0.08	9.8	7.9E-06
2	9 34	50	45	44	52.70	63.30	-0.02	0.02	0.00	0.10	9.3	6.5E-06
4	7 10	50	45	44	52.20	64.80					9.0	
4	7 20	50	45	44	50.85	66.15	-0.01	0.01	0.00	0.12	8.5	7.9E-06
4	7 36	50	45	44	49.15	67.85	-0.02	0.02	0.00	0.13	8.0	6.5E-06
4	7 37	50	45	44	49.00	63.00					8.7	
4	7 48	50	45	44	47.80	64.25	-0.01	0.01	0.00	0.14	8.4	6.6E-06
4	8 4	50	45	44	46.20	65.80	-0.02	0.02	0.00	0.16	7.9	6.2E-06
4	8 20	50	45	44	44.80	67.20	-0.01	0.01	0.00	0.17	7.4	5.8E-06
4	8 43	50	45	44	43.05	69.00	-0.02	0.02	0.00	0.19	6.9	5.5E-06
4	9 9	50	45	44	41.10	70.90	-0.02	0.02	0.00	0.21	6.3	5.7E-06
4	8 59	50	45	44	63.60	70.90					9.8	

TRIAXIAL PERMEABILITY DATA SHEET

SHANNON & WILSON, INC.

ject Combustion Engineering Test. by KMH-11/19/98

Job No. E-1039-01 Boring WS-26 Sample 13.0-15.0 Checked by [illegible] - 12/7/98

Description Grey fat CLAY, with some Fe stains, some sm Fe nodules, weathered shells, slickensides

Depth Permeant tap water Test Method ASTM 5084-90

Permeameter No. 5 Standpipe Vol (cc/cm) Inflow: 1.280 Outflow: 1.281

4	9	24	50	45	44	61.15	73.35	-0.02	0.02	0.00	0.24	9.0	5.3E-06
4	10	23	50	45	44	56.20	78.20	-0.05	0.05	0.00	0.28	7.5	5.1E-06
4	11	3	50	45	44	53.20	81.20	-0.03	0.03	0.00	0.31	6.6	5.4E-06
4	11	4	50	45	44	53.20	70.00					8.3	
4	11	53	50	45	44	49.30	73.90	-0.04	0.04	0.00	0.35	7.1	5.3E-06
4	12	36	50	45	44	46.40	76.80	-0.03	0.03	0.00	0.38	6.2	5.2E-06
4	13	6	50	45	44	44.60	78.60	-0.02	0.02	0.00	0.40	5.6	5.2E-06

TRIAXIAL PERMEABILITY DATA SHEET

SHANNON & WILSON, INC.

ect Combustion Engineering — Test. by KMH/KDM-11/20/98

Job No. E-1039-01 — Boring WS-27 — Sample 21.0-23.0 — Checked by [illegible] -12/7/98

Description Dark grey fat CLAY, with occa sm roots & root holes, rare Fe stains, sl blocky

Depth — Permeant tap water — Test Method ASTM 5084-90

Permeameter No. 17 — Standpipe Vol (cc/cm) Inflow: 1.298 Outflow: 1.293

UPALINE

	Before Test	After Test		Before Test	After Test
Sample Diameter (in)	2.885	2.891	Tare No.	AB2	96
Sample Length (in)	2.731	2.741	Tare Wt. (g)	2.63	83.40
Sample Area (cm^2)	42.17	42.35	Wet Soil + Tare (g)	74.00	634.27
Sample Volume (CC)	292.55	294.85	Dry Soil + Tare (g)	56.59	496.60
Sample Wt. (g)	546.80	550.87	Water Content (%)	32.3	33.3
Wet Density (pcf)	116.6	116.6	Porosity	0.461	
Dry Density (pcf)	88.2	87.4	Pore Volume (CC)	134.76	
Effective Consolidation (psi)	5 min	6 max	Degree of Saturation	100	
			Specific Gravity	2.62	

Read Time hr	min	Pcell psi	Pin psi	Pout psi	Readings (cm) hin	hout	Inflow PV	Outflow PV	Storage PV	Total PV	i	K cm/s
1	8	50	45	44	59.60	75.40	—	—	—	—	7.9	—
1	8 0.5	50	45	44	55.20	79.80	-0.04	0.04	0.00	0.04	6.6	6.2E-04
1	8 1.0	50	45	44	51.95	83.05					4.6	
1	8 1.5	50	45	44	49.25	85.75	-0.03	0.03	0.00	0.07	3.9	6.5E-04
1	8 2.0	50	45	44	47.20	87.80	-0.02	0.02	0.00	0.09	3.3	5.9E-04
1	8 2.5	50	45	44	45.35	89.70	-0.02	0.02	0.00	0.11	2.7	6.4E-04
1	8 3.0	50	45	44	43.75	91.30	-0.02	0.02	0.00	0.12	2.3	6.6E-04
1	8 3.5	50	45	44	65.60	80.00					7.0	
1	8 4.0	50	45	44	61.60	84.00	-0.04	0.04	0.00	0.16	5.9	6.3E-04
1	8 4.5	50	45	44	58.40	87.20					6.0	
1	8 5.0	50	45	44	55.80	89.80	-0.03	0.02	0.00	0.18	5.2	4.8E-04
1	8 5.5	50	45	44	53.50	92.10	-0.02	0.02	0.00	0.21	4.6	4.8E-04
1	8 6.0	50	45	44	51.60	94.00	-0.02	0.02	0.00	0.22	4.0	4.5E-04
1	8 6.5	50	45	44	50.00	95.60	-0.02	0.02	0.00	0.24	3.6	4.3E-04
1	8 7.0	50	45	44	48.60	97.00	-0.01	0.01	0.00	0.25	3.2	4.3E-04
1	8 7.5	50	45	44	47.40	98.20	-0.01	0.01	0.00	0.27	2.8	4.1E-04
2	8	50	45	44	85.30	90.80					9.3	

TRIAXIAL PERMEABILITY DATA SHEET

SHANNON & WILSON, INC.

ject Combustion Engineering Test. by KMH/KDM-11/20/98

Job No. E-1039-01 Boring WS-27 Sample 21.0-23.0 Checked by [illegible] -12/7/98

Description Dark grey fat CLAY, with occa sm roots & root holes, rare Fe stains, sl blocky

Depth Permeant tap water Test Method ASTM 5084-90

Permeameter No. 17 Standpipe Vol (cc/cm) Inflow: 1.298 Outflow: 1.293

UPALINE

2	8	0.5	50	45	44	81.10	94.90	-0.04	0.04	0.00	0.30	8.1	4.9E-04
2	8	1.0	50	45	44	77.95	98.05	-0.03	0.03	0.00	0.33	7.2	4.2E-04
2	8	2.0	50	45	44	72.35	103.60	-0.05	0.05	0.00	0.39	5.6	4.5E-04
2	8	2.5	50	45	44	72.35	87.00					8.0	
2	8	3.0	50	45	44	69.00	90.30	-0.03	0.03	0.00	0.42	7.1	4.5E-04
2	8	3.5	50	45	44	66.00	93.30	-0.03	0.03	0.00	0.45	6.2	4.6E-04
2	8	4.0	50	45	44	67.55	79.80					8.4	
2	8	4.5	50	45	44	63.85	83.40	-0.04	0.03	0.00	0.48	7.3	4.8E-04
2	8	5.0	50	45	44	60.75	86.50	-0.03	0.03	0.00	0.51	6.4	4.6E-04
2	8	5.5	50	45	44	58.00	89.25	-0.03	0.03	0.00	0.54	5.6	4.7E-04
2	8	6.0	50	45	44	60.10	76.60					7.8	
2	8	6.5	50	45	44	57.00	79.90	-0.03	0.03	0.00	0.57	6.8	4.5E-04

TRIAXIAL PERMEABILITY DATA SHEET

SHANNON & WILSON, INC.

ect Combustion Engineering — Test. by KMH/KDM-10/30/98

Iob No. E-1039-01 — Boring WS-28 — Sample 16.5-18.5 — Checked by KMH - 12/7/98

Description Dark grey lean CLAY, with some roots & root holes, some Fe stains, sl blocky

Depth — Permeant tap water — Test Method ASTM 5084-90

Permeameter No. 6 — Standpipe Vol (cc/cm) Inflow: 1.266 Outflow: 1.279

	Before Test	After Test		Before Test	After Test
Sample Diameter (in)	2.882	2.881	Tare No.	AB3	94
Sample Length (in)	1.994	1.990	Tare Wt. (g)	2.63	83.35
Sample Area (cm^2)	42.09	42.06	Wet Soil + Tare (g)	85.65	489.94
Sample Volume (CC)	213.16	212.58	Dry Soil + Tare (g)	66.39	392.83
Sample Wt. (g)	402.92	406.59	Water Content (%)	30.2	31.4
Wet Density (pcf)	118.0	119.3	Porosity	0.464	
Dry Density (pcf)	90.6	90.8	Pore Volume (CC)	98.97	

Effective Consolidation (psi) 5 min — 6 max

Degree of Saturation 99

Specific Gravity 2.71

Read Time hr	min	Pcell psi	Pin psi	Pout psi	Readings (cm) hin	hout	Inflow PV	Outflow PV	Storage PV	Total PV	i	K cm/s
1	8 8	50	45	44	61.40	70.60	—	—	—	—	12.1	—
1	8 11	50	45	44	57.95	74.00	-0.04	0.04	0.00	0.04	10.7	5.1E-05
1	8 15	50	45	44	54.40	77.55	-0.05	0.05	0.00	0.09	9.3	4.5E-05
1	8 20	50	45	44	50.80	81.15	-0.05	0.05	0.00	0.14	7.9	4.2E-05
2	10	50	45	44	56.20	66.90					11.8	
2	10 6	50	45	44	49.00	74.00	-0.09	0.09	0.00	0.23	9.0	5.8E-05
2	10 8	50	45	44	47.05	76.00	-0.02	0.03	0.00	0.25	8.2	5.8E-05
2	10 9	50	45	44	46.15	76.90	-0.01	0.01	0.00	0.27	7.8	5.7E-05
2	10 11	50	45	44	44.40	78.70	-0.02	0.02	0.00	0.29	7.1	6.0E-05
2	10 12	50	45	44	43.50	79.60	-0.01	0.01	0.00	0.30	6.8	6.5E-05
2	10 13	50	45	44	42.60	80.50	-0.01	0.01	0.00	0.31	6.4	6.9E-05
2	11	50	45	44	60.25	70.40					11.9	
2	11 1	50	45	44	58.85	71.80	-0.02	0.02	0.00	0.33	11.3	6.1E-05
2	11 2	50	45	44	57.50	73.15	-0.02	0.02	0.00	0.35	10.8	6.2E-05
2	11 3	50	45	44	56.20	74.45	-0.02	0.02	0.00	0.36	10.3	6.2E-05
2	11 4	50	45	44	54.90	75.75	-0.02	0.02	0.00	0.38	9.8	6.5E-05
2	11 5	50	45	44	53.70	76.95	-0.02	0.02	0.00	0.40	9.3	6.3E-05

TRIAXIAL PERMEABILITY DATA SHEET

SHANNON & WILSON, INC.

ject Combustion Engineering Test. by KMH/KDM-10/30/98

Job No. E-1039-01 Boring WS-28 Sample 16.5-18.5 Checked by KMH - 12/7/98

Description Dark grey lean CLAY, with some roots & root holes, some Fe stains, sl blocky

Depth Permeant tap water Test Method ASTM 5084-90

Permeameter No. 6 Standpipe Vol (cc/cm) Inflow: 1.266 Outflow: 1.279

2	11	6	50	45	44	52.60	78.05	-0.01	0.01	0.00	0.41	8.9	6.1E-05
2	11	7	50	45	44	51.55	79.10	-0.01	0.01	0.00	0.42	8.4	6.1E-05
2	11	8	50	45	44	50.50	80.15	-0.01	0.01	0.00	0.44	8.0	6.4E-05
2	11	10	50	45	44	48.50	82.15	-0.03	0.03	0.00	0.46	7.2	6.6E-05
2	11	12	50	45	44	46.65	84.00	-0.02	0.02	0.00	0.49	6.5	6.8E-05
4	8		50	45	44	61.90	71.35					12.0	
4	8	3	50	45	44	57.50	75.75	-0.06	0.06	0.00	0.54	10.3	6.6E-05
4	8	28	50	45	44	57.40	68.00					11.8	
4	8	31	50	45	44	52.90	72.30	-0.06	0.06	0.00	0.60	10.1	6.8E-05
4	8	40	50	45	44	52.90	70.10					10.5	
4	8	54	50	45	44	39.35	83.60	-0.17	0.17	0.00	0.77	5.1	6.5E-05
4	8	55	50	45	44	38.70	84.20	-0.01	0.01	0.00	0.78	4.9	6.3E-05
4	8	56	50	45	44	38.10	84.85	-0.01	0.01	0.00	0.79	4.7	6.6E-05

TRIAXIAL PERMEABILITY DATA SHEET

SHANNON & WILSON, INC.

;ect Combustion Engineering — Test. by KDM-11/19/98

Job No. E-1039-01 — Boring WS-29 — Sample 20.0-22.0 — Checked by KWH - 12/7/98

Description Dark grey lean CLAY, with some sand, some sm roots & root holes, occa thin f sand stringers, sl blocky

Depth — Permeant tap water — Test Method ASTM 5084-90

Permeameter No. 11 — Standpipe Vol (cc/cm) Inflow: 1.290 Outflow: 1.289

	Before Test	After Test		Before Test	After Test
Sample Diameter (in)	2.868	2.860	Tare No.	KT1	52
Sample Length (in)	2.797	2.773	Tare Wt. (g)	2.63	83.17
Sample Area (cm^2)	41.68	41.45	Wet Soil + Tare (g)	99.49	628.33
Sample Volume (CC)	296.10	291.93	Dry Soil + Tare (g)	74.89	497.24
Sample Wt. (g)	553.62	545.16	Water Content (%)	34.0	31.7
Wet Density (pcf)	116.7	116.5	Porosity	0.483	
Dry Density (pcf)	87.0	88.5	Pore Volume (CC)	143.13	
Effective Consolidation (psi)	5 min	6 max	Degree of Saturation	95	
			Specific Gravity	2.70	

Read Time / hr min	Pcell psi	Pin psi	Pout psi	Readings (cm) hin	hout	Inflow PV	Outflow PV	Storage PV	Total PV	i	K cm/s
1 10 42	50	45	44	60.00	61.40	—	—	—	—	9.7	—
1 13 59	50	45	44	58.95	62.40	-0.01	0.01	0.00	0.01	9.4	2.8E-07
1 18 2	50	45	44	57.60	63.70	-0.01	0.01	0.00	0.02	9.0	3.0E-07
2 7 41	50	45	44	53.15	68.10	-0.04	0.04	0.00	0.06	7.8	3.3E-07
2 17 17	50	45	44	50.60	70.70	-0.02	0.02	0.00	0.08	7.1	3.1E-07
3 9 25	50	45	44	46.05	75.05	-0.04	0.04	0.00	0.12	5.8	3.7E-07
3 15 35	50	45	44	44.70	76.40	-0.01	0.01	0.00	0.14	5.4	3.3E-07
5 10 13	50	45	44	40.10	81.00	-0.04	0.04	0.00	0.18	4.1	1.9E-07
7 10 55	50	45	44	68.80	70.10					9.7	
7 13 42	50	45	44	68.20	70.70	-0.01	0.01	0.00	0.18	9.5	1.9E-07
7 16 11	50	45	44	67.70	71.20	0.00	0.00	0.00	0.19	9.4	1.8E-07
9 15 10	50	45	44	59.20	79.55	-0.08	0.08	0.00	0.26	7.0	1.9E-07
9 15 22	50	45	44	58.35	74.15					7.7	
10 15 15	50	45	44	54.88	77.65	-0.03	0.03	0.00	0.29	6.7	1.7E-07
10 18 17	50	45	44	54.40	78.10	0.00	0.00	0.00	0.30	6.6	2.0E-07
11 7 49	50	45	44	52.50	79.85	-0.02	0.02	0.00	0.31	6.1	1.8E-07
11 13 3	50	45	44	51.90	80.50	-0.01	0.01	0.00	0.32	5.9	1.7E-07

TRIAXIAL PERMEABILITY DATA SHEET

SHANNON & WILSON, INC.

ject Combustion Engineering Test. by KDM-11/19/98

Job No. E-1039-01 Boring WS-29 Sample 20.0-22.0 Checked by [illegible] - 12/7/98

Description Dark grey lean CLAY, with some sand, some sm roots & root holes, occa thin f sand stringers, sl blocky

Depth Permeant tap water Test Method ASTM 5084-90

Permeameter No. 11 Standpipe Vol (cc/cm) Inflow: 1.290 Outflow: 1.289

11	15	19	50	45	44	51.60	80.80	0.00	0.00	0.00	0.32	5.8	2.0E-07
12	9	32	50	45	44	49.45	82.90	-0.02	0.02	0.00	0.34	5.2	1.8E-07
12	14	41	50	45	44	48.95	82.90					5.1	
13	9	50	50	45	44	47.05	85.25	-0.02	0.02	0.00	0.36	4.5	2.0E-07
14	8	5	50	45	44	44.95	87.25	-0.02	0.02	0.00	0.38	3.9	1.9E-07

TRIAXIAL PERMEABILITY DATA SHEET

SHANNON & WILSON, INC.

ect Combustion Engineering — Test. by KMH-11/20/98

Job No. E-1039-01 — Boring WS-32 — Sample 12.0-14.0 — Checked by [illegible] 12/7/98

Description Brown & grey lean CLAY, with numerous Fe stains, some sm Fe nodules, some roots & rootholes, blocky

Depth — Permeant tap water — Test Method ASTM 5084-90

Permeameter No. 9 — Standpipe Vol (cc/cm) Inflow: 1.302 Outflow: 1.311

	Before Test	After Test		Before Test	After Test
Sample Diameter (in)	2.875	2.885	Tare No.	KT2	74
Sample Length (in)	2.293	2.301	Tare Wt. (g)	2.63	85.24
Sample Area (cm^2)	41.88	42.17	Wet Soil + Tare (g)	79.60	564.06
Sample Volume (CC)	243.93	246.49	Dry Soil + Tare (g)	63.05	461.51
Sample Wt. (g)	478.42	478.82	Water Content (%)	27.4	27.3
Wet Density (pcf)	122.4	121.2	Porosity	0.410	
Dry Density (pcf)	96.1	95.3	Pore Volume (CC)	100.04	
Effective Consolidation (psi)	5 min	6 max	Degree of Saturation	100	
			Specific Gravity	2.61	

Read Time hr	min	Pcell psi	Pin psi	Pout psi	Readings (cm) hin	hout	Inflow PV	Outflow PV	Storage PV	Total PV	i	K cm/s
1	23	50	45	44	73.60	75.50	—	—	—	—	11.7	—
1	35	50	45	44	70.30	78.70	-0.04	0.04	0.00	0.04	10.6	1.3E-05
1	43	50	45	44	68.50	80.50	-0.02	0.02	0.00	0.07	10.0	1.1E-05
3	10	50	45	44	66.05	74.65					10.6	
3	5	50	45	44	64.05	76.65	-0.03	0.03	0.00	0.09	9.9	2.0E-05
3	9	50	45	44	62.55	78.15	-0.02	0.02	0.00	0.11	9.4	2.0E-05
3	12	50	45	44	61.45	79.20	-0.01	0.01	0.00	0.13	9.0	2.0E-05
3	13	50	45	44	61.45	74.00					9.9	
3	17	50	45	44	60.05	75.40	-0.02	0.02	0.00	0.14	9.4	1.9E-05
3	20	50	45	44	58.90	76.55	-0.01	0.02	0.00	0.16	9.0	2.2E-05
3	23	50	45	44	57.85	77.60	-0.01	0.01	0.00	0.17	8.7	2.1E-05
3	26	50	45	44	56.85	78.65	-0.01	0.01	0.00	0.19	8.3	2.1E-05
3	27	50	45	44	56.85	70.00					9.8	
3	30	50	45	44	55.85	71.00	-0.01	0.01	0.00	0.20	9.5	1.8E-05
3	33	50	45	44	54.85	72.00	-0.01	0.01	0.00	0.21	9.1	1.9E-05
3	36	50	45	44	53.80	73.00	-0.01	0.01	0.00	0.23	8.8	2.0E-05
3	39	50	45	44	52.85	73.95	-0.01	0.01	0.00	0.24	8.5	1.9E-05

TRIAXIAL PERMEABILITY DATA SHEET

SHANNON & WILSON, INC.

ject Combustion Engineering — Test. by KMH-11/16/98

Job No. E-1039-01 — Boring WS-32 — Sample 25.0-26.0 — Checked by KMH -12/7/98

Description Grey-brown lean CLAY, with some Fe stains, some sm roots & root holes

Depth — Permeant tap water — Test Method ASTM 5084-90

Permeameter No. 10 — Standpipe Vol (cc/cm) Inflow: 1.301 Outflow: 1.301

	Before Test	After Test		Before Test	After Test
Sample Diameter (in)	2.882	2.889	Tare No.	KT3	81
Sample Length (in)	2.585	2.586	Tare Wt. (g)	2.63	82.76
Sample Area (cm^2)	42.09	42.29	Wet Soil + Tare (g)	81.26	599.66
Sample Volume (CC)	276.34	277.79	Dry Soil + Tare (g)	62.15	470.00
Sample Wt. (g)	516.49	516.90	Water Content (%)	32.1	33.5
Wet Density (pcf)	116.6	116.1	Porosity	0.482	
Dry Density (pcf)	88.3	87.0	Pore Volume (CC)	133.13	
Effective Consolidation (psi)	5 min	6 max	Degree of Saturation	95	
			Specific Gravity	2.73	

Read Time y hr min	Pcell psi	Pin psi	Pout psi	Readings (cm) hin	hout	Inflow PV	Outflow PV	Storage PV	Total PV	i	K cm/s
1 8 28	50	45	44	67.60	63.45	—	—	—	—	11.3	—
1 8 31	50	45	44	64.75	66.40	-0.03	0.03	0.00	0.03	10.5	4.6E-05
3 10	50	45	44	57.90	60.75					9.2	
3 10 2	50	45	44	56.75	61.85	-0.01	0.01	0.00	0.04	8.9	3.2E-05
3 10 4	50	45	44	55.80	62.80	-0.01	0.01	0.00	0.05	8.6	2.8E-05
3 10 7	50	45	44	54.55	64.10	-0.01	0.01	0.00	0.06	8.2	2.6E-05
3 10 9	50	45	44	53.80	64.85	-0.01	0.01	0.00	0.07	8.0	2.4E-05
3 10 13	50	45	44	52.50	66.15	-0.01	0.01	0.00	0.08	7.6	2.2E-05
3 10 17	50	45	44	51.25	67.45	-0.01	0.01	0.00	0.09	7.2	2.2E-05
4 9	50	45	44	69.05	79.40					9.1	
4 9 4	50	45	44	67.45	81.00	-0.02	0.02	0.00	0.11	8.6	2.3E-05
4 9 7	50	45	44	66.35	82.10	-0.01	0.01	0.00	0.12	8.3	2.2E-05
4 9 11	50	45	44	64.90	83.60	-0.01	0.01	0.00	0.14	7.9	2.3E-05
4 9 12	50	45	44	64.90	76.90					8.9	
4 9 17	50	45	44	63.15	78.70	-0.02	0.02	0.00	0.15	8.3	2.1E-05
4 9 28	50	45	44	59.55	82.40	-0.04	0.04	0.00	0.19	7.2	2.2E-05
4 9 33	50	45	44	58.15	83.75	-0.01	0.01	0.00	0.20	6.8	2.0E-05

TRIAXIAL PERMEABILITY DATA SHEET

SHANNON & WILSON, INC.

pct Combustion Engineering Test. by KMH-11/16/98

Job No. E-1039-01 Boring WS-32 Sample 25.0-26.0 Checked by CMLH -12/7/98

Description Grey-brown lean CLAY, with some Fe stains, some sm roots & root holes

Depth Permeant tap water Test Method ASTM 5084-90

Permeameter No. 10 Standpipe Vol (cc/cm) Inflow: 1.301 Outflow: 1.301

4 10	50	45	44	49.20	68.35					7.8	
4 10 7	50	45	44	47.00	70.55	-0.02	0.02	0.00	0.22	7.1	2.2E-05
4 10 13	50	45	44	45.40	72.10	-0.02	0.02	0.00	0.24	6.6	2.0E-05
4 10 19	50	45	44	43.90	73.60	-0.01	0.01	0.00	0.25	6.2	2.0E-05
4 10 23	50	45	44	42.90	74.60	-0.01	0.01	0.00	0.26	5.9	2.1E-05

TRIAXIAL PERMEABILITY DATA SHEET

SHANNON & WILSON, INC.

ject Combustion Engineering — Test. by KDM-11/24/98

Job No. E-1039-01 — Boring WS-33 — Sample 20.0-22.0 — Checked by KWH -12/7/98

Description Dark brown & grey fat CLAY, with some Fe nodules, occa Fe stains, occa sm roots

Depth — Permeant tap water — Test Method ASTM 5084-90

Permeameter No. 16 — Standpipe Vol (cc/cm) Inflow: 1.312 Outflow: 1.308

	Before Test	After Test		Before Test	After Test
Sample Diameter (in)	2.866	2.876	Tare No.	LB22	82
Sample Length (in)	2.573	2.585	Tare Wt. (g)	2.63	83.50
Sample Area (cm^2)	41.62	41.91	Wet Soil + Tare (g)	70.12	621.59
Sample Volume (CC)	272.01	275.19	Dry Soil + Tare (g)	55.64	506.51
Sample Wt. (g)	534.74	538.09	Water Content (%)	27.3	27.2
Wet Density (pcf)	122.7	122.0	Porosity	0.415	
Dry Density (pcf)	96.4	95.9	Pore Volume (CC)	112.91	
Effective Consolidation (psi)	5 min	6 max	Degree of Saturation	100	
			Specific Gravity	2.64	

Read Time y hr min	Pcell psi	Pin psi	Pout psi	Readings (cm) hin	hout	Inflow PV	Outflow PV	Storage PV	Total PV	i	K cm/s
1 11 1	50	45	44	68.05	70.95	—	—	—	—	10.3	—
1 16 11	50	45	44	67.80	71.20	0.00	0.00	0.00	0.00	10.2	4.1E-08
3 15 36	50	45	44	66.15	72.75	-0.02	0.02	0.00	0.02	9.8	3.0E-08
4 9 21	50	45	44	65.60	73.15	-0.01	0.00	0.00	0.03	9.6	2.4E-08
4 18 17	50	45	44	65.40	73.40	0.00	0.00	0.00	0.03	9.5	2.3E-08
5 7 49	50	45	44	65.00	73.80	0.00	0.00	0.00	0.03	9.4	2.7E-08
5 18 12	50	45	44	64.65	74.05	0.00	0.00	0.00	0.04	9.3	2.7E-08
6 9 32	50	45	44	64.20	74.50	-0.01	0.01	0.00	0.04	9.2	2.8E-08
7 9 31	50	45	44	63.55	74.95	-0.01	0.01	0.00	0.05	9.0	2.2E-08
8 8 6	50	45	44	63.05	75.30	-0.01	0.00	0.00	0.05	8.9	1.8E-08
9 7 34	50	45	44	62.55	75.65	-0.01	0.00	0.00	0.05	8.8	1.8E-08
10 8 31	50	45	44	62.05	76.05	-0.01	0.00	0.00	0.06	8.6	1.8E-08
10 18 4	50	45	44	61.85	76.25	0.00	0.00	0.00	0.06	8.6	2.1E-08
11 7 51	50	45	44	61.60	76.50	0.00	0.00	0.00	0.06	8.5	1.9E-08
11 17 45	50	45	44	61.45	76.65	0.00	0.00	0.00	0.07	8.4	1.6E-08
12 9 35	50	45	44	61.15	76.90	0.00	0.00	0.00	0.07	8.4	1.8E-08
12 16 23	50	45	44	61.00	77.00	0.00	0.00	0.00	0.07	8.3	1.9E-08

TRIAXIAL PERMEABILITY DATA SHEET

SHANNON & WILSON, INC.

'ect Combustion Engineering Test. by KDM-11/24/98

Job No. E-1039-01 Boring WS-33 Sample 20.0-22.0 Checked by [illegible] - 12/7/98

Description Dark brown & grey fat CLAY, with some Fe nodules, occa Fe stains, occa sm roots

Depth Permeant tap water Test Method ASTM 5084-90

Permeameter No. 16 Standpipe Vol (cc/cm) Inflow: 1.312 Outflow: 1.308

13	9	20	50	45	44	60.65	77.15	0.00	0.00	0.00	0.07	8.2	1.6E-08
15	8	19	50	45	44	59.85	77.85	-0.01	0.01	0.00	0.08	8.0	1.7E-08
16	8		50	45	44	59.35	78.20	-0.01	0.00	0.00	0.08	7.9	2.0E-08
17	8	39	50	45	44	58.85	78.50	-0.01	0.00	0.00	0.09	7.8	1.8E-08

TRIAXIAL PERMEABILITY DATA SHEET

SHANNON & WILSON, INC.

ect Combustion Engineering — Test. by KDM-11/19/98

Job No. E-1039-01 — Boring WS-34 — Sample 30.7-32.0 — Checked by [illegible] 12/7/98

Description Dark grey lean CLAY, with some f sand, occa thin f sand stringers; rare sm roots — 1/1/00

Depth — Permeant tap water — Test Method ASTM 5084-90

Permeameter No. 9 — Standpipe Vol (cc/cm) Inflow: 1.302 Outflow: 1.311

	Before Test	After Test		Before Test	After Test
Sample Diameter (in)	2.845	2.825	Tare No.	LB24	54
Sample Length (in)	2.741	2.708	Tare Wt. (g)	2.63	82.71
Sample Area (cm^2)	41.01	40.44	Wet Soil + Tare (g)	77.94	643.57
Sample Volume (CC)	285.54	278.15	Dry Soil + Tare (g)	62.70	540.85
Sample Wt. (g)	571.82	560.86	Water Content (%)	25.4	22.4
Wet Density (pcf)	125.0	125.8	Porosity	0.408	
Dry Density (pcf)	99.7	102.8	Pore Volume (CC)	116.61	
Effective Consolidation (psi)	5 min	6 max	Degree of Saturation	95	
			Specific Gravity	2.70	

Read Time y hr min	Pcell psi	Pin psi	Pout psi	Readings (cm) hin	hout	Inflow PV	Outflow PV	Storage PV	Total PV	i	K cm/s
1 10 49	50	45	44	64.90	68.70	---	---	---	---	9.6	---
3 15 35	50	45	44	63.50	69.95	-0.02	0.01	0.00	0.01	9.2	2.4E-08
4 9 15	50	45	44	63.00	70.30	-0.01	0.00	0.00	0.02	9.1	2.3E-08
4 18 19	50	45	44	62.80	70.55	0.00	0.00	0.00	0.02	9.0	2.4E-08
5 7 45	50	45	44	62.45	70.90	0.00	0.00	0.00	0.02	8.9	2.6E-08
5 18 14	50	45	44	62.20	71.15	0.00	0.00	0.00	0.03	8.8	2.4E-08
6 9 34	50	45	44	61.80	71.40	0.00	0.00	0.00	0.03	8.7	2.1E-08
6 14 42	50	45	44	61.65	71.55	0.00	0.00	0.00	0.03	8.7	3.0E-08
7 9 45	50	45	44	61.00	72.00	-0.01	0.01	0.00	0.04	8.5	3.0E-08
8 8 7	50	45	44	60.50	72.45	-0.01	0.01	0.00	0.04	8.4	2.2E-08
9 7 49	50	45	44	59.90	72.90	-0.01	0.01	0.00	0.05	8.2	2.4E-08
10 8 29	50	45	44	59.45	73.25	-0.01	0.00	0.00	0.05	8.1	1.8E-08
11 7 52	50	45	44	59.00	73.70	-0.01	0.01	0.00	0.06	8.0	2.1E-08
12 9 37	50	45	44	58.45	74.05	-0.01	0.00	0.00	0.06	7.9	2.0E-08
12 16 24	50	45	44	58.35	74.15	0.00	0.00	0.00	0.06	7.8	1.7E-08
15 8 20	50	45	44	57.05	75.00	-0.01	0.01	0.00	0.07	7.5	1.9E-08
16 8 5	50	45	44	56.65	75.35	0.00	0.00	0.00	0.07	7.4	1.9E-08

TABLE 2

COMBUSTION ENGINEERING
MISSOURI STATE ROUTE P
HEMATITE, MISSOURI

Geometric Mean - NSSSC Monitoring Wells/Piezometers
Summary of Results of Single Well Hydraulic Conductivity Testing

Table 2a - Feet/Minute

Well ID	Hvorslev Method Feet/minute	Bouwer-Rice Method Feet/minute	Geomean of Two Methods Feet/minute
WS-22	1.37E-04	1.96E-03	5.18E-04
WS-24	2.72E-05	6.85E-04	1.37E-04
WS-28	1.71E-05	5.53E-04	9.74E-05
WS-33	1.12E-04	1.45E-03	4.03E-04
PZ-1	1.34E-05	1.27E-03	1.30E-04
GEOMEAN	**3.95E-05**	**1.06E-03**	**2.05E-04**

Table 2b - Feet/Day

Well ID	Hvorslev Method Feet/day	Bouwer-Rice Method Feet/day	Geomean of Two Methods Feet/day
WS-22	1.97E-01	2.82E+00	7.46E-01
WS-24	3.92E-02	9.87E-01	1.97E-01
WS-28	2.47E-02	7.97E-01	1.40E-01
WS-33	1.61E-01	2.09E+00	5.80E-01
PZ-1	1.93E-02	1.83E+00	1.88E-01
GEOMEAN	**5.68E-02**	**1.53E+00**	**2.95E-01**

Table 2c - Centimeters/Second

Well ID	Hvorslev Method cm/sec	Bouwer-Rice Method cm/sec	Geomean of Two Methods cm/sec
WS-22	6.96E-05	9.94E-04	2.63E-04
WS-24	1.38E-05	3.48E-04	6.94E-05
WS-28	8.71E-06	2.81E-04	4.95E-05
WS-33	5.69E-05	7.37E-04	2.05E-04
PZ-1	6.80E-06	6.45E-04	6.62E-05
GEOMEAN	**2.00E-05**	**5.41E-04**	**1.04E-04**

TABLE 3

COMBUSTION ENGINEERING
MISSOURI STATE ROUTE P
HEMATITE, MISSOURI

Geometric Mean - DSCC Monitoring Wells/Piezometers
Summary of Results of Single Well Hydraulic Conductivity Testing

Table 3a - Feet/Minute

Well ID	Hvorslev Method Feet/minute	Bouwer-Rice Method Feet/minute	Geomean of Two Methods Feet/minute
WS-23	4.34E-04	4.09E-03	1.33E-03
WS-25	1.82E-04	2.26E-03	6.41E-04
WS-27	2.54E-04	5.74E-03	1.21E-03
WS-29	3.80E-04	6.97E-03	1.63E-03
WS-32	9.48E-05	3.11E-03	5.43E-04
WS-34	2.90E-04	4.99E-03	1.20E-03
PZ-2	9.48E-05	3.11E-03	5.43E-04
GEOMEAN	2.13E-04	4.04E-03	9.29E-04

Table 3b - Feet/Day

Well ID	Hvorslev Method Feet/day	Bouwer-Rice Method Feet/day	Geomean of Two Methods Feet/day
WS-23	6.24E-01	5.88E+00	1.92E+00
WS-25	2.61E-01	3.26E+00	9.23E-01
WS-27	3.66E-01	8.27E+00	1.74E+00
WS-29	5.48E-01	1.00E+01	2.35E+00
WS-32	2.00E+00	2.92E+01	7.65E+00
WS-34	2.49E-01	4.75E+00	1.09E+00
PZ-2	1.37E-01	4.48E+00	7.82E-01
GEOMEAN	4.18E-01	7.19E+00	1.73E+00

Table 3c - Centimeters/Second

Well ID	Hvorslev Method cm/sec	Bouwer-Rice Method cm/sec	Geomean of Two Methods cm/sec
WS-23	2.20E-04	2.08E-03	6.76E-04
WS-25	9.22E-05	1.15E-03	3.26E-04
WS-27	1.29E-04	2.92E-03	6.13E-04
WS-29	1.93E-04	3.54E-03	8.27E-04
WS-32	7.07E-04	1.03E-02	2.70E-03
WS-34	8.78E-05	1.68E-03	3.84E-04
PZ-2	4.82E-05	1.58E-03	2.76E-04
GEOMEAN	1.47E-04	2.53E-03	6.11E-04

APPENDIX E

Field Capacity Calculation

$$p_e = p_t - \theta_r \cdot \qquad (4.4)$$

Therefore, the effective porosity is related to the total porosity and the field capacity according to the following expression:

Several aspects of the soil system influence the value of its effective porosity: (1) the adhesive water on minerals, (2) the absorbed water in the clay-mineral lattice, (3) the existence of unconnected pores, and (4) the existence of dead-end pores. The adhesive water in the soil is that part of the water present in the soil that is attached to the surface of the soil grains through the forces of molecular attraction (Marsily 1988). The sum of the volumes of the adhesive and absorbed water plus the water that fills the unconnected and dead-end pores constitute the volume of the adsorbed water, V_{iw}, that is unable to move through the system.

A detailed list of representative porosity values (total porosity and effective porosity) is presented in Table 3.2.

4.2 MEASUREMENT METHODOLOGY

Determination of the effective porosity, p_e, of soils can be accomplished indirectly by measuring the total porosity, p_t, and the field capacity, θ_r, and then calculating p_e from Equation 4.4. The total porosity is obtained indirectly by measuring the soil densities according to the method described in Section 3.2. To determine the field capacity of the soils, the soil sample is first saturated with water and is then allowed to drain completely under the action of gravity until it gets to its irreducible saturation. The value of θ_r can then be obtained according to the methods used for measuring volumetric water content (Section 6.2).

4.3 RESRAD DATA INPUT REQUIREMENTS

To use RESRAD, the user is required to define (or to use the default values) of the effective porosity of three distinct materials: (1) contaminated zone, (2) saturated zone, and (3) unsaturated zone. In RESRAD, the effective porosity values are entered as decimal fractions rather than as percentages. As a default value, RESRAD adopts the value of $p_e = 0.2$ for all three materials. These default values are provided for generic use of the RESRAD code. For more accurate utilization of the model, site-specific data should be used.

If site-specific data are not available and the soil type is known, Table 3.2 can be used for estimating effective porosity. However, if no information is available on soil type, then the values of effective porosity should be experimentally determined according to the method presented in Section 4.2. Effective porosity values should not be greater than total porosity values. Total porosity is discussed in Section 3.

Problem: Calculate Field Capacity of Soil

Formula: $P_e = P_t - 2_r$

Where: P_e = Effective Porosity

P_t = Total Porosity

2_r = Field Capacity

Given: $P_e = 0.281$ (from default value for silty-clay from Table 3.3-1 of "Development of Probabilistic RESRAD 6.0 and RESAD-Build 3.0 Computer Codes, "November 2000).

$P_t = 0.446$ (Shannon & Wilson Data)

2_r = Unknown

Solve for 2_r $P_e = P_t - 2_r$

$- 2_r = P_e - P_t$

$2_r = P_t - P_e$

$2_r = 0.446 - 0.281$

$2_r = 0.165$

Field Capacity = 0.165

water content and residual water content to develop distributions for effective porosity by subtraction. Table 3.3-1 gives the distributions and the defining parameters for effective porosity for the 12 soil textural classes and for the generic soil type.

The distribution to be used for cases when the type of soil is not known (the RESRAD default distribution) was obtained as the weighted average of the distributions for the individual soil classes. The same weighting factor scheme as discussed for the generic soil type in Section 3.1 was used. The probability density function of the weight average was plotted, and the parameters of the normal distribution were chosen to represent the weighted average curve over the range of interest. The probability density function for the effective porosity for this generic soil type is shown in Figure 3.3-1. When a site-specific analysis is being conducted, the distribution for the soil type present at the site should be used. For consistency, distributions corresponding to the same soil type selected for this parameter should also be selected for the following parameters: soil density, total porosity, hydraulic conductivity, and the soil b parameter.

Table 3.3-1 Distribution Type and Parameters for Effective Porosity by Soil Type

Soil Type	Distribution	Mean	Standard Deviation	Lower Limit	Upper Limit
Sand	Normal	0.383	0.0610	0.195	0.572
Loamy sand	Normal	0.353	0.0913	0.0711	0.635
Sandy loam	Normal	0.346	0.0915	0.0629	0.628
Sandy clay loam	Normal	0.289	0.0703	0.0723	0.507
Loam	Normal	0.352	0.101	0.0414	0.663
Silt loam	Normal	0.383	0.0813	0.132	0.634
Silt	Normal	0.425	0.110	0.0839	0.766
Clay loam	Normal	0.315	0.0905	0.0349	0.594
Silty clay loam	Normal	0.342	0.0705	0.124	0.560
Sandy clay	Normal	0.281	0.0513	0.122	0.439
Silty clay	Normal	0.289	0.0735	0.0623	0.517
Clay	Normal	0.311	0.0963	0.0138	0.609
Generic soil type[a]	Normal	0.355	0.0906	0.075	0.635

[a] *Parameters for the generic soil type were derived from the distribution* enveloping all soil types. The lower and upper limits correspond to the 0.001 and 0.999 quantile values, respectively.

Sources: Carsel and Parrish (1988); Meyer et al. (1997).

APPENDIX F

Representative Values of Soil-Specific Exponential b Parameter

conductivity function.

TABLE 13.1 Representative Values of Soil-Specific Exponential b Parameter

Texture	Soil-Specific Exponential Parameter, *b*
Sand	4.05
Loamy sand	4.38
Sandy loam	4.90
Silty loam	5.30
Loam	5.39
Sandy clay loam	7.12
Silty clay loam	7.75
Clay loam	8.52
Sandy clay	10.40
Silty clay	10.40
Clay	11.40

Source: Clapp and Hornberger (1978).

APPENDIX G

Well Pump Intake Calculations and Supporting Documentation

WELL PUMP INTAKE CALCULATIONS

WELL PUMP INTAKE CALCULATIONS BASED ON DSCC WELLS	
MW or Piez	**Depth bgs (feet)**
WS-23	38.52
WS-25	38.21
WS-27	32.46
WS-29	27.79
WS-32	35.22
WS-34	35.45
PZ-2	33.49
OB-1	26.20
OB-2	37.00
BR3-OB	24.30
Average (feet bgs)	**32.86**
Pump Height (feet bgs)	**30.86**
Pump Height (meters bgs)	**9.41**

Pump is assumed to located 2 feet off the bottom of the well.

WESTINGHOUSE ELECTRIC CO. LLC
HEMATITE, MISSOURI FACILITY

REMEDIAL INVESTIGATION/FEASIBILITY STUDY WORK PLAN
TABLE 5 - MONITORING WELL/PIEZOMETER CONSTRUCTION DATA

WELL DESIGNATION	DATE INSTALLED	SCREEN/CASING MATERIAL	WELL CASING DIAMETER (INCHES O.D.)	GRADE ELEVATION (FEET AMSL)	TOP OF CASING ELEVATION (FEET AMSL)	WELL BOTTOM ELEVATION (FEET AMSL)	DEPTH OF WELL (FEET BGS)	DEPTH OF WELL (FEET BTOC)	SCREEN LENGTH (FEET)	SCREENED INTERVAL (FEET BGS)	HYDROSTRATIGRAPHIC ZONE MONITORED
WS-7	Unknown	PVC/Unknown	4	432.25	432.28	409.77	22.48	22.51	Unknown	Unknown	Unconsolidated
WS-8	Unknown	PVC/Unknown	4	431.71	433.70	414.04	17.67	19.66	Unknown	Unknown	Unconsolidated
WS-9	Unknown	PVC/Unknown	4	431.77	432.84	406.47	25.30	26.37	Unknown	Unknown	Unconsolidated
RMC-9	Unknown	PVC/Unknown	2	433.51	436.07	Unknown	Unknown	Unknown	Unknown	Unknown	Unconsolidated
WS-13	Unknown	PVC/PVC	2	434.02	435.80	Unknown	Unknown	20.70	Unknown	Unknown	Unconsolidated
WS-14	Unknown	PVC/PVC	2	433.56	435.65	Unknown	Unknown	25.58	Unknown	Unknown	Unconsolidated
WS-15	Unknown	PVC/PVC	2	430.58	432.76	406.79	23.79	25.97	Unknown	Unknown	Unconsolidated
WS-16	Unknown	PVC/PVC	2	430.19	432.25	410.55	19.64	21.70	Unknown	Unknown	Unconsolidated
WS-17B	26-Jun-96	PVC/PVC	2	433.39	435.36	412.85	20.54	22.51	13.00	7.0-20.0	Unconsolidated
WS-22	24-Sep-98	PVC/PVC	2	438.22	441.12	421.96	16.26	19.16	5.00	10.5-15.5	NSSSC/Unconsolidated
WS-23	24-Sep-98	PVC/PVC	2	438.15	441.16	399.63	38.52	41.53	10.00	28.52-38.52	DSCC/Unconsolidated
WS-24	23-Sep-98	PVC/PVC	2	436.76	439.64	420.00	16.76	19.64	10.00	5.5-15.5	NSSSC/Unconsolidated
WS-25	23-Sep-98	PVC/PVC	2	436.55	439.09	398.34	38.21	40.75	10.00	28.4-38.4	DSCC/Unconsolidated
WS-26	28-Sep-98	PVC/PVC	2	430.48	433.53	415.32	15.16	18.21	10.00	5.0-15.0	NSSSC/Unconsolidated
WS-27	28-Sep-98	PVC/PVC	2	430.69	433.56	398.23	32.46	35.33	10.00	21.8-31.8	DSCC/Unconsolidated
WS-28	25-Sep-98	PVC/PVC	2	425.71	428.61	409.87	15.84	18.74	10.00	6.5-16.5	NSSSC/Unconsolidated
WS-29	25-Sep-98	PVC/PVC	2	425.32	428.20	397.53	27.79	30.67	7.00	20.4-27.4	DSCC/Unconsolidated
WS-30	15-Oct-98	PVC/PVC	2	425.41	428.27	376.20	49.21	52.07	10.00	38.9-48.9	Jefferson City-Cotter Dolomite
WS-31	13-Oct-98	PVC/PVC	2	424.95	427.63	343.54	81.41	84.09	10.00	71.3-81.3	Jefferson City-Cotter Dolomite
WS-32	30-Sep-98	PVC/PVC	2	433.20	436.11	397.98	35.22	38.13	5.00	30.8-35.8	DSCC/Unconsolidated
WS-33	22-Sep-98	PVC/PVC	2	434.23	437.12	416.32	17.91	20.80	10.00	7.6-17.6	NSSSC/Unconsolidated
WS-34	21-Sep-98	PVC/PVC	2	434.21	436.96	398.76	35.45	38.20	10.00	25.6-35.6	DSCC/Unconsolidated
PZ-1	28-Sep-98	PVC/PVC	2	431.75	434.74	407.85	23.90	26.89	10.00	13.5-23.5	NSSSC/Unconsolidated
PZ-2	28-Sep-98	PVC/PVC	2	431.63	434.81	398.14	33.49	36.67	10.00	23.5-33.5	DSCC/Unconsolidated
PZ-3	13-Oct-98	PVC/PVC	2	433.23	435.85	372.28	60.95	63.57	10.00	50.3-60.3	Jefferson City-Cotter Dolomite
PZ-4	13-Oct-98	PVC/PVC	2	438.17	440.71	378.86	59.31	61.85	10.00	49.3-59.3	Jefferson City-Cotter Dolomite
OB-1	15-May-02	PVC/PVC	2	426.67	429.64	400.47	26.20	29.17	16.20	10.0-26.2	Unconsolidated
OB-2	28-May-02	PVC/PVC	2	427.71	430.52	390.71	37.00	39.81	27.00	10.0-37.0	Unconsolidated

Note
O.D. = Outside Diameter
AMSL = Above Mean Sea Level
BGS = Below Ground Surface
BTOC = Below Top of Casing
1 .SC = Near-Surface, Silt; Silty-Clay
DSCC = Deep, Silty-Clay; Clay

WESTINGHOUSE ELECTRIC CO. LLC
HEMATITE, MISSOURI FACILITY

REMEDIAL INVESTIGATION/FEASIBILITY STUDY WORK PLAN
TABLE 5 - MONITORING WELL/PIEZOMETER CONSTRUCTION DATA

WELL DESIGNATION	DATE INSTALLED	SCREEN/CASING MATERIAL	WELL CASING DIAMETER (INCHES O.D.)	GRADE ELEVATION (FEET AMSL)	TOP OF CASING ELEVATION (FEET AMSL)	WELL BOTTOM ELEVATION (FEET AMSL)	DEPTH OF WELL (FEET BGS)	DEPTH OF WELL (FEET BTOC)	SCREEN LENGTH (FEET)	SCREENED INTERVAL (FEET BGS)	HYDROSTRATIGRAPHIC ZONE MONITORED
BR1-JC	06-Jun-02	PVC/PVC	1	439.29	442.08	332.29	107.00	109.79	10.00	97.0-107.0	Jefferson City-Cotter Dolomite
BR1-RB	24-Jul-02	PVC/PVC	2	440.03	442.63	275.03	165.00	167.60	40.00	125-165	Roubidoux Formation
BR2-JC	23-Jul-02	PVC/PVC	1	428.64	431.33	313.64	115.00	117.69	5.00	105-115	Jefferson City-Cotter Dolomite
BR2-RB	24-Jul-02	PVC/PVC	2	428.23	431.50	93.23	335.00	338.27	40.00	295-335	Roubidoux Formation
BR3-OB	23-Jul-02	PVC/PVC	2	418.65	421.72	394.35	24.30	27.37	11.10	13.2-24.3	DSCC/Unconsolidated
BR3-RB	24-Jul-02	PVC/PVC	2	418.12	420.73	228.12	190.00	192.61	40.00	150-190	Roubidoux Formation
BR4-JC	24-Jul-02	PVC/PVC	2	432.11	434.51	327.11	105.00	107.40	10.00	95-105	Jefferson City-Cotter Dolomite
BR4-RB	24-Jul-02	PVC/PVC	2	431.95	434.93	191.95	240.00	242.98	40.00	200-240	Roubidoux Formation

Note
O.D. = Outside Diameter
AMSL = Above Mean Sea Level
BGS = Below Ground Surface
BTOC = Below Top of Casing
NSSSC = Near-Surface, Silt; Silty-Clay
DSCC = Deep, Silty-Clay; Clay

APPENDIX H

Well Pumping Rate Calculation and Supporting Documentation

LEGGETTE, BRASHEARS & GRAHAM, INC.

Scenario 1: Area of Contamination = 6432 M^2

Assume: 4 Adults
4 head of cattle

225 liters/adult/day
160 liters/head/day

225 x 4 = 900 liters/day
160 x 4 = 640 liters/day

Total 1540 liters/day or 562,100 liters/yearly

Conversion:

1 liter = 0.001 M^3

562,1000 liters = 562 M^3

Pumping Rate Requirements: 562 M^3/year

Scenario 2: Area of Contamination = 77458 M^2

Assume: 4 Adults
10 head of cattle

from above:
225 x 4 = 900 liters/day
160 x 10 = 1600 liters/day

Total 2500 liters/day of 912,500 liters/yearly

Pumping Rate Requirements: 913 M^3/year

Table 3.10-1 Example Calculations for Estimating the Well Pumping Rate

Water Use Component	General Case	Water Use as a Function of Land Area		
		100 m^2	2,400 m^2	10,000 m^2
Household	225 × 4 L/d = 328.7 $m^3 yr^{-1}$	328.7 $m^3 yr^{-1}$	328.7 $m^3 yr^{-1}$	328.7 $m^3 yr^{-1}$
Livestock	50+160 L/d = 76.7 $m^3 yr^{-1}$	76.7 $m^3 yr^{-1}$	76.7 $m^3 yr^{-1}$	76.7 $m^3 yr^{-1}$
Irrigation of vegetable plot				
Contaminated fraction	f_p = min(Area/2000, 0.5)	0	0.5	0.5
Irrigation rate	I_r (m yr^{-1})	0	0.1125 m yr^{-1}	0.1125 m yr^{-1}
Irrigation water	$f_p \times I_r \times 2000$	0	112.5 $m^3 yr^{-1}$	112.5 $m^3 yr^{-1}$
Irrigation of pasture				
Contaminated fraction	f_m = Area/20,000 ≤ 1	0	0.065	0.445
Irrigation rate	I_r (m yr^{-1})	0	0.1125 m yr^{-1}	0.1125 m yr^{-1}
Irrigation water	$f_m \times I_r \times 20{,}000$	0	146.3 $m^3 yr^{-1}$	1001 $m^3 yr^{-1}$
Drinking water	409.5 × 4 L/yr = 1.64 $m^3 yr^{-1}$ (Section 5.2)	1.64 $m^3 yr^{-1}$	1.64 $m^3 yr^{-1}$	1.64 $m^3 yr^{-1}$
Total ($m^3 yr^{-1}$)		407	666	1519

PRINCIPLES OF CONTROLLED GRAZING

David W. Pratt, U.C.C.E. Farm Advisor

LIVESTOCK & RANGE REPORT NO. 932 SPRING, 1993

Napa & Solano Counties U.C.C.E., Livestock/Range Management Program

GRASS FARMING

Ranching is really the business of converting sunlight energy into forage and forage into harvestable livestock products in a sustainable manner. From this perspective we see that those of us in the livestock business are also in the grass business. Allan Nation, editor of the Stockman Grass Farmer would say we are "grass farmers" and our livestock are the four legged combines with which we harvest our crop.

Most of us have considered the livestock business, not the grass business, as our primary occupation. As a result, our focus has been on the animal. We have a relatively poor understanding of how our crop grows and responds to grazing. An understanding of this relationship is fundamental to successful grass farming.

GREEN LEAVES CAPTURE SUNLIGHT

Sustainable production in ranching starts with using plants to capture sunlight energy. When sunlight falls on bare soil, rocks, or anything but growing plants, its energy cannot be harvested.

Principle: Maintain 100% green plant cover in pastures for as long as possible.

THE "S" SHAPED CURVE

The efficiency with which plants convert the sun's energy into green leaves and the ability of animals to harvest and use energy from those leaves depends on the phase of growth of the plants.

After grazing, plants go through three phases of growth that form an "S" shaped curve (figure 1). **Phase I** occurs after plants have been severely grazed. After grazing, fewer leaves are left to intercept sunlight and plants require more energy for growth than they are able to produce through photosynthesis. So, to compensate, energy is mobilized from the roots. The roots become smaller and weaker as energy is used to grow new leaves.

FIGURE 1. PLANT GROWTH AFTER GRAZING (THE 'S' SHAPED CURVE)

number of head per acre:

STOCK DENSITY = HEAD ÷ ACRE

For example if 50 steers are grazing a 10 acre paddock the stock density is 5 head/acre:

STOCK DENSITY = 50 HEAD ÷ 10 ACRES = 5 head / acre

In his book Holistic Resource Management, Allan Savory says, "Low density, not overgrazing or overstocking, should bear the blame for many serious range and production problems, including trailing, successional shifts toward brush and weeds, pest outbreaks, poor animal performance, and high supplemental feed costs...". To understand why, let's take another look at the two one acre paddocks described earlier (Figure 2).

The two paddocks had identical stocking rates (100 animal days per acre), but they were grazed for different periods of time and the stock densities were drastically different.

In the first paddock, with one animal grazing for 100 days (stock density 1 animal/acre), utilization was uneven, with some plants overgrazed and others undergrazed. In the other paddock, where one hundred animals grazed for one day (stock density 100 animals/acre), utilization was more uniform and there was no overgrazing. Shortening the graze period reduced overgrazing, but it was the increase in stock density that resulted in more even utilization.

Overgrazing is a function of time.

Uniformity of utilization is a function of stock density.

Pastures with low stock density usually appear "patchy" with some patches grazed very short and other patches consisting of rank, "wolfy," phase III vegetation. Some ranchers mow pastures to keep vegetation uniform and palatable. Others use fire to remove old, stemmy, ungrazed material. What they usually really need is higher stock density.

High stock density increases the uniformity of utilization and maintains forage in a more palatable, nutritious, digestible condition.

Stock density increases as the number of animals in a paddock increase or as paddock size decreases.

Principle: Use the highest stock density possible.

Twenty head per acre is the minimum stock density needed to uniformly graze irrigated pasture. Higher is better. Stock densities of over 50 cattle per acre are not uncommon on well managed irrigated pastures. Two head per acre is a reasonable target on more remote ranges. Again, higher is better.

HERD EFFECT

If you haven't already seen the movie *Dances With Wolves*, get out the popcorn and rent it tonight. When it gets to the scene where they are tracking the buffalo, stop the tape and reread this section.

After the buffalo stampeded through, the range literally looked plowed. This is a natural phenomena called herd effect. When animals are spread out and calm, their hooves tend to compact the soil. When they are concentrated and excited, they tend to knock down old standing vegetation and break up the soil.

Herd effect will not happen just by increasing stock density. To achieve this effect it is usually necessary to stimulate animals in some way. It can be done by herding through or feeding on the area where you want this impact.

Evaluating Methods for Performing

Final Status Surveys for Land Areas at the Hematite Facility

April 2006

Prepared by:

Wayne C. Gaul, Ph.D, CHP, CHMM
Claude M. Wiblin, CHP
J. Stewart Bland, CHP

DO-06-003

CHESAPEAKE NUCLEAR SERVICES, INC.
A J.STEWART BLAND COMPANY

788 Sonne Drive, Annapolis, MD 21401
Phone: 410-266-9174 FAX: 410-266-5811 www.chesnuc.com

Table of Contents

Page

1. Executive Summary 1
2. Introduction and Scope 3
3. References 3
4. Radionuclide Distribution 4
4.1 Expected Distribution of Radionuclides of Interest 6
4.2 Expected Distribution within the Limestone Fill 7
4.3 Expected Distribution within the Sediment 7
4.4 Expected Distribution on the Surface 7
4.4.1 Expected Distribution in Surface Locations with BD Prefix 8
4.4.2 Expected Distribution in Surface Locations with BP Prefix 8
4.4.3 Expected Distribution in Surface Locations with CB Prefix 8
4.4.4 Expected Distribution in Surface Locations with DM Prefix 9
4.4.5 Expected Distribution in Surface Locations with EP Prefix 9
4.4.6 Expected Distribution in Surface Locations with GS Prefix 10
4.4.7 Expected Distribution in Surface Locations with LF Prefix 10
4.4.8 Expected Distribution in Surface Locations with NB Prefix 10
4.4.9 Expected Distribution in Surface Locations with OA Prefix 11
4.4.10 Expected Distribution in Surface Locations with PL Prefix 11
4.4.11 Expected Distribution in Surface Locations with RR Prefix 11
4.4.12 Expected Distribution in Surface Locations with SW Prefix 12
4.5 Expected Distribution for the Sub-Surface Soil 12
4.5.1 Expected Distribution in Sub-surface Locations With BLD Prefix 12
4.5.2 Expected Distribution in Sub-surface Locations with BD Prefix 13
4.5.3 Expected Distribution in Sub-surface Locations with BP Prefix 13
4.5.4 Expected Distribution in Sub-surface Locations with CB Prefix 13
4.5.5 Expected Distribution in Sub-surface Locations with DM Prefix 14
4.5.6 Expected Distribution in Sub-surface Locations with EP Prefix 14
4.5.7 Expected Distribution in Sub-surface Locations with LF Prefix 14
4.5.8 Expected Distribution in Sub-surface Locations with NB Prefix 15
4.5.9 Expected Distribution in Sub-surface Locations with OA Prefix 15
4.5.10 Expected Distribution in Sub-surface Locations with PL Prefix 15
4.5.11 Expected Distribution in Sub-surface Locations with RR Prefix 16
4.5.12 Expected Distribution in Sub-surface Locations with SW Prefix 16
4.6 Summary of Site Radionuclide Distribution and Spatial Variability 16
5.0 Instruments and Final Status Survey Requirements 19
6.0 Detector Efficiency Modeling 21
6.1 Detector Characteristics 21
6.2 Detector Modeling 26
6.2.1 Sodium Iodide (NaI(Tl)) Detectors 26
6.2.2 High Purity Germanium (HpGe) Detector 27
6.2.3 Cadmium Zinc Telluride (CdZnTe) Detector 27

6.2.4 FIDLER Model 28
7.1 Detector Response to Individual Nuclides 29
7.1.1 Am-241 29
7.1.2 Np-237 and Short Lived Daughters 30
7.1.3 U-234 31
7.1.4 U-235 plus Short Lived Daughters 32
7.1.5 U-238 plus Short Lived Daughters 33
7.1.6 Pu-239 35
7.1.7 Th-232 plus Entire Decay Chain 35
7.2 Limestone Fill Area 38
7.3 Sediment Area 39
7.4 Surface Area 41
7.5 Sub Surface Area 42
8.0 Surrogate Scanning Radionuclides 43
9.0 Detector Response Evaluations 48
9.1 Detector Response 48
9.2 Limestone Fill and Sediment Areas 48
9.3 Surface Area 49
9.4 Sub-Surface Area 50
10.0 Scan Minimum Detectable Levels 52
10.1 Minimum Detectable Count Rate (MDCR) 52
10.2 Minimum Detectable Activity Level 54
11.0 Conclusions 59

1. EXECUTIVE SUMMARY

This evaluation report investigates methods and instruments capable of performing the final status survey for the Hematite Former Fuel Cycle Facility (Hematite). This evaluation is needed because the identified radionuclides are not readily detected using conventional methods due to the low energy photons and the low decay abundance. The varying mix of radionuclides throughout the facility has been evaluated as part of the site characterization. These data were used for establishing the distribution of radionuclide contaminants for the different areas of the site. The distributions showed that the principal radionuclide(s) that contributed to the total contamination and DCGL contribution varied significantly in different areas. Examining the decay characteristics, it was identified that U-235 and U-238 were the likely radionuclides to be used as surrogates for performing the radiation scan as required by MARSSIM for final status surveys. Therefore modeling was performed such that an accurate representation of a detector's ability to respond to the radiation throughout the site could be determined. All photons from the radionuclides were modeled; however, the most prominent photons were used to determine if an energy window could be used to enhance detector performance for the radionuclide mix.

Numerous detectors were evaluated for modeling and, based on a review of detection characteristics, four were selected for detailed modeling/evaluation. The detectors modeled were considered off the shelf instruments and included a Cadmium Zinc Telluride (CZT), Field Instrument to Detect Low Energy Radiation (FIDLER), High Purity Germanium (HpGe) and a more conventional 2" x 2" NaI(Tl). These detectors were chosen because the CZT is relatively new and has a high Z and has a good resolution; the FIDLER was chosen because it is designed to detect the low energies, which are abundant at the site; the HpGe was chosen because of its spectroscopic ability in an attempt to use it to advantage with this radionuclide mix; and the NaI was chosen because it is a field standard for final status surveys.

The Monte Carlo N-Particle (MCNP) radiation transport code, version 5, was used for establishing a correlation between a source, as defined by the radionuclide distribution in each area, and each detector. The modeling of source and detector geometry was used for establishing the corresponding detection efficiency. Different photon energy bins are established in the modeling at 5 keV intervals to be used for surrogate modeling. The actual primary and scatter energy spectra were calculated. The results of this modeling yielded correlations for the evaluated detectors in terms of counts per minute per pCi/g for all radionuclides of interest. This modeling included the key radionuclides identified at the Hematite site, including Np-237, U-234, U-235 and U-238, Th-232, Am-241 and Pu-239. Short-lived progeny were included. The contributions based on identified radionuclide abundances for specific areas at the site were evaluated for determining detector response as a function of gamma energy.

Knowing the detector's energy response characteristics (i.e., cpm per pCi/gm as a function of gamma energy), the efficiency of the detector can be determined for the radionuclide mix of a specific area. These data also support an evaluation of surrogate radionuclides to be used as indicators of relative activity. Using techniques detailed in MARSSIM, the minimum detectable count rate and the corresponding minimum detectable activity were determined for each detector and related to the specific area at the Hematite facility. It was found that use of U-235 and/or U-238 as surrogates were appropriate in the majority of areas. Observation intervals (scan speeds)

ranging from one to ten seconds were investigated to determine the different affect the different interval had on the ability of the detection percentage of the DCGL. This information gave an indication of what observation interval could be used for improving the detection levels while minimizing scan times.

Background count rates were varied from 500 cpm to 10,000 cpm to determine the percentage of the DCGL would pass at different observation intervals. The observation interval, in seconds, was plotted against percentage passing for different background count rates. This representation showed the effect on the minimum detectable activity for different scan observation intervals and different background levels. It also showed that there appears to be an optimum scan interval between 4 and 6 seconds for typical background levels. For example, it was calculated that at a scan observation interval of 4 seconds in a 2000 cpm background, the FIDLER with an appropriately set energy window should meet the MARSSIM scan criteria of <50% DCGL in 19 of the 28 areas used for evaluating the Hematite site. At 1000 cpm background and 10 second interval, 21 identified areas were modeled as meeting the criteria. This evaluation is used for illustrative purposes only since many areas did not appear to have sufficient soil sample data to provide reliable indication of radionuclide distribution. The results of these evaluations support a conclusion that setting an appropriate energy window on a FIDLER type detector greatly increases scanning efficiency (i.e., lower detection level) and can likely be used for performing MARSSIM scan surveys for most of the areas. Actual field studies are needed for refining the modeling, evaluating actual background levels, and demonstrating the capabilities of the recommended methods.

2. INTRODUCTION AND SCOPE

The Hematite facility presents a unique set of radionuclides which possess different concentrations and distribution throughout the site which pose problems in detection at levels that are considered protective of the health and safety of the public. Chesapeake Nuclear Services has performed an analysis of the site radiological characterization data and dose modeling to determine appropriate commercially available radiation detection instrumentation for performing the final status survey (FSS) of land areas throughout the site. This document is intended to provide the technical basis for selection of the instrumentation and determining the appropriate sensitivity to meet the final release criteria for the site.

3. REFERENCES

3.1 Westinghouse Electric Co., *Hematite Soil Survey Plan*, Rev. 1 (Draft), License SNM-33, Docket Number 70-36, January 2005.

3.2 Westinghouse Electric Co., *Hematite Decommissioning Plan*, Rev. 1, January 2005.

3.3 NUREG-1575, *Multi-Agency Radiation Survey and Site Investigation Manual* (MARSSIM), Rev. 1, August 2000.

3.4 NUREG-1757, *Consolidated NMSS Decommissioning Guidance*, Vol. 2, (2003).

3.5 J.F.Briesmeister, Editor, *MCNP[1]-A General Monte Carlo N-Particle Transport Code – Version 5*, Los Alamos National Laboratory report LA-UR-03-1987 (Revised June 30, 2004).
[1](MCNP is a registered trademark of the Regents of the University of California, Los Alamos National Laboratory).

3.6 "MCNP Homepage," http://laws.lanl.gov/x5/MCNP/index.html (2004).

3.7 ICRU Report 53, Gamma-Ray Spectrometry in the Environment, December 1994, International Commission on Radiation Units and Measurements, Bethesda, MD.

3.8 Miller KM, et al; In Situ gamma ray spectrometry for the measurement of uranium in surface soils, Health Physics, 67:140-150; 1994.

3.9 Rybacek K, et al; In-situ determination of deposited radionuclide activity: Improved method using derived depth distributions from the measured photon spectra. Health Physics, 62: 519-528; 1992.

3.10 Stevenson KA, et al; Estimate of excess uranium in surface soil surrounding the feed materials production center using a requalified data base; Health Physics, 65: 283-287; 1993.

3.11 Marianno CM, et al; An Experimental Determination of Fidler scanning efficiency at specific speeds; Health Physics, 84(2): 197-202, Feb. 2003.

3.12 Abelquist, E. W., Scan MDCs for Multiple Radionuclides in Class 1 Areas, Health Physics, Supplement 3, S141-S146; 2003.

3.13 Nuclear Regulatory Commission, 1997, "Minimum Detectable Concentrations with Typical Radiation Survey Instruments for Various Contaminants and Field Conditions," NUREG/CR-1507, Final, NRC, Washington, DC.

3.14 Nuclear Regulatory Commission, 1998, "Human Performance of Radiological Survey Scanning," NUREG/CR-6364, NRC, Washington, DC.

4. RADIONUCLIDE DISTRIBUTION

The key radionuclides at the Hematite site are given in Reference 3.1. The values for the Derived Concentration Guidance Levels (DCGLs) of these key radionuclides are given in Table 4.1, which are each based on the 25 mrem/yr criterion. This gives the resulting dose at the peak year, based on the exposure model utilized, of 25 mrem for each radionuclide if the soil was contaminated to the level given in the table. It is therefore necessary to use the "sum-of-the-fractions" rule when a mixture of radionuclides is present. This necessarily reduces the allowable DCGL values for the radionuclides to allow for the mixture of radionuclides such that the sum-of-the-fractions for all the radionuclides present in the soil is less than one. The Characterization Data did not differentiate between Pu-239 and Pu-240; this report considers them all as Pu-239.

Table 4.1, Site-Specific, Radionuclide-Specific, Soil Derived Concentration Guidance Levels

Radionuclide	Units	DCGL	
		Surface Source	Volumetric Source
Am-241	pCi/g	117	40
Np-237+D	pCi/g	1.4	0.11
Pu-239	pCi/g	129	43
Tc-99	pCi/g	140	23
Th-232+C	pCi/g	2.9	1.5
U-234	pCi/g	518	188
U-235+D	pCi/g	63	35
U-238+D	pCi/g	224	127

"+D" = plus short-lived decay products
"+C" = plus entire decay chain (Th-232 assumed to be in equilibrium with Ra-228+D and Th-228+D)

The key radionuclides and the more abundant key gamma photons considered in the Hematite list of site specific radionuclides is given in Table 4.2. All decay characteristics of these nuclides are given in Appendix 1.

Table 4.2, Key Gammas for Radionuclides

Radionuclide	Energy, MeV	Decay Probability
Am-241	0.0139 0.02635 0.05954	42.7% 2.4% 35.9%
Np-237+D	0.0133 0.02937 0.0865	59.19% 13.99% 12.6%
Pa-233	0.0136 0.31198	48.9% 38.6%
U-233	0.013	3.9226%
Pu-239	0.0136 0.113	4.41% 0.05%
Th-232+C	0.0123	8.39%
Ra-228	0.00667	0.000621%
Ac-228	0.0130 0.3383 0.9111 0.9691	39.11% 11.36 27.7% 16.662%
Th-228	0.084371	1.21%
Ra-224	0.24098	3.95%
Pb-212	0.0748 0.0873 0.2386	8.04% 10.7% 44.65%
Bi-212	0.727	11.83%
Tl-208 (36%)	0.510 0.583 0.861 2.6147	21.6% 0.842% 0.125% 99.8%
U-234	0.0130 0.0532 0.1214	10.50% 0.12% 0.04%
U-235+D	0.013 0.1857	30.91% 54%
Th-231	0.0133 0.0842	70.8% 6.435%
Pa-231	0.0274 0.144	9.3% 10.5%
U-238+D	0.013	8.831%

Table 4.2, Key Gammas for Radionuclides		
Radionuclide	**Energy, MeV**	**Decay Probability**
	0.0664	0.097%
Th-234	0.0633	3.81%
	0.0768	0.128%
	0.0924	2.72%
	0.0928	2.688%
	0.1128	0.242
Pa-234m	0.0136	0.4433%
(99.84%)	0.0947	0.116%
	0.0984	0.187%
	0.766	0.21%
	0.926	0.3739%
	1.001	0.5891%
Pa-234	0.0947	0.025%
(0.16%)	0.0984	0.041%

"+D" = plus short-lived decay products
"+C" = plus entire decay chain (Th-232 assumed to be in equilibrium with Ra-228+D and Th-228+D)

4.1 Expected Distribution of Radionuclides of Interest

The distribution of primary interest is that which would be expected to exist in the soil remaining upon completion of the remediation work. This distribution may be different from the distribution associated with the most contaminated soil as these more elevated areas will probably be remediated. The data reviewed included sample results from the Limestone Fill, Sediment, Surface Soil, and Sub-surface Soil. The Limestone Fill, Sediment, Surface Soil and Sub-surface Soil areas were treated as volumetric sources. An attempt was made to subdivide data into 12 smaller areas for each of the Surface and Sub-surface areas.

For this review, any individual sample was considered remediated if it would result in an implied annual dose greater than 3.5 times the unity fraction DCGL (> 87.5 mrem). It is not unreasonable to expect that some multiples of the DCGL may remain and that concentration values of 3.5 times the unity DCGL may be in any mix. The "3.5" is not intended to bound future elevated area DCGL values and is only a review starting point. For some distributions, the removal of sample results would reduce the number available for review to three or fewer. In these instances, a remediation divisor was applied to individual results to reduce the overall DCGL factor to 1; assuming that remediation efforts had not changed the mix but did reduce the overall concentration.

In many instances, both alpha results and gamma results were reported for the same radionuclide concentration; the higher value was always used. Further, values below minimum detection limits were treated as real numbers. However, all resulting negative DCGLs multiples were set to zero.

4.2 Expected Distribution within the Limestone Fill

Table 4.3 represents the expected radionuclide distribution for the Limestone Fill area. A remediation divisor of 4.4 was applied to results for two of the three samples. Note there were no results for U-234 or Pu-239 for this area

Table 4.3, Radionuclide Distribution In Limestone Fill Area (pCi/g)

Statistics	Tc-99	U-235	U-238	Th-232	Am-241	Np-237
Minimum	21.3	0.00	0.43	0.02	0.0000	0.0000
Maximum	22.7	1.7	4.5	0.71	0.08	0.015
Mean	21.8	0.60	1.8	0.26	0.03	0.006
Median	21.4	0.12	0.5	0.04	0.00	0.004
Standard Deviation	0.8	0.9	2.3	0.40	0.05	0.008
# of Samples	3	3	3	3	3	3

4.3 Expected Distribution within the Sediment

Table 4.4 represents the expected radionuclide distribution for the Sediment area. One sample was removed as it had a multiple of about 6.5 times the DCGL.

Table 4.4, Radionuclide Distribution In Sediment Area (pCi/g)

Statistics	Tc-99	U-234	U-235	U-238	Th-232	Am-241	Np-237	Pu-239
Minimum	-0.23	0.25	0.02	0.29	0.01	-0.49	-7.10	0.000
Maximum	255	291	15	61	1.56	0.14	0.09	0.006
Mean	22.9	40.4	2.1	8.1	0.7	-0.1	-0.7	0.004
Median	1.5	1.3	0.2	1.0	0.6	0.0	0.0	0.004
Standard Deviation	67.6	95.3	4.8	18.2	0.4	0.2	1.9	0.003
# of Samples	14	14	14	14	14	14	14	4

4.4 Expected Distribution on the Surface

Table 4.5 is presented with all results to show the large distribution of concentrations for the surface area. Due to the large standard deviations and multiples of DCGLs, this area was further reviewed by location of sample identified by the first two letters of the sample identification location.

Table 4.5, Radionuclide Distribution in Surface Soil (pCi/g)

Statistics	Tc-99	U-234	U-235	U-238	Th-232	Am-241	Np-237	Pu-239
Minimum	-0.29	0.76	-0.29	-0.48	-0.05	-1.77	-39.60	-0.002
Maximum	17100	103	308	705	36.4	3.80	0.58	0.033
Mean	216	18.3	14.1	37.4	1.5	0.18	-1.39	0.008
Median	1.57	1.45	0.39	2.04	1.00	0.01	0.00	0.007
Standard Deviation	1623	36.0	44.2	111	4.37	0.70	4.53	0.008
# of Samples	115	9	115	115	115	115	115	30

4.4.1 Expected Distribution in Surface Locations with BD Prefix

Table 4.6 gives the results for the surface locations with the BD prefix. For this sub-area, a remediation divisor of 5.4 was applied to three of the four samples. Note that no results were available for U-234 and Pu-239.

Table 4.6, Radionuclide Distribution in Surface Soil Area with BD Prefix (pCi/g)

Statistics	Tc-99	U-234	U-235	U-238	Th-232	Am-241	Np-237	Pu-239
Minimum	3.52		3.63	4.26	0.06	0.03	-0.01	
Maximum	106		19	80	0.335	0.704	0.010	
Mean	57		11	41	0.197	0.351	0.006	
Median	59.75		11.31	39.37	0.19	0.33	0.01	
Standard Deviation	48		9	41	0	0	0.01	
# of Samples	4	0	4	4	4	4	4	0

4.4.2 Expected Distribution in Surface Locations with BP Prefix

Table 4.7 represents the expected radionuclide distribution for samples with the BP prefix. A remediation divisor was not applied to this data.

Table 4.7, Radionuclide Distribution in Surface Soil Area with BP Prefix (pCi/g)

Statistics	Tc-99	U-234	U-235	U-238	Th-232	Am-241	Np-237	Pu-239
Minimum	0.18	2.22	-0.22	1.03	0.59	-0.19	-3.25	0.002
Maximum	68.30	2.22	53.50	53.90	1.45	0.57	0.12	0.007
Mean	10.53	2.22	8.35	9.27	1.08	0.07	-0.30	0.005
Median	1.13	2.22	0.32	2.27	1.15	0.04	-0.04	0.007
Standard Deviation	21		18	17	0.27	0.21	0.98	0.003
# of Samples	11	1	11	11	11	11	11	3

4.4.3 Expected Distribution in Surface Locations with CB Prefix

There was only one sample identified with this prefix; the results are listed below in Table 4.8. Note that no results were available for U-234.

Table 4.8, Radionculide Distribution in Surface Soil Area with CB Prefix (pCi/g)

Location	Tc-99	U-234	U-235	U-238	Th-232	Am-241	Np-237	Pu-239
CB-01-00-SL	5.15		2.87	18.40	1.26	-0.14	0.01	0.002

4.4.4 Expected Distribution in Surface Locations with DM Prefix

There were only two samples for this sub-area, given in Table 4.9. Remediation divisors of 4.5 and 19 were applied to the results of sample numbers DM-01-00-SL and DM-02-00-SL; respectively. Note that no results were available for U-234 and Pu-239.

Table 4.9, Radionuclide Distribution in Surface Soil Area with DM Prefix (pCi/g)

Statistics	Tc-99	U-234	U-235	U-238	Th-232	Am-241	Np-237	Pu-239
Minimum	7.96		16.21	22.67	-0.01	0.15	0.003	
Maximum	8		53	24	1.7	0.51	0.005	
Mean	8		34.4	23.2	0.8	0.33	0.004	
Median	8.03		34.44	23.20	0.83	0.33	0.004	
Standard Deviation	0		25.8	1	1.18	0.25	0.002	
# of Samples	2	0	2	2	2	2	2	0

4.4.5 Expected Distribution in Surface Locations with EP Prefix

Table 4.10 represents the expected radionuclide distribution for samples with the EP prefix. Three samples were removed from consideration for exceeding the DCGLs with multiples of 8 to 124.

Table 4.10, Radionuclide Distribution in Surface Soil Area with EP Prefix (pCi/g)

Statistics	Tc-99	U-234	U-235	U-238	Th-232	Am-241	Np-237	Pu-239
Minimum	5.24	103	0.74	4.12	0.40	-0.06	-0.04	0.000
Maximum	219	103	96.50	92.30	1.91	1.04	0.58	0.030
Mean	87	103	22.03	44.15	1.16	0.39	0.15	0.011
Median	59.90	103	6.97	28.30	1.26	0.23	0.04	0.008
Standard Deviation	75		30.2	36.4	0.48	0.43	0.22	0.011
# of Samples	9	1	9	9	9	9	9	5

4.4.6 Expected Distribution in Surface Locations with GS Prefix

Table 4.11 represents the expected radionuclide distribution for samples with the GS prefix. Note that no results were available for U-234 and Pu-239. No individual sample result caused the DCGL to be exceeded.

Table 4.11, Radionuclide Distribution in Surface Soil Area with GS Prefix (pCi/g)

Statistics	Tc-99	U-234	U-235	U-238	Th-232	Am-241	Np-237	Pu-239
Minimum	-0.11		-0.18	-0.48	0.23	-0.10	-9.52	
Maximum	0.43		0.10	1.61	0.99	0.11	-1.30	
Mean	0.12		-0.06	0.67	0.73	-0.01	-5.03	
Median	0.02		-0.07	0.79	0.74	-0.01	-3.73	
Standard Deviation	0		0.1	1	0.31	0.09	3.40	
# of Samples	5	0	5	5	5	5	5	0

4.4.7 Expected Distribution in Surface Locations with LF Prefix

Table 4.12 represents the expected radionuclide distribution for samples with the LF prefix. Note that no results were available for U-234 and Pu-239. No individual sample result caused the DCGL to be exceeded.

Table 4.12, Radionuclide Distribution in Surface Soil Area with LF Prefix (pCi/g)

Statistics	Tc-99	U-234	U-235	U-238	Th-232	Am-241	Np-237	Pu-239
Minimum	0.90		0.12	0.52	0.31	-0.11	-6.69	
Maximum	12		1	2	1.4	0.30	0.13	
Mean	5		0.3	1.4	0.9	0.05	-1.33	
Median	2.38		0.28	1.23	0.79	0.03	-0.03	
Standard Deviation	5		0.2	1	0.44	0.15	3.00	
# of Samples	5	0	5	5	5	5	5	0

4.4.8 Expected Distribution in Surface Locations with NB Prefix

Table 4.13 represents the expected radionuclide distribution for samples with the NB prefix. Note that no results were available for U-234 and Pu-239. No individual sample result caused the DCGL to be exceeded.

Table 4.13, Radionuclide Distribution in Surface Soil Area with NB Prefix (pCi/g)

Statistics	Tc-99	U-234	U-235	U-238	Th-232	Am-241	Np-237	Pu-239
Minimum	-0.29	0.76	-0.29	-0.45	0.13	-0.63	-10.60	0.00
Maximum	13	52	3	10	1.5	0.54	0.12	0.03
Mean	1	9.6	0.3	1.8	0.9	0.01	-1.19	0.01
Median	0.40	1.10	0.16	1.50	1.00	0.00	0.00	0.01
Standard Deviation	3	20.9	0.7	2	0.35	0.21	2.54	0.01
# of Samples	27	9	115	115	115	115	115	30

4.4.9 Expected Distribution in Surface Locations with OA Prefix

Table 4.14 represents the expected radionuclide distribution for samples with the OA prefix. Four samples were removed from consideration for exceeding the DCGLs by multiples of 3.8 to 5.1.

Table 4.14, Radionuclide Distribution in Surface Soil Area with OA Prefix (pCi/g)

Statistics	Tc-99	U-234	U-235	U-238	Th-232	Am-241	Np-237	Pu-239
Minimum	0.15	1.93	0.00	-0.47	0.12	-0.55	-12.00	0.001
Maximum	109	1.93	39	165	1.4	0.98	0.14	0.01
Mean	14	1.93	2.7	10.7	0.9	-0.04	-0.99	0.01
Median	1.57	1.93	0.35	1.76	0.98	-0.04	0.00	0.01
Standard Deviation	27		7.7	32	0.28	0.28	2.43	0.00
# of Samples	33	1	33	33	33	33	33	8

4.4.10 Expected Distribution in Surface Locations with PL Prefix

Table 4.15 represents the expected radionuclide distribution for samples with the PL prefix. Note that no results were available for U-234 and only one for Pu-239. No individual sample result caused the DCGL to be exceeded.

Table 4.15, Radionuclide Distribution in Surface Soil Area with PL Prefix (pCi/g)

Statistics	Tc-99	U-234	U-235	U-238	Th-232	Am-241	Np-237	Pu-239
Minimum	1.58		0.04	1.35	0.82	-0.08	-4.08	0.01
Maximum	38		2	8	1.4	0.07	0.00	0.01
Mean	14		1.0	3.8	1.1	0.02	-1.37	0.01
Median	2.96		0.39	2.04	1.22	0.06	-0.04	0.01
Standard Deviation	21		1.3	4	0.28	0.09	2.35	
# of Samples	3	0	3	3	3	3	3	1

4.4.11 Expected Distribution in Surface Locations with RR Prefix

Table 4.16 represents the expected radionuclide distribution for samples with the RR prefix. Note that no results were available for U-234 and only one for Pu-239. Only one individual sample result caused the DCGL to be exceeded by a factor of about 2.7.

Table 4.16, Radionuclide Distribution in Surface Soil Area with RR Prefix (pCi/g)

Statistics	Tc-99	U-234	U-235	U-238	Th-232	Am-241	Np-237	Pu-239
Minimum	0.18		0.58	1.03	1.41	0.18	-0.01	0.00
Maximum	15		58	248	1.7	0.86	0.11	0.00
Mean	6		19.8	84.6	1.5	0.43	0.07	0.00
Median	1.76		0.83	4.87	1.42	0.25	0.11	0.00
Standard Deviation	8		33.0	141	0.14	0.37	0.07	
# of Samples	3	0	3	3	3	3	3	1

4.4.12 Expected Distribution in Surface Locations with SW Prefix

Table 4.17 represents the expected radionuclide distribution for samples with the RR prefix. Note that no results were available for U-234 and only one for Pu-239. Only one individual sample result caused the DCGL to be exceeded slightly by a factor of about 1.02.

Table 4.17, Radionuclide Distribution in Surface Soil Area with SW Prefix (pCi/g)

Statistics	Tc-99	U-234	U-235	U-238	Th-232	Am-241	Np-237	Pu-239
Minimum	0.37		0.25	1.30	0.73	-0.29	-0.03	0.01
Maximum	22		12	32	1.6	0.01	0.10	0.01
Mean	10		3.8	11.2	1.3	-0.15	0.04	0.01
Median	9.60		1.60	5.77	1.35	-0.17	0.05	0.01
Standard Deviation	12		5.5	14	0.39	0.15	0.06	
# of Samples	4	0	4	4	4	4	4	1

4.5 Expected Distribution for the Sub-Surface Soil

Table 4.18 is presented with all results to show the large distribution of concentrations for the sub-surface area. Due to the large standard deviations and multiples of DCGLs, this area was further reviewed by location of sample identified by the first two or three letters of the sample identification location.

Table 4.18, Radionuclide Distribution in Sub-surface Soil (pCi/g)

Statistics	Tc-99	U-234	U-235	U-238	Th-232	Am-241	Np-237	Pu-239
Minimum	-0.83	0.49	-0.54	-1.90	-0.09	-0.72	-17.80	-0.01
Maximum	131	315	18	71	174	15	0.353	8
Mean	1.45	30.87	0.37	1.54	1.32	0.03	-1.61	0.20
Median	0.33	1.08	0.12	0.83	0.94	0.00	-0.04	0.00
Standard Deviation	7.48	79.10	1.59	4.92	8.79	0.79	3.05	1.22
# of Samples	353	31	381	381	389	404	381	45

4.5.1 Expected Distribution in Sub-surface Locations With BLD Prefix

Table 4.19 represents the expected radionuclide distribution for samples with the BLD prefix. One sample was removed from consideration for exceeding the DCGL by a multiple of about 4.3.

Table 4.19, Radionuclide Distribution in Sub-surface Soil Area with BLD Prefix (pCi/g)

Statistics	Tc-99	U-234	U-235	U-238	Th-232	Am-241	Np-237	Pu-239
Minimum	7.50	17.80	-0.40	-0.57	0.11	-0.29	0.000	-0.009
Maximum	7.50	188.00	17.90	71.00	1.31	0.70	0.008	0.008
Mean	7.50	102.90	1.82	6.55	0.75	0.05	0.002	0.002
Median	7.50	102.90	0.44	1.70	0.87	0.01	0.002	0.003
Standard Deviation		120.35	3.72	13.39	0.42	0.19	0.002	0.004
# of Samples	1	2	29	29	36	36	15	18

4.5.2 Expected Distribution in Sub-surface Locations with BD Prefix

Table 4.20 represents the expected radionuclide distribution for samples with the BD prefix. One sample was removed from consideration for exceeding the DCGL by a multiple of about 3.9.

Table 4.20, Radionuclide Distribution in Sub-surface Soil Area with BD Prefix (pCi/g)

Statistics	Tc-99	U-234	U-235	U-238	Th-232	Am-241	Np-237	Pu-239
Minimum	-0.01	1.08	-0.37	-0.25	0.63	-0.18	-9.11	0.003
Maximum	1.61	1.73	0.55	2.15	1.52	0.27	0.094	0.003
Mean	0.55	1.35	0.15	0.90	1.05	0.00	-1.11	0.003
Median	0.43	1.24	0.22	0.97	1.10	-0.02	-0.05	0.003
Standard Deviation	0.50	0.34	0.25	0.56	0.28	0.14	2.41	
# of Samples	16	3	16	16	16	16	16	1

4.5.3 Expected Distribution in Sub-surface Locations with BP Prefix

Table 4.21 represents the expected radionuclide distribution for samples with the BP prefix. Note that no results were available for Pu-239.

Table 4.21, Radionuclide Distribution in Sub-surface Soil Area with BP Prefix (pCi/g)

Statistics	Tc-99	U-234	U-235	U-238	Th-232	Am-241	Np-237	Pu-239
Minimum	-0.83	0.94	-0.26	-1.29	0.17	-0.41	-9.08	
Maximum	4	1	1	2	1	1	0.052	
Mean	0.30	0.94	0.13	0.72	0.96	-0.06	-2.30	
Median	0.05	0.94	0.11	0.90	1.01	-0.05	-0.43	
Standard Deviation	1.02		0.23	0.70	0.30	0.24	2.95	
# of Samples	28	1	28	28	28	28	28	0

4.5.4 Expected Distribution in Sub-surface Locations with CB Prefix

Table 4.22 represents the expected radionuclide distribution for samples with the CB prefix. Note that no results were available for Pu-239.

Table 4.22, Radionuclide Distribution in Sub-surface Soil Area with CB Prefix (pCi/g)

Statistics	Tc-99	U-234	U-235	U-238	Th-232	Am-241	Np-237	Pu-239
Minimum	0.04	2.48	0.14	-0.86	0.78	-0.16	-0.04	
Maximum	1	2	0	1	2	0	0.026	
Mean	0.32	2.48	0.28	0.39	1.17	-0.03	0.00	
Median	0.13	2.48	0.28	0.89	1.07	-0.10	0.00	
Standard Deviation	0.41		0.14	1.09	0.45	0.17	0.03	
# of Samples	3	1	3	3	3	3	3	0

4.5.5 Expected Distribution in Sub-surface Locations with DM Prefix

Table 4.21 represents the expected radionuclide distribution for samples with the DM prefix. Note the different amount of samples with U-234 and Pu-239 results.

Table 4.21, Radionuclide Distribution in Sub-surface Soil Area with DM Prefix (pCi/g)

Statistics	Tc-99	U-234	U-235	U-238	Th-232	Am-241	Np-237	Pu-239
Minimum	-0.44	0.49	-0.54	-1.90	-0.09	-0.72	-17.30	-0.001
Maximum	7.49	1.70	0.77	2.74	1.70	0.73	0.162	-0.001
Mean	0.35	0.87	0.08	0.66	0.79	-0.02	-1.66	-0.001
Median	0.26	0.83	0.10	0.69	0.83	0.00	-0.05	-0.001
Standard Deviation	0.65	0.30	0.22	0.70	0.41	0.20	3.13	
# of Samples	207	11	207	207	207	207	207	1

4.5.6 Expected Distribution in Sub-surface Locations with EP Prefix

Table 4.22 represents the expected radionuclide distribution for samples with the EP prefix. One sample result was removed from considerations for exceeding the DCGL by a multiple of about seven.

Table 4.22, Radionuclide Distribution in Sub-surface Soil Area with EP Prefix (pCi/g)

Statistics	Tc-99	U-234	U-235	U-238	Th-232	Am-241	Np-237	Pu-239
Minimum	0.06	2.42	-0.27	-1.87	0.06	-0.45	-17.80	-0.001
Maximum	17	3	2	11	2	1	0.135	0.007
Mean	5.41	2.55	0.29	1.99	1.05	0.05	-2.60	0.004
Median	3.84	2.55	0.11	1.17	1.07	-0.01	-0.18	0.005
Standard Deviation	4.77	0.18	0.54	3.26	0.36	0.27	4.17	0.004
# of Samples	28	2	28	28	28	28	28	3

4.5.7 Expected Distribution in Sub-surface Locations with LF Prefix

Table 4.23 represents the expected radionuclide distribution for samples with the LF prefix. Only one sample had results for U-234 and Pu-239.

Table 4.23, Expected Distribution in Sub-surface Soil Area with LF Prefix (pCi/g)

Statistics	Tc-99	U-234	U-235	U-238	Th-232	Am-241	Np-237	Pu-239
Minimum	0.14	5.62	-0.28	-0.44	0.31	-0.71	-12.90	0.004
Maximum	4	6	0	2	1	0	0.212	0.004
Mean	1.27	5.62	0.09	0.73	0.88	-0.13	-2.20	0.004
Median	0.60	5.62	0.14	0.72	1.01	-0.12	-0.26	0.004
Standard Deviation	1.55		0.21	0.76	0.35	0.24	3.51	
# of Samples	16	1	16	16	16	16	16	1

4.5.8 Expected Distribution in Sub-surface Locations with NB Prefix

Table 4.24 represents the expected radionuclide distribution for samples with the NB prefix. One sample was removed from consideration for exceeding the DCGL by a multiple of about 3.7.

Table 4.24, Radionuclide Distribution in Sub-surface Soil Area with NB Prefix (pCi/g)

Statistics	Tc-99	U-234	U-235	U-238	Th-232	Am-241	Np-237	Pu-239
Minimum	-0.44	0.49	-0.54	-1.90	-0.09	-0.72	-17.30	-0.001
Maximum	7.49	1.70	0.77	2.74	1.70	0.73	0.162	-0.001
Mean	0.35	0.87	0.08	0.66	0.79	-0.02	-1.66	-0.001
Median	0.26	0.83	0.10	0.69	0.83	0.00	-0.05	-0.001
Standard Deviation	0.65	0.30	0.22	0.70	0.41	0.20	3.13	
# of Samples	207	11	207	207	207	207	207	1

4.5.9 Expected Distribution in Sub-surface Locations with OA Prefix

Table 4.25 represents the expected radionuclide distribution for samples with the OA prefix. Note that no results were available for Pu-239.

Table 4.25, Radionuclide Distribution in Sub-surface Soil Area with OA Prefix (pCi/g)

Statistics	Tc-99	U-234	U-235	U-238	Th-232	Am-241	Np-237	Pu-239
Minimum	-0.44	0.75	-0.25	0.10	0.39	-0.15	-2.64	
Maximum	1.67	0.75	0.32	2.05	1.61	0.12	0.121	
Mean	0.45	0.75	0.12	1.11	1.08	-0.01	-0.88	
Median	0.37	0.75	0.12	0.90	1.17	-0.01	-0.39	
Standard Deviation	0.69		0.18	0.68	0.37	0.09	1.09	
# of Samples	8	1	8	8	8	8	8	0

4.5.10 Expected Distribution in Sub-surface Locations with PL Prefix

Table 4.26 represents the expected radionuclide distribution for samples with the PL prefix. Note there is only one sample with Pu-239.

Table 4.26, Radionuclide Distribution in Sub-surface Soil Area with PL Prefix (pCi/g)

Statistics	Tc-99	U-234	U-235	U-238	Th-232	Am-241	Np-237	Pu-239
Minimum	-0.05	1.08	-0.15	-1.09	0.03	-0.63	-6.85	0.00
Maximum	4.54	4.44	0.64	1.71	1.39	0.33	0.086	0
Mean	0.95	2.76	0.15	0.32	0.92	-0.08	-2.13	0.00
Median	0.71	2.76	0.08	0.29	1.04	-0.09	-0.82	0.00
Standard Deviation	1.19	2.38	0.23	0.87	0.44	0.28	2.71	
# of Samples	12	2	12	12	12	12	12	1

4.5.11 Expected Distribution in Sub-surface Locations with RR Prefix

The following table represents the expected radionuclide distribution for samples with the RR prefix.

Table 4.27, Expected Distribution in Sub-surface Soil Area with RR Prefix (pCi/g)

Statistics	Tc-99	U-234	U-235	U-238	Th-232	Am-241	Np-237	Pu-239
Minimum	0.08	0.75	0.06	-0.38	0.67	-0.04	-2.64	0.00
Maximum	0	3	1	1	1	1	0.072	0
Mean	0.17	1.78	0.21	0.60	0.99	0.26	-0.43	0.00
Median	0.12	1.78	0.16	0.55	1.02	0.22	0.02	0.00
Standard Deviation	0.11	1.45	0.18	0.66	0.24	0.25	1.09	
# of Samples	6	2	6	6	6	6	6	1

4.5.12 Expected Distribution in Sub-surface Locations with SW Prefix

Table 4.28 represents the expected radionuclide distribution for samples with the RR prefix. Note that no results were available for Pu-239. One sample was removed from consideration for exceeding the DCGL by a multiple of about 5.

Table 4.28, Radionuclide Distribution in Sub-surface Soil Area with SW Prefix (pCi/g)

Statistics	Tc-99	U-234	U-235	U-238	Th-232	Am-241	Np-237	Pu-239
Minimum	0.01	0.87	-0.42	-0.52	-0.16	-0.47	-9.18	
Maximum	0.91	1	0.53	2.95	1.41	0.24	0.107	
Mean	0.39	1	0.13	1.07	1.01	-0.06	-2.46	
Median	0.40	1	0.11	1.14	1.08	-0.05	-0.04	
Standard Deviation	0.25		0.27	1.03	0.38	0.19	3.52	
# of Samples	15	1	15	15	15	15	15	0

4.6 Summary of Site Radionuclide Distribution and Spatial Variability

Table 4.29 is the summary of the expected distributions giving the sum of the activity means for each area and the indicated fraction of each radionuclide for a specific area. The distribution is also given with the Tc-99 activity removed. Tables 4.30 and 4.31 give the expected distribution for the sub units within the surface and sub-surface areas. These tables indicate the total mean activities for the various areas across the site range from 1.5 to 286 pCi/g with the Tc-99 contribution, without the Tc-99 the activity ranges from 2.7 to 71.5 pCi/g. As a fraction of these mean activity totals, Tc-99 ranges from 4 to 89%, U-234 from 0 to 90%, U-235 from 1 to 22%, U-238 from 4 to 67%, Th-232 from 0.5 to 10%, Am-241 from 0 to 1%, Np-237 from 0 to 0.2%, and Pu-239 from 0.0 to 0.6%. These tables indicate a lack of U-234 data for several areas including those surface areas where U-234 could be of interest as concentrations were identified in several corresponding sub-surface areas. The following discrepancies must be noted: (a) no results were available for a corresponding surface area for the "BLD" sub-surface area, (b) no results were available for a corresponding sub-surface area for the "GS" (gas station) surface

area, however, no radiological issues are expected but chemical issues may be present, and (c) blank areas in the tables indicate that no results were provided for review. When the mean activity of a particular radionuclide result was a negative value it was considered as zero for this section of the report.

Table 4.29, Summary of Activity Distribution By Area

Area	Total of Mean Activities (pCi/g)	Fraction of Total of Mean Activities for Area Samples							
		Tc-99	U-234	U-235	U-238	Th-232	Am-241	Np-237	Pu-239
Limestone Fill	24.5	89.0%		2.4%	7.4%	1.1%	0.10%	0.024%	
w/o Tc-99	2.7			22.3%	66.8%	9.6%	1.1%	0.22%	
Sediment	74.2	30.9%	54.4%	2.8%	10.9%	0.94%	0.0%	0.0%	0.005%
w/o Tc-99	51.30		78.7%	4.1%	15.8%	1.4%	0.0%	0.0%	0.008%
Surface	286.1	75.1%	6.4%	4.9%	13.0%	0.5%	0.1%	0.0%	0.003%
w/o Tc-99	71.5		25.6%	19.7%	52.3%	2.1%	0.3%	0.0%	0.011%
Sub-Surface	35.8	4.1%	86.3%	1.0%	4.3%	3.7%	0.1%	0.0%	0.6%
w/o Tc-99	34.3		89.9%	1.08%	4.49%	3.85%	0.09%	0.00%	0.58%

Table 4.30, Summary of Activity Distributions of the Different Surface Areas

Area	Total of Mean Activities (pCi/g)	Fraction of Total of Mean Activities for Surface Samples							
		Tc-99	U-234	U-235	U-238	Th-232	Am-241	Np-237	Pu-239
BD	110.0	0.521		0.103	0.370	0.002	0.003	<0.001	
BP	31.5	0.334	0.070	0.265	0.294	0.034	0.002	<0.001	<0.001
CB	27.7	0.186		0.104	0.664	0.045	<0.001	<0.001	<0.001
DM	66.8	0.120		0.515	0.347	0.012	0.005	<0.001	
EP	257.8	0.337	0.400	0.085	0.171	0.005	0.002	0.001	<0.001
GS	1.5	0.077		0.000	0.442	0.481	<0.001	<0.001	
LF	7.2	0.629		0.048	0.193	0.123	0.007	<0.001	
NB	13.8	0.087	0.693	0.023	0.127	0.068	0.001	<0.001	0.001
OA	30.6	0.470	0.063	0.087	0.350	0.030	<0.001	<0.001	<0.001
PL	20.1	0.704		0.047	0.191	0.056	0.001	<0.001	<0.001
RR	112.0	0.050		0.177	0.756	0.013	0.004	0.001	<0.001
SW	26.8	0.391		0.142	0.418	0.047	<0.001	0.001	<0.001

Table 4.31, Summary of Distributions of the Different Sub-surface Areas									
Area	Total of Mean Activities (pCi/g)	Fraction of Total of Mean Activities for Sub-surface Samples							
		Tc-99	U-234	U-235	U-238	Th-232	Am-241	Np-237	Pu-239
BLD	119.6	0.063	0.860	0.015	0.055	0.006	<0.001	<0.001	
BD	4.0	0.137	0.337	0.038	0.225	0.262	<0.001	<0.001	0.001
BP	3.1	0.097	0.309	0.044	0.237	0.313	<0.001	<0.001	
CB	4.6	0.068	0.535	0.061	0.084	0.251	<0.001	<0.001	
DM	99.5	0.069	0.793	0.026	0.102	0.010	0.001	<0.001	<0.001
EP	11.3	0.477	0.224	0.026	0.176	0.093	0.004	<0.001	<0.001
LF	8.6	0.148	0.654	0.011	0.085	0.102	<0.001	<0.001	<0.001
NB	2.8	0.128	0.318	0.028	0.240	0.286	<0.001	<0.001	<0.001
OA	3.5	0.128	0.213	0.034	0.316	0.309	<0.001	<0.001	
PL	5.1	0.186	0.542	0.029	0.062	0.181	<0.001	<0.001	<0.001
RR	4.0	0.042	0.444	0.052	0.150	0.248	0.064	<0.001	<0.001
SW	3.5	0.111	0.250	0.039	0.309	0.290	<0.001	<0.001	

5.0 INSTRUMENTS AND FINAL STATUS SURVEY REQUIREMENTS

The Multi-Agency Radiation Survey and Site Investigation Manual (MARSSIM, Reference 3.3) provides information on planning, conducting, evaluating, and documenting building surface and surface soil final status radiological surveys. The MARSSIM contains information on planning final status survey measurements and the selection instruments (Chapter 4), field measurement methods and instrumentation (Chapter 6) and sampling and preparation for laboratory measurements (Chapter 7).

Instrumentation requirements in MARSSIM are general in scope leaving implementation to the user as indicated in paragraph 6.1 of MARSSIM: "Selecting instrumentation requires evaluation of both site and radionuclide specific parameters and conditions. Instruments should be stable and reliable under the environmental and physical conditions where they are used, and their physical characteristics (size and weight) should be compatible with the intended application. The instrument and measurement method should be able to detect the type of radiation of interest, and should, in relation to the survey or analytical technique, be capable of measuring levels that are less than the derived concentration guideline level (DCGL)." The guidance provides a thought process which if paralleled should provide acceptable end results regardless of the instruments selected for use.

Specific recommendations include:

> Scanning and direct measurement techniques should be capable of detecting levels below the established DCGLs- detection limits of 10-50% of the DCGL should be the target. (MARSSIM 6.2.2.6)
>
> Direct *in situ* measurements for photon emitting radionuclides are usually at a specified distance from the surface and for a specified period of time. A calibrated detector measures the fluence rate of primary photons at specific energies that are characteristic of a particular radionuclide. For outdoor measurements, the distribution profile of contaminants (even in the top six inches) must be evaluated and considered. (MARSSIM 6.4.1.1)

MARSSIM provides a discussion on scanning for photon emitters in soil by the use of sodium iodide survey meters (NaI(Tl)) detectors). This topic includes detector distance from the soil and movement of it in a serpentine pattern while walking to achieve a scan rate of 0.5 m/s (MARSSIM 6.4.2.1). Modeling using a radiation shielding or transport code of a small area of elevated activity is used to determine the net response. The dimensions of the soil slug, the density and the dose point above the surface are described in detail. (MARSSIM 6.7.2.1) NUREG-1507, Reference 3.4 provides a detailed example of how the scan MDC can be determined for enriched uranium.

Systematic measurements and sampling in conjunction with surface scanning are used to obtain adequate assurance that small areas of elevated radioactivity will satisfy the release criterion of the DCGL for elevated measurement comparison ($DCGL_{EMC}$). The procedure is applicable for all radionuclides (considers surrogate and related radionuclide such as Tc-99) and is

implemented for survey units classified as Class 1. Additional samples (measurements) may be needed when the concentration that can be detected by scanning, MDC_{scan}, is larger than the DCGL for wide areas ($DCGL_W$). If the MDC_{scan}, is larger than the $DCGL_W$, the number of samples or direct measurements will probably increase. This means more time and dollars spent in an individual survey unit. The method in section 5.5.2.4 of MARSSIM to determine whether additional samples are needed is the industry standard. Obviously, if scanning is a major factor in the final status survey, the lower the MDC_{scan}, the better.

6.0 DETECTOR EFFICIENCY MODELING

An evaluation of different type detectors that are commercially available for radionuclide identification and measurement by photon detection was performed. From an initial identification of detectors, those with identified characteristics that had capabilities for field application for the radionuclides of concern at Hematite were selected for detailed modeling and evaluation.

6.1 Detector Characteristics

The crystal that detects the radiation can be composed of a wide array of materials. Below is a general list of the most common materials available and a general discussion of the important properties of each material. Tables 6.1 and 6.2 give further characteristics.

NaI(Tl) scintillation crystals are used in most standard applications for detection of γ-radiation because of their unequalled high light output and the excellent match of the emission spectrum to the sensitivity of photomultiplier tubes, resulting in a good energy resolution. They can also be manufactured in large sizes.

CsI(Tl) has the advantage that it is non-hygroscopic, does not cleave and can be read out using silicon photodiodes instead of photomultiplier tubes. These Scintillator Photodiode Detectors are compact, very stable, do not require any high voltage, are rugged, and can be operated in high magnetic fields. Because of their compact size these detectors are frequently used in arrays or matrices in particle physics research.

CsI(Na) is a non-hygroscopic, moderately high light output scintillator mainly used for applications where mechanical stability and good energy resolution are required. Below 60° C it is an alternative to NaI(Tl) with a slightly decreased scintillation response, see Figure 6.1.

Bismuth germanate ($Bi_4Ge_3O_{12}$) has the extreme high density of 7.13 g /cm^3 and has a high Z value which makes these crystals very suited for the detection of natural radioactivity (U, Th, K), for high energy physics applications (high photofraction) or in compact Compton suppression spectrometers. They need to operate at low temperatures to optimize their efficiency as can be seen in Figure 6.1.

Figure 6.1, Temperature Dependence of the Scintillation Yield for NaI(Tl), CsI(Tl), and BGO
(adapted from Scionix Scintillation Detector Catalog, Scionix Holland B.V.)

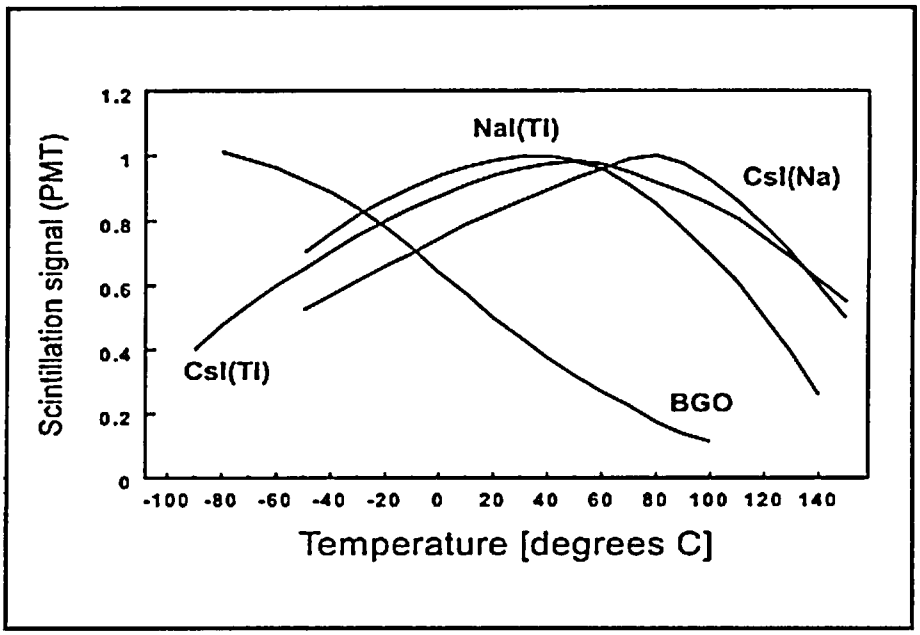

YAP:Ce is a high density (5.5 g/cm^3) oxide crystal with a decay time about 10 times shorter than NaI(Tl). It is used in detectors for high count rate (up to several MHz) X-ray spectrometry. The non-hygroscopic nature of this material allows the use of thin mylar entrance windows and guarantees a long lifetime of the detector.

CaF_2(Eu), europium doped calcium fluoride, is a low density scintillation crystal with a moderately high light output. Thanks to its low Z value it is well suited for the detection of electrons (beta particles) with a high efficiency (low backscatter fraction). CaF_2 (Eu) is a crystal that is also used in *phoswich* scintillation detectors in combination with NaI(Tl). The phoswich detector is used in the FIDLER.

Organic (plastic) scintillators consist of a transparent host material (a plastic) doped with a scintillating organic molecule (e.g. POPOP : p-bis [2-(5-phenyloxazolyl)] benzene). Radiation is absorbed by the host material, mostly via Compton effect because of the low density and Z-value of organic materials. Therefore, plastic scintillators are mostly used for the detection of β- and other particles. Furthermore plastic scintillators are mainly used when large detector volumes are required e.g. in security or health physics applications. The cost of large plastic scintillation detectors (per volume) is much lower than that of equivalent size NaI(Tl) detectors; plastic scintillators can be manufactured in meter long slabs.

Cadmium zinc telluride (CZT: CdZnTe) is a wide band gap semiconductor that is fabricated into detectors that provide two key advantages for use in portable instrumentation. The high density of the crystal provides excellent stopping power over a wide range of energies. The ability to operate at room temperature without the need for liquid nitrogen cooling allows the construction of compact devices. The resolution of CZT is intermediate between scintilators and Germanium devices. CZT detectors can be fabricated into a variety of shapes and small sizes making it possible to produce detectors capable of meeting the requirements of a wide assortment of applications unsupported by the other detector types.

High purity germanium (HpGe) detectors are semiconductor diodes having a p-i-n structure in which the intrinsic (I) region is sensitive to ionizing radiation, particularly x rays and gamma rays. Under reverse bias, an electric field extends across the intrinsic or depleted region. When photons interact with the material within the depleted volume of a detector, charge carriers (holes and electrons) are produced and are swept by the electric field to the P and N electrodes. This charge, which is in proportion to the energy deposited in the detector by the incoming photon, is converted into a voltage pulse by an integral charge sensitive preamplifier.

Since photoelectron statistics (or electron-hole pair statistics) plays a key role in the accurate determination of the energy of the radiation, the use of scintillation materials with a high light output is preferred for all spectroscopic applications. The scintillator emission wavelength should be matched to the sensitivity of the light detection device that is used (PMT or photodiode).

Table 6.1, Physical Characteristics

Material	Density [g/cm^3]	Emission Maximum [nm]	Decay Constant[1]	Refractive Index[2]	Conversion Efficiency[3]	Hygroscopic
NaI(Tl)	3.67	415	0.23 ms	1.85	100	yes
CsI(Tl)	4.51	550	0.6/3.4 ms	1.79	45	no
CsI(Na)	4.51	420	0.63 ms	1.84	85	slightly
CsI (undoped)	4.51	315	16 ns	1.95	4 - 6	no
CaF2 (Eu)	3.18	435	0.84 ms	1.47	50	no
^{6}LiI (Eu)	4.08	470	1.4 ms	1.96	35	yes
^{6}Li - glass	2.6	390 - 430	60 ns	1.56	4 - 6	no
CsF	4.64	390	3 - 5 ns	1.48	5 - 7	yes
BaF_2	4.88	315	0.63 ms	1.5	16	no
YAP (Ce)	5.55	350	27 ns	1.94	35 - 40	no
BGO	7.13	480	0.3 ms	2.15	15 - 20	no
$CdWO_4$	7.9	470 / 540	20 / 5 ms	2.3	25 - 30	no
Plastics	1.03	375 - 600	1 - 3 ms	1.58	25 - 30	no

(1) Effective average decay time for gammas, micro-seconds
(2) At the wavelength of maximum emission

(3) Relative scintillation signal at room temperature for gammas when coupled to a photomultiplier tube

Table 6.2, Commonly Used Scintillation Materials with Specific Applications

Material	Important Properties	Major Applications
NaI(Tl)	Very high light output, good energy resolution	General scintillation counting, health physics, environmental monitoring, high temperature use
CsI(Tl)	Non-hygroscopic, rugged, long wavelength emission	Particle and high energy physics, general radiation detection, photodiode readout, phoswiches
CsI(Na)	High light output, rugged	Geophysical, general radiation detection
CsI(undoped)	Fast, non-hygroscopic, radiation hard, low light output	Poor light output
CaF_2 (Eu)	Low Z, high light output	Beta detection, alpha/beta phoswiches
^{6}LiI(Eu)	High neutron cross-section, high light output	Thermal neutron detection and spectroscopy
^{6}Li - glass	High neutron cross-section, non-hygroscopic	Thermal neutron detection
BaF_2	Ultra-fast sub-ns UV emission	Positron life time studies, physics research, fast timing
YAP(Ce)	High light output, low Z, fast	MHz X-ray spectroscopy, synchrotron physics
BGO	High density and Z	Particle physics, geophysical research, PET, anti-Compton spectrometers, high natural background
$CdWO_4$	Very high density, low afterglow, radiation hard	DC measurement of X-rays (high intensity), readout with photodiodes, Computerized Tomography (CT)
Plastics	Fast, low density and Z, high light output	Particle detection, beta detection

After looking at the various detectors and detector configurations that could be developed with these materials the final modeling was done with just NaI(Tl), HpGe and the CdZnTe detectors.

Table 6.3, Reasoning Behind Not Modeling	
Material	**Reason Not Modeled**
CsI(Tl)	Relatively poor light output, small detector size
CsI(Na)	Small detector size
CsI(undoped)	Very poor light output greatly decreasing efficiency
CaF_2 (Eu)	Low Z, poor light output
^{6}LiI(Eu)	Poor light output
^{6}Li - glass	Very poor light output greatly decreasing efficiency
CsF	Very poor light output greatly decreasing efficiency
BaF_2	Poor light output greatly decreasing efficiency
YAP(Ce)	Small detector size
BGO	Poor light output, responds best at lower temperature
$CdWO_4$	Small detector size
Plastics	Poor light output and poor gamma sensitivity

6.2 Detector Modeling

MCNP Version 5, References 3.5 and 3.6, is a general purpose radiation transport computer code, which has been released to the Radiation Safety Information Computational Center. MCNP is developed and supported by the Eolus team at Los Alamos National Laboratory (LANL) to support Accelerated Strategic Computing Initiative (ASCI) projects. MCNP is a general-purpose Monte Carlo N–Particle code that can be used for neutron, photon, electron, or coupled neutron/photon/electron transport.

The actual primary and scatter energy spectrum was calculated. The amount of gammas that reached the detector was determined as the gamma flux across the detector face in gammas/sec/cm^2. This allowed the energy (MeV) deposited in the detector to be determined. With the amount of energy deposited the relative efficiency of the detector could be determined for the source term at a specific site. The model collected photon and electron interactions within the detector.

6.2.1 Sodium Iodide (NaI(Tl)) Detectors

Figure 6.3 shows the typical model used for the NaI detector scintillation detector. The assumption is that the housing and scintillation material is the same density throughout. The detector is a 2" tall by 2" diameter right circular cylinder. The density is given above. The thallium is doped at 0.02% uniform throughout the crystal.

Figure 6.3, Typical Scintillation Detector Geometry

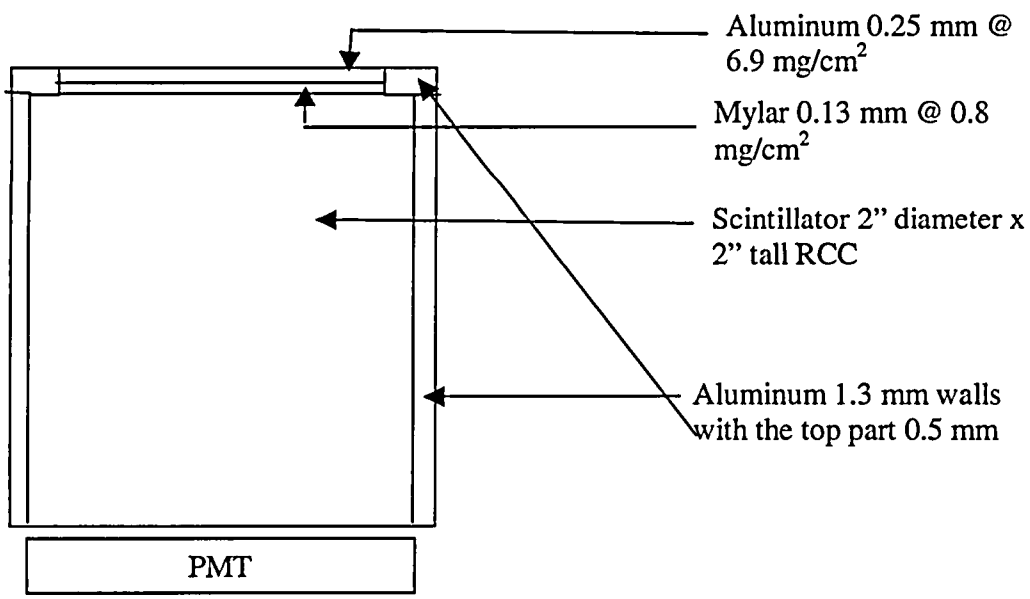

6.2.2 High Purity Germanium (HpGe) Detector

The HpGe detector was chosen as a field instrument because of its greater spectroscopy ability which may be needed to differentiate the Hematite radionuclides from background material. A shallow detector was chosen (3 cm thick) because it would be more sensitive to the low energy photons and help decrease Compton interference. The model was a right circular cylinder (RCC)3" diameter; radius = 3.81 cm and 3 cm tall. The aluminum support ring was 0.5 mm thick and 5mm wide. The aluminum encasing was a1.3 mm thick wall. The Germanium density was 5.33 g/cc, Al density was 2.7 g/cc, and the Beryllium window 0.2 mm thick with a density of 1.8 g/cc. See Figure 6.4.

Figure 6.4, Typical Germanium Detector Model

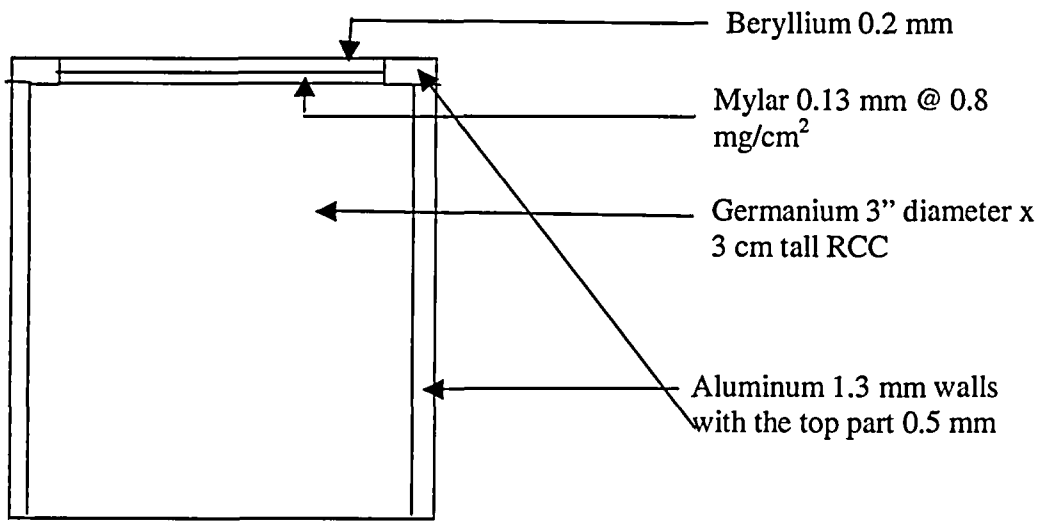

6.2.3 Cadmium Zinc Telluride (CdZnTe) Detector

The CdZnTe Co-Planar Grid (CPG) detector is made possible by recent advances in the CdZnTe detector manufacturing processes. The CPG electrode design provides the basis for a significant increase in the size and detection efficiency of CdZnTe detectors while achieving high energy resolution. These large volume CdZnTe detectors have the electrode geometry and charge collection efficiency to offer the high resolution necessary for nuclear spectroscopy. The CPG detectors are ideal for applications requiring high efficiency, high resolution, room temperature operation. Their compact size and rugged design allows their use in harsh or restrictive environments. The crystal density is 5.78 g/cm^3. They typically have a carbon fiber window which is 0.5 mm thick and a density thickness of 1.2.g/cm^2. These are smaller detectors and are modeled with the dimensions of Figure 6.5.

Figure 6.5, CdZnTe Detector Model

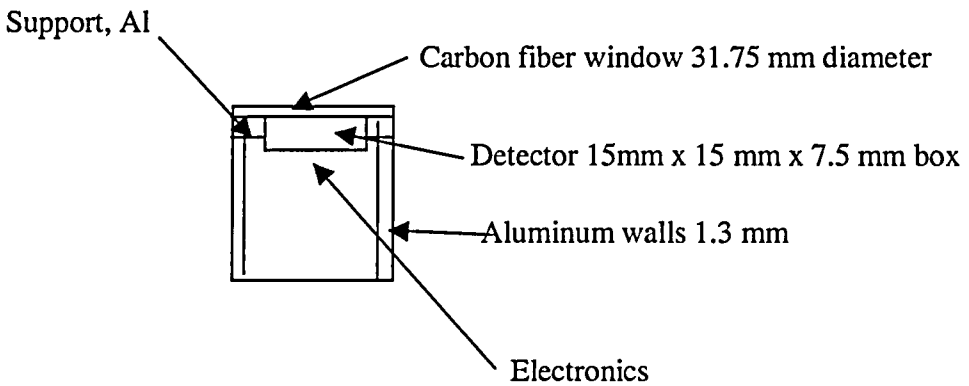

6.2.4 FIDLER Model

The FIDLER (Field Instrument to Detect Low-Energy Radiation) is a thin window, thin crystal NaI(Tl) detector. Its dimensions are 5 inch diameter with a thickness of 0.07 inches (127 mm X 1.67 mm right circular cylinder). It is encased in a 0.02 inch (0.50 mm) aluminum housing with a 0.10 inch beryllium window. It is specifically designed to detect low energy by being thin enough to let high energy photons pass through the crystal without detection. It can be used with a single channel analyzer set to a specific low energy from a specific radionuclide such as the 17 keV L X-ray from americium. It was modeled as described n Figure 6.6.

Figure 6.6, FIDLER Detector Model

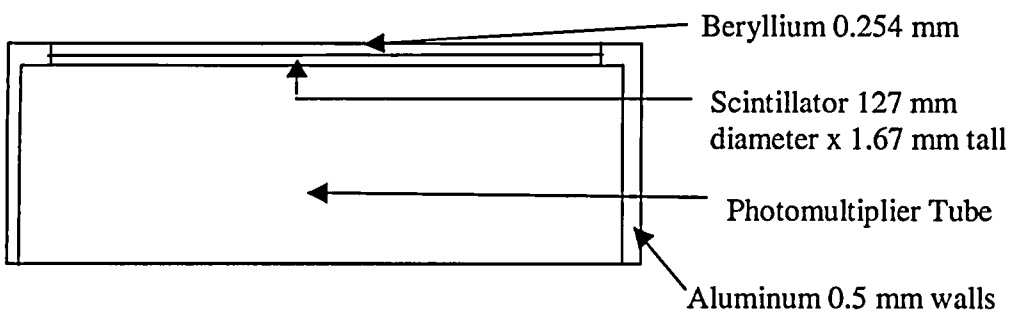

7.0 DETECTION LEVEL EVALUATION

To evaluate the response of the detector to the different radiations, each detector's response to the nuclides in Table 4.1 was modeled. The detectors were modeled at a ten centimeter height above the soil. The detector was looking down at the soil surface cylindrical area of elevated activity which was 0.25 m^2 with a radius of 28 cm. The depth of the area of elevated activity is 15 cm. This gave a soil volume of 0.0375 cubic meters. The soil density was 1.6 grams per cubic centimeter which gives a total soil mass of 60,000 grams. Where available, vendor data was used for the configuration of the detector materials and specifications. Due to the possibility of significant variation of radionuclides within the contaminated area each nuclide (with daughters) was modeled with the response of each proposed detector.

The source was defined as uniformly distributed radioactive emissions within a soil geometry. The chemical composition of soil was taken from ICRU Report 53, "Gamma-Ray Spectrometry in the Environment", Reference 3.7. Type 1 soil, as presented in Table 7.1 is that as used in ICRU Report 53 for its evaluations, considered typical soil. A typical soil density of 1.6 g/ml was assumed. The activity modeled was placed uniformly throughout the soil.

Table7.1, Soil Composition for ICRU Type 1 Soil

Element	Relative Weight Percents
H	2.2
C	< 0.1
O	57.5
N	< 0.1
Al	8.5
Si	26.2
Fe	5.6

7.1 Detector Response to Individual Nuclides

The detectors were modeled to determine the response to each individual radionuclide and the short lived daughter photons were added to Np-237, U-235, and U-238. The entire chain of radionuclides in the Th-232 chain was added to the Th-232 response.

7.1.1 Am-241

The response of each of the detectors modeled to Am 241 is given in Figure 7.1 and shows the response of the FIDLER and HpGe detectors are more responsive to these low energy photons. The small size of the CZT detector contributes significantly to the poor response. Setting a detector window from 40 to 65 keV would allow a preference of Am-241 photons to be detected.

Figure 7.1, Detector Response to Am-241

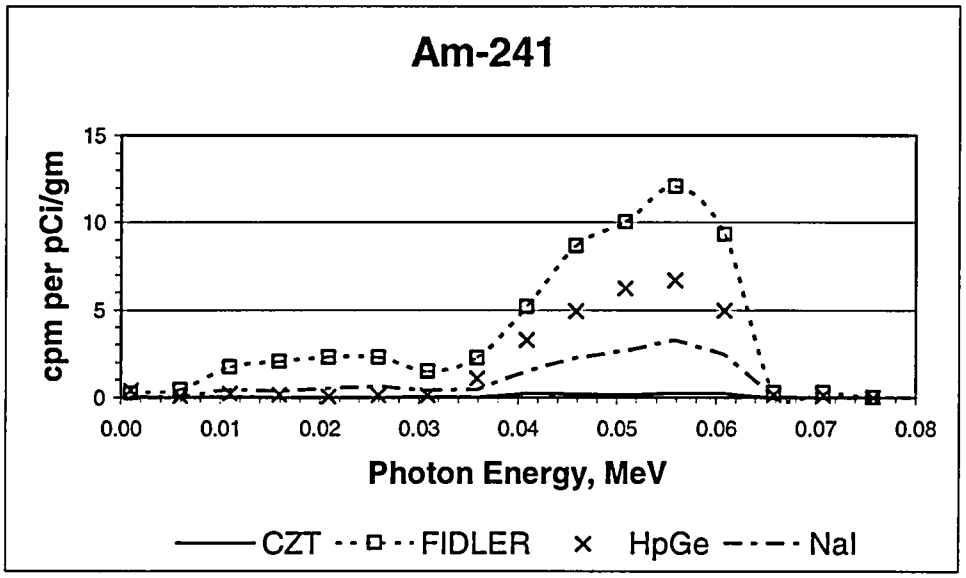

Looking at more detail on the makeup of the graph the most prominent photons were evaluated for their response within the energy bin that best describes the photon energy. This is given in Table 7.2.

Table 7.2, Specific Photon Energy Detector Response for Am-241

Am-241		Detector MCNP Results (cpm per pCi/gm)			
Photon Energy MeV	Probability of Decay	CZT	FIDLER	HpGe	NaI
0.0139	42.7%	0.00E+00	2.03E+00	1.52E-01	3.56E-01
0.026345	2.4%	0.00E+00	2.29E+00	1.27E-01	6.35E-01
0.059537	35.9%	2.54E-01	1.21E+01	6.71E+00	3.28E+00

7.1.2 Np-237 and Short Lived Daughters

The response of the different detectors to Np-237 and the immediate short lived daughters Pa-233 and U-233 is given in Figure 7.2. Note the response of the FIDLER and HpGe is better at the low energies. There is a slight contribution from the Pa-133 at the 0.31 MeV area for the HpGe detector. Setting a detector window between 60 and 110 keV would capture the majority of the Np-237 photons. The HpGe could have a window set at 300 to 320 keV.

Figure 7.2, Detector Response to Np-237 plus Daughters

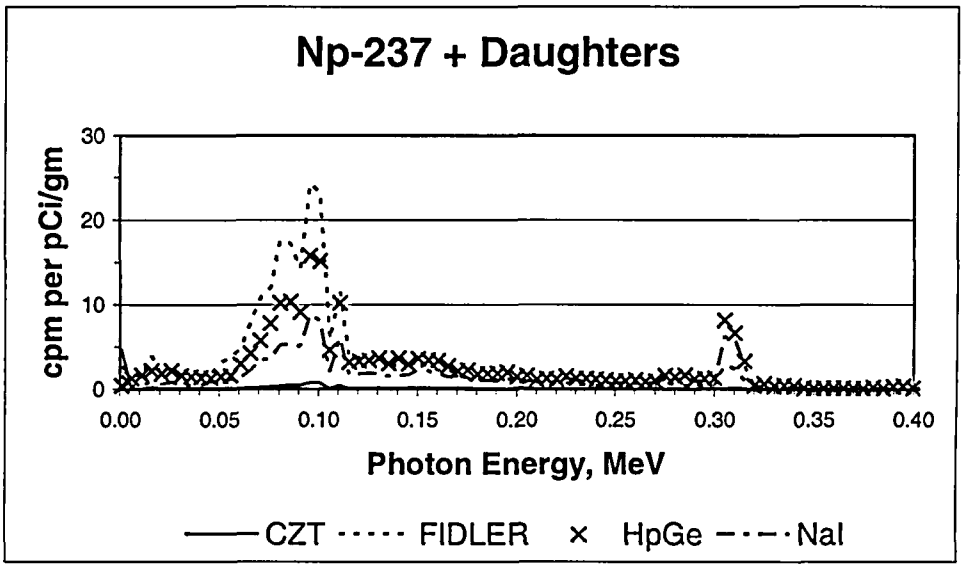

Looking at the most prevalent photons in the decay series their relative contribution is given in Table 7.3. The low energy photons have a much larger response with the 86.5 keV and.98.4 keV photons readily visible in the low energy range and the 312 keV photon detected in the higher energy range by the HpGe and NaI detectors.

Table 7.3, Specific Photon Energy Detector Response for Np-237 and Progeny

Np-237 + Pa-233 + U-233		Detector MCNP Results (cpm per pCi/gm)			
Photon Energy MeV	Probability of Decay	CZT	FIDLER	HpGe	NaI
0.0133	59.19%	Included below			
0.0136	48.92%	1.85E-01	3.90E+00	2.16E+00	7.65E-01
0.0294	13.99%	7.91E-02	2.21E+00	2.16E+00	8.17E-01
0.0865	12.60%	4.22E-01	1.72E+01	1.04E+01	5.33E+00
0.0947	10.84%	Included below			
0.0984	17.57%	6.86E-01	2.43E+01	1.58E+01	8.83E+00
0.3120	38.60%	7.91E-02	2.79E+00	8.20E+00	6.25E+00

7.1.3 U-234

The decay of U-234 is given in Figure 7.3 which shows several specific peaks for the FIDLER . The HpGe and NaI have a noticeable response also. The multiple peaks due to the contribution of the 0.013 MeV photon are easily identified. Looking at the graph would suggest several windows can be set for a detector, however, the relatively low cpm per pCi per gram suggests

significant contribution from background would interfere unless the U-234 concentration was high.

Figure 7.3, Detector Response to U-234

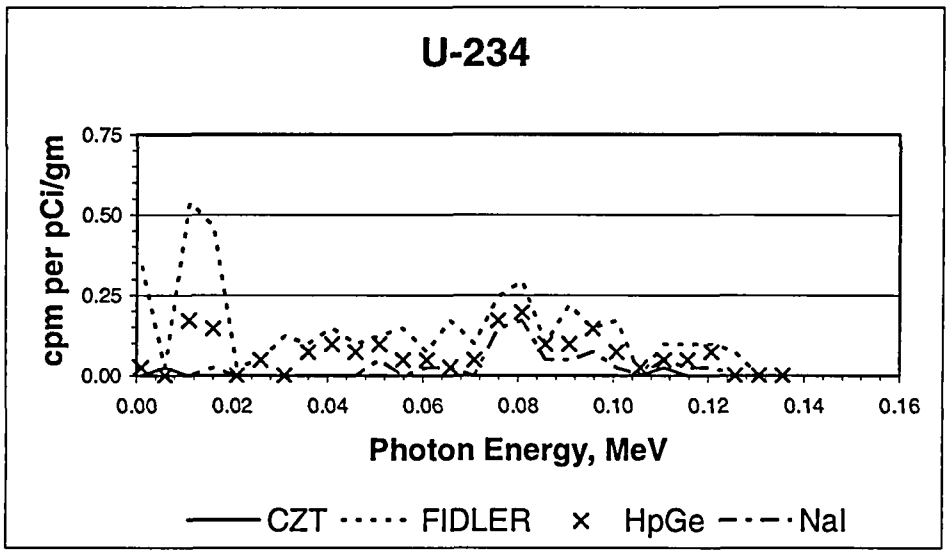

Looking at more detail on the makeup of the graph by looking at the individual photon response is given in Table 7.4. Due to the extremely low photon abundance all responses are lower and the CZT detector response was negligible.

Table 7.4, Specific Photon Energy Detector Response for U-234

U-234		Detector MCNP Results cpm per pCi/gm			
Photon Energy MeV	Probability of Decay	CZT	FIDLER	HpGe	NaI
0.0130	10.50%	0.00E+00	4.64E-01	1.46E-01	2.44E-02
0.0532	0.12%	0.00E+00	1.22E-01	9.76E-02	4.88E-02
0.1214	0.04%	0.00E+00	9.76E-02	7.32E-02	2.44E-02

7.1.4 U-235 plus Short Lived Daughters

The decay of U-235 and the immediate short lived daughters Th-231 and Pa-231 is given in Figure 7.4. The 185 keV photon presents a recognizable peak and would be appropriate to set a detector window at 180 to 190 keV.

Figure 7.4, Detector Response to U-235 plus Daughters

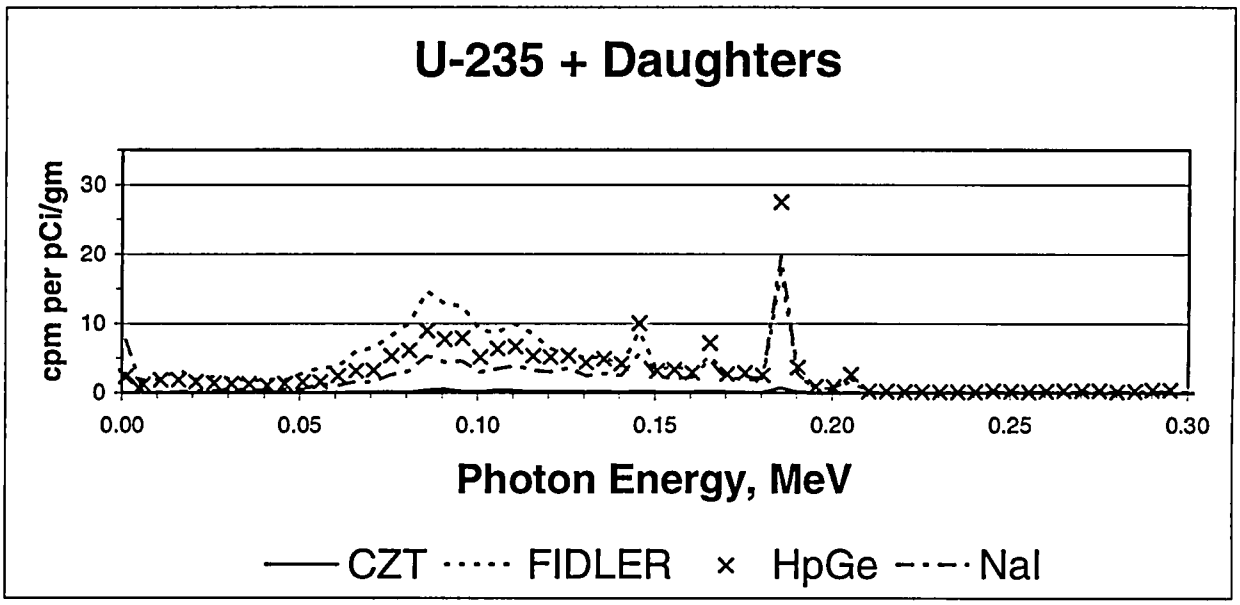

A more detailed response per photon is given in Table 7.5. The large response of the HpGe to the 0.186 MeV peak is particularly noticeable, with good response from the FIDLER and NaI detectors also.

Table 7.5, Specific Photon Energy Detector Response for U-235

U-235 + Th-231 + Pa-231		Detector MCNP Results cpm per pCi/gm			
Photon Energy MeV	Probability of Decay	CZT	FIDLER	HpGe	NaI
0.013	30.9%	Included below			
0.0133	70.8%	1.04E-01	3.73E+00	2.37E+00	1.07E+00
0.027	9.3%	5.22E-02	2.32E+00	1.38E+00	3.13E-01
0.084	6.4%	4.17E-01	1.47E+01	9.00E+00	5.29E+00
0.144	10.50%	2.61E-01	8.84E+00	1.00E+01	5.58E+00
0.185	54.0%	6.78E-01	1.74E+01	2.76E+01	1.97E+01

7.1.5 U-238 plus Short Lived Daughters

The detector response to U-238 plus the immediate short lived daughters of Th-234, Pa-234m, and Pa-234 is given in Figure 7.5. The FIDLER has a noticeably higher response due to the low energy photons, however, a response from the HpGe and NaI is noticeable. Setting a detector window from 60 to 75 keV and 80 to 100 keV would give preferential detection to the two peaks from the U-238 and daughters.

Figure 7.5, Detector Response to U-238 plus Daughters

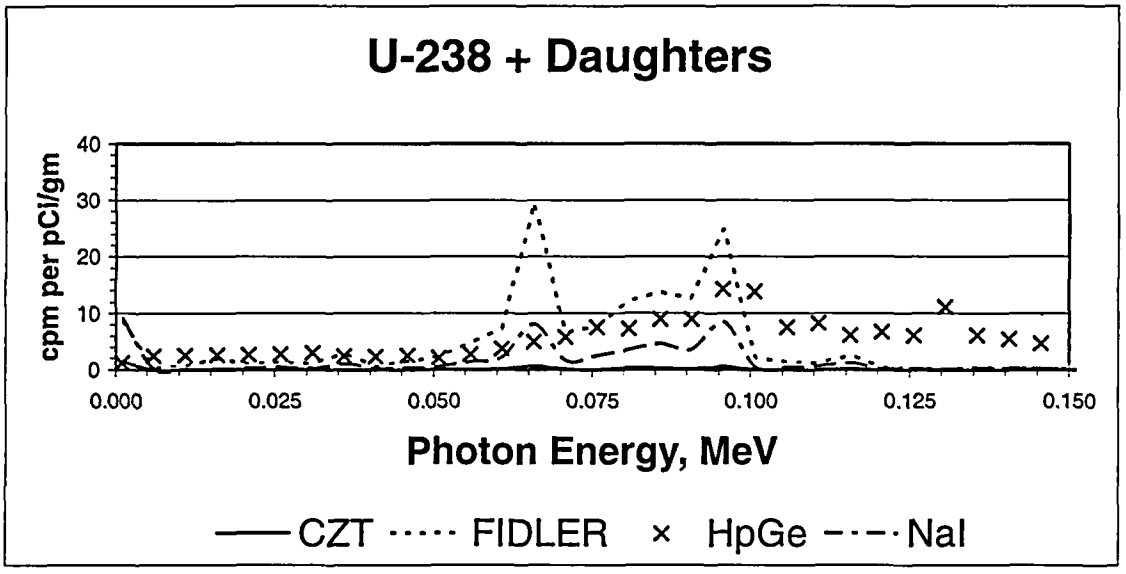

Looking at more detail on the makeup of the graph the most prominent photons were evaluated for their response within their energy bin and is given in Table 7.6.

Table 7.6, Specific Photon Energy Detector Response for U-238 plus Daughters

U-238 + Th-234 + Pa-234m + Pa-234		Detector MCNP Results cpm per pCi/gm			
Photon Energy MeV	Probability of Decay	CZT	FIDLER	HpGe	NaI
0.013	8.83%	Included below			
0.0133	9.57%	Included below			
0.0136	0.625%	5.16E-02	2.68E+00	5.16E+00	2.84E-01
0.0633	3.81%	Included below			
0.0664	0.097%	8.52E-01	3.68E+01	8.74E+00	1.03E+01
0.0768	0.128%	4.13E-01	1.22E+01	7.28E+00	3.56E+00
0.0924	2.72%	Included below			
0.0928	2.69%	Included below			
0.0947	0.141%	Included below			
0.0984	0.228%	7.49E-01	3.76E+01	2.34E+01	1.22E+01
0.1110	0.087%	Included below			
0.1128	0.24%	1.81E-01	3.64E+00	1.44E+01	1.86E+00
0.7664	0.207%	0.00E+00	0.00E+00	4.41E-01	5.16E-02
0.926	0.374%	0.00E+00	2.58E-02	2.87E+00	3.87E-01
1.001	0.589%	0.00E+00	0.00E+00	0.00E+00	0.00E+00

7.1.6 Pu-239

The detector response to Pu-239 is given in Figure 7.6, which shows a similar relative response of the FIDLER, HpGe and NaI detectors. The formation of multiple peaks from simultaneous addition of the 0.0136 MeV photon can be seen. The relative low abundance of the Pu-239 photons would make it difficult to detect in a high background area but a window set at 65 to105 keV may prove beneficial. Table 7.7 gives a more detail response of the detectors to the two photons from Pu-239.

Figure 7.6, Detector Response to Pu-239

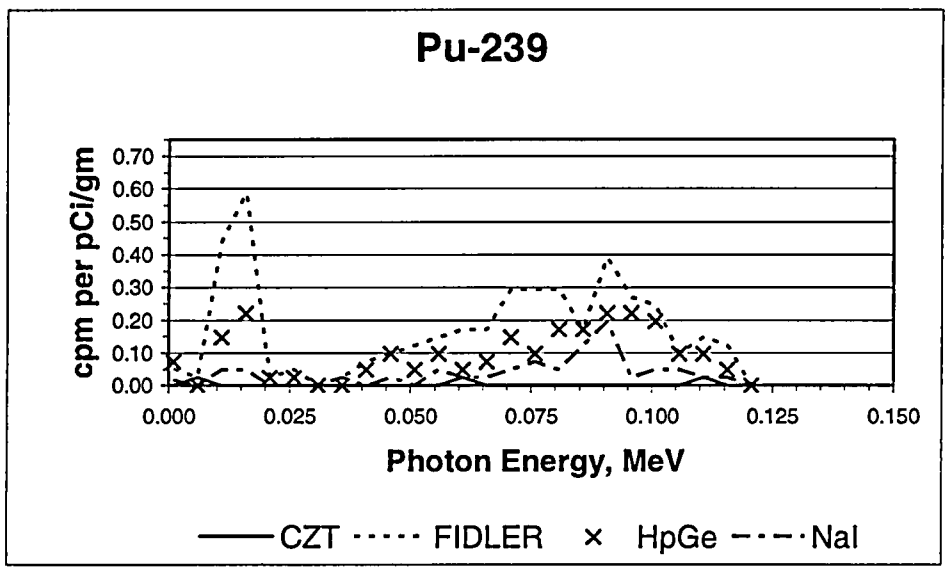

Table 7.7, Specific Photon Energy Detector Response for Pu-239					
Pu-239		Detector MCNP Results cpm per pCi/gm			
Photon Energy MeV	Probability of Decay	CZT	FIDLER	HpGe	NaI
0.0136	4.41%	0.00E+00	5.88E-01	2.20E-01	4.90E-02
0.113	0.05%	2.45E-02	1.47E-01	9.79E-02	2.45E-02

7.1.7 Th-232 plus Entire Decay Chain

The response of the detectors to Th-232 plus its decay chain daughters is given in Figure 7.7. The photon energy was modeled out to 3 MeV to try to capture the 2.6 MeV photon from the Tl-208 and other higher energy photons from the complete chain. No noticeable response was seen by the detectors above 1 MeV. To determine if the model was working properly the amount of gammas reaching the detectors was determined and the gamma flux at the detectors was as expected in the model, but the response of the relatively small volume of the detectors did stop the entire high energy photon in the detector, therefore, there was no detector response.

Figure 7.7, Detector Response to Th-232 Plus Progeny

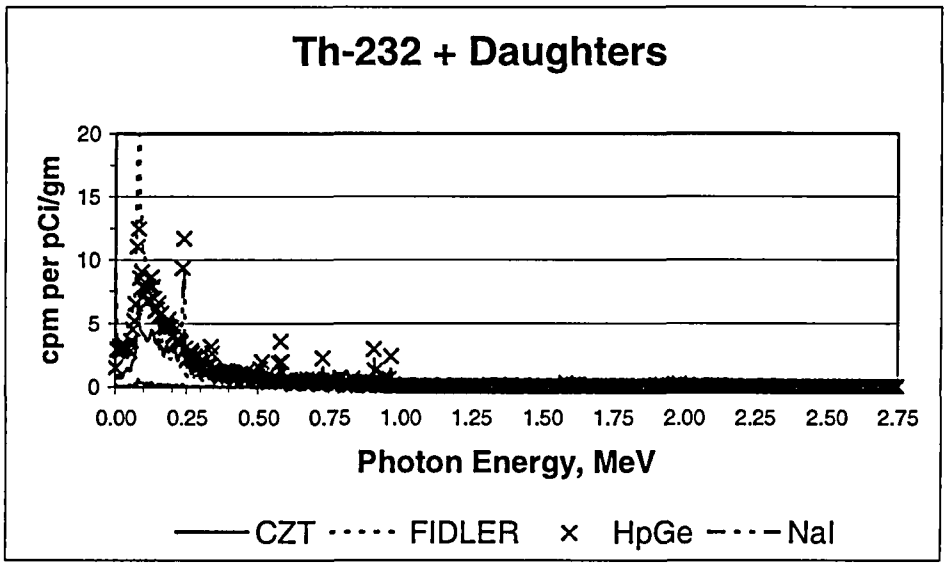

It is more informative to look at the graph in parts that separate the low energy area from the higher energy photon area. The low energy photon area from 0 to 1.0 MeV is given in Figure 7.8, while the high energy area, 1.0 MeV to 2.75 MeV, is given in Figure 7.9. Note there is no contribution from the CZT in the high energy region. A more detailed analysis of the prominent photons is given in Table 7.8.

Figure 7.8, Detector Response to Low Energy Photons from Th-232 Plus Progeny

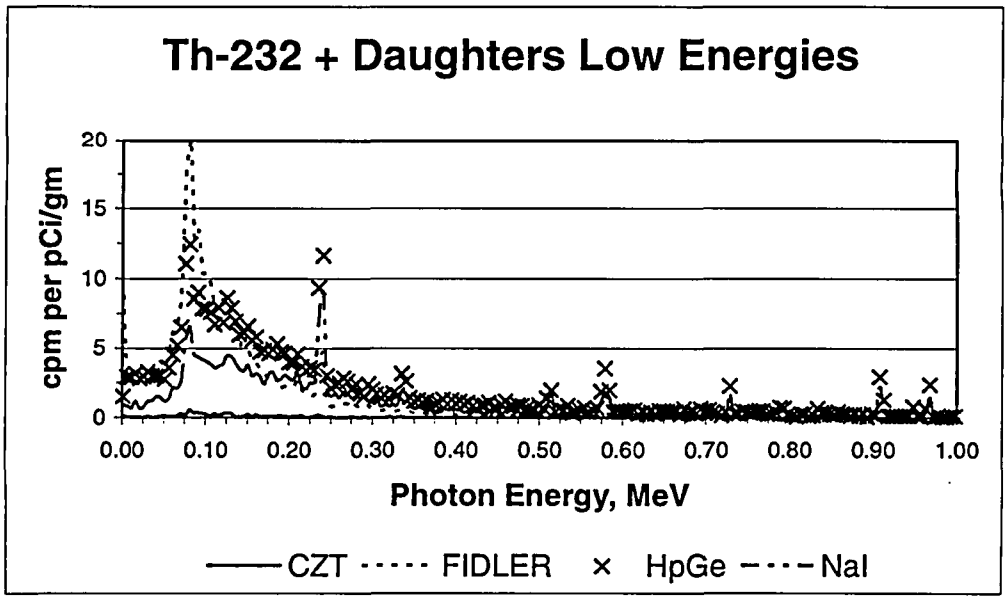

Figure 7.9, Detector Response to High Energy Photons from Th-232 Plus Progeny

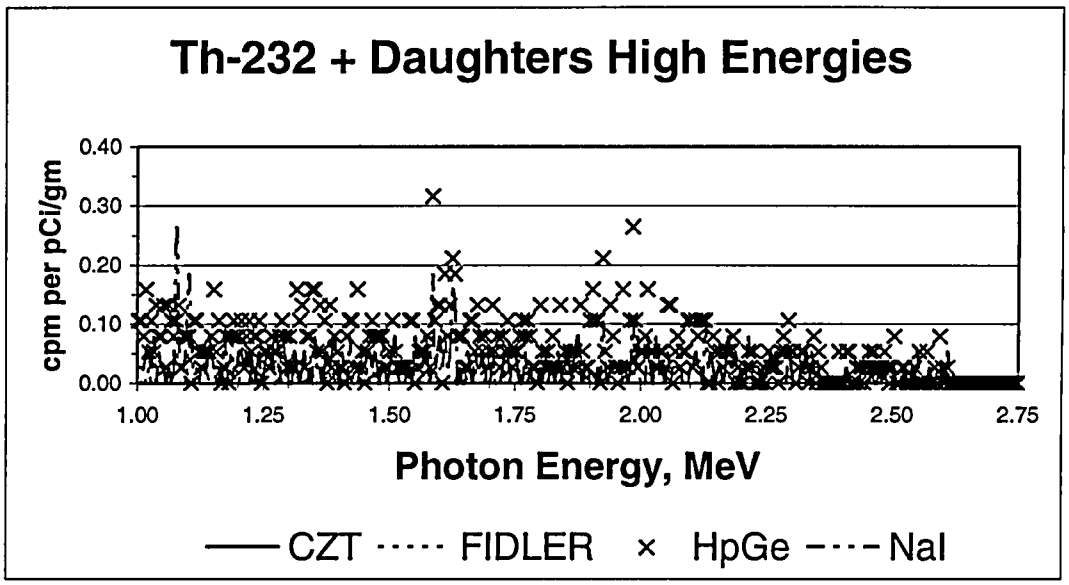

Table 7.8, Specific Photon Energy Detector Response for Th-232 plus Progeny					
Th-232 + Daughters		Detector MCNP Results cpm per pCi/gm			
MeV	Probability	CZT	FIDLER	HpGe	NaI
0.0123	8.39%	Included below			
0.0130	39.11%	1.58E-01	4.65E+00	3.17E+00	1.19E+00
0.0748	10.7%	7.13E-01	3.35E+01	1.11E+01	5.65E+00
0.0873	8.04%	5.02E-01	2.74E+01	9.03E+00	4.36E+00
0.239	44.6%	3.70E-01	7.05E+00	1.17E+01	9.03E+00
0.3383	11.36%	2.64E-02	1.29E+00	3.14E+00	1.87E+00
0.727	11.83%	0.00E+00	2.90E-01	2.93E+00	2.24E+00
0.9111	27.70%	2.64E-02	3.17E-01	2.27E+00	1.66E+00
0.9691	16.62%	2.64E-02	1.06E-01	2.38E+00	1.43E+00

Specific areas at the Hematite facility (Limestone Fill, Sediment, Sub surface and Surface) were modeled and graphed to determine the response of the detectors for the specific area and to also look at the response as a function of the relative nuclide contribution. This was done by tabulating the specific radionuclide contribution, without the Tc-99 contribution (Table 4.29) and multiplying the photon contribution, in a specific energy bin, by the percentage activity of that radionuclide for that area. For example, for the Limestone Fill area U-235 plus short lived daughters contribute 22.3% of the activity, U-238 and short lived daughters contribute 66.8%, Th-232 plus chain daughters contributes 9.6%, Am-241 contributes 1.1% and Np-237 contributes 0.22%. Each of these percentages was multiplied by the photon contribution from the specific

energy bin. These contributions were totaled for each energy bin for each detector and plotted. Although the photon energy was modeled out to 2 MeV (3 MeV for the Th-232 chain) the contribution from the lower energies was plotted because the higher energies did not register sufficient photons to rise above background. Typically the HpGe detector responded with a greater response than the NaI and the FIDLER responded better at the low energies. The response of each detector was modeled to determine the contribution of each radionuclide in the specific area of interest. Sub areas in the surface and sub-surface area were not graphed because of the relatively few samples in numerous sub areas.

7.2 Limestone Fill Area

The limestone fill area has a predominant contribution from U-238 and U-235. These nuclides provide a large contribution in the Compton region by depositing more photons there. The efficiency of the FIDLER and HpGe detectors to the low energy photons can be seen in Figure 7.10.

Figure 7.10, Limestone Fill Area Detector Response to All Nuclides Present

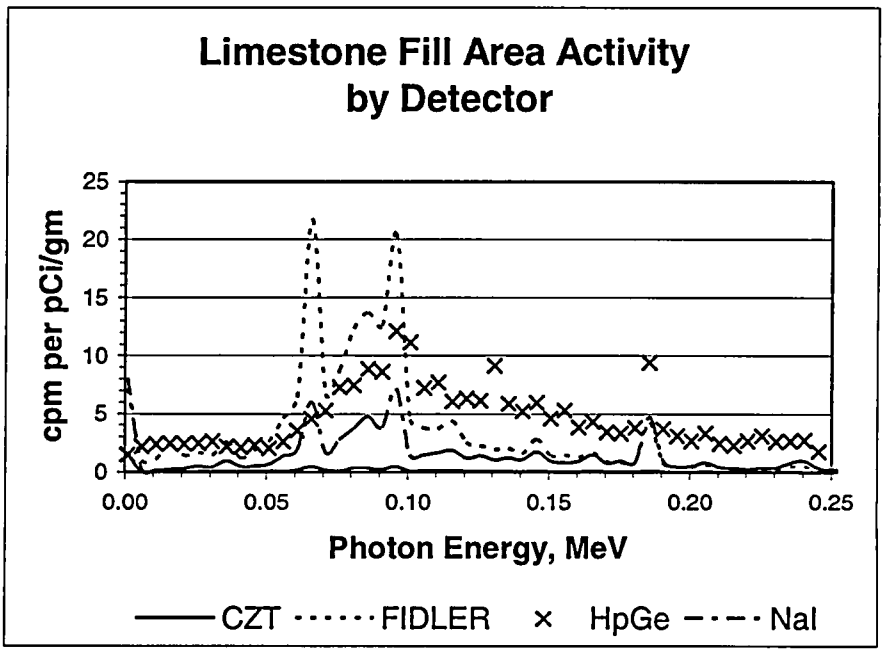

Looking at the contribution from each radionuclide in the Limestone Fill area clearly shows the U-238 contribution as dominant, Figure 7.10. Figure 7.11 show the response of the FIDLER detector to each radionuclide plus daughters in the chain for the limestone fill area. The predominant radionuclide is the U-238 as expected, however the U-235 contribution is noticeable.

Figure 7.11, Limestone Fill Area Response for FIDLER by Individual Nuclide Contribution

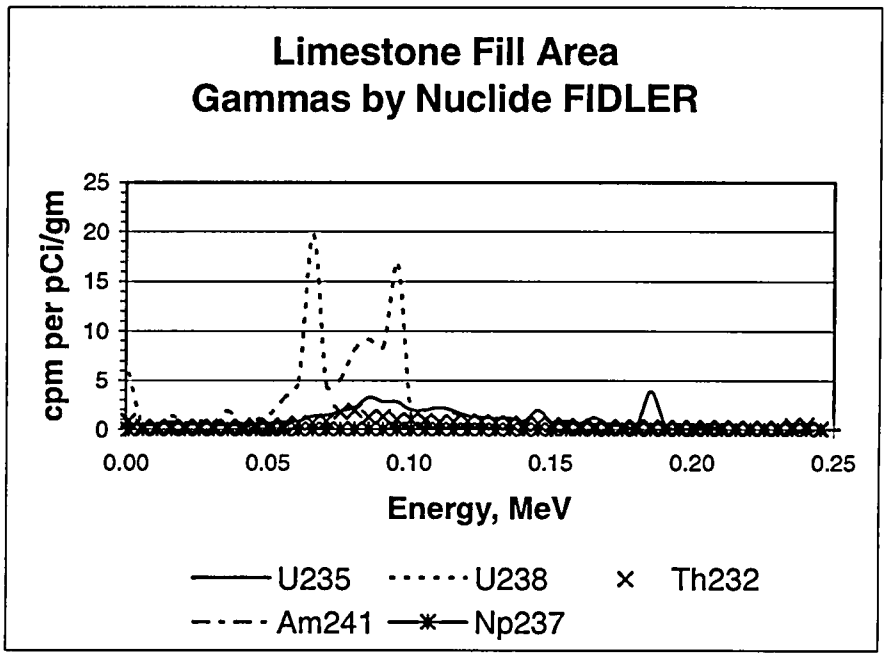

7.3 Sediment Area

The sediment fill area has a predominant nuclide contribution that is from U-234 with U-238 being the secondary contributor. However, the U-238 photons are more noticeable because of the low photon abundance for U-234. The response of the different detectors to the sediment area nuclide mix is given in Figure 7.12. Figure 7.13 shows that the U-238 contribution is predominant, however, there is a discernable U-235 contribution.

Figure 7.12, Sediment Area Activity Detected For Each Detector

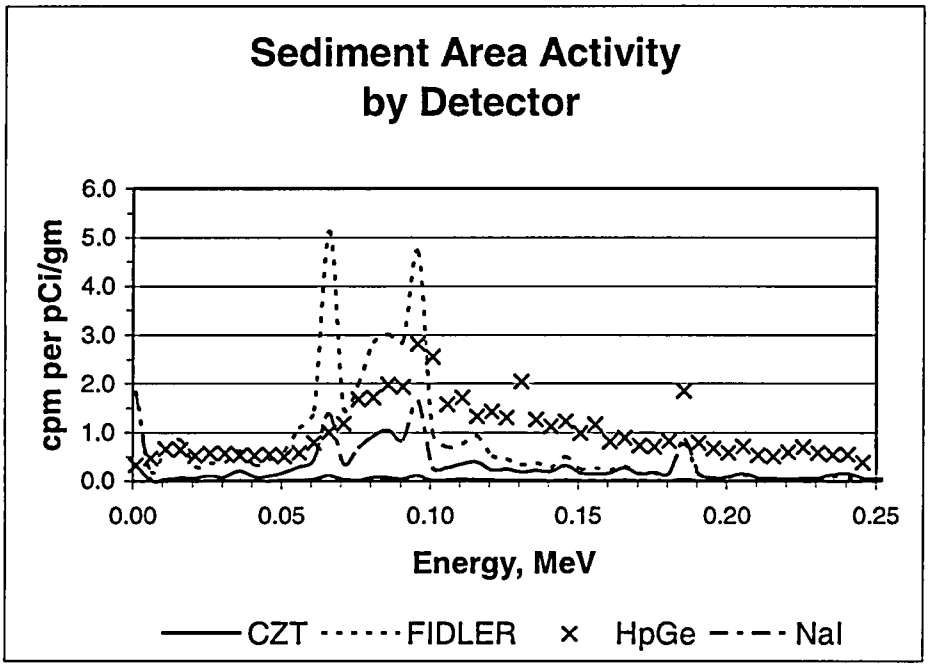

Figure 7.13, Sediment Area Response for FIDLER by Individual Nuclide Contribution

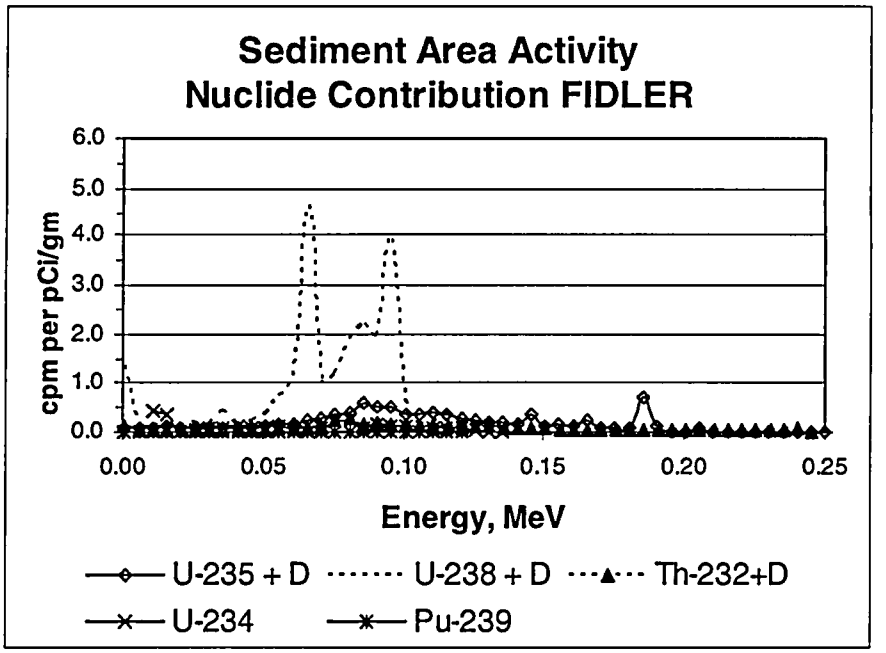

7.4 Surface Area

The surface area had predominant contribution from the U-238 with secondary contribution from the U-234. The response of the detectors to the surface area nuclide mix is given in Figure 7.14.

Figure 7.14, Surface Area Activity Detected For Each Detector

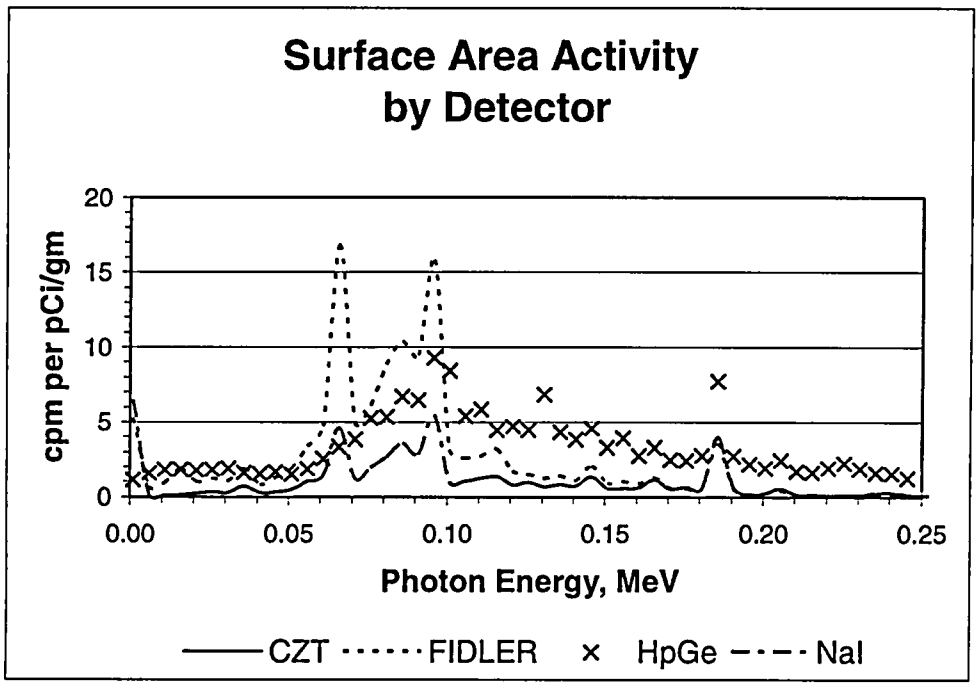

The similar contribution from U-238 is noticed in this graph, as is the 185 keV peak contributed by the U-235 photon.

7.5 Sub Surface Area

The sub surface area has a predominant nuclide contribution that is from U-234 with a very slight U-238 as the secondary contributor. The response of the detectors to the sub surface area nuclide mix is given in Figure 7.15.

Figure 7.15, Sub Surface Area Activity Detected For Each Detector

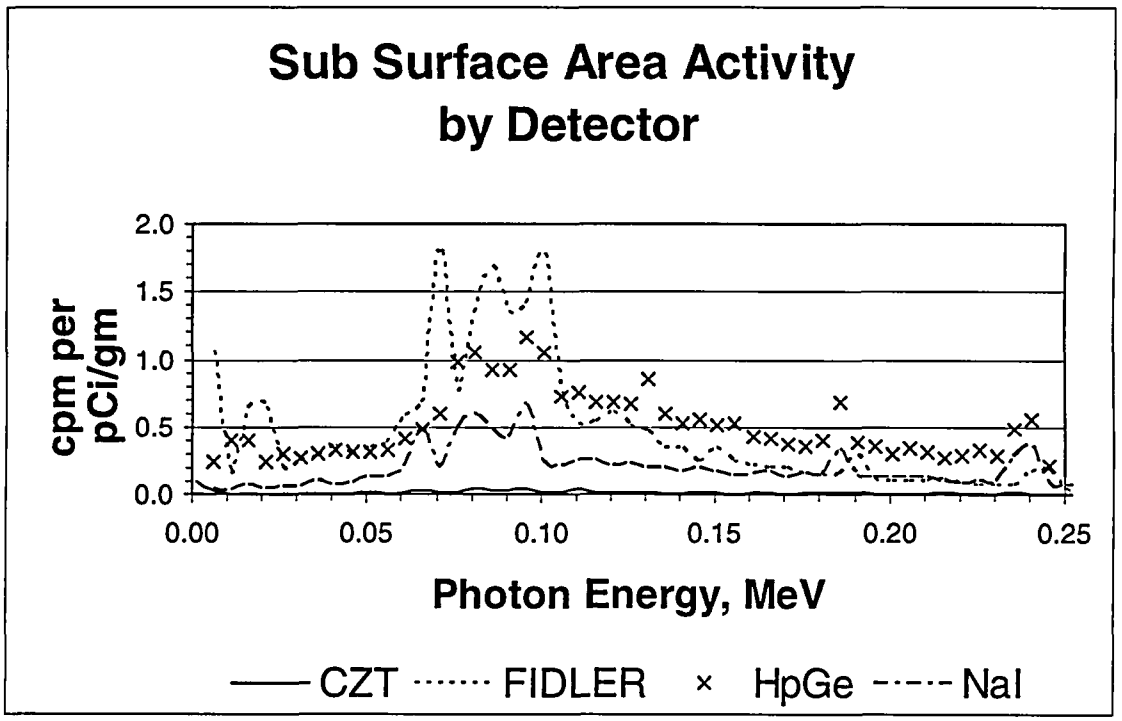

The predominant radionuclide characteristic peaks of the U-238 contribution is noticeable. A peak at about the 220 keV range is noticeable for the HpGe and NaI detectors.

8.0 SURROGATE SCANNING RADIONUCLIDES

This section reviews the potential use for surrogate radionuclides based on the major contributors of activity in each sub-area from the results of characterization samples collected at Hematite. This selection of potential surrogate radionuclides at Hematite is made understanding that surface evaluations will be considered as volumetric readings. The probable mix used in this evaluation by individual sub-area should reflect the final status. The frequency that a radionuclide appears as the major, 2nd or 3rd largest contributor to total activity is presented in Table 8.1.

Table 8.1 Major Activity Contributors for Different Areas

Major Contributors to Activity				
	Sub Surface	**Surface**	**Limestone**	**Sediment**
Tc-99	9	13	1	1
Th-232	10	3	0	0
U-238	8	13	1	1
U-235	0	8	1	0
U-234	13	3	0	1

Excluding Tc-99 and U-234 as non-gamma and low abundance emitters, respectively, the choices for surrogates are U-235, U-238, and Th-232 since the Am-241, Np-237 and Pu-239 represent such small activity fractions or the selection of a Gross Activity DCGL. The final choice will be dependent upon the MDCscan (actual) and the respective DCGL.

When using a surrogate measurement for multiple radionuclides, it is necessary to determine if the radionuclide activity concentrations have a fairly constant ratio throughout the survey unit. In accordance with Appendix I of MARSSIM, the correlation coefficient, r, will be computed for the activity concentrations of selected surrogates and each of the additional radionuclides and compared to applicable acceptance criteria. In order to improve the correlation among radionuclide activity concentrations, the radionuclides of concern will be separated into appropriate groups for evaluation. For example, U-235 might be analyzed as a surrogate radionuclide for other radionuclides, including U-234, U-238, and Tc-99. Similarly, a surrogate radionuclide might be selected for Th-232 and its decay chain and for the transuranic radionuclides. Calculation of the correlation coefficient, r, will reveal if the selected surrogate radionuclide has an acceptable correlation with the other radionuclides in its group. If a plot of the points has an underlying linear pattern, they are correlated; the computation will indicate if it is closer to zero than one. As an example, this comparison was performed for certain sample data from the DM Sub-surface are and the results are shown in Table 8.2. It is expected that a considerable mixing of soil will be performed during the excavation phase and that ratios will improve by the time of final status survey.

Table 8.2, DM Area Comparison For Correlation

DM Area Comparison	Correlation
Tc-99/U-235	0.50
Tc-99/U-238	0.50
U-238/U-235	1.00
Th-232/U-235	0.44

Because there is not a simple, fixed ratio of the various radionuclides to a single radionuclide, it will be necessary to use a combination of the methods for related and unrelated radionuclides, described in Appendix I of MARSSIM, to accommodate the use of multiple surrogate radionuclides.

Scaling factors are the calculated ratios of a correlated radionuclide activity concentration to that of the surrogate radionuclide activity concentration. Representative scaling factors must be developed later that are representative of the situation that will exist at the final cleanup stage. MARSSIM recommends calculating scaling factors at the 95 percent confidence level. If the scaling factor is underestimated (i.e., low), then the contribution of the related radionuclide to the final dose estimate will be underestimated. For purposes of initial planning and selection of instrumentation, scaling factors were not considered. Later it will be possible to reevaluate the radionuclide distribution, based on the final sample distribution results, for the purpose of determining instrument response.

At final status survey, the ratios of the expected correlated radionuclide activity concentrations to that of the surrogate radionuclide activity concentration will then be calculated. For final status survey considerations for survey instrumentation, correlations are assumed to be acceptable. However, instrument response should be planned from the following parameters as determined for each radionuclide ratio:

- average
- median
- minimum
- maximum
- standard deviation (σ)
- percent coefficient of variation (%CV)

Using the above information, the radionuclide specific scaling factors will then be calculated at the 95 percent confidence level using the following equation:

$$SF_i = R_i + 1.96\ \sigma_i$$

Where:

SF_i = scaling factor of radionuclide i to the surrogate radionuclide

R_i = average activity concentration ratio of radionuclide i to the surrogate radionuclide
σ_i = standard deviation of the average activity concentration ratio

MARSSIM provides estimates for scan MDCs of enriched uranium (EU) for a NaI detector and these are indicated below in Table 8.3. Note that these values are for the sum of U-234, U-235, and U-238 and an apparent full-open energy window. MARSSIM also indicated a background of 10k cpm for a 2x2 NaI.

Table 8.3 Scan MDC For Different Uranium Enrichments

% EU	pCi/g
3	96
20	107
50	118
75	132

For most of the areas, the sum of U-234, U-235, and U-238 activities and DCGLs will be well below those indicated in the MARSSIM Scan MDCs table above. MARSSIM also lists the NaI scan MDC for Th-232 with progeny at 1.8 pCi/g which is greater than the volume DCGL. MARSSIM requires additional direct measurements (or samples) per survey unit whenever the scan MDC is greater than the DCGL. The number of additional samples is dependent on actual site-specific conditions, such as area factors, background, efficiencies, and scan time. The method in section 5.5.2.4 of the MARSSIM is used to determine whether additional samples are needed is described below.

The area factor is the multiple of the DCGL that is permitted in a limited portion of the survey unit. The ratio of the MDCscan to the DCGL establishes the area factor (the multiple of the DCGL) that can be detected by scanning (MARSSIM equation 5-4):

$$areafactor = \frac{MDCscan}{DCGL}$$

Using the methods in MARSSIM, the size of the area corresponding to the area factor, A_{EC}, can be determined. The number of sample points that may be needed to detect this area of elevated measurement concentration, N_{EMC}, in a survey unit is:

$$N_{EMC} = \frac{A}{A_{EC}}$$

where:

N_{EMC} = number of sample points
A = area of the survey unit
A_{EC} = area of concentration greater than DCGL

If N_{EMC} is larger than N, additional samples are required to demonstrate that areas of elevated concentrations meet the radiological criteria for license termination.

Additional consideration can be given to known information concerning the site based on historical site assessment and site characterization data. If it is known that a maximum concentration is not likely to be exceeded, the size of the area corresponding to an equivalent area factor for this concentration may be used for A_{EC} in the equation above. Similarly, based on knowledge of how the radioactive material was handled or dispersed on the site, it may be possible to estimate the smallest area likely to have elevated concentrations. If this is so, that area can be used. Likewise, knowledge of how the residual radioactivity would be likely to spread or diffuse after deposition could be used to determine an area A_{EC}.

The goal is to develop an MDCscan below the DCGL. Even if the MDCscan is capable of detecting levels below the established DCGLs; MARSSIM recommends that detection limits of 10-50% of the DCGL should be the target. Areas at Hematite that require development of area factors will be those where the final MDCscan is greater than the surrogate or gross DCGL. Although area factors are beyond the scope of this report, MARSSIM paragraph 5.5.2.4 with its Table 5.6 provide illustration data and application.

Considering the low values for gross activity DCGLs and the potentially very low values for many of the surrogate DCGLs (see following table), the selection of the surrogate and the appropriate instrument is made by selecting the instrument with the lowest MDCscan with the highest activity fraction or multiple of the potential surrogates of the survey unit. The use of selected energy regions of interest (i.e., detector energy window) can reduce background levels while also allowing for the detection of the key gammas for the radionuclides of concern. When two or more radionuclides are involved at the same energy emission, it may well be that the gross MDA_{mod} may be the best choice as further discrimination can not be made. Different scanning windows may be required for the different mixes in individual sub-areas.

Table 8.4 presents the mean activity per sub-area, the respective Gross Activity DCGL, and Surrogate DCGLs for U-238, Th-232, and U-235. The table also lists the three highest activity contributors for each of the sub-areas. Gross Activity DCGLs were calculated with equation 4-4 of MARSSIM; the modified DCGLs for surrogates were calculated with equation I-14 on the MARSSIM page I-32. All eight radionuclides identified in the characterization were included in the DCGL calculations: Tc-99, U-234, U-235, U-238, Th-232, Am-241, Np-237, Pu-239. The contributions from Am-241, Np-237, and Pu-239 were included even though they are negligible from an activity standpoint. The sum of mean activity column has an assumed background of 0.36 pCi/g for U-234, 0.04 pCi/g for U-235, 0.36 pCi/g for U-238, and 0.38 pCi/g for Th-232 which were subtracted from the mean values for this table.

Table 8.4, Mean Activity Per Sub-Area, Respective Gross Activity DCGL, and Surrogate DCGLs

Area	Sum of Mean Activity*	Gross Activity DCGL	U-238 Surrogate $DCGL_{mod}$	Th-232 Surrogate $DCGL_{mod}$	U-235 Surrogate $DCGL_{mod}$	Major Contributor	2nd Largest Contributor	3rd Largest Contributor
Limestone and Sediment Fill as a Volumetric Source								
Fill	23.8	23.1	1.4	N/A	0.54	Tc-99	U-238	U-235
Sed	73.1	47.6	5.1	0.20	1.37	U-234	Tc-99	U-238
Surface as a Volumetric Source								
BD	109.4	34.8	12.8	N/A	3.61	Tc-99	U-238	U-235
BP	30.4	24.4	7.2	0.56	6.68	Tc-99	U-238	U-235
CB	26.9	23.5	15.8	0.77	2.47	U-238	Tc-99	U-235
DM	66.1	35.6	12.3	0.24	18.55	U-235	U-238	Tc-99
EP	256.6	35.6	6.1	0.11	3.05	U-234	Tc-99	U-238
GS	0.8	3.2	1.3	1.45	N/A	Th-232	U-238	Tc-99
LF	6.4	11.7	1.9	0.91	0.55	Tc-99	U-238	Th-232
NB	12.7	25.6	2.8	1.14	0.55	U-234	U-238/Tc-99	Th-232
OA	29.5	25.8	9.1	0.46	2.29	Tc-99	U-238	U-235
PL	19.3	16.5	3.0	0.64	0.78	Tc-99	U-238	U-235
RR	111.2	39.0	29.5	0.39	6.92	U-238	U-235	Tc-99
SW	26.0	16.4	6.8	0.55	2.38	U-238	Tc-99	U-235
All	287.3	96.6	3.3	0.14	1.26	Tc-99	U-238	U-234
Subsurface as a Volumetric Source								
BLD	118.4	95.3	5.0	0.30	0.33	U-234	Tc-99	U-238
BD	2.9	5.9	1.1	1.39	0.13	U-234	Th-232	Tc-99
BP	1.9	4.7	0.9	1.42	0.15	U-234	Th-232	U-238
CB	3.5	6.3	0.1	1.41	0.42	U-234	Th-232	Tc-99
DM	98.4	77.9	7.7	0.47	0.34	U-234	U-238	Tc-99
EP	10.2	14.3	2.3	0.94	0.14	Tc-99	U-234	U-238
LF	7.4	17.8	0.9	1.19	0.08	U-234	Tc-99	Th-232
NB	1.6	5.5	1.0	1.39	0.08	U-234	Th-232	Tc-99
OA	2.4	4.7	1.5	1.41	0.08	U-238	Th-232	U-234
PL	4.0	9.6	N/A	1.29	0.26	U-234	Tc-99	Th-232
RR	2.9	6.6	0.6	1.40	0.28	U-234	Th-232	U-238
SW	2.3	5.2	1.6	1.41	0.10	U-238	Th-232	U-234
All	36	31.6	1.4	1.16	0.17	U-234	U-238/Tc-99	Th-232

9.0 DETECTOR RESPONSE EVALUATIONS

Using the information provided in Sections 7.0 and 8.0 it is appropriate to determine how the detectors should respond at different locations throughout the site. Due to the poor response of the CZT detector it is not included in this evaluation. Tc-99 is not used either because of no gamma component.

9.1 Detector Response

Looking at the Figures in Section 7.0 for each radionuclide a determination of the approximate response of the detectors to that radionuclide can be calculated by summing the response within a window. It is assumed that U-235 and U-238 are the primary radionuclides of concern. This was done for the three primary detectors and is given in Table 9.1.

Table 9.1, Projected Detector Response for Specific Energy Windows

Nuclide	Window	Detector Response cpm per pCi/gm		
		FIDLER	HpGe	NaI
U-235	65 – 100 keV	83.3	50.0	53.9
	180 – 190 keV	21.7	33.7	48.4
U-238	60 – 100 keV	117	75.5	35.3
	60 – 75 keV	51.1	22.1	14.4
	80 - 100 keV	65.7	53.5	20.9
Th-232	70 -90 keV	73.0	47.6	23.8
	230 – 240 keV	10.5	24.5	18.6

This data can be used to determine a potential response in relation to the surrogate DCGL by multiplying the projected response in a specific window by the surrogate DCGL for the specific area. The model energy bins for the windows chosen in Table 9.1 was summed for each specific area and multiplied by the appropriate $DCGL_{mod}$ to determine the potential detector response.

9.2 Limestone Fill and Sediment Areas

From the data supporting Figure 7.10 for the Limestone Fill area and Figure 7.12 for the Sediment area the cpm per pCi per gram for the Limestone Fill and Sediment areas should give a noticeable response for the three detectors selected. This potential detector response at the $DCGL_{mod}$ for U-238 is given in Table 9.2 for a volumetric source. The potential detector response at the $DCGL_{mod}$ for U-235 is given in Table 9.3.

Table 9.2, Detector Response for U-238 in Limestone Fill and Sediment Areas				
Area	Surrogate $DCGL_{mod}$ (pCi/g)	Detector Response cpm per $DCGL_{mod}$ 60 – 100 keV		
		FIDLER	HpGE	NaI
Limestone	1.4	164	106	49
Sediment	5.1	597	385	180

Table 9.3, Detector Response for U-235 in Limestone Fill and Sediment Areas							
Area	Surrogate $DCGL_{mod}$ (pCi/g)	Detector Response cpm per $DCGL_{mod}$ 65 – 100 keV			Detector Response cpm per $DCGL_{mod}$ 180 – 190 keV		
		FIDLER	HpGE	NaI	FIDLER	HpGE	NaI
Limestone	0.54	45	27	29	12	18	26
Sediment	1.37	114	69	74	30	46	66

9.3 Surface Area

The surface area has 12 different sub areas that each have specific $DCGL_{mod}$. This data was used with the data from the model supporting Figure 7.14 to determine the potential response of the different instruments. This potential detector response at the $DCGL_{mod}$ is given in Table 9.4 for the U-238 window and Table 9.5 for the two U-235 windows.

Table 9.4, Detector Response for U-238 in Surface Area				
Area	Surrogate $DCGL_{mod}$ (pCi/g)	Detector Response (cpm per $DCGL_{mod}$) 60 – 100 keV		
		FIDLER	HpGE	NaI
BD	12.8	1,498	966	452
BP	7.2	842	544	254
CB	15.8	1,849	1,193	558
DM	12.3	1,439	929	434
EP	6.1	714	461	215
GS	1.3	152	98	46
LF	1.9	222	143	67
NB	2.8	328	211	99
OA	9.1	1,065	687	321
PL	3	351	227	106
RR	29.5	3,452	2,227	1,041
SW	6.8	796	513	240
All	3.3	386	249	116

Table 9.5, Detector Response for U-235 in Surface Area							
Area	Surrogate $DCGL_{mod}$ (pCi/g)	Detector Response (cpm per $DCGL_{mod}$) 65 – 100 keV			Detector Response (cpm per $DCGL_{mod}$) 180 – 190 keV		
		FIDLER	HpGE	NaI	FIDLER	HpGE	NaI
BD	3.61	301	181	195	78	122	175
BP	6.68	556	334	360	145	225	323
CB	2.47	206	124	133	54	83	120
DM	18.55	1,545	928	1000	403	625	898
EP	3.05	254	153	164	66	103	148
GS	N/A						
LF	0.55	46	28	30	12	19	27
NB	0.55	46	28	30	12	19	27
OA	2.29	191	115	123	50	77	111
PL	0.78	65	39	42	17	26	38
RR	6.92	576	346	373	150	233	335
SW	2.38	198	119	128	52	80	116
All	1.26	105	63	68	27	42	61

9.4 Sub-Surface Area

The sub surface area has 12 sub areas that each has a specific $DCGL_{mod}$. This data was used with the data from the model supporting Figure 7.15 to determine the potential response of the different instruments. This potential detector response at the $DCGL_{mod}$ is given in Table 9.6 for the U-238 window and Table 9.7 for the two U-235 windows.

Table 9.6, Detector Response for U-238 in Sub-Surface Area				
Area	Surrogate $DCGL_{mod}$ (pCi/g)	Detector Response (cpm per $DCGL_{mod}$) 60 – 100 keV		
		FIDLER	HpGE	NaI
BLD	5	585	378	177
BD	1.1	129	83	39
BP	0.9	105	68	32
CB	0.1	12	8	4
DM	7.7	901	581	272
EP	2.3	269	174	81
LF	0.9	105	68	32
NB	1	117	76	35
OA	1.5	176	113	53
PL	N/A			
RR	0.6	70	45	21
SW	1.6	187	121	56
All	1.4	164	106	49

Table 9.7, Detector Response For U-235 In The Sub-Surface Area							
Area	Surrogate $DCGL_{mod}$ (pCi/g)	Detector Response (cpm per $DCGL_{mod}$) 65 – 100 keV			Detector Response (cpm per $DCGL_{mod}$) 180 – 190 keV		
		FIDLER	HpGE	NaI	FIDLER	HpGE	NaI
BLD	0.33	27	17	18	7	11	16
BD	0.13	11	7	7	3	4	6
BP	0.15	12	8	8	3	5	7
CB	0.42	35	21	23	9	14	20
DM	0.34	28	17	18	7	11	16
EP	0.14	12	7	8	3	5	7
GS	0.08	7	4	4	2	3	4
LF	0.08	7	4	4	2	3	4
NB	0.08	7	4	4	2	3	4
OA	0.26	22	13	14	6	9	13
PL	0.28	23	14	15	6	9	14
RR	0.1	8	5	5	2	3	5
SW	0.17	14	9	9	4	6	8
All	1.26	217	116	68	52	81	61

10.0 SCAN MINIMUM DETECTABLE LEVELS

10.1 Minimum Detectable Count Rate (MDCR)

The minimum detectable concentrations (MDCs) may be calculated for scanning instruments using the method provided in MARSSIM for calculating MDCs that address both Type I and Type II errors (i.e., elimination of false negatives and false positives), using the following formula:

$$Scan\ MDCR_{surveyor} = \frac{MDCR}{\sqrt{p}\,\epsilon_i}$$

where MDCR is the minimum detectable count rate in counts per minute (cpm), ε_i is the instrument efficiency (cpm/μR/hour), and p is the surveyor efficiency, dimensionless. The approaches described in the paper by E.W. Abelquist, "Scan MDCs for Multiple Radionuclides in Class 1 Areas" (Reference 3.12), has been used to guide the development of scan MDCs.

Based on laboratory studies (References 3.13 and 3.14), the value of p has been estimated to be between 0.5 and 0.75. The value of 0.5 is conservative and is used here. In addition:

$$MDCR = s_i \times (60/i)$$

where s_i is the minimal number of net source counts required for a specified level of performance for the interval i, in seconds, and:

$$s_i = d'\sqrt{b_i}$$

where d′ is the value selected from MARSSIM Table 6.5 based on the required true positive (1-β) and false positive rates (α), and b_i is the number of background counts in the scan intervals (where b_i = b*scan time in seconds*1 min/60 s). The value of d′ used here to calculate the detector sensitivity values is 1.9, corresponding to an alpha of 0.05 and beta of 0.40. This value of d′ will result in about 60 percent true positives and about 5 percent false positives.

Using the above described methodology along with the modeled detector response, the MDCR can calculated for varying scan speed and background. If a surveyor scan speed of 0.5 m/s is chosen, the surveyor will take approximately 2 seconds to traverse the area. Similarly at a slower rate of 0.25 m/s the detector will have a 4 second view on the area. And at 0.1 m/s the detector will have a 10 second field of view. This correlation is presented in Table 10.1 and Figure 10.1. Note: this evaluation is for illustrative purposes based on modeling where background variation is considered to following normal counting statistics. No consideration has been given to varying background levels associated with varying natural levels of radioactive materials in the soil.

Table 10.1, Minimum Detectable Count Rate at Various Scan Times and Background Levels								
	Minimum Detectable Count Rate, cpm							
Scan Time=	1 sec	2 sec	3 sec	4 sec	5 sec	6 sec	8 sec	10 sec
Background								
100	147	104	85	74	66	60	52	47
500	329	233	190	165	147	134	116	104
1000	465	329	269	233	208	190	165	147
1500	570	403	329	285	255	233	202	180
2000	658	465	380	329	294	269	233	208
2500	736	520	425	368	329	300	260	233
3000	806	570	465	403	360	329	285	255
3500	871	616	503	435	389	355	308	275
4000	931	658	537	465	416	380	329	294
4500	987	698	570	494	442	403	349	312
5000	1041	736	601	520	465	425	368	329
5500	1091	772	630	546	488	446	386	345

Figure 10.1, Minimum Detectable Count Rate at Varying Scan Times and Background Levels

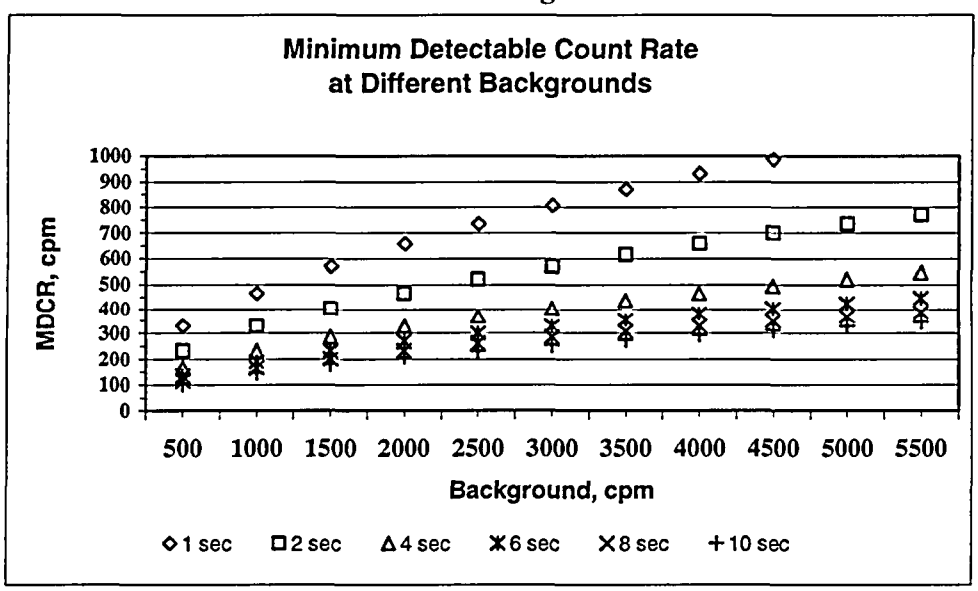

As can be seen, once the scan time decreases less than 4 seconds the MDCR increases rapidly. This data can be used to determine the necessary scan speed to reach an appropriate MDCR depending on the background of the specific area being surveyed.

10.2 Minimum Detectable Activity Level

From the modeling provided the minimum detectable activity, in pCi/gram, can be determined by dividing the minimum detectable count rate from Table 10.1 by the detector response of cpm per pCi/gm for a specific radionuclide within a specific energy window. For example, from Table 9.1 the FIDLER response for U-238, within the 60 – 100 keV window, is projected to be 117 cpm per pCi/gram. If we divide the MDCR by this and plot it for different background counts per minute we get the graph in Figure 10.2 which represents the minimum detectable U-238 activity at different backgrounds and at different scan times (scan speeds). Table 10.2 shows the numerical data.

Figure 10.2, Minimum Detectable Activity for U-238 at Different Scan Times and Background Levels with FIDLER Detector

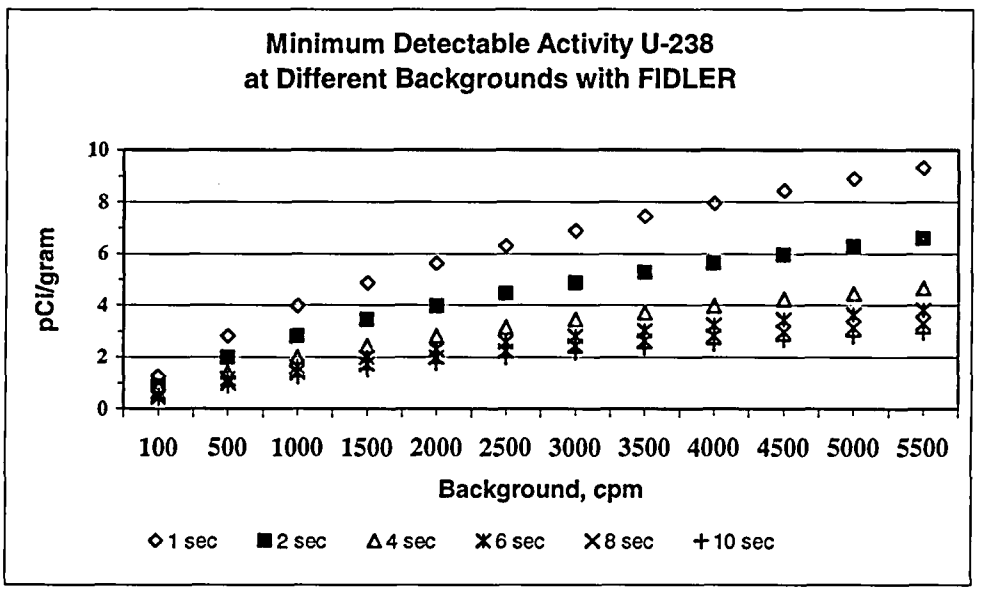

Table 10.2, Minimum Detectable Activity for U-238 with FIDLER, pCi/gm								
Scan Time= Background	1 sec	2 sec	3 sec	4 sec	5 sec	6 sec	8 sec	10 sec
100	1.26	0.89	0.73	0.63	0.56	0.51	0.44	0.40
500	2.81	1.99	1.62	1.41	1.26	1.15	0.99	0.89
1000	3.97	2.81	2.30	1.99	1.78	1.62	1.41	1.26
1500	4.87	3.44	2.81	2.44	2.18	1.99	1.73	1.54
2000	5.62	3.97	3.25	2.81	2.51	2.30	1.99	1.78
2500	6.29	4.44	3.63	3.15	2.81	2.56	2.22	1.99
3000	6.89	4.87	3.97	3.44	3.08	2.81	2.44	2.18
3500	7.44	5.26	4.30	3.72	3.32	3.03	2.63	2.35
4000	7.96	5.62	4.59	3.97	3.56	3.25	2.81	2.51
4500	8.44	5.97	4.87	4.22	3.78	3.44	2.98	2.67
5000	8.90	6.29	5.14	4.44	3.97	3.63	3.15	2.81
5500	9.32	6.60	5.38	4.67	4.17	3.81	3.30	2.95

This can also be done with the NaI detector and is given for U-238 in Figure 10.3 and Table 10.3.

Figure 10.3, Minimum Detectable Activity for U-238 at Different Scan Times and Background with 2X2 Inch NaI Detector.

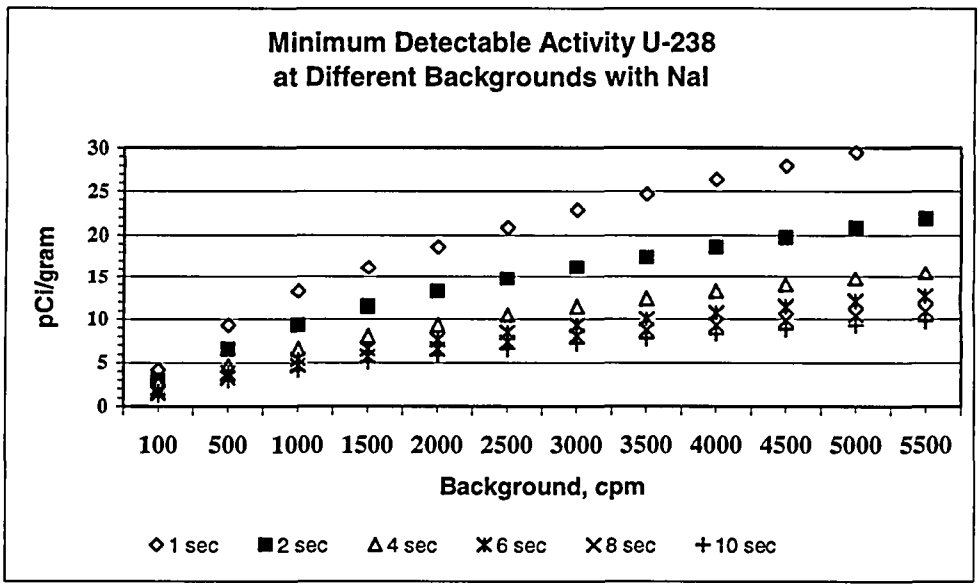

Table 10.3, Minimum Detectable Activity for U-238 with 2X2 Inch NaI, pCi/gm								
Scan Time= Background	1 sec	2 sec	3 sec	4 sec	5 sec	6 sec	8 sec	10 sec
100	4.17	2.95	2.41	2.08	1.86	1.70	1.47	1.32
500	9.32	6.60	5.38	4.67	4.16	3.80	3.29	2.95
1000	13.17	9.32	7.62	6.60	5.89	5.38	4.67	4.16
1500	16.15	11.42	9.32	8.07	7.22	6.60	5.72	5.10
2000	18.64	13.17	10.76	9.32	8.33	7.62	6.60	5.89
2500	20.85	14.73	12.04	10.42	9.32	8.50	7.37	6.60
3000	22.83	16.15	13.17	11.42	10.20	9.32	8.07	7.22
3500	24.67	17.45	14.25	12.32	11.02	10.06	8.73	7.79
4000	26.37	18.64	15.21	13.17	11.78	10.76	9.32	8.33
4500	27.96	19.77	16.15	13.99	12.52	11.42	9.89	8.84
5000	29.49	20.85	17.03	14.73	13.17	12.04	10.42	9.32
5500	30.91	21.87	17.85	15.47	13.82	12.63	10.93	9.77

Figures 10.4 and 10.5 apply the same logic to determine the minimum detectable activity for U-235 with a FIDLER and NaI detector respectively. The 65 – 100 keV window was used. The Tabular data is given in Table 10.4 and 10.5, respectively

Figure 10.4, Minimum Detectable Activity for U-235 at Different Scan Times and Background Levels with FIDLER

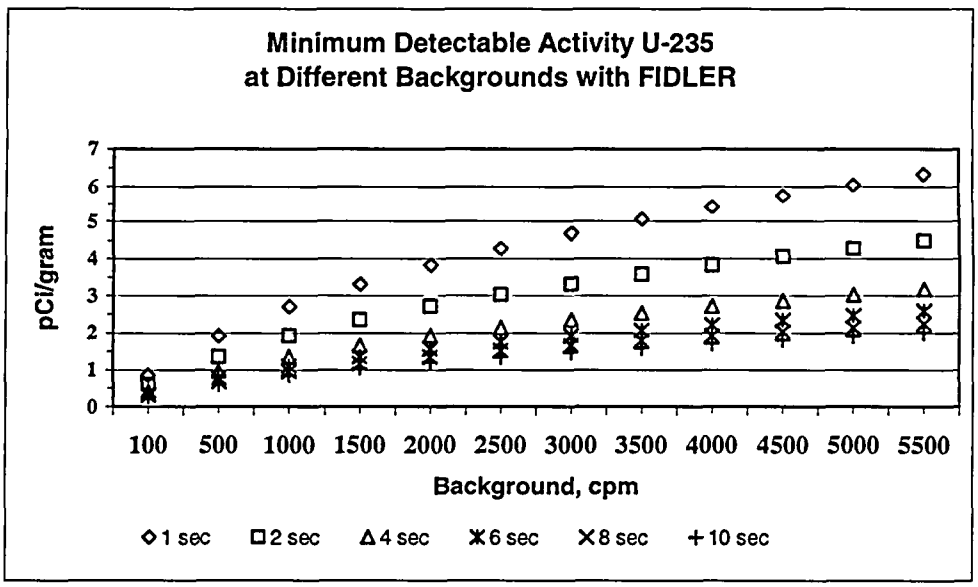

Table 10.4, Minimum Detectable Activity for U-235 with FIDLER pCi/gm								
Scan Time= Backgrond	1 sec	2 sec	3 sec	4 sec	5 sec	6 sec	8 sec	10 sec
100	0.86	0.61	0.49	0.43	0.38	0.35	0.30	0.27
500	1.91	1.35	1.10	0.96	0.86	0.78	0.68	0.61
1000	2.71	1.91	1.56	1.35	1.21	1.10	0.96	0.86
1500	3.31	2.34	1.91	1.66	1.48	1.35	1.17	1.05
2000	3.83	2.71	2.21	1.91	1.71	1.56	1.35	1.21
2500	4.28	3.03	2.47	2.14	1.91	1.75	1.51	1.35
3000	4.69	3.31	2.71	2.34	2.10	1.91	1.66	1.48
3500	5.06	3.58	2.92	2.53	2.26	2.07	1.79	1.60
4000	5.41	3.83	3.12	2.71	2.42	2.21	1.91	1.71
4500	5.74	4.06	3.31	2.87	2.57	2.34	2.03	1.82
5000	6.05	4.28	3.49	3.03	2.71	2.47	2.14	1.91
5500	6.35	4.49	3.66	3.17	2.84	2.59	2.24	2.01

Figure 10.5, Minimum Detectable Activity for U-235 at Different Scan Times and Background Levels with 2X2 Inch NaI Detector

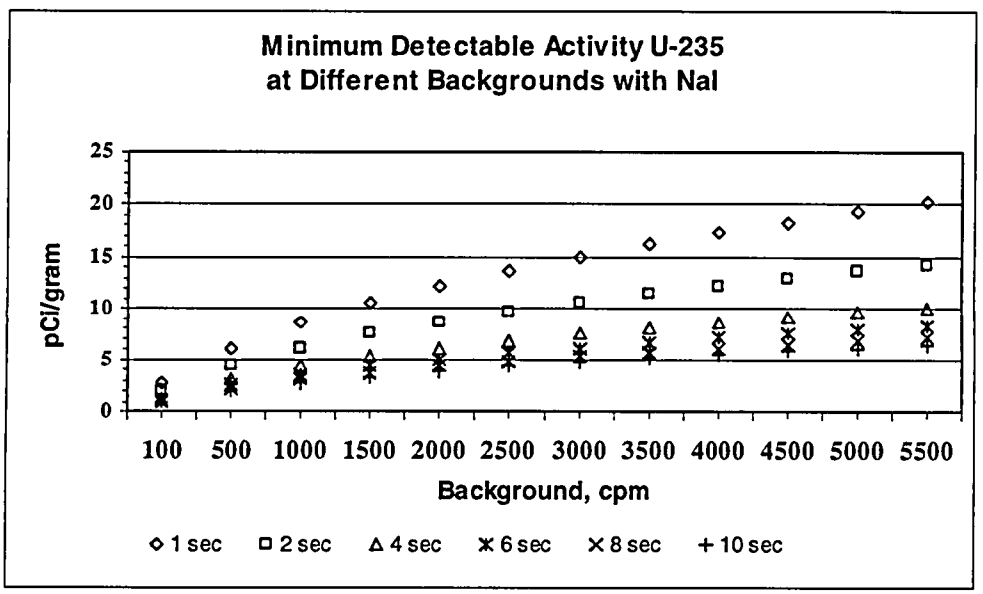

Table 10.5, Minimum Detectable Activity for U-235 with 2X2 Inch NaI, pCi/gm								
Scan Time= Background	1 sec	2 sec	3 sec	4 sec	5 sec	6 sec	8 sec	10 sec
100	2.73	1.93	1.58	1.37	1.22	1.11	0.97	0.86
500	6.11	4.32	3.53	3.05	2.73	2.49	2.16	1.93
1000	8.63	6.11	4.99	4.32	3.86	3.53	3.05	2.73
1500	10.58	7.48	6.11	5.29	4.73	4.32	3.74	3.34
2000	12.21	8.63	7.05	6.11	5.46	4.99	4.32	3.86
2500	13.65	9.65	7.88	6.83	6.11	5.57	4.83	4.32
3000	14.96	10.58	8.63	7.48	6.69	6.11	5.29	4.73
3500	16.15	11.42	9.33	8.08	7.22	6.59	5.71	5.11
4000	17.27	12.21	9.97	8.63	7.72	7.05	6.11	5.46
4500	18.32	12.95	10.58	9.16	8.19	7.48	6.48	5.79
5000	19.31	13.65	11.15	9.65	8.63	7.88	6.83	6.11
5500	20.25	14.32	11.69	10.12	9.06	8.27	7.16	6.40

11.0 CONCLUSIONS

The results of this evaluation show that the use of a FIDLER-type detector operated with a limited energy window for reducing background levels provides improved detection capability for the suite of radionuclides at the Hematite site. The surrogate radionuclides and energy windows are U-238 with a 60 keV – 100 keV window and U-235 with a 65 keV – 100 keV window.

An evaluation was performed for identifying areas that could likely be scanned with the FIDLER with the specified energy window and meeting the scanning criteria suggested in MARSSIM of 10% - 50% of the DCGL. The FIDLER response in terms of cpm per pCi/gm was determined for the key radionuclides. The Minimum Detectable Count Rates (MDCR) for different background levels and observation times were divided by this response to provide a minimum detectable activity (MDA), in pCi/gm. The MDA was divided by the gross DCGL for the specific area, and sub area, to determine the DCGL fraction, i.e. what percentage of the DCGL the detector should see with the window properly set. If this fraction was less than 50% it passes the MARSSIM test.

This evaluation was done for the limestone fill area and the sediment area. The surface and sub surface areas had sample results from different locations within these large areas that were labeled as sub areas within the larger area and the sub areas for the surface and sub surface locations were evaluated separately and in total. The results, presented in Table 11.1, indicate that for 20 out of 28 (71%) of the areas the MDA fraction of the DCGL meets the MARSSIM criteria for a 10 second observation interval at a background of 2000 cpm. With a background of 2000 cpm and a 4 second observation interval 19 of 28 (68%) met the criteria. However, it should be noted this includes sub areas where the sample data may not give a true representation because of the low number of samples taken. Also note that the presence of Tc-99 in these sub areas may have significant influence as a non gamma emitter. This can be seen if you look at the first four rows of Table 11.1 where only two of the large areas are less than the 50% criteria, but when the sub areas are included the number greatly increases

This evaluation was done for different observation times and at different backgrounds. The effect of background and observation time on the number of areas with the MDA greater than 50% of the DCGL is given in Table 11.2. Figure 11.1 is a graph of the percentage of the areas that meet the MARSSIM criteria at different observation intervals and background cpm and shows that increasing the observation time to greater than 4 seconds provides minimal benefit for the fraction of areas that meet the MARSSIM MDA criteria. Therefore, the areas requiring more time can be identified up front and surveyed longer to meet the required criteria, while saving time at the other areas.

Table 11.1, Percentage of the DCGL Detected						
	Background (cpm) / Observation Interval (sec)					
Area	**500 /10**	**1000/10**	**2000/10**	**500/4**	**1000/4**	**2000 /4**
Limestone	45.0%	63.5%	89.9%	71.3%	100.7%	142.2%
Sediment	47.1%	66.6%	94.3%	74.8%	105.6%	149.1%
Surface	63.9%	90.3%	127.7%	101.3%	143.1%	202.0%
Sub-Surface	52.5%	74.2%	104.9%	83.2%	117.5%	166.0%
Surface						
BD	26.7%	37.8%	53.5%	42.4%	59.9%	84.6%
BP	10.8%	15.3%	21.6%	17.1%	24.2%	34.2%
CB	6.6%	9.4%	13.3%	10.5%	14.8%	21.0%
DM	10.6%	15.0%	21.2%	16.9%	23.8%	33.6%
EP	114.5%	161.8%	229.0%	181.6%	256.5%	362.2%
GS	2.4%	3.3%	4.7%	3.8%	5.3%	7.5%
LF	9.7%	13.7%	19.3%	15.3%	21.6%	30.6%
NB	14.4%	20.4%	28.8%	22.9%	32.3%	45.6%
OA	11.8%	16.7%	23.6%	18.8%	26.5%	37.4%
PL	19.9%	28.2%	39.9%	31.6%	44.7%	63.1%
RR	12.7%	17.9%	25.4%	20.1%	28.4%	40.1%
SW	12.2%	17.3%	24.5%	19.4%	27.4%	38.7%
Sub-Surface						
BLD	73.1%	103.4%	146.3%	116.0%	163.9%	231.4%
BD	6.4%	9.1%	12.9%	10.2%	14.4%	20.4%
BP	5.3%	7.4%	10.5%	8.3%	11.8%	16.6%
CB	10.2%	14.4%	20.4%	16.2%	22.8%	32.3%
DM	42.1%	59.5%	84.1%	66.7%	94.2%	133.1%
EP	13.9%	19.7%	27.8%	22.1%	31.2%	44.1%
LF	15.3%	21.7%	30.6%	24.3%	34.3%	48.5%
NB	4.6%	6.5%	9.2%	7.3%	10.3%	14.6%
OA	5.2%	7.3%	10.3%	8.2%	11.6%	16.3%
PL	12.4%	17.5%	24.8%	19.7%	27.8%	39.3%
RR	7.3%	10.3%	14.5%	11.5%	16.3%	23.0%
SW	5.0%	7.1%	10.0%	7.9%	11.2%	15.8%
Number Meeting MARSSIM Criteria						
	24	21	20	21	20	19

Table 11.2, Percentage of Areas Not Meeting MARSSIM Criteria				
	Background			
Observation Time	500	1000	1500	2000
1	32.1%	57.1%	71.4%	71.4%
2	28.6%	32.1%	42.9%	57.1%
3	25.0%	32.1%	32.1%	42.9%
4	25.0%	28.6%	32.1%	32.1%
5	25.0%	28.6%	28.6%	32.1%
6	25.0%	25.0%	28.6%	32.1%
8	17.9%	25.0%	28.6%	28.6%
10	14.3%	25.0%	25.0%	28.6%

Figure 11.1, Fraction of Areas Meeting MARSSIM Criteria at Different Observation Times and Background Levels

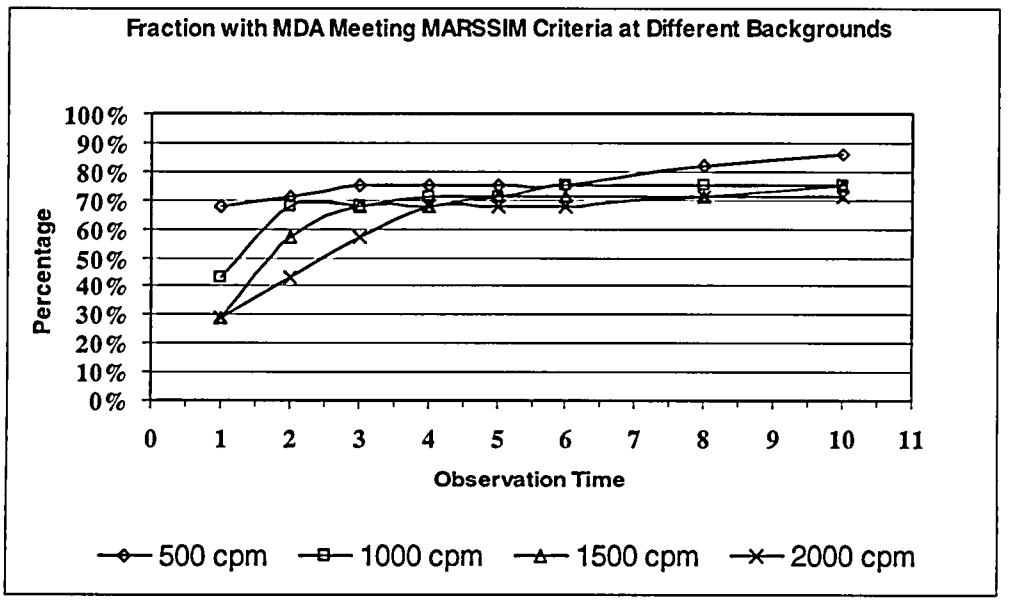

In summary, field measurements and correlation of the modeled data and instrument response to the actual radionuclides would be beneficial in providing the necessary confirmation checks. The required DCGL should be able to be detected with a properly set up FIDLER detector in most of the areas with a reasonable scan time if the background can be maintained low. Variability is expected and the scanning should be able to use surrogate radionuclides to successfully get an indication of activity present in soil.

Evaluation of a 2X2 Inch NaI(Tl) and FIDLER Detectors for Decommissioning Surveys at the Westinghouse Hematite Site

Detector Modeling and Field Studies

FINAL
April 2006

DO-06-002

Prepared by:

J. Stewart Bland, CHP
Jamie K. Doan
Wayne C. Gaul, PhD, CHP, CHMM

CHESAPEAKE NUCLEAR SERVICES, INC.
A J. STEWART BLAND COMPANY

788 Sonne Drive • Annapolis, MD 21401
410-266-9174 • 410-266-5811 (facsimile)
www.chesnuc.com

Evaluation of a 2X2 Inch NaI(Tl) and FIDLER Detectors for Decommissioning Surveys at the Westinghouse Hematite Site

Detector Modeling and Field Studies

1.0 Introduction and Background

The purpose of the study was to perform a field evaluation of NaI(Tl) and Fidler detectors for potential use in performing walkover scan surveys in a spectral mode at the Hematite Former Fuel Cycle Facility (Hematite). The results of this evaluation include an evaluation of detector detection capability and a comparison of field measurements with detector response modeling as previously reported in Chesapeake Nuclear Services May 2005 report, "Evaluating Methods for Performing Final Status Surveys for Land Areas at the Hematite Facility."

While the standard gamma walkover survey in a gross mode can identify elevated levels in comparison to a reference area, the results of the survey can be misleading due to spatial variations in background radiation levels that occur within a survey area, mainly attributable to varying levels of naturally occurring radioactive materials (NORM). Using suitable gamma spectral analysis techniques (detectors and instrumentation), specific gamma energies or regions of interest, corresponding to the photopeaks for the radionuclides of concern, can be evaluated. This technique improves the detection capability in the presence of varying ambient background levels by specifically targeting only those gammas associated with the radionuclide(s) of concern.

This evaluation consisted of a detailed study in a controlled test environment and data collection in several outside areas around the site. The test environment consisted of five B-12 boxes (labeled DM-01 thru DM-05) filled with homogenized soil of known concentrations. Boxes were placed in the west side of the main warehouse. Concentrations previously had been determined through detailed sampling and analysis. The field part consisted of measurements collected at five locations from areas in the west and southwest areas of the site. These locations were selected to reflect a combination of background and likely impacted areas.

2.0 Instrumentation Setup

Spectral data was obtained with an URSA-II multi-channel analyzer using the URSA-II pocket PC software on a TDS Recon handheld computer to collect the data. Three different detectors were tested in this study. The three detectors used in the study were a Ludlum 44-10 2x2 inch NaI(Tl), an Alpha Spectra Fidler[1] with a beryllium window, and a Scionix Fidler-type detector with an aluminum window.

A simple, but suitable for the scope of this study, energy calibration was performed with a 1 μCi Cs-137 source providing both a high (661 keV) and low (32 keV) energy peak. The fine gain adjust was performed periodically to correct for slight energy response shifts that can occur as a function of temperature in NaI(Tl) detectors. Response checks were performed prior to the collecting spectra and at the close of business each day to verify operability.

[1] Fidler, which stands for field instrument to detect low energy radiation, consists of a thin window, thin crystal NaI(Tl) detector. For the Alpha Spectra Fidler the crystal was a 127 mm diameter and 1.67 mm height right circular cylinder with a 0.254 mm Be window. The Scionix crystal was essential the same size but with a 0.0025 mm Al window.

3.0 Results for Test Boxes

Five (5) B-12 boxes filled with soil containing varying levels of contaminants representative of the Hematite site have been configured at the site for detector testing purposes. To provide a baseline measurement, a single 10 minute count was collected for each detector with the detector suspended from a tripod in the middle of the box at a height of approximately 10 centimeters above the box soil surface. Spectra were collected for each detector for each of the five boxes. Additional spectra measurements were collected with the 2x2 inch NaI(Tl) detector and Alpha Spectra Fidler detector for count time intervals more representative of typical scanning methods. These measurements provide data that can be used for evaluating detection capability as a function of scan time interval. For boxes DM-02, DM-04 and DM-05, ten spectra were collected for each of the following time intervals: one minute, twelve seconds, eight seconds and four seconds.

Using the URSA-II desktop gamma spectral analysis software, spectral data were visually evaluated to determine appropriate regions of interest. The regions of interest were correlated with nuclides present in the boxes. Based on the results of previous modeling (ref. 1), it was identified that the radionuclide U-235 provides the best combination of an energetic gamma emission (185.7 keV) with relatively high abundance (54%) for use in performing field scanning. The nearest competing peaks to the 185.7 keV from U-235 (of significant abundance) are Pb-212 at 238.6 keV (Th-232 progeny) and the 144 keV from U-235 itself with a 10.5% abundance. Ra-226 has a competing peak at 186 keV with 3.28% abundance and should be present only in background quantities.

As observable in Figures 1 through 3, the 185.7 keV peak is distinguishable with all three detectors with the 2x2 inch NaI(Tl) detector clearly providing the best response at this energy level.[2] These figures represent spectra collected for ten minutes on the highest activity box, DM-05. Note: for display purposes, all spectra shown in this report are graphed using a moving average trend line with a period of ten for visually smoothing the display. Additionally, the peak labels and energies have been manually included on the graphs for illustrative purposes.

While longer count times provide more counts and better statistics for evaluating spectral data, they are not practical in performing walkover surveys. To evaluate the effect of scan time on detection level (i.e., decreased detection capability attributable to reduced counts in the designated region of interest), ten spectra were collected for each of the following time intervals: one (1) minute, twelve (12) seconds, eight (8) seconds, and four (4) seconds. Figures 4 through 7 show example spectra collected on box DM-05 with the 2x2 inch NaI(Tl) detector for each of these time intervals.

[2] It is of interest to note that the Al window Fidler produced a spectrum with poorer resolution, which likely is a result of the characteristics of the specific crystal and the detector photomultiplier tube. This result highlights the importance of carefully selecting quality scintillation crystals and testing of resolutions prior to use for spectral analysis.

Figure 1
2x2 NaI Detector Response for Box DM-05
10-min Spectrum

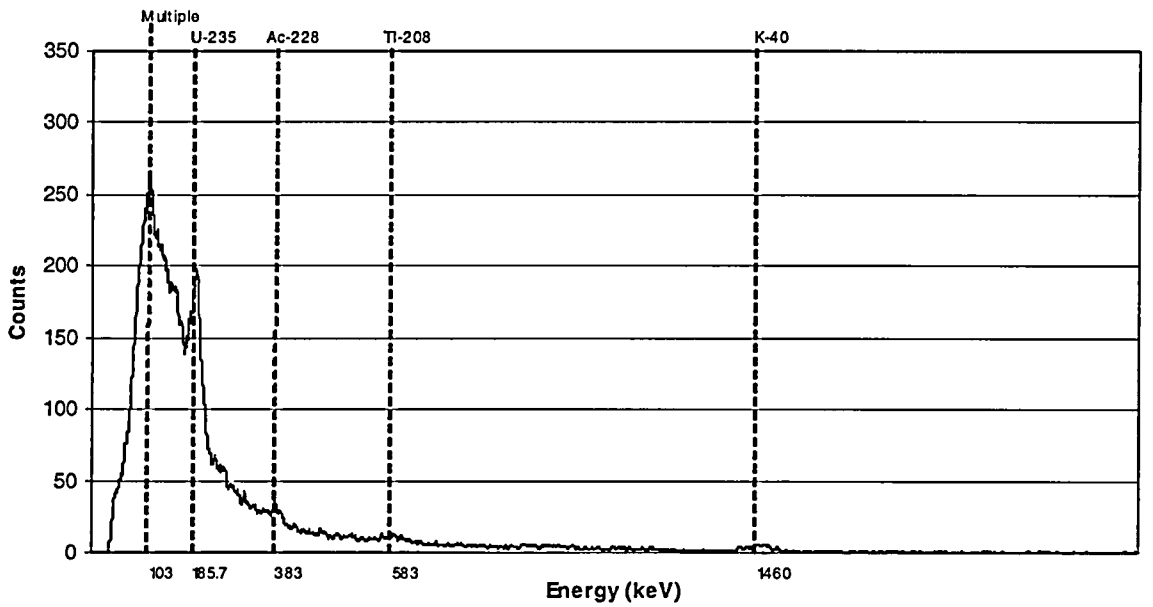

Figure 2
Fidler - Beryllium Detector Response for Box DM-05
10-min Spectrum

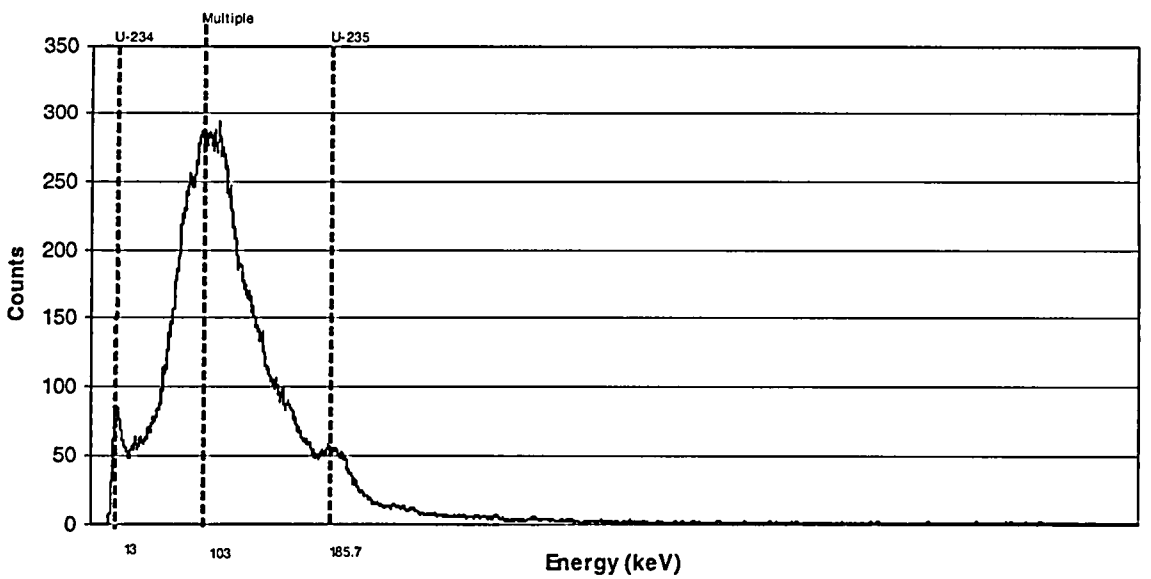

Figure 3
Fidler - Aluminum Detector Response for Box DM-05
10-min Spectrum

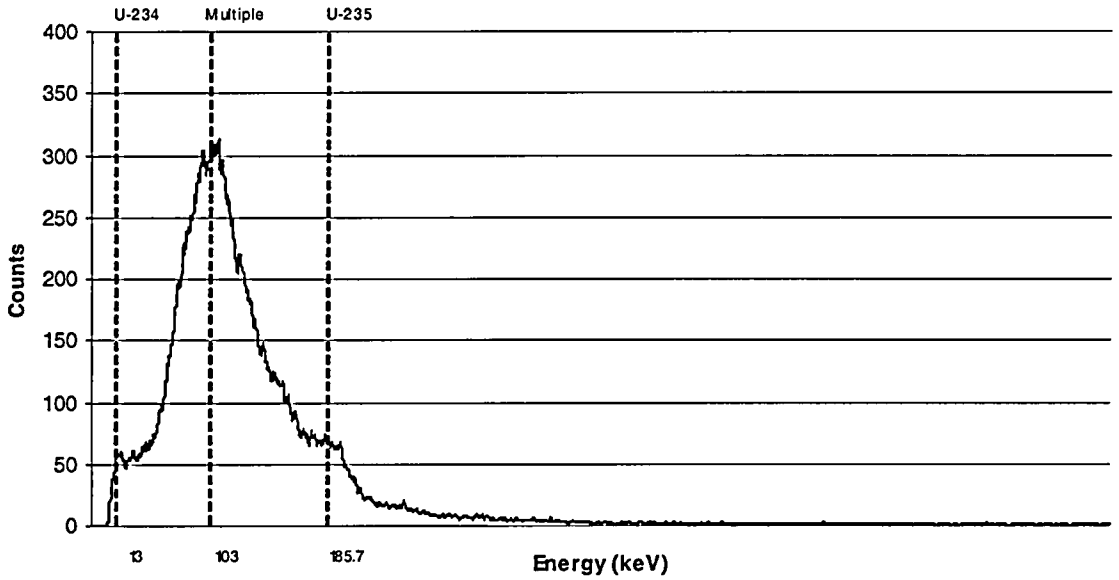

While the 185.7 keV U-235 peak is visible for the 4 and 8 second, its limited number of net counts yields poor statistics and a resulting very limited capability for quantitative analysis. The 12-second spectrum allows for a more statistically reliable quantitative assessment to be performed. Tables 1 and 2 provide a summary of the analysis performed for the region of interest for the 185.7 keV peak. The region of interest starts at around 170 keV and ends at 210 keV. As can be observed in Figures 2 and 3, there appears to be some visible tailing on the high energy side. To account for this, a slightly higher percent of the ROI energies are above the peak energy (i.e., 185 keV minus 15 keV plus 25 keV). Observable regions of interest appeared to vary slightly from one spectrum to the next. This phenomenon was attributable to counting statistics, especially where there were limited numbers of interactions for the shorter counting times. The region of interest as used for the analysis was selected by repeatedly examining the data set under varying ROIs. The 4-second spectrum was not included due to the inability to consistently identify the desired peak.

Figure 4
2x2 NaI Detector for Box DM-05
1-min Spectrum

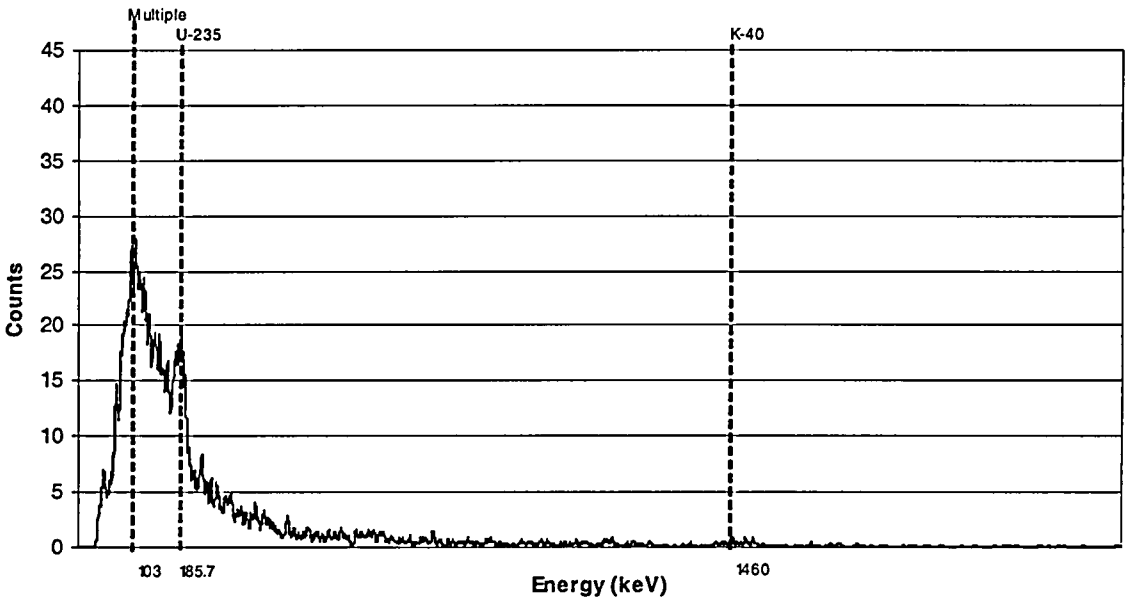

Figure 5
2x2 NaI Detector for Box DM-05
12-second Spectrum

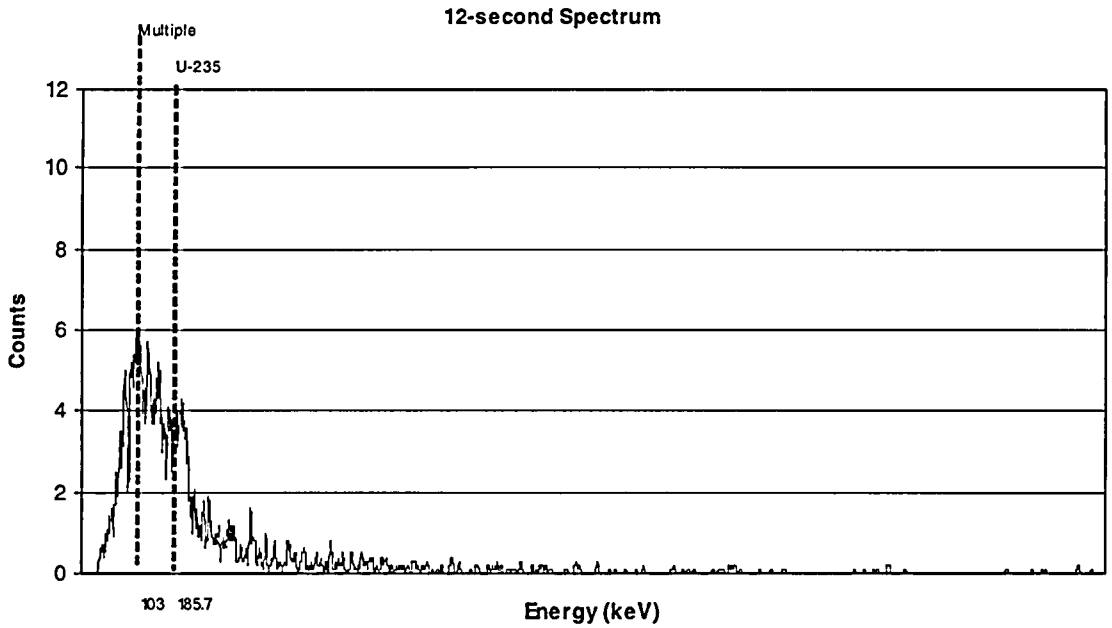

Figure 6
2x2 NaI Detector for Box DM-05
8-second Spectrum

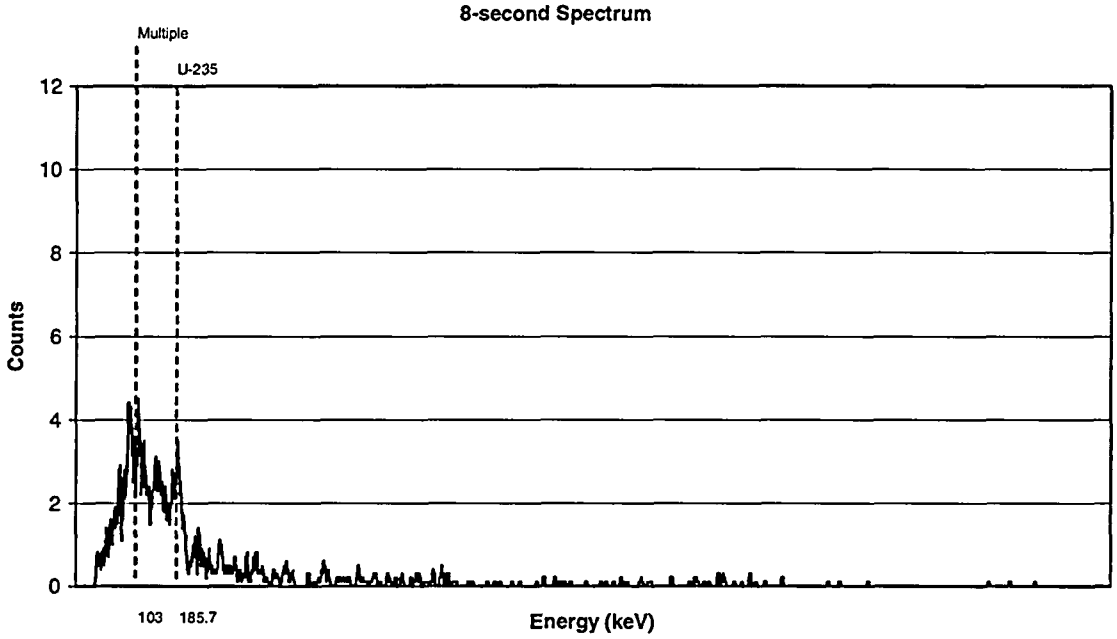

Figure 7
2x2 NaI Detector for Box DM-05
4-second Spectrum

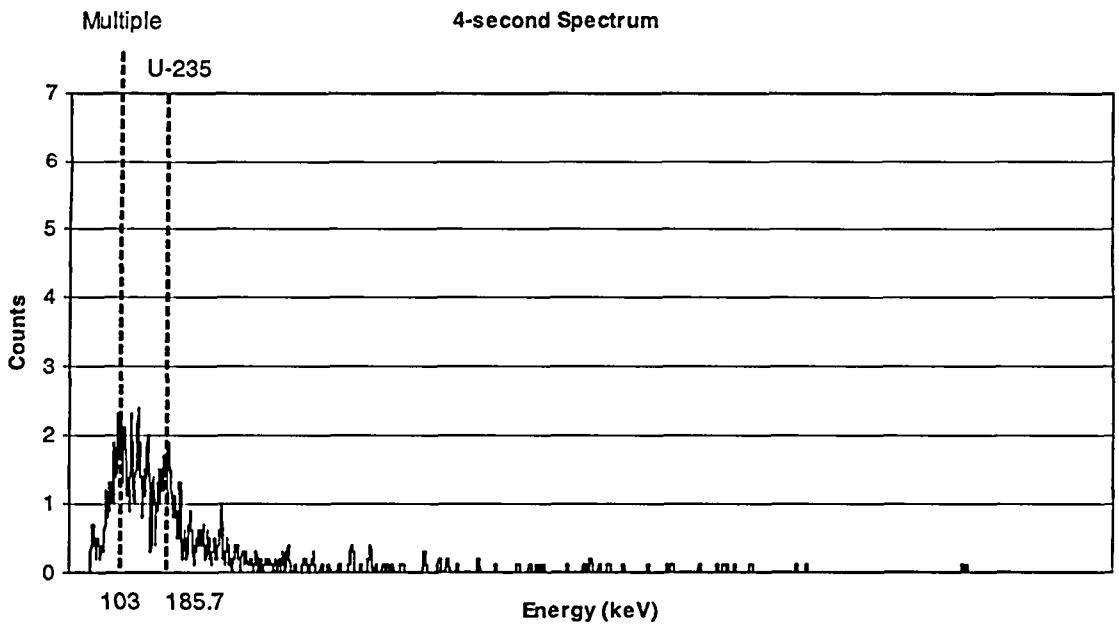

Table 1 2X2 Inch NaI(Tl) Detector Response for the 185.7 keV Region of Interest for Box DM-05 (gross counts per minute for the 185.7 keV region of interest)				
Time =	10 min*	1 min	12 s	8s
Minimum		1146	1123	1142
Maximum		1243	1290	1366
Average	1249	1202	1210	1261
Standard Deviation		29 (2.4%)	51 (4.2%)	70 (5.5%)

* A single 10-minute count.

Table 2 2X2 Inch NaI(Tl) Detector Net Response (Compton subtracted) for the 185.7 keV Region of Interest for Box DM-05 (net counts per minute)				
Time =	10 min	1 min	12 s	8s
Minimum		208	58	-53
Maximum		450	632	874
Average	385	285	343	418
Standard Deviation		74 (26%)	196 (57%)	296 (71%)

As shown in the Table 1, the gross counts per minute in the region of interest remain consistent throughout. The 1-minute, 12-second, and 8-second intervals are all within two standard deviations of the 10-minute interval, showing that the gross count rate in the region of interest selected remains consistent regardless of the count time. The data in Table 2 for the Compton subtracted ROI show statistically significant data. The net results, following subtraction of the Compton component, change significantly as the count time decreases. This variation reflects the difficulty in performing Compton subtraction, where very low total counts in the ROI compared with adjacent channels used for the background subtract significantly impact on the resultant statistics. This issue is discussed in more detail in Section 4.

To obtain a conversion factor of counts per minute to pCi/g for U-235, the region of interest was evaluated against known concentrations of U-235 for each of the test boxes using the 10-minute count interval with the 2x2 inch NaI(Tl) detector. Results of the soil analysis for the test boxes are presented in Table 3. Box DM-01 is considered a background box and is not included in the determination of the conversion factor.

Table 3 Summary of Analytical Information for Soil Boxes		
Box ID	**Box Description**	**U-235 (pCi/g ± 1 σ)***
DM-01	Background	0.103**
DM-02	Spike	1.873 ± 0.369
DM-03	1.2 x Background	1.953 ± 0.377
DM-04	1.5 x Background	2.290 ± 0.279
DM-05	2.5 x Background	4.980 ± 0.811

* counting statistics only; no consideration given to sampling error that may result from spatial variation.
** calculated value based on measured U-238 and assumed equilibrium conditions.

Since the 2x2 inch NaI(Tl) detector provides the best visual identification for the region of interest, conversion factors were determined for only this detector. Using the same region of interest described earlier (173 - 210 keV), the net counts per minute in the region of interest were calculated for soil boxes DM-02 thru DM-05. These values were then divided by the soil analysis results, pCi/g, from the above table to determine the conversion factor. The results, as presented in Table 4 below, show all correlations within 1 standard deviation of each other.

Table 4
Conversion Factor Based on 10-minute Spectra for 2x2 NaI Detector

Box ID	ROI Net cpm (± 1σ)*	cpm per pCi/g
DM-02	121 (± 26)	64.6 (±18.8)
DM-03	139 (± 24)	71.3 (± 18.4)
DM-04	130 (± 26)	56.8 (± 13.3)
DM-05	385 (± 28)	77.3 (± 13.8)
	Average	67.5 (± 8.1)

* One sigma error based on counting errors of the spectral data.

The same evaluation was made for boxes DM-02, DM-04 and DM-05 for the 1-minute count intervals. The average of the ten 1-minute counts was used to determine the net ROI counts per minute. The Compton component was subtracted. Those results are presented in Table 5.

Table 5
Conversion Factor Based on Ten 1-minute Spectra for a 2x2 NaI Detector

Box ID	ROI Net cpm (± 1σ)*	cpm per pCi/g
DM-02	124.5 (± 65.7)	66.5 (± 37.4)
DM-04	127.9 (± 99.6)	55.8 (± 44.0)
DM-05	285.4 (± 73.7)	57.3 (± 17.5)
	Average	59.88 (± 15.1)

* One sigma error based on the ten 1-minute count data set.

4.0 Results for Field Study

Several exterior areas were selected for additional evaluation following completion of the soil box survey. The five areas included a location approximately 40 feet north of the small warehouse in the southwest corner of the facility and 60 feet west of the large warehouse, a location approximately 30 feet north of the pond where previous surveys had indicated elevated levels, two background locations in the grass area on the west side of the property, and a location in the red barn. A single 10-minute spectrum was collected at each location with the 2x2 inch NaI(Tl) and Alpha Spectra Fidler (Beryllium window) detectors. To be consistent with standard scanning methods (and previous modeling), the detectors were mounted on a tripod with detector face approximately 10 cm above the soil surface.

A key observation from observing field response and reviewing the spectra is that temperature plays a key role by affecting the gain of the detector, which can cause a shift in the energy response as related to channel and gamma energy designation. Temperatures outside were 15-20°F warmer than those observed indoor, where the temperature was environmentally controlled. This environmental factor (temperature) causes an apparent shift in the peak energies as observed by the identified ROI. This topic is further addressed in a later section.

The findings of this portion of the survey further supported the use of a pre-defined ROI with Compton subtract as the better method for analysis. The spectrum, presented below in Figure 8, is for an outside area that had been identified as representative of background (based on soil analysis). This area is not expected to contain elevated levels of uranium isotopes resulting from facility operations; and the spectrum reflects this condition where the U-235 peak is not prominent.

Figure 9 shows a spectrum from a location to the north of the on-site pond that has been identified as containing slightly elevated levels of U-235. The spectrum for this pond location has a clear peak at 185.7 keV, indicating the presence of U-235. The gross count rate for the background spectrum was 9,875 cpm; while the gross count rate for the pond location was 6,931 cpm. The observable, physical characteristics of the soils in these two areas appeared to be similar (typical soil and grass), but the gross count rate was 42% higher in the supposedly background location than the impacted location with elevated levels of U-235. Visually comparing these two spectra, the peaks associated with Ac-228 and Tl-208 (progeny of Th-232 decay) in the background spectrum indicate a higher composition of naturally occurring radiation compared to the pond location.

A common technique in performing land surveys is to establish a typical site/area background level based on gross instrument response (e.g., gross count rate). As discussed above, this technique has very limited ability to distinguish residual low level uranium isotope contamination due to typical background variation. Even the technique of using gross energy window has limitations when a Compton subtract routine is not included. Compton scatter can lead to increased counts in the energy window, leading to false positive indications of elevated levels of contaminant. When evaluating the U-235 185.7 keV region of interest for these two spectra, it is apparent that a simple, typical background subtract for a given region will not be sufficient in determining the presence of uranium. For this example, the gross count rates in the region of interest were 705 and 905 cpm for the pond location and background location, respectively.

The distinction between gross and net count rate is achieved by applying standard spectral analysis technique for Compton subtract.[3] The net count rate (10-minute, Compton subtracted) was 60.4 (± 23.9) cpm for the pond location and 0.6 (± 28.2) cpm for the background location. Based upon the average conversion factor from Table 4, the activity at the pond location is 0.89 (± 0.37) pCi/g U-235. If a gross background subtract method were applied, no elevated U-235 level would be identified. Table 6 summarizes this discussion.

Table 6
Comparison of Field Survey Locations with 2X2 Inch NaI(Tl) Detector

Survey Location	Gross cpm	Gross ROI cpm	Net ROI cpm
Background	9,875	905 (± 95)	0.6 (± 28.2)
North of Pond	6,931	705 (± 84)	60.4 (± 23.9)
Red Barn	(to be added)	1144 (± 107)	429 (± 25.9)

[3] This technique involves selecting a number of channels on each side of the peak region of interest to represent the average Compton base. A linear interpellation is applied between the low-side and high-side to establish the underlying Compton component, which is then subtracted from the gross counts in the ROI to yield the net.

Figure 8
2x2 NaI Detector Background Location
10 - minute Spectrum

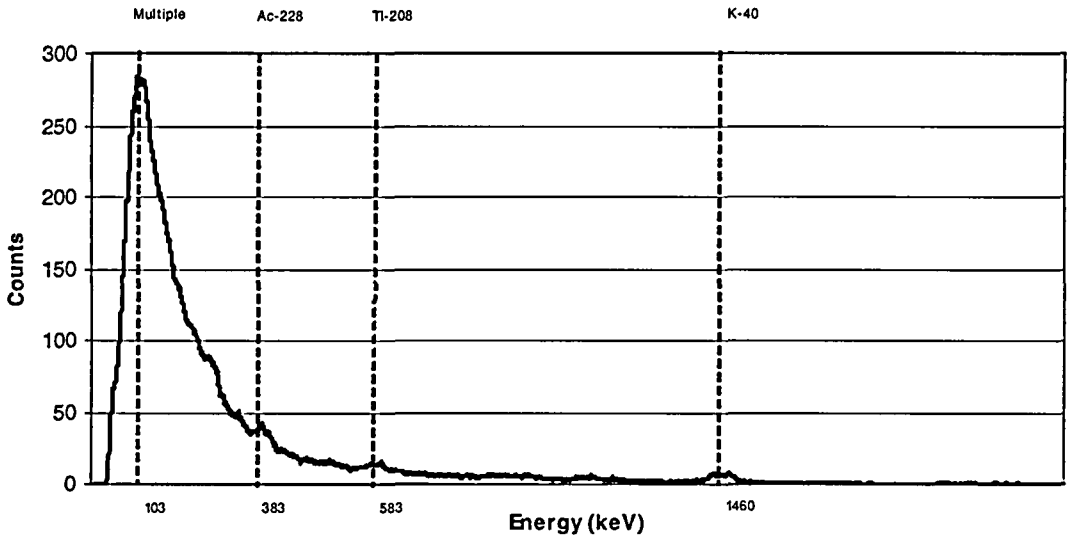

Figure 9
2x2 NaI Detector Pond Location
10 - minute Spectrum

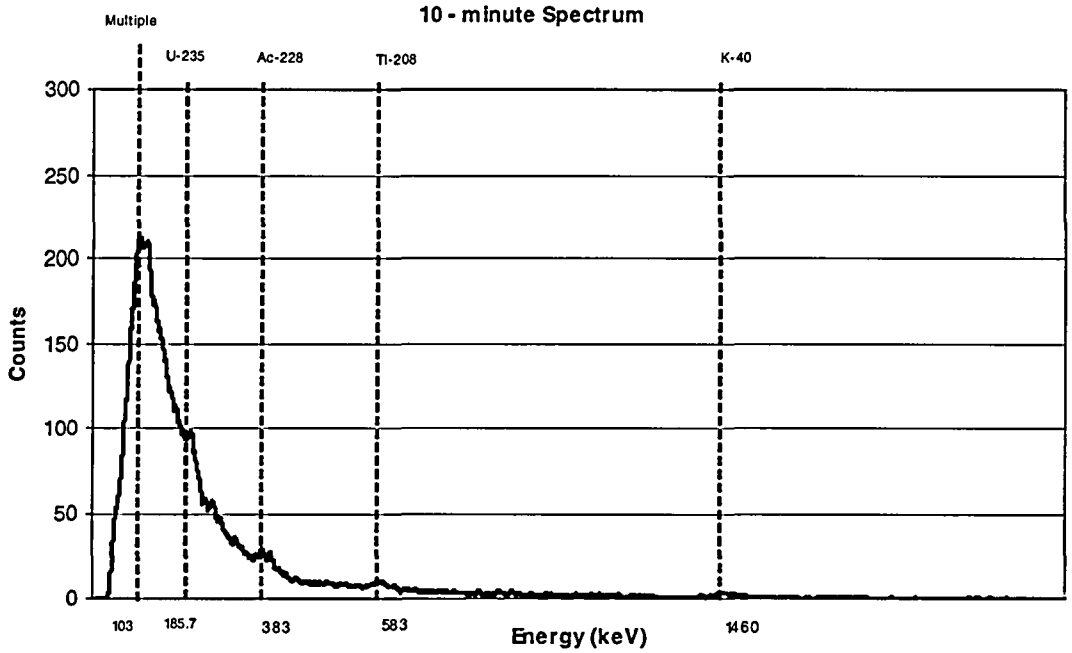

The final exterior location observed was inside the red barn at the north end of the property. This area had been identified as a potentially contaminated area. A ten-minute spectrum was collected for both the 2x2 inch NaI(Tl) and the Fidler (Be window) detector. The spectra are presented below in Figure 10 for the NaI and Figure 11 for the Fidler. The results indicate a clear difference between this location and the other locations, both outdoors and in the test boxes. This is clearly evident from observing the U-234 13 keV peak in Figure 11.

When evaluating the 185.7 keV U-235 peak for the 2x2 inch NaI(Tl) spectrum, the centroid was observed to be at approximately 196.8 keV. This represents a shift of approximately +10 keV from the data collected in the controlled environment. As discussed earlier, the exterior temperatures were 15 to 20°F warmer than inside the building where the test boxes were surveyed. This spectral shift has a significant impact on the evaluation of the region of interest. Applying the same region of interest (173 – 210 keV) used on the test boxes yields 1,179 gross cpm with a net (Compton subtracted) value of 297 cpm. Due to the shift in the peak centroid, the region of interest was not accurate. A new region of interest was established at 180 – 217 keV. The results were 1,144 gross cpm and 429 net cpm in the new region of interest. Applying the conversion factor established in Table 4 of 67.5 cpm per pCi/g U-235, the correlation is 4.4 pCi/g for the initial ROI and 6.4 pCi/g using the adjusted ROI, which reflects the gain shift, or a 45% difference. This comparison illustrates the importance of monitoring and compensating for any gain shift periodically while collecting spectra (scanning or static) in the field. This parameter must be controlled in performing field spectroscopy.

The spectrum collected using the Fidler detector shows a pronounced peak at 13 keV, likely associated with U-234 at 10.5% abundance, U-235 at 30.9% abundance, and Th-231 at 70.8% abundance. This region cannot be quantitatively evaluated due to the limited field of view at the low energies and the multiple radionuclide input. Examining the 185.7 keV, U-235 region of interest, the peak appears to be slightly wider for the outdoor area compared to the controlled area.[4] When comparing the red barn spectrum with the box DM-05 spectrum, a shift in the ROI was noted, caused by the change in temperature. For the DM-05 spectrum the region of interest was set at 172 – 205 keV; and for the red barn the ROI used was 171 – 210 keV. The results are 758 cpm gross and 129 (± 33.2) cpm net for the DM-05 test box and 746 cpm gross and 165 (± 35.7) cpm net for the red barn. Based upon this evaluation, the U-235 activity for the red barn would be approximately 6.6 (± 2.4) pCi/g.[5] This value compares favorably with the value calculated above for the 2x2 inch NaI(Tl) detector of 6.4 (± 0.9) pCi/g.[6]

[4] Increasing temperature of NaI(Tl) detectors slightly broadens the peak shape, decreasing resolution.
[5] This correlation is based on the DM-05 box measurement, where the net response for the Fidler was 129 (± 33.2) cpm with the box content being 4.98 pCi/g U-235, for a resulting 25.9 (± 7.9) cpm per pCi/g U-235.
[6] Correlation is based on the average value from Table 4, where the 2X2 inch NaI(Tl) detector response was calculated to be 67.5 (± 8.1) cpm per pCi/g.

Figure 10
2x2 NaI Detector Red Barn
10-minute Spectrum

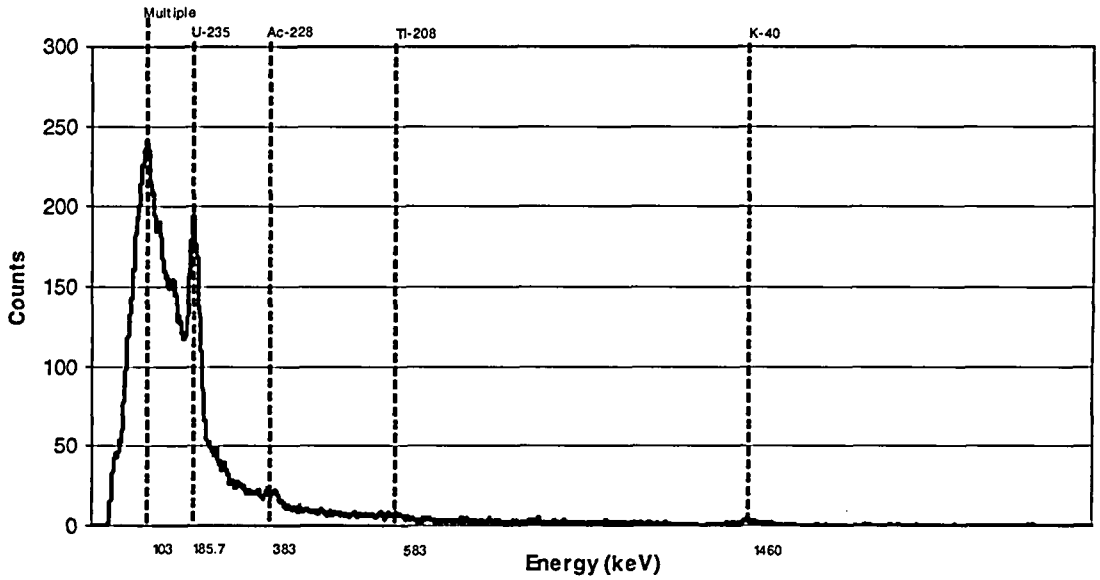

Figure 11
Fidler - Beryllium Detector Red Barn
10-minute Spectrum

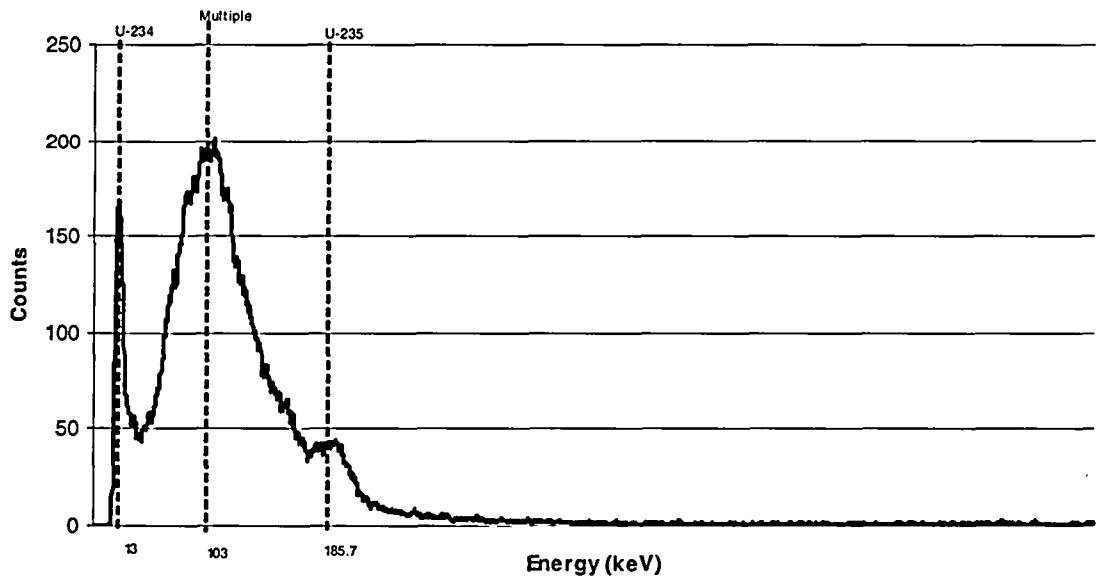

5.0 Comparison of Measurements with NCMP Modeling

The May 2005 report, "Evaluating Methods for Performing Final Status Surveys for Land Areas at the Hematite Facility," was based on the default MARSSIM surface scanning geometry of the right circular cylinder with a radius of 0.56 meter and 15 cm depth. Modeling using the MCNP code was performed for calculating the response for 2x2 inch NaI(Tl), Fidler and Ge detectors. The detector modeling assumed an energy window of 180 – 190 keV for the quantification of the 185.7 keV gamma of U-235. The calculated response for the 2X2 inch NaI(Tl) detector for U-235 and the immediate short lived daughters, Th-231 and Pa-231, is summarized in Table 7.

Table 7
Calculated Response of 2X2 Inch NaI Detector for U-235 Window

Modeling	Window	Detector Response (cpm per pCi/gm)
Initial Modeling (1 m^2, 15 cm depth source)	180 – 190 keV	48.4
Revised Modeling (B-12 box geometry)	170 – 210 keV	52.9

When the source was remodeled to reflect the geometry of the B-12 boxes with a 45 cm soil depth, the resultant correlation for the NaI(Tl) detector increased to 52.9 cpm per pCi/g, representing about a 9% increase from that noted above for the initial 1 m^2, 15 cm depth source geometry. This remodeled value is approximately 20% lower than the correlation based on field measurements.

Based on the measurements for the soil boxes, the correlation for the 2x2 inch NaI(Tl) detector was measured to be 67.5 (± 8.1) cpm per pCi/g U-235. This value is approximately 20% higher than that determined through modeling. There are several potential causes for this difference: one being the method used by the gamma spectral analysis software in stripping the underlying Compton continuum; and another being the potential presence of other radionuclides that also contribute counts in the 170 – 210 keV energy window. For example, Ra-226 has a 186 keV gamma with 3.3% abundance. This radionuclide will add approximately 1 cpm in the U-235 ROI for each pCi/g of soil activity.[7]

The window used to obtain the field measured, empirical conversion factor was over a broader range of energies (i.e., 170 keV to 210 keV) compared with that assumed for the original modeling (i.e., 180 to 190 keV). As discussed above, there remains a potential for some counts in the Compton continuum to be included in the net counts as determined by the gamma spectral analysis software. Regardless, considering errors in sampling, analysis, and statistical measurements, the results of the field measurements provide good data for verifying the applicability of spectral scanning for improving the detection capability for U-235 at the hematite site.

6.0 Conclusions

From the initial modeling study, it was determined that a properly set-up NaI detector with a reasonable scan speed and reasonable background should be able to achieve detection capability consistent with DCGL values for many of the areas The results of this field study support the conclusions of the initial study and further support the feasibility of using spectral

[7] This correlation is based on the MCNP calculated detector efficiency of approximately 8.6E-06 counts per disintegration for the 185 keV gamma in the B-25 box geometry.

scanning for enhancing the scanning MDC for decommissioning surveys at Hematite. With a multichannel analyzer and the ability to remove the Compton interference, the effect of background variation can be addressed (via Compton subtraction) and improved detection capability can be realized, much more so than simply using gross count mode.

The collection of data in a spectral mode requires additional controls beyond those required for routine gross count rate operation. Due to the short time intervals involved in spectral scanning, the quality of the counting statistics is not as good as they are over longer time intervals, i.e., fewer total counts. As shown in the summary data in Table 2, standard deviations increase noticeably between the one minute and eight second data sets. The required scan time interval will need to be evaluated for each particular area at the site to ensure adequate statistics for meeting the required MDC, which will be based on the area radionuclide mix and corresponding DCGL.

In determining the appropriate region of interest by which the data should be analyzed, slight variations in the upper and lower bounds of the window can have a significant impact on the quantitative results, which emphasizes the importance of maintaining control of spectral shifts that can be caused by environmental factors, such as temperature. Procedural controls will be needed for routinely evaluating fine gain to ensure that the peak energies of the check source are maintained in the correct channel. The importance of maintaining quality controls is essential in the evaluation of the large quantity of data that will be accumulated.

Remedial Investigation
Task Specific Work Plan

Burial Pits

Rev. 0

Prepared for:

Westinghouse

Westinghouse Electric Company
Hematite Facility
3300 State Road P
Festus, MO 63028

Prepared by:

RIVERFRONT ENVIRONMENTAL

Riverfront Environmental, Inc.
1139 Olive Street, Suite 300
St. Louis, MO 63101

March 2005

TABLE OF CONTENTS

1.0 INTRODUCTION 1
1.1 Purpose and Scope 1
1.1.1 Purpose 1
1.1.2 Scope 1
1.2 Site Background 2
2.0 INFORMATION SOURCES 4
2.1 Inter-Office Memos 4
2.1.1 1965 Memo 4
2.1.2 1969 Memo 5
2.2 Burial Pit Logbook 5
2.3 Hematite Long-Range Site Plan 6
2.4 Aerial Photographs 7
2.5 Geophysical Surveys 8
2.5.1 1998 Geophysical Survey 8
2.5.2 2002 Geophysical Survey 9
2.6 Soil Sampling (April 2004 & June 2004) 10
2.6.1 Surface Soil Sampling 10
2.6.2 Subsurface Soil Sampling 10
2.6.3 Subsurface Wipe Sample 10
2.7 Groundwater Sampling (July-August 2004) 11
3.0 FACTORS TO BE CONSIDERED IN SAMPLING OF WASTE MATERIALS IN BURIAL PITS 12
3.1 Trenching 12
3.2 Borings 12

4.0 SUMMARY AND CONCLUSIONS 13

LIST OF TABLES

Table 1	Summary of Chlorinated VOCs Detected in Subsurface Soil Samples from Burial Pit Areas Collected in June 2004 by SAIC
Table 2	Summary of Radioisotopes Detected in Subsurface Soil Samples from Burial Pit Areas Collected in June 2004 by SAIC

LIST OF FIGURES

Figure 1	TCE Levels in Temporary Monitoring Wells (July/August 2004)
Figure 2	PCE Levels in Temporary Monitoring Wells (July/August 2004)

LIST OF ATTACHMENTS

ATTACHMENT A	United Nuclear Corporation Inter-office memos (1965, 1969)
ATTACHMENT B	Electronic Data Tool
ATTACHMENT C	Hematite Long-Range Site Plan (1969)
ATTACHMENT D	Aerial Photographs (1960, 1966, 1974, 1975, 1976, and 2002)
ATTACHMENT E	Allgeier, Martin, and Associates, Inc Report (September 1998)
ATTACHMENT F	Geophex Ltd. Report (January 14, 2003)
ATTACHMENT G	Burial Pit Sampling Locations
ATTACHMENT H	Analytical Data Summary
ATTACHMENT I	Analytical Results – Wipe Sample from DPT Shoe (Analysis dated 8/16/2004)

Acronyms & Abbreviations

ADC	Aero-Data Corporation
AEC	Atomic Energy Commission
ASCS	Air and Soil Conservation Service
bgs	below ground surface
CERCLA	Comprehensive Environmental Response Compensation and Liability Act
EM	Electromagnetic
FS	Feasibility Study
GPR	Groundwater Penetrating Radar
MSA	Mine Safety Appliances
MoDOT	Missouri Department of Transportation
NRC	U.S. Nuclear Regulatory Commission
ppb	Parts Per Billion
PCE	Perchloroethene
RI	Remedial Investigation
SVOC	Semi-Volatile Organic Compound
TCE	Trichloroethene
TSWP	Task Specific Work Plan
^{234}U	Uranium-234
^{235}U	Uranium-235
^{238}U	Uranium-238
UF_6	Uranium Hexafluoride
UFP	Uranium Fluoride Production
UNC	United Nuclear Corporation
VOC	Volatile Organic Compound
WEC	Westinghouse Electric Company

1.0 INTRODUCTION

This Task Specific Work Plan (TSWP) provides the evaluation of available data related to the burial pits located at the former nuclear materials manufacturing plant at Hematite, Missouri, herein referred to as the Hematite Facility or Facility. During the 1960's and 1970's, the operators of the Hematite Facility buried site-related chemical and radiological wastes in unlined pits excavated at the site. After waste disposal, the pits were covered with on-site soils.

This TSWP is intended to summarize available records and results of investigations to date regarding the burial pits, including information from the following sources:

- Burial pit logs;
- Geophysical surveys;
- Aerial photograph interpretation;

and

- Analytical results from samples taken during the on-going remedial investigation (RI).

This TSWP also evaluates the reasonableness and/or necessity of conducting additional characterization into the nature and extent of contamination within the burial pits in order to evaluate remedial alternatives.

1.1 Purpose and Scope

1.1.1 Purpose

The overall purpose of the RI is to characterize the various environmental media at the Hematite Facility sufficiently to allow for the development and evaluation of remedial alternatives during the Feasibility Study (FS). The purpose of this TSWP is to summarize existing information that describes the locations and contents of the burial pits located on the Hematite Facility grounds and to evaluate the necessity of gathering additional data to evaluate remedial actions.

1.1.2 Scope

Historical documents provide information about procedures that were followed, as well as burial pit contents and locations. A logbook was kept that provides a detailed inventory of the materials placed in the pits, and a 1969 drawing identified the area of existing and future pit locations. Additional information has been obtained since the time the burial pits were closed and covered through the interpretation of historical aerial photographs, geophysical survey data, and analysis of soil and groundwater from or nearby the burial pit area.

This TSWP specifically summarizes the following items:

- A logbook that was kept between 1965 and 1970, which provides a detailed inventory of materials placed in the burial pits;
- Aerial photographs taken during the 1960's and 1970's previously analyzed and interpreted;
- Geophysical surveys (including magnetic, electromagnetic, and ground penetrating radar) performed in 1998 and 2002; and
- Analytical data from samples taken from surficial soil, subsurface soil, and groundwater in the burial pit area and a wipe sample during the ongoing RI.

The analyses of the aerial photographs and geophysical data were performed by third party consultants, and this report does not attempt to provide additional analysis or interpretation of existing data. Where possible, correlations between data sources are identified (e.g., aerial photos and logbook entries from the same date.)

1.2 Site Background

The Hematite Facility is a 228-acre property owned by the Westinghouse Electric Company (WEC) and located in eastern Missouri in Jefferson County, east of the town of Hematite. The Facility is southeast of State Route P between hills to the northwest and a terrace/floodplain of Joachim Creek, a tributary of the Mississippi River. The surface topography of the terrace deposit slopes gently to the southeast and blends with the alluvial floodplain deposits of Joachim Creek. Both grassy areas and wooded areas cover these two deposits; the terrace deposits are primarily grass-covered, and the alluvial deposits are primarily wooded.

Operations at the Hematite Facility throughout its history have included the manufacture of uranium metal and uranium compounds from natural and enriched uranium for use as nuclear fuel. Specifically, operations included the conversion of uranium hexafluoride (UF_6) gas of various ^{235}U enrichments to uranium oxide, uranium carbide, uranium dioxide pellets, and uranium metal. These products were manufactured for use by the federal government and government contractors and by commercial and research reactors approved by the Atomic Energy Commission (AEC). Research and development was also conducted at the facility, as were uranium scrap recovery processes.

The Facility was used for these manufacturing activities for approximately 47 years, i.e., from 1954 through 2001. Westinghouse ceased operations at the Facility in June 2001 and is now proceeding with decommissioning and characterization activities.

As part of the RI, surface and subsurface soil samples were collected around the burial pit area for analysis of both chemical and radiological constituents. These soil investigations have delineated the outer extent of impacted soils in the vicinity of the burial pits, as well as elsewhere at the Facility. Similarly, well installation and groundwater monitoring have been conducted as

part of the RI that identifies the extent of groundwater impacts associated with the Hematite Facility.

2.0 INFORMATION SOURCES

This report summarizes the following information sources regarding the burial pits:

- Inter-Office Memos of United Nuclear Corporation (UNC) dated July 19, 1965, and October 10, 1969.
- Burial Pit Logbook; used from July 16, 1965 to August 24, 1970.
- Hematite Plant Long Range Site Plan Map from UNC dated September 11, 1969.
- Aerial photographs, from 1960's to 1970's identifying several burial pits and/or features interpreted as burial pit scars.
- Geophysical surveys from 1998 and 2002, identifying anomalies in soil strata related to burial pits.
- Soil sampling data from the 2004 RI, showing results for radiological constituents and volatile organic compounds (VOCs) from surface sampling in burial pit areas and subsurface sampling around the perimeter of the burial pits.
- Groundwater sampling data from the RI sampling conducted from July through August 2004, showing results for chlorinated VOCs from temporary wells around the perimeter of burial pits.

Each information source is discussed in detail in the following sections.

2.1 Inter-Office Memos

Two inter-office memos from UNC, the owner and operator of the Facility at that time, were issued on July 19, 1965 (1965 memo) and October 10, 1969 (1969 memo). In general, the memos document the procedures governing the disposal practices for the burial pits. Copies of the memos are included in this report in Attachment A. These procedures are described in Sections 2.1.1 and 2.1.2, respectively.

2.1.1 1965 Memo

The 1965 memo presented the criteria governing the size, spacing, depth, and maintenance of records for the burial pits, as well as the maximum uranium content and the containerization of wastes. No criteria were provided regarding the construction, lining, or capping of the pits, and it is inferred that the pits were unlined. The memo also detailed the standard operating procedures for determining whether a waste should be sent to the burial pits or to an off-site disposal facility.

According to the 1965 UNC memo, the burial pits were to be excavated to a depth of 4 feet below ground surface (bgs) with a minimum of 6 feet separating each pit. Additionally, no more than 12 pits were to be filled per year, all wastes entering the burial pits were to be tagged

showing enrichment and total uranium mass, and records were to be maintained for each burial (see Section 2.2 – Burial Logbook). The memo did not, however, specify limitations on the lateral extent of a pit or its total volumetric capacity.

The maximum amount of radioactivity allowed in each pit was limited to 50 microcuries. The described procedure also specified the maximum mass of uranium or thorium allowed in each pit when the enrichment of the waste was known. The final mass of uranium for each pit was recorded in the logbooks.

The 1965 procedures dictated that the wastes were to be placed in appropriate containers to reduce the spread of radioactive contaminants in the burial pits. Visible contamination on the external surfaces of the containers and equipment was to be removed. The uranium content of each buried waste was to be determined by chemical analysis, gamma counting, or engineering estimate. The logbooks provide engineering estimates of uranium content for each log entry (waste type and volume) disposed of in the burial pits.

The procedure also provided criteria for on-site or off-site disposal of waste. In general, trash from the plant area, non-process equipment, glass from labs (packed in 55-gallon drums), acid insolubles, Mine Safety Appliances (MSA) filters and other solid process wastes were disposed of in the burial pits. Process equipment was disposed off-site at AEC-licensed commercial burial facilities or scrap dealers. These disposal criteria are consistent with the types of waste material recorded in the logbook.

2.1.2 1969 Memo

This memo provided the procedural process for conducting gamma counts on plant residues, as well as the handling and labeling of materials.

2.2 Burial Pit Logbook

The burial pit logbook consists of two volumes that contain entries recorded during the operational period from July 16, 1965 to August 24, 1970. The logbook contains approximately 15,000 entries listing the date of burial, pit number, the particular disposal item, the enrichment of the item, the uranium mass content, and other logging codes. According to the logbook, forty pits were created and filled between 1965 and 1970. Some pits were open for as short a time as two weeks while others were open for up to four months.

According to the logbook, the primary waste types disposed of on-site included various solids such as trash, empty bottles, floor tile, rags, drums, bottles, glass wool, lab glassware, acid insolubles, and filters. Chemical wastes were also disposed of in the pits including hydrochloric acid, hydrofluoric acid, potassium hydroxide, trichloroethene (TCE), alcohols, oils, and waste water. The uranium mass of each item varied between 0 to 63 grams. Enrichment measurements or estimates of each item were generally not recorded in the logbook. Based upon the logbook, the mass of uranium disposed in each pit varied, ranging from 178.08 grams to 801.8 grams.

The data from the original logbooks has been entered into an electronic format for use as a tool for assessing waste information. A copy of this electronic tool is included in Attachment B. According to the tool, the enrichment of the various wastes ranges from 1.65% to 97.0% The five most frequent entries are

- Acid insolubles (2,050 entries)
- Glass wool (2,080 entries)
- Gloves and liners (900 entries)
- Red Room trash (570 entries)
- Lab trash (515 entries)

The five entries with highest recorded grams uranium) are

- Acid Insoluble (one entry at 63 grams)
- Wood Filters (4 entries ranging from 22 to 44 grams)
- Metal shavings (one entry at 41 grams)
- Leco Crucibles (4 entries ranging from 29-31.6 grams)
- Reactor Tray (one entry at 40.4 grams)
-

2.3 Hematite Long-Range Site Plan

The Long Range Site Plan for the Hematite Facility, dated September 11, 1969, is a drawing of the facility showing the layout of the various buildings and process areas of the plant at that time (Attachment C). The drawing also shows the previously constructed burial pits and future burial pit locations, presumably with respect to the date of the drawing.

In the 1969 drawing, the plant is divided into several process areas. The northeastern and eastern portions of the plant are labeled on the site plan as the "UFP" area. While the acronym "UFP" is not defined on the drawing, Westinghouse interprets this to mean "uranium fluoride production", based on site process knowledge. The past burial pits are shown to be located northeast of the UFP area, while the future burial pits are immediately southeast of the past burial pits and directly east of the UFP area. Also depicted on the drawing is a 430 foot contour line (mean sea level) adjacent to the burial pit area and labeled as 'Site Perimeter". The intermittent creek is located to the east of this contour line, indicating that there was physical separation between the burial pits and the creek.

By observing the date that each burial pit was used from the logbook along with the date of the Site Plan drawing, it can be inferred that the first 31 pits were all located in the past burial pit location northeast of the UFP area, while the remaining pits were are located in the future burial pit location east of the UFP area. Therefore, the evidence indicates that, while the individual locations of the burial pits are unknown, all of the burial pits for which entries exist in the logs are likely to be consolidated within these two areas.

2.4 Aerial Photographs

Aerial photographs taken between the years of 1954 and 2002 were previously analyzed by Aero-Data Corporation (ADC) for indications of burial pits and burial pit scars. ADC did not identify any burial pits or burial pit scars in the photographs taken in 1954, 1956, 1957, 1959, 1962, 1971, 1973, 1979, 1985, 1990, 1991, 1996, 1998, and 2002. The photographs taken in 1960, 1966, 1974, 1975, and 1976 indicate either active burial pits or potential markings of past burial pits (scars). These photographs are included in this TSWP in Attachment D. The photographs are discussed individually in the sections below.

1960 Aerial Photograph
The 1960 aerial was photographed on November 3, 1960, by the Missouri Department of Transportation (MoDOT). In this photograph, one burial pit was identified approximately 150 feet northeast from the north corner of the UFP area. The approximate dimensions of the pit are 50 feet long (northeast to southwest) and 20 feet wide (northwest to southeast). This pit was not identified by ADC, but drawn on the photograph and labeled "first pits" by an unknown source. The shading and shape of the marking on the photograph appear to be consistent with subsequent burial pit markings. Therefore, the identified pit is included in this discussion as a possible burial pit. The existence of this pit is indicative of pit usage prior to the implementation of the burial pit logbook and procedures.

1966 Aerial Photograph
The 1966 aerial was photographed on September 24, 1966, by the U.S. Department of Agriculture, Air and Soil Conservation Service. In this photograph, one additional burial pit was identified approximately 200 feet northeast from the north corner of the UFP area. The interpreted dimensions of the pit are 60 feet long (northwest to southeast) and 20 feet wide (northeast to southwest). The pit is shown amidst a large cleared area. Correlating the date of the photograph with the burial pit logbook indicates the pit identified should be pit number 5.

1974 Aerial Photograph
The 1974 aerial was photographed on January 25, 1974, by MoDOT. In this photograph, two additional burial pits and three burial pits scars were identified. The burial pits lie approximately 150 feet northeast of the east corner of the fence line. The dimensions of the pits are approximately 20 feet by 40 feet and 25 by 66 feet. The burial pit scars lay from 200 to 300 feet northeast of the east corner of the fence line. In general, the dimensions of each scar are 20 feet by 50 feet.

1975 Aerial Photograph
The 1975 aerial photograph was taken on January 25, 1974, by the Surdex Corporation. Three additional burial pit scars were identified approximately 150 feet northeast and east of the UFP area. Two of pit scars lie 150 feet northeast of the northeast face of the UFP area and are each 20 feet wide (northeast to southwest) by 100 feet long (northwest to southeast). The third pit scar lies to the east of the east corner of the UFP area and is 30 feet wide (northeast to southwest) by 200 feet long (northwest to southeast).

1976 Aerial Photograph
The 1976 aerial was photographed on February 23, 1976, by the U.S. Department of the Interior, Geological Survey. One burial pit scar was identified approximately 200 feet northeast of the north corner of the UFP area. The pit scar measures approximately each 20 feet wide (northeast to southwest) by 20 feet long (northwest to southeast).

2002 Aerial Photograph
The 2002 aerial was photographed on February 22, 2002, by the Surdex Corporation. This photograph shows the burial pits and scars identified in the previous photographs, with the exception of the pit identified on the 1960 photograph.

In total, three burial pits and seven burial pits scars were identified from the historical aerial photographs. Only the burial pit identified in the 1966 aerial photograph can be correlated with dates in burial pit logbook to show that the pit should be pit 5. In general the pit locations identified or interpreted on the photos are consistent with burial ground locations on the long range site plan of 1969. However, the photos show no regular pattern of pit location or orientation.

Disturbed soil is visible in the vicinity of the burial pits in several of the photographs. Thus, it is apparent that the area in the vicinity of the burial pits has been regraded on several occasions. These regrading efforts included the addition of soil cover atop the area where the burial pits were excavated and filled. Analysis of the existing photographs suggests that up to 15 feet of soil of soil cover were added atop the burial pits in some areas. These soil cover activities appear to have been conducted as part of overall site operations and were not specific to NRC regulations regarding amount of cover materials to be placed over pits. The regrading efforts were not documented in site records.

2.5 Geophysical Surveys

2.5.1 *1998* Geophysical Survey

On August 10 through 13, 1998, a geophysical investigation was conducted by Berkshire Environmental, a subcontractor of Allgeier, Martin, and Associates, Inc. A copy of the investigation report, dated September 1998, is included in Attachment E.

The investigation used electromagnetic (EM) and magnetic methods over the suspected burial pit area to determine the areal extent of buried materials, assess the contents of these pits, determine the number and location of disposal pits, delineate the burial pits laterally, and explore for possible inorganic soil or groundwater contamination related to the pits. Results of the survey revealed several EM and magnetic anomalies that were interpreted to be burial pits. However, the exact number of burial pits could not be determined. The investigation also showed a high percentage of metallic material within the top 10 feet of soil. The lateral delineation of the burial pits in this investigation is consistent with the burial pit boundaries shown on the 1969 Hematite Long-Range Site Plan.

2.5.2 2002 Geophysical Survey

On December 16 and 17, 2002, a preliminary geophysical survey was conducted by Geophex Ltd. (Geophex). A copy of the Geophex report, dated January 14, 2003, is included in Attachment F.

The purpose of the investigation was to test the effectiveness of three geophysical methods including EM, magnetic, and ground penetrating radar (GPR) for determining the location of the burial pits at the site. According to Geophex, ground penetrating radar proved effective in identifying only surficial anomalies, while EM and magnetic methods were successful in identifying subsurface anomalies.

Surveying was conducted in three areas around the site. The first grid, Grid 1, measured 100 feet by 150 feet and was located northeast of the UFP building. The second grid, Grid 2, measured 130 feet by 150 feet and was located east of the site and northwest of the Missouri Pacific Railroad. The third grid, Grid 3, measured 80 feet by 150 feet and was located southwest of the Facility buildings and southeast of the barn in an area of the site where no reported burial operations took place. Grids 1 and 2 were located in select areas where analysis of historical aerial photographs showed burial pits or burial pit scars.

Grid 1
The electromagnetic survey of Grid 1 identified three trench-like anomalies and eight smaller subsurface anomalies. The magnetic data from this grid also indicated significant amounts of buried ferrous materials in the areas identified by the EM survey.

Grid 2
The electromagnetic survey of Grid 2 identified several subsurface anomalies varying in size. The magnetic data from this grid also indicated buried ferrous materials in the areas identified in the EM survey. An additional area of buried ferrous material not identified by the EM survey was located in the north corner of the grid by the magnetic survey.

Grid 3
The electromagnetic and magnetic survey of Grid 3 did not identify any subsurface anomalies. Anomalies detected were all attributed to surface features such as manhole covers, concrete, and a water tank.

The results of the investigation showed metallic anomalies in Grid 1 and Grid 2 not attributed to surface features, while Grid 3 anomalies were all attributed to surface features. These results are consistent with the 1969 Hematite Long-Range Site Plan which shows Grid 1 and Grid 2 located within the burial pit area, while Grid 3 is located on an undeveloped portion of the site.

In summary, available geophysical methods could identify some subsurface features that were likely buried waste materials (i.e., ferrous and non-ferrous metals), but these geophysical surveys were not successful in delineating individual burial pit boundaries. Furthermore, the geophysical methods identified only ferrous and non-ferrous metal anomalies, materials not always present in

the buried waste, and the effectiveness of the geophysical methods was limited by the amount of cover soils atop the burial pits.

2.6 Soil Sampling (April 2004 & June 2004)

As part of the RI, surface and subsurface soil samples were collected in the vicinity of the burial pits. Two soil sampling events were conducted by SAIC in April 2004 and June 2004. The April 2004 sampling event focused on surficial soil sampling atop suspected burial pit areas. The June 2004 sampling event focused on subsurface soil sampling on the perimeter of the burial pit areas. An aerial photograph showing the sampling locations is displayed in the figure contained in Attachment G. The samples were analyzed for VOCs, semi-volatile organic compounds (SVOCs), and select radioisotopes. The data will be presented in the RI, but is also summarized in Attachment H. The two sampling events and results are discussed in the following sections.

2.6.1 Surface Soil Sampling

Surficial soil samples were collected atop suspected burial pit areas on April 28, 29, and May 3, 2004. A total of twelve soil samples were collected during this time period. The samples were analyzed for VOCs, SVOCs, and select radioisotopes. The compounds that were analyzed for were either not detected or detected in trace amounts in the soil samples. Various sources indicate that the burial pits were covered with 4 to 15 feet of clean soil cover, thus, the clean analytical results for surface soil samples may be indicative of cover placement activities.

2.6.2 Subsurface Soil Sampling

Subsurface soil samples were collected on the perimeter of suspected burial pit areas on June 15, 28, 29, and 30, 2004. A total of thirty soil samples at depths ranging from 5 to 33 feet bgs were collected from seven borings during this time period. The samples were analyzed for VOCs, SVOCs, and select radioisotopes.

The VOC analysis of the subsurface soil samples identified detectable levels of chlorinated compounds including perchloroethene (PCE), TCE, cis-1,2-dichloroethene, 1,1-dichloroethane, chloroethane, vinyl chloride, and methylene chloride. Table 1 summarizes the VOC concentrations in parts per billion (ppb) at each applicable sampling point. Concentrations of SVOCs were either not detected or detected in trace amounts in the samples. The analytical results for the select radioisotopes showed detectable concentrations for isotopic uranium, isotopic thorium, neptunium-237, americium-241, and technetium-99. The identification of VOCs and radioisotopes in subsurface soils is consistent with the conclusion that these constituents are also present in burial pit waste.

2.6.3 Subsurface Wipe Sample

One RI boring, DS-01(BP-15) was identified as possibly being located within a burial pit. During probe advancement, a yellowish material was encountered at a 10-12 foot interval and

drilling was stopped. Soil samples from the probe were not collected, but a wipe sample was taken of the residue smeared on the shoe of the probing rod. The wipe sample was analyzed for isotopic uranium. Attachment I provides the analytical results for the wipe sample. The results of the analysis show detectable concentrations of ^{234}U, ^{235}U, and ^{238}U, consistent with low enriched uranium (approximately 2%). These results are consistent with the fact that low enriched isotopic uranium is expected to be present within the burial pits.

2.7 Groundwater Sampling (July-August 2004)

Groundwater samples were collected from temporary wells around the perimeter of the burial pit area from July 9 through August 4, 2004. The samples were analyzed for chlorinated VOCs including TCE and PCE by a mobile laboratory. VOCs are expected to be an indicator of contaminant migration from the burial pits through groundwater. Concentrations of TCE ranged up to 1,500 ppb, while concentrations of PCE peaked at 2,000 ppb at the perimeter of the burial pit area. Figures 1 and 2 show the concentrations of TCE and PCE, respectively, in each temporary monitoring well. The results of this investigation are consistent with the conclusion that chlorinated VOCs are present within the burial pits.

The data provided by the temporary wells provides an initial definition of the delineation of the nature and extent of groundwater VOC contamination migrating from the burial pit area. Several temporary wells, as shown on Figures 1 and 2, serve to bound the VOC contamination to the east and south (e.g., BP-21 (nondetect), NB-61 (nondetect) and NB-71 (nondetect). Additional definition will be presented in the Remedial Investigation report in terms of bounding the source both laterally and vertically fro both radiological and VOC constituents.

3.0 FACTORS TO BE CONSIDERED IN SAMPLING OF WASTE MATERIALS IN BURIAL PITS

The following section identifies concerns and issues related to performance of intrusive field activities in or near burial pit locations.

3.1 Trenching

The excavation of test pits or test trenching is the conventional technique for investigating former waste disposal pits or landfills. Test pitting is often used both to delineate the extent of buried waste as well as a means to collect samples of such waste.

The Hematite Facility, however, is being closed in accordance with U.S. Nuclear Regulatory Commission (NRC) requirements, and the NRC has prohibited trenching into potentially contaminated soils unless this activity is being conducted under an NRC-approved Decommissioning Plan. Accordingly, until the Decommissioning Plan is approved, trenching is not available as a technique to determine the lateral extent of the burial pits or to collect samples of materials buried in these pits.

3.2 Borings

Soil borings advanced using augers and a rotary drill rig or using hydraulic push techniques (e.g., Geoprobes®) could theoretically be used to investigate the burial pits. Examination of materials retrieved from soil borings (i.e., native soil versus waste) would be expected to provide some information regarding the extent of subsurface waste. Auger borings could retrieve many of the type of materials buried in the pits, but the degree to which this information was representative would be highly uncertain given the heterogeneity of the materials in the pits. The ability of Geoprobe borings to retrieve waste samples is questionable.

Moreover, advancing soil boring into unknown wastes raises significant concerns regarding environmental contamination and workers' health and safety. Certain wastes known to be present in the burial pits present a considerable risk if encountered in an uncontrolled manner. For example, because the exact location of any individual container is unknown, there is always the possibility that drilling could puncture or break a sealed container, resulting in releases both to the subsurface environmental and in exposure to workers.

Based on the heterogeneity of pit materials and the limited effiency of field equipment to retrieve representative samples in an effective and safe manner, random sampling of the burial pit area would provide limited benefit. Data obtained would be inadequate to provide significant waste characterization. In addition, the high risks and increased costs of such work greatly outweigh the potential benefits.

4.0 SUMMARY AND CONCLUSIONS

The purpose of this report has been to summarize historical and current information related to defining the nature and extent of waste contained in burial pits at the Hematite Facility. Knowledge of the waste characteristics of the material in the burial pits is needed to assess this area as a potential source of contamination as part of the RI.

The report summarizes the contemporaneous information (i.e., burial pit logs and memos describing the wastes that were placed into the pits, historical aerial photographs of the site) as well as information gathered after the pits were closed (i.e., geophysical surveys performed in the vicinity of the burial pits, and analytical results of soil and groundwater samples collected from perimeter locations around the pits). This report has summarized information related to the locations and sizes of the burial pits as well as the general contents of the pits.

Available means to supplement the current information are limited by the NRC prohibition against test trenching until the Facility Decommissioning Plan is approved. Boring techniques are likely to have limited effectiveness in characterizing the subsurface wastes and present significant concerns regarding potential environmental releases of contaminants and worker health and safety risks.

Information from the various sources is generally consistent and provides an adequate basis for delineating the burial pits and characterizing the waste materials in these pits. The available information is adequate for purposes of the RI and for proceeding with the evaluation of alternatives in the FS, without performing additional burial pit characterization.

TABLES

Table 1. Subsurface VOC Summary - Summary of Chlorinated VOCs Detected in Subsurface Soil Samples from Burial Pit Areas Collected in June 2004 by SAIC(concentrations in ppb)

Sample ID	Perchloroethene	Trichloroethene	cis-1,2-Dichloroethene	1,1-Dichloroethene	1,1-Dichloroethane	Chloroethane	Vinyl Chloride
BP-13-35-SL	--	--	--	--	--	--	--
BP-17-15-SL	9.1	7.3	14	--	--	--	--
BP-17-23-SL	--	14	39	12	--	--	--
BP-17-31-SL	--	--	57	23	--	--	--
BP-19-13-SL	21	6.7	19	--	--	--	--
BP-19-25-SL	--	--	46	150	210	--	--
BP-19-29-SL	--	--	8.3	51	130	--	--
BP-20-19-SL	42	7.2	--	--	--	--	--
BP-20-27-SL	--	--	--	--	--	--	--
BP-21-07-SL	--	--	--	--	--	--	--
BP-21-07-SL-FD	--	--	--	--	--	--	--
BP-21-13-SL	29	11	--	--	--	--	--
BP-21-24-SL	22	12	--	30	19	--	--
BP-21-34-SL	--	--	--	--	--	--	--
BP-22-13-SL	46	20	12	--	--	--	--
BP-22-23-SL	45	29	22	--	--	--	--
BP-22-33-SL	11	170	85	--	50	29	15

Note: -- = analyte was either not analyzed for or the concentration was below detection limits.
This table was adapted from previously existing tables; the original laboratory reports were unavailable.

Table 2. Summary of Radioisotopes Detected in Subsurface Soil Samples from Burial Pit Areas Collected in June 2004 by SAIC(concentrations in pci/g)

Sample Probe ID		Isotope						
		Tc-99	Th-228	Th-232	U-234	U-235	Np-237	Am-241
BP-13-05-SL	Value					0.319±0.406		
	MDL					0.664		
BP-13-05-SL	Value	0.59±0.51			0.943±0.178	0.0476±0.0262	-0.0627±0.172	0.0101±0.421
	MDL	0.811			0.0215	0.017	0.332	0.772
BP-13-11-SL	Value	0.416±0.494				0.084±0.395	-0.716±11.9	0±0.388
	MDL	0.806				0.7	21.5	0.714
BP-13-15-SL	Value	0.323±0.496				-0.142±0.407	-0.0373±0.178	0.0503±0.152
	MDL	0.82				0.779	0.343	0.263
BP-13-25-SL	Value	0.361±0.498				0.387±0.459	0.0425±0.199	-0.405±0.621
	MDL	0.819				0.744	0.355	1.18
BP-13-35-SL	Value	0.587±0.517				0.124±0.377	-4.33±11.1	0.135±0.389
	MDL	0.824				0.658	20.6	0.68
BP-17-05-SL	Value	4.26±1.26	1.07±0.218	1.16±0.232		0.35±0.515	-0.829±14.4	-0.0325±0.141
	MDL	1.31	0.0612	0.0247		0.856	26	0.263
BP-17-15-SL	Value	2.46±1.02				0.287±0.366	0.022±0.0983	-0.2±0.369
	MDL	1.31				0.598	0.183	0.723
BP-17-23-SL	Value	1.66±0.892				-0.256±0.382	-9.08±9.98	-0.348±0.393
	MDL	1.26				0.757	20.2	0.808
BP-17-31-SL	Value	0.311±0.758				-0.151±0.504	-7.89±13.6	-0.0477±0.142
	MDL	1.29				0.939	25.9	0.265
BP-18-05-SL	Value	0.0413±0.75				0.177±0.501	0.0141±0.223	-0.301±0.611
	MDL	1.32				0.868	0.402	1.15
BP-18-15-SL	Value	-0.051±0.738				0.715±0.573	-0.0425±0.242	0.00301±0.158
	MDL	1.32				0.873	0.454	0.284
BP-18-25-SL	Value	0.34±0.775				0.0919±0.502	-2.38±13.9	0.452±0.651
	MDL	1.32				0.889	25.5	1.08
BP-18-31-SL	Value	0.39±0.741				-0.115±0.265	-4.27±7.14	-0.173±0.268
	MDL	1.25				0.523	14.3	0.555
BP-19-05-SL	Value	-0.232±0.714				0.148±0.365	0.0515±0.132	-0.36±0.349
	MDL	1.3				0.629	0.231	0.717
BP-19-13-SL	Value	-0.195±0.716				0.0967±0.433	-4.4±12.1	0.577±0.54
	MDL	1.3				0.759	22.3	0.852
BP-19-25-SL	Value	0.217±0.774				0.156±0.365	-0.0343±0.139	-0.123±0.398
	MDL	1.34				0.631	0.269	0.757
BP-19-29-SL	Value	0.00358±0.717				0.571±0.437	-0.356±0.17	-0.0467±0.123
	MDL	1.27				0.653	0.327	0.231
BP-20-03-SL	Value	-0.721±0.766				-0.108±0.469	-4.9±12	-0.0997±0.13
	MDL	1.46				0.864	22.5	0.252
BP-20-19-SL	Value	-0.0758±0.825				0.111±0.507	-0.0791±0.19	-0.188±0.576
	MDL	1.47				0.888	0.366	1.06
BP-20-27-SL	Value	-0.425±0.822				-0.0223±0.298	-0.0726±0.123	-0.095±0.296
	MDL	1.52				0.556	0.249	0.58
BP-21-07-SL	Value	-0.286±0.806				0.118±0.411	-7.71±10.7	-0.092±0.155
	MDL	1.47				0.727	21.4	0.292
BP-21-07-SL-FD	Value	-0.579±0.759				-0.0517±0.491	-2.01±13.3	0.176±0.616
	MDL	1.43				0.886	24.1	1.06
BP-21-13-SL	Value	-0.518±0.78				0.0821±0.373	-3.31±9.64	0.0673±0.393
	MDL	1.46				0.659	18.2	0.703
BP-21-24-SL	Value	-0.828±0.769				0.176±0.506	0.0359±0.201	0.0559±0.153
	MDL	1.49				0.877	0.364	0.264
BP-21-34-SL	Value	-0.413±0.792				0.469±0.37	-0.0471±0.156	0.112±0.434
	MDL	1.47				0.554	0.3	0.766
BP-22-05-SL	Value	-0.216±0.823				0.0127±0.393	-7.77±10.4	0.244±0.46
	MDL	1.49				0.713	20.4	0.781
BP-22-13-SL	Value	0.0553±0.805				0.0521±0.442	-3.38±12.6	-0.414±0.518
	MDL	1.42				0.787	23.1	1
BP-22-23-SL	Value	-0.158±0.752				0.17±0.344	-0.146±9.09	-0.368±0.357
	MDL	1.36				0.589	16.6	0.733
BP-22-33-SL	Value	0.374±0.853				-0.145±0.381	-3.15±10	0.0101±0.105
	MDL	1.45				0.722	18.8	0.189

Note: Blank cells indicate analysis was not performed for the particular analyte. This table was adapted from previously existing tables; the original laboratory reports were unavailable.

FIGURES

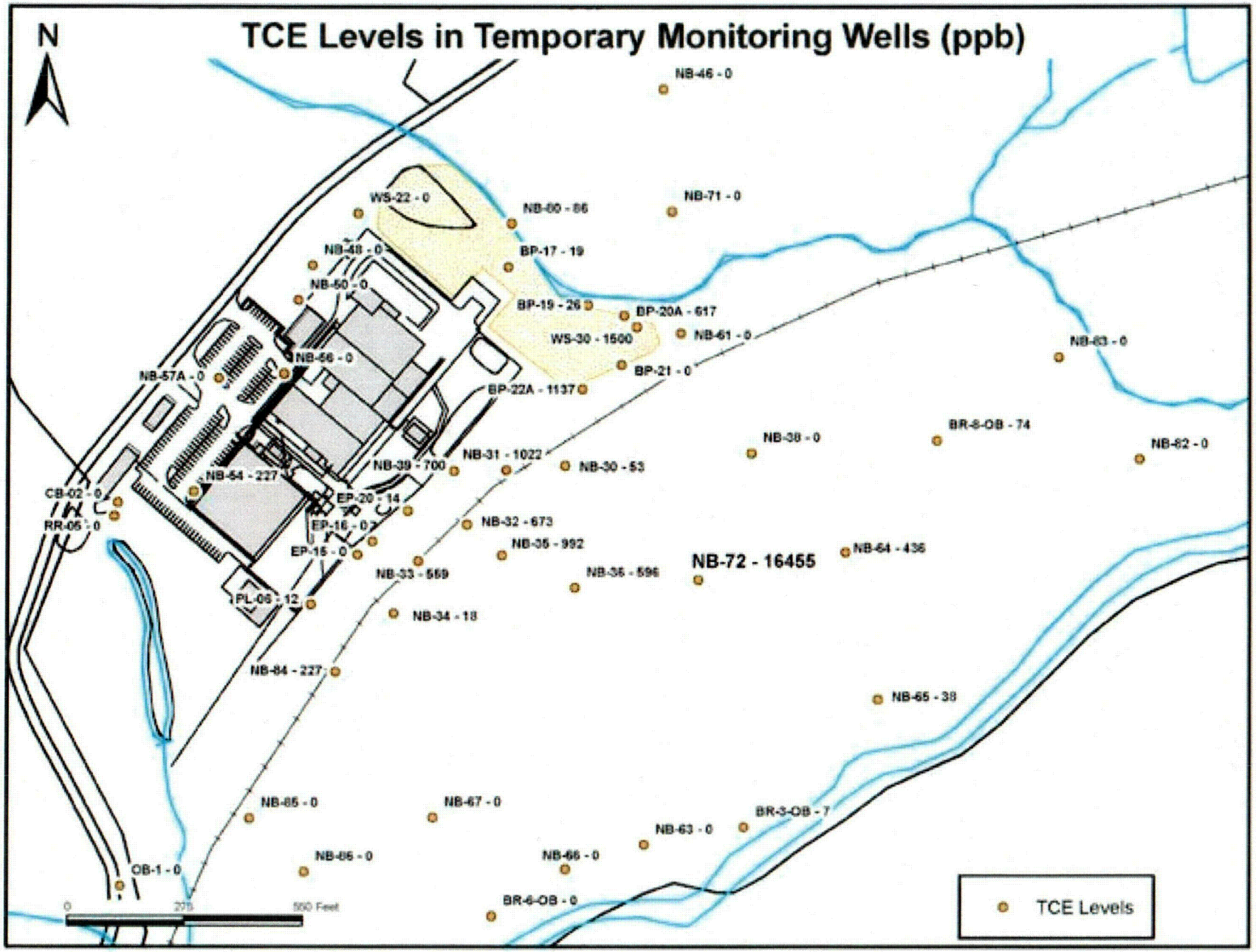
TCE Levels in Temporary Monitoring Wells (ppb)
N
NB-46 - 0
WS-22 - 0
NB-60 - 86
NB-71 - 0
NB-48 - 0
BP-17 - 19
NB-50 - 0
BP-19 - 26
BP-20A - 617
WS-30 - 1500
NB-61 - 0
NB-63 - 0
NB-56 - 0
NB-57A - 0
BP-21 - 0
BP-22A - 1137
BR-8-OB - 74
NB-38 - 0
NB-62 - 0
NB-31 - 1022
NB-30 - 53
NB-39 - 700
NB-54 - 227
CB-02 - 0
EP-20 - 14
RR-05 - 0
EP-16 - 0
NB-32 - 673
NB-35 - 992
EP-15 - 0
NB-64 - 436
NB-72 - 16455
NB-33 - 569
NB-36 - 596
PL-06 - 12
NB-34 - 18
NB-84 - 227
NB-65 - 38
NB-85 - 0
NB-67 - 0
BR-3-OB - 7
NB-63 - 0
NB-86 - 0
NB-66 - 0
OB-1 - 0
BR-6-OB - 0
0
275
550 Feet
TCE Levels

Figure 1

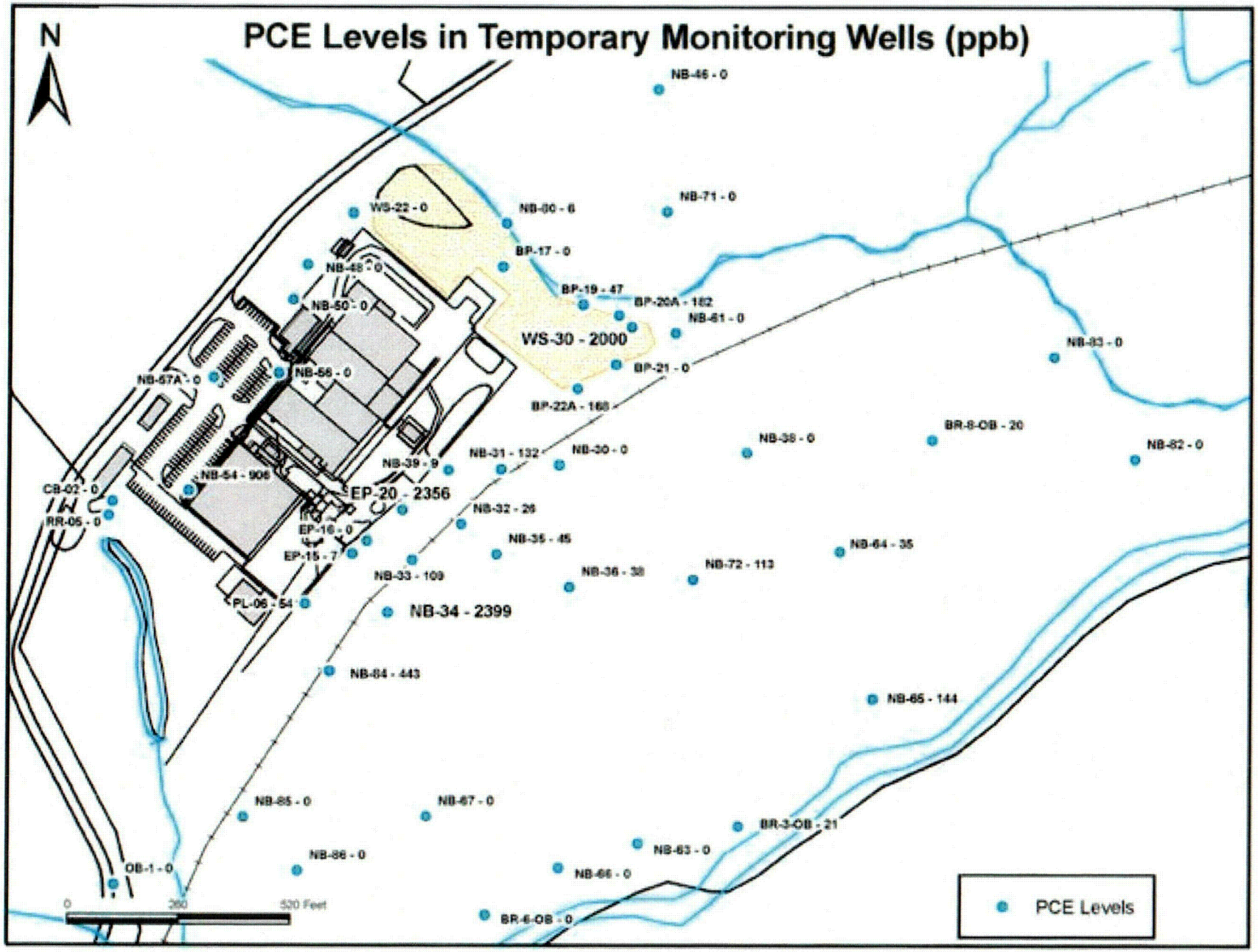
N
PCE Levels in Temporary Monitoring Wells (ppb)
NB-46 - 0
NB-71 - 0
WS-22 - 0
NB-60 - 6
BP-17 - 0
NB-48 - 0
NB-50 - 0
BP-19 - 47
BP-20A - 182
NB-61 - 0
WS-30 - 2000
NB-83 - 0
BP-21 - 0
NB-57A - 0
NB-58 - 0
BP-22A - 168
BR-8-OB - 20
NB-38 - 0
NB-82 - 0
NB-31 - 132
NB-30 - 0
NB-39 - 9
NB-54 - 906
CB-02 - 0
EP-20 - 2356
RR-05 - 0
NB-32 - 26
EP-16 - 0
NB-35 - 45
NB-64 - 35
EP-15 - 7
NB-33 - 109
NB-36 - 38
NB-72 - 113
PL-06 - 54
NB-34 - 2399
NB-84 - 443
NB-65 - 144
NB-85 - 0
NB-67 - 0
BR-3-OB - 21
NB-63 - 0
NB-86 - 0
OB-1 - 0
NB-66 - 0
0
260
520 Feet
BR-6-OB - 0
PCE Levels

Figure 2

ATTACHMENT A

INTER-OFFICE MEMO

UNITED NUCLEAR CORPORATION

TO	E. F. SANDERS	AT	HEMATITE	DATE	JULY 19, 1965
FROM	L. J. SWALLOW	AT	HEMATITE	COPY TO	D. F. CRONIN D. G. DARR R. M. HAMMOND J. A. RODE J. P. ROSSER F. G. STENGEL
SUBJECT	BURIAL OF RESIDUES AND CONTAMINATED MATERIAL				

THE FOLLOWING IS A SUMMARY OF THE CRITERIA WE AGREED TO FOR THE BURIAL OF LOW LEVEL WASTES AND CONTAMINATED EQUIPMENT.

1. AEC REGULATIONS

MAXIMUM QUANTITY PER BURIAL PIT: 50 MICROCURIES

ENRICHMENT	GRAMS U
>50 - 100%	790
>25 - <50	2000
>20 - <25	5000
>15 - <20	6000
>10 - <15	8000
> 6 - <10	12000
5	22000
4	26000
3	32000
2	40000
1	59000
NATURAL AND DEPLETED	150000
THORIUM	450000

IF MORE THAN ONE ENRICHMENT IS INVOLVED IN THE BURIAL THEN THE QUANTITY OF URANIUM OF EACH ENRICHMENT BURIED MUST BE LIMITED SUCH THAT:

$$\frac{X_1}{Ax_1} + \frac{X_2}{Ax_2} + --- + \frac{X_N}{Ax_N} = 1.00$$

WHERE: X_1, X_2, X_N IS THE QUANTITY OF U (IN GRAMS) OF EACH ENRICHMENT TO BE BURIED. Ax_1, Ax_2, Ax_N IS THE ALLOWABLE QUANTITY TO BURY OF THE CORRESPONDING ENRICHMENT.

BURIAL DEPTH: ALL MATERIAL BURIED IS A MINIMUM OF 4 FEET BELOW GRADE.

BURIAL FREQUENCY: NOT MORE THAN 12 PER CALENDAR YEAR.

SEPARATION OF BURIAL PITS: A MINIMUM OF SIX FEET BETWEEN PITS.

RECORDS: EACH ITEM SHALL BE TAGGED SHOWING ENRICHMENT, TOTAL U CONTENT.

A WRITTEN RECORD SHALL BE MAINTAINED BY THE RESPONSIBLE SUPERVISOR OF EACH BURIAL. THIS RECORD WILL LIST THE INDIVIDUAL ITEMS BURIED, TOTAL CONTENT AND DATE OF BURIAL.

NOTE: THERE IS NO REGULATION ON THE SIZE OF THE PIT.

II. UNC REGULATIONS

A. CONTAINERS: PROCESS RESIDUES (SUCH AS ACID INSOLUBLES), MSA FILTERS, CONTAMINATED TRASH, ETC., WILL BE PACKAGED IN SUITABLE CONTAINERS TO PREVENT THE SPREAD OF RADIOACTIVE CONTAMINATION DURING THE BURIAL PROCESS.

VISIBLE CONTAMINATION: VISIBLE CONTAMINATION ON EXTERNAL SURFACES OF ALL CONTAINERS OR EQUIPMENT SHALL BE REMOVED.

DETERMINING U CONTENT: THE URANIUM CONTENT OF EACH ITEM BURIED SHALL BE DETERMINED BY EITHER SAMPLE AND CHEMICAL ANALYSIS, GAMMA COUNTING OR ENGINEERING ESTIMATE.

III. SOP FOR PARTICULAR TYPES OF MATERIAL

A. GENERAL TRASH FROM PLANT AREA

THIS INCLUDES PAPER, RAGS, EMPTY BOTTLES, ETC.

PACKAGE IN POLY BAGS AND GAMMA COUNT.

LESS THAN OR EQUAL 4 GM 93% ENRICHED U (OR EQUIVALENT) PER BAG: BURY

GREATER THAN 4 GRAMS 93% U PER BAG:

1. IF CONCENTRATED -- LOCATE AND REMOVE.
2. IF DISPERSED: BURY.

B. PROCESS EQUIPMENT

1. REMOVE VISIBLE EXTERNAL CONTAMINATION.
2. REMOVE INTERNAL ACCUMULATIONS AS PRACTICAL.

3. MAKE "ENGINEERING ESTIMATE" OF TOTAL U OR GAMMA COUNT.

4. DISPOSE OF THROUGH AEC LICENSED COMMERCIAL BURIAL FACILITIES OR SCRAP DEALERS.

C. NON-PROCESS EQUIPMENT FROM PLANT AREAS (PIPING, FURNACE COILS, INSULATION FROM NON-PROCESS PIPING, ETC.)

1. REMOVE VISIBLE CONTAMINATION AND BURY. ASSUME NO U VALUE.

D. GLASS FROM CHEM LAB

1. RINSE AND COLLECT IN 55 GALLON DRUM. KEEP SEPARATE FROM OTHER TRASH.

BURY ASSUMING NO U VALUE.

E. ACID INSOLUBLES, MSA FILTERS, OTHER SOLID PROCESS RESIDUES

1. DETERMINE U CONTENT AND BURY WITHIN AEC LIMITS LISTED IN SECTION I ABOVE OR FORWARD TO LICENSED COMMERCIAL BURIAL FACILITIES.

F. OTHER

ITEMS NOT SPECIFICALLY FITTING THE ABOVE LISTED CATAGORIES WILL BE DISPOSITIONED AS THEY OCCUR BY THE HEALTH PHYSICS DEPARTMENT.

LJSWALLOW/JB

INTER-OFFICE MEMO

UNITED NUCLEAR CORPORATION

PH-69-131

TO Distribution AT Hematite DATE October 10, 1969

FROM E. F. Sanders AT Hematite COPY TO

SUBJECT Proposed Gamma Count Area SOP

I have outlined my recommendation for handling gamma count residues in the attachment. The following items are required to implement this system.

1) An operator assigned to the gamma count area as his major function.

2) New (smaller) trash receptacles in the process areas.

3) A place and system for disposal of low enriched liquids.

4) A supplemental system to schedule and handle materials which require reprocessing.

5) Hoods (one for hi enriched materials and one for low enriched materials) to cut up filters or otherwise prepare combustible materials for burning.

6) More burning capacity in both hi enriched and low enriched areas.

Gene

EFS/ah

attachments

Distribution: R. M. Barto
T. J. Collopy
J. P. Colton
B. C. Derreberry
L. C. Schuckenbrock
L. J. Swallow

UNITED NUCLEAR CORPORATION
Chemical Products

October 10, 1969

GAMMA COUNT PROCEDURE

A. HANDLING AND ROUTING OF MATERIALS TO BE COUNTED

1. Item Plant

Item residues will be brought either to the inside "residue rack" or to the outside "To Be Counted" area and recorded on the gamma count list as spelled out in the item residue SOP. The material control operator will transport these materials to the proper area once each shift.

2. Other Plant Residues

Residues from other plant areas will be tagged with the appropriate radioactivity tag and transported to the "To Be Counted" area as soon as they are dispositioned for counting by the foreman or the scrap engineer.

3. Process Area Trash

Trash will be picked up by the operator assigned to the gamma count area on a daily basis. Trash is placed in poly bags, tagged with the proper burial tag and transported to the "To Be Counted" area. (Non-contaminated trash is picked up by porters in office areas or by yard man in shipping - Receiving area and transported to holding area for burial).

B. HANDLING OF COUNTED RESIDUES

1. Item Plant Residues

a) Once each shift, the foreman will check the gamma count list and disposition the counted residues as per the item residue SOP. He will mark materials dispositioned for burial, "OK To Bury" on the container tag.

b) Once each day, the gamma count area operator will take each residue dispositioned for burial to the "For Burial" area.

c) Once each day, the gamma count area operator will take liquid residues dispositioned for discard to the Red Room Filtrate tank and discard it, logging it in to the filtrate system log book.

d) Once each shift, the material control operator will return the containers back to the item plant that are so dispositioned.

e) On a daily basis, the material control operator will transfer the containers dispositioned to the south vault as per the item residue SOP.

2. Other Plant Residues and Trash

a) Each day at approximately 10:00 A.M., the gamma count area operator will go through all residues. The following materials will be recorded on Sheet #1 and put in the Jeep:

(1) Counted residues marked "OK To Bury".

(2) Trash counted at less than 4 grams.

(3) Other plant solid residues with less than 1 gram (for plant liquid residues less than 1 gram see (b) below, do not record on Sheet #1).

(4) One copy of the Sheet #1 goes to the Item material control operator, one copy to ~~L. Vario~~ P. Sparks, one copy to SWOPP MCO, one copy to the burial log and one copy to T. J. Collopy.

b) After (a) above is complete, the following materials will be recorded on Sheet #2. If the container does not have a residue number, record the number on the container tag and on the Sheet #2 as per the note on the bottom of Sheet #2.

(1) Trash counted at 4 grams or greater.

(2) Plant residues counted at 1 gram or greater.

(3) Counted liquid residues.

(4) One copy of the Sheet #2 goes to T. J. Collopy and other copy stays with the gamma count area operator.

c) On a daily basis, the scrap engineer will disposition the materials on the Sheet #2 and return the sheet to the gamma count area operator to disposition the materials according to the list.

d) The gamma count area operator will disposition the containers as follows:

(1) Materials for burial will be marked "OK To Bury" and transported to the "For Burial" area.

(2) Hi enriched liquids for discard to filtrate tank will be logged in to the red room filtrate system and discarded.

(3) Low enriched liquids for discard - - - - - - - - - - - - - - - - ?

(4) Materials for transfer to the South Vault will be transported to the vault with a transfer ticket. 31

(5) Materials for reprocessing will be taken to storage until reprocessing time is scheduled.

(6) Hi enriched trash bags will be taken to the red room utility hood, one at a time. The contents of the container will be separated as follows:

(a) Non-contaminated or slightly contaminated trash into a poly bag, retagged with a burial tag and marked as trash.

(b) Highly contaminated trash into a poly bottle and retagged with an appropriate residue tag.

(c) Sample bottles or other containers to be "knocked out", cleaned up and put into a poly bag, retagged with a burial tag and marked as trash.

(d) All uranium powders, either from (c) or from other sources in the original container collected, put into a poly bottle and tagged with an appropriate residue tag.

(e) Items (a), (b), and (c) will be taken to the "To Be Counted" area. Item (c) will be weighed and put on the shelf for recovery.

(7) Lo enriched trash bags will be taken to the scrap recycle area and handled as described in (6) above.

ah

ATTACHMENT B

ATTACHMENT C

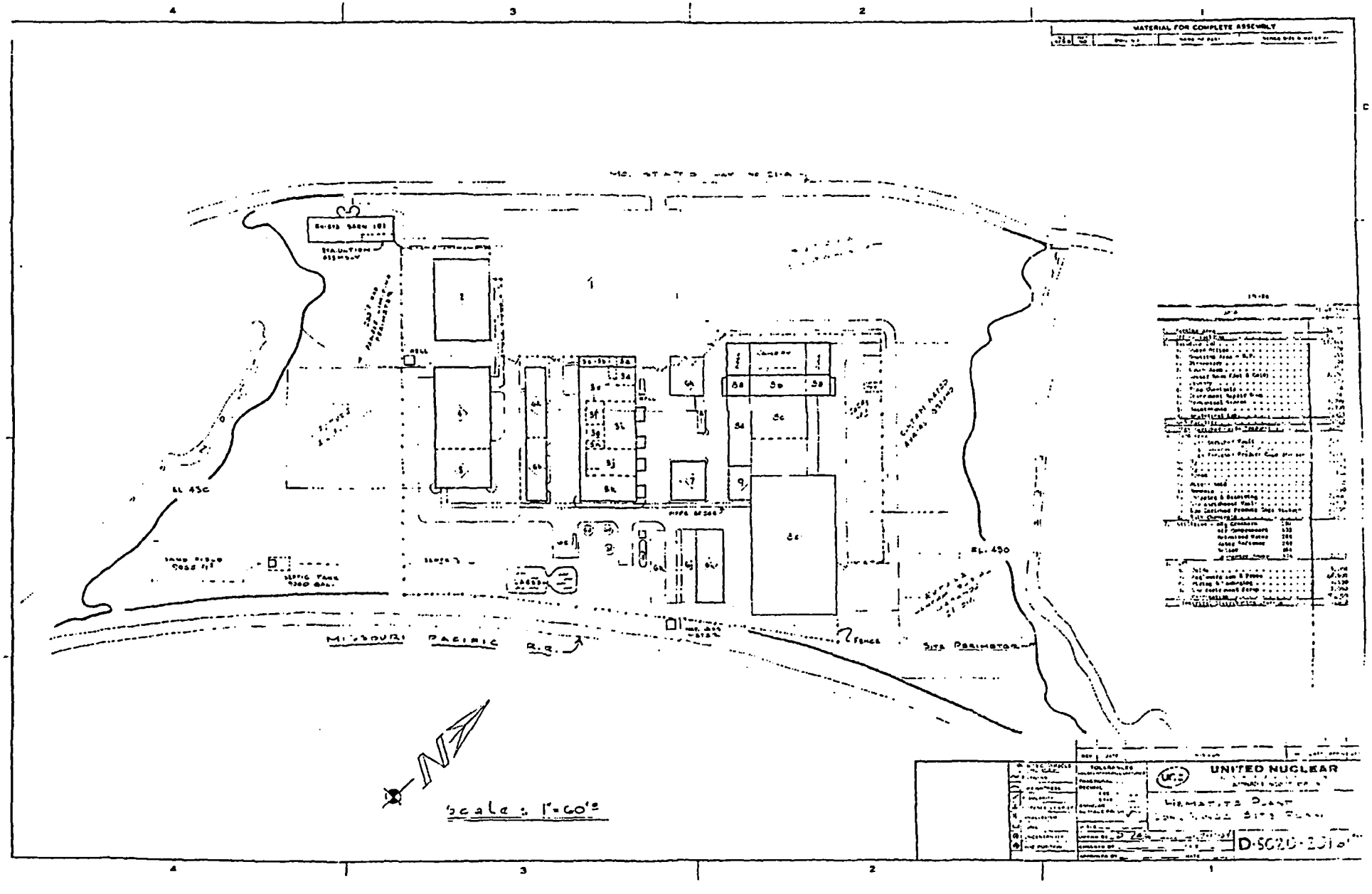
MATERIAL FOR COMPLETE ASSEMBLY
EL 450
EL 450
MISSOURI PACIFIC R.R.
FENCE
SITE PERIMETER
PIPE BRIDGE
SEPTIC TANK
LAGOON
CONTAIN AREA ANNUAL SPILLS
N
Scale: 1"=60'
UNITED NUCLEAR
HEMATITE PLANT
D-5020-2316

ATTACHMENT D

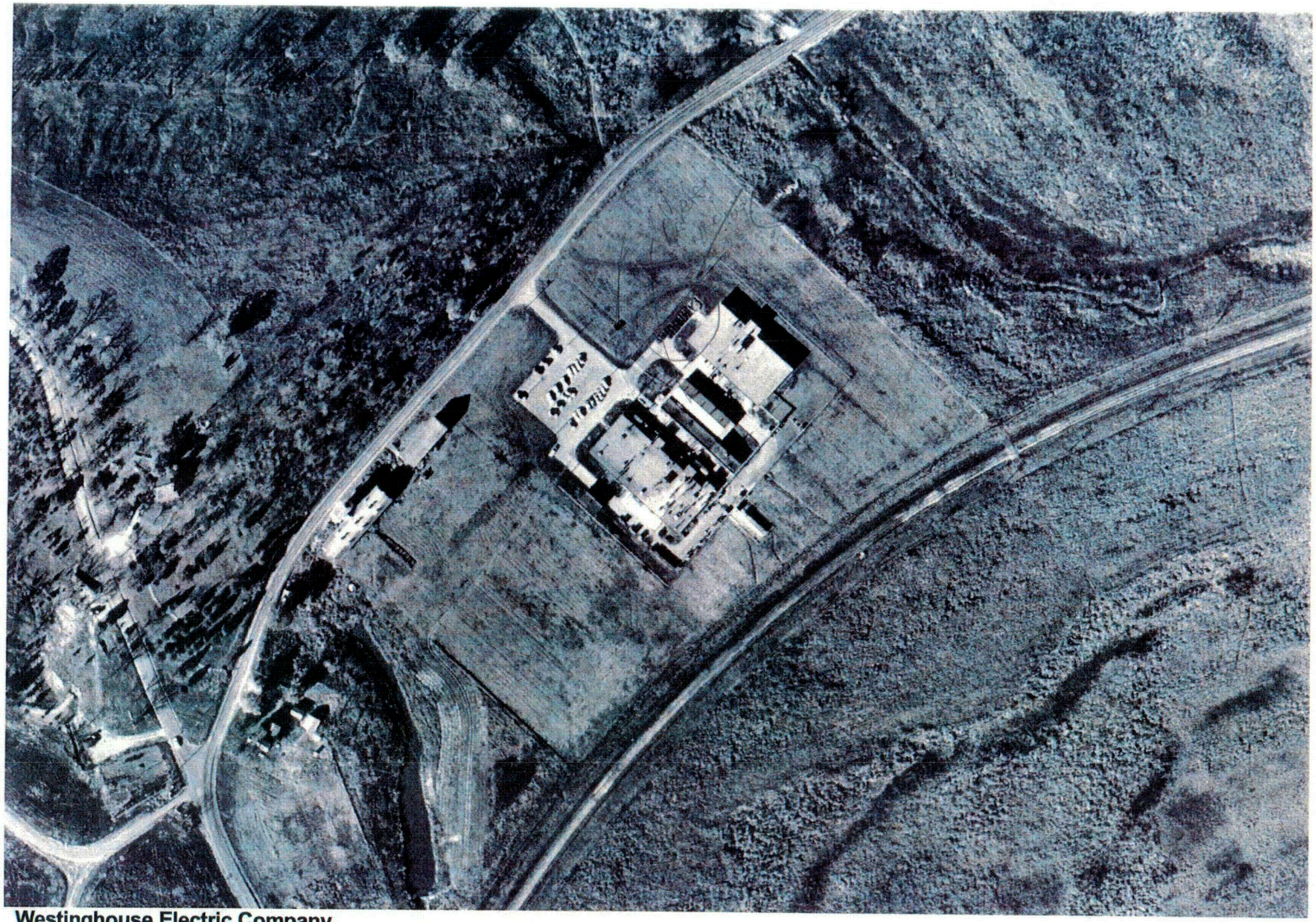

Westinghouse Electric Company
Hematite Plant - Festus, MO
11/3/1960
Photo Source: Missouri DOTD

N W E S

100 0 100 Feet

AERO-DATA CORP.
ENVIRONMENTAL
REMOTE SENSING CONSULTING SERVICES
AERIAL PHOTO ACQUISITION
INTERPRETATION and MAPPING

Westinghouse Electric Company
Hematite Plant - Festus, MO
9/24/1966
Photo Source: ASCS

Pit
Pit Scar

N
W E
S

100 0 100 Feet

AERO-DATA CORP.
ENVIRONMENTAL
REMOTE SENSING CONSULTING SERVICES
AERIAL PHOTO ACQUISITION
INTERPRETATION and MAPPING

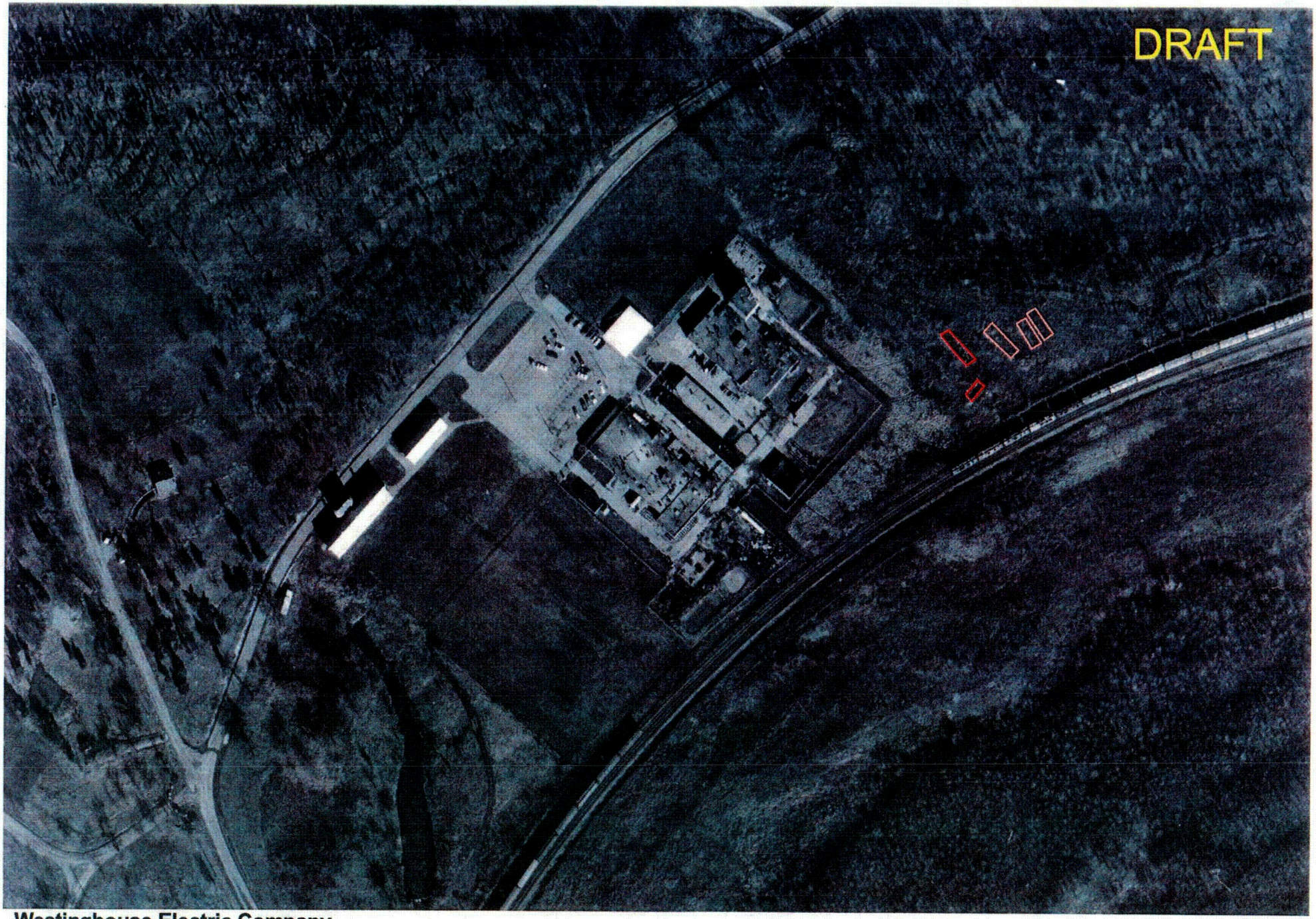

Westinghouse Electric Company
Hematite Plant - Festus, MO
1/25/1974
Photo Source: Missouri DOTD

Pit
Pit Scar

N W E S

100 0 100 Feet

AERO-DATA CORP.
ENVIRONMENTAL
REMOTE SENSING CONSULTING SERVICES
AERIAL PHOTO ACQUISITION
INTERPRETATION and MAPPING

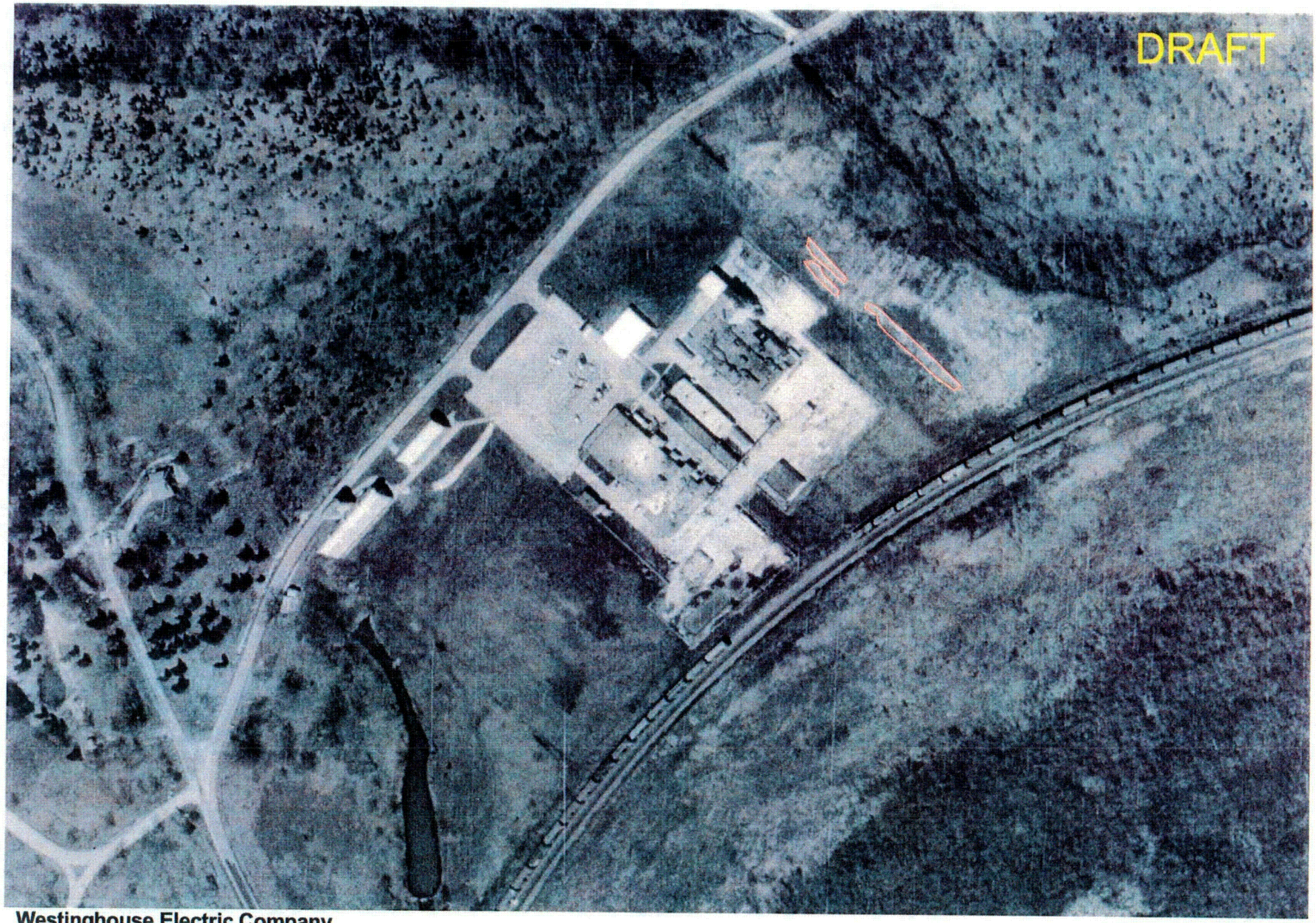

Westinghouse Electric Company
Hematite Plant - Festus, MO
4/6/1975
Photo Source: Surdex Corp.

Pit
Pit Scar

N
W E
S

100 0 100 Feet

AERO-DATA CORP.
ENVIRONMENTAL
REMOTE SENSING CONSULTING SERVICES
AERIAL PHOTO ACQUISITION
INTERPRETATION and MAPPING

Westinghouse Electric Company
Hematite Plant - Festus, MO
2/23/1976
Photo Source: USGS

Pit
Pit Scar

N
W E
S

100 0 100 Feet

AERO-DATA CORP.
ENVIRONMENTAL
REMOTE SENSING CONSULTING SERVICES
AERIAL PHOTO ACQUISITION
INTERPRETATION and MAPPING

Westinghouse Electric Company
Hematite Plant - Festus, MO
2/22/2002
Photo Source: Surdex Corp.

Historical Trenches and Trench Scars from 9/24/1966 through 2/23/1976

Pit
Pit Scar

N W E S

100 0 100 Feet

AERO-DATA CORP.
ENVIRONMENTAL
REMOTE SENSING CONSULTING SERVICES
AERIAL PHOTO ACQUISITION
INTERPRETATION and MAPPING

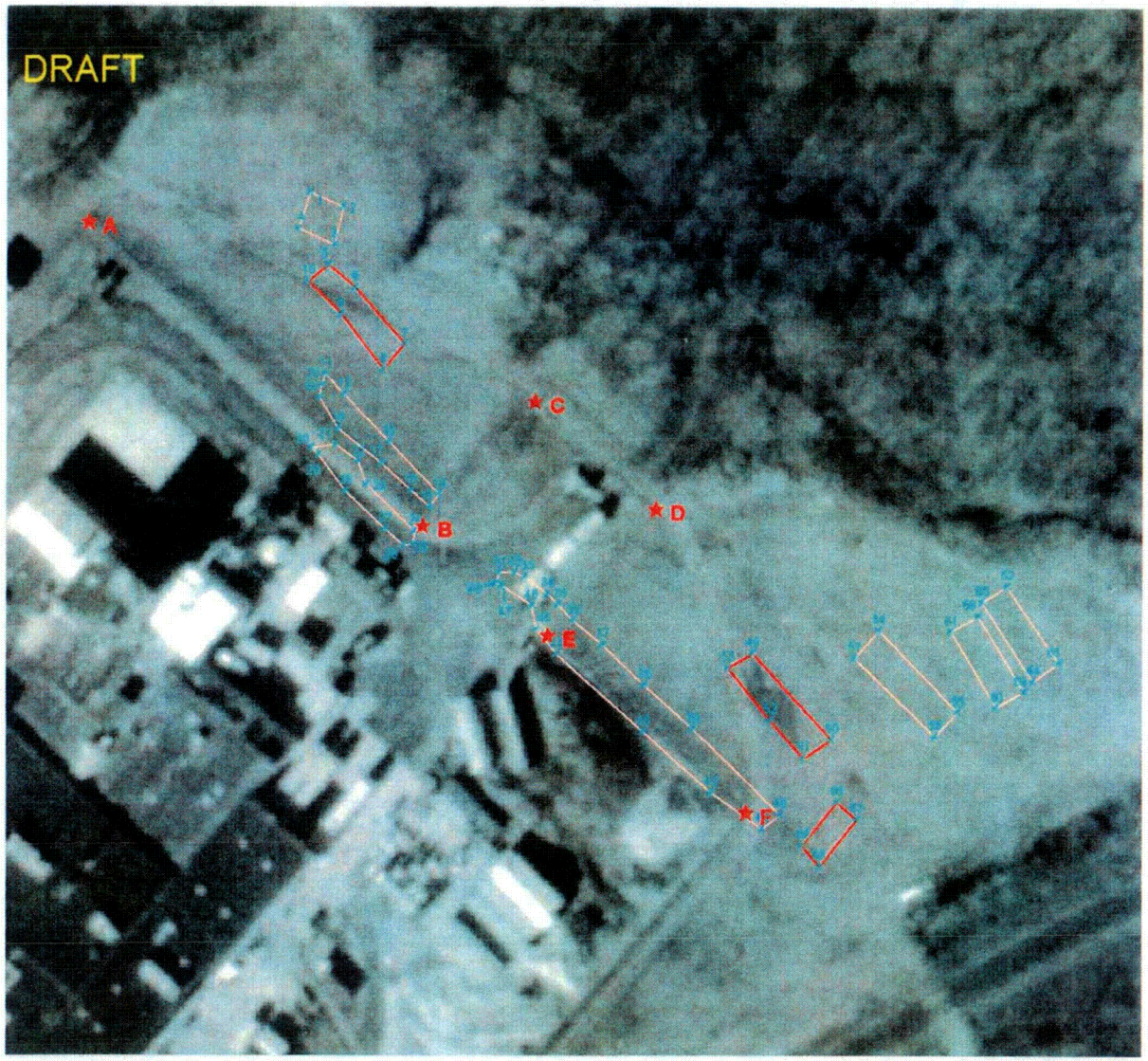

Westinghouse Electric Company
Hematite Plant - Festus, MO
2/22/2002
Photo Source: Surdex Corp

Historical Trenches and Trench Scars from 9/24/1966 through 2/23/1976

Pit
Pit Scar

Pit Edge Points
Fence Points

All Distances in Feet

Fence Line Points from Point A to Points B-F

Name	Distance	Bearing
A	0.00	0.00
B to A	248.52	131.52
C to A	265.52	111.32
D to A	350.26	116.36
E to A	339.24	131.41
F to A	484.70	131.40

From Fence Point "C"

Id_	Distance	Bearing	Id_	Distance	Bearing
1	167.55	312.26	38	166.20	158.86
2	148.96	314.72	39	198.86	154.14
3	139.17	307.32	40	262.57	149.08
4	160.46	305.46	41	264.29	151.77
5	135.66	302.92	42	234.15	155.61
6	116.48	301.81	43	189.86	161.76
7	78.30	293.23	44	138.89	175.21
8	85.09	281.39	45	124.53	179.90
9	117.02	293.80	46	111.84	181.26
10	140.93	297.35	47	102.48	190.55
11	116.57	277.04	48	102.05	192.26
12	105.25	271.82	49	182.44	139.12
13	83.52	254.37	50	246.40	138.51
14	73.63	225.80	51	244.41	142.73
15	81.91	224.88	52	216.68	143.42
16	84.12	234.32	53	179.99	143.99
17	91.19	248.04	54	226.76	123.54
18	109.56	262.08	55	287.78	126.14
19	118.88	270.81	56	286.02	129.73
20	118.06	274.12	57	224.85	128.64
21	112.23	257.74	58	270.69	115.69
22	102.60	251.32	59	312.45	120.45
23	103.23	243.77	60	303.99	123.37
24	97.23	222.65	61	261.19	118.82
25	103.05	220.55	62	278.54	111.28
26	106.93	222.24	63	322.16	116.33
27	108.25	229.58	64	313.94	119.14
28	115.42	244.73	65	269.25	114.06
29	123.11	256.15	66	274.71	142.79
30	125.96	258.32	67	288.55	142.14
31	95.94	191.79	68	297.86	148.29
32	94.82	187.15	69	283.36	148.69
33	96.34	183.58	C	0.00	0.00
34	105.38	176.49			
35	111.81	173.75			
36	121.87	170.20			
37	138.16	164.45			

From Fence Point "D"

Id_	Distance	Bearing	Id_	Distance	Bearing
1	256.43	312.03	38	96.23	183.89
2	237.76	313.55	39	121.65	170.42
3	227.90	308.98	40	179.80	157.63
4	249.02	307.64	41	183.44	161.39
5	223.93	306.35	42	157.18	168.91
6	204.63	306.04	43	121.53	183.33
7	165.05	302.99	44	96.52	214.65
8	167.97	296.83	45	93.20	225.32
9	203.47	301.47	46	86.83	232.54
10	228.13	302.85	47	94.92	243.91
11	196.36	291.91	48	97.10	245.21
12	182.65	289.96	49	95.04	146.16
13	151.38	283.95	50	158.52	142.38
14	119.52	273.68	51	158.13	148.97
15	124.28	270.44	52	130.96	151.43
16	135.18	274.22	53	95.12	155.57
17	153.09	279.36	54	139.30	118.42
18	180.42	284.09	55	199.47	123.72
19	195.03	288.13	56	197.21	128.89
20	196.21	290.12	57	136.16	126.71
21	179.63	281.29	58	186.80	108.20
22	165.75	279.07	59	225.89	116.09
23	159.64	274.81	60	216.39	120.00
24	132.95	264.60	61	175.61	112.39
25	134.87	261.77	62	197.60	102.30
26	139.82	261.71	63	237.57	110.67
27	149.31	265.70	64	227.95	114.32
28	171.13	273.26	65	186.42	105.81
29	188.34	279.02	66	188.31	148.06
30	192.77	280.01	67	201.82	146.76
31	92.89	247.92	68	214.26	155.14
32	85.79	245.86	69	200.12	156.20
33	81.46	242.87	D	0.00	0.00
34	75.73	232.42			
35	75.28	226.16			
36	76.31	216.82			
37	79.73	201.67			

40 0 40 Feet

AERO-DATA CORP

ATTACHMENT E

AN INTEGRATED GEOPHYSICAL INVESTIGATION AT COMBUSTION ENGINEERING

HEMATITE, MISSOURI

September, 1998

AM
ALLGEIER, MARTIN & ASSOCIATES, INC.
Consulting Engineers
Joplin, Missouri

TABLE OF CONTENTS

Section		Page No.
	TABLE OF CONTENTS	i
	LIST OF FIGURES	ii
1.0	OVERVIEW	1
2.0	GEOPHYSICAL THEORY	1
	2.1 Magnetics	1
	2.2 Time-Domain Electromagnetic Induction - EM-61	2
	2.3 Frequency-Domain Electromagnetic Induction - EM-31 & EM-34	2
3.0	FIELD DESIGN	3
4.0	INTERPRETATION and RESULTS	4
	4.1 Magnetic Gradient	4
	4.2 EM-61	4
	4.3 EM-31	5
	4.4 EM-34	5
	4.5 Integrated Interpretations	6
5.0	SUMMARY and CONCLUSIONS	7
6.0	REFERENCES CITED	8
7.0	CLOSING	8
Appendix A	Summary of Interpreted Anomaly Coordinates	

LIST OF FIGURES

Figure 1	**Geophysical Instrumentation (Magnetic Gradient & EM-61)**
Figure 2	**Geophysical Instrumentation (EM-31 & EM-34)**
Figure 3	**Surveyed Control Grid**
Figure 4	**Magnetic Data Reference Map**
Figure 5	**EM-61 Data Reference Map**
Figure 6	**EM-31 & EM-34 Data Reference Map**
Figure 7	**Magnetic Gradient Contour Map**
Figure 8	**EM-61 Lower Coil Contour Map**
Figure 9	**EM-61 Differential Contour Map**
Figure 10	**Ground Conductivity Contour Map**
Figure 11	**In-Phase Contour Map**
Figure 12	**EM-34 Profile - Line A**
Figure 13	**EM-34 Profile - Line B**
Figure 14	**EM-34 Profile - Line C**
Figure 15	**EM-34 Profile - Line D**
Figure 16	**Combined Anomaly Map**

AN INTEGRATED GEOPHYSICAL INVESTIGATION
AT
COMBUSTION ENGINEERING
HEMATITE, MISSOURI

1.0 INTRODUCTION

Leggette, Brashears, and Graham, Inc. (LB&G) contracted with Allgeier, Martin & Associates, Inc. (AMA) to conduct an integrated geophysical investigation at the Combustion Engineering (CE) facility in Hematite, Mo. AMA in turn contracted with Berkshire Environmental, Inc. (Berkshire) to collect magnetic gradient, time domain electromagnetic (Geonics EM-61), and frequency-domain electromagnetic (Geonics EM-31 and EM-34) data at the site. This data was collected on August 10th through 13th, 1998 over an irregularly shaped area of approximately 3.1 acres. The objectives of the geophysical investigation were to: 1) characterize the areal extent of buried materials; 2) determine the number and location of disposal trenches and characterize their contents; 3) determine the lateral extent of trenches for drilling purposes; and 4) explore for possible inorganic soil or groundwater contamination related to the trenches.

The following report is largely a result of an interpretive collaboration between AMA and Berkshire. Much of the procedure description and discussion of results was provided by Berkshire in their report to AMA.

Results of the geophysical investigation revealed numerous interpreted burial trenches. The position and lateral limits of identified trenches is defined primarily by ferrous and some non-ferrous materials within the backfill. Correlation between magnetic gradient, EM-61, and EM-31 (in-phase) maps is consistent with buried ferrous materials, while ground conductivity responses mapped via EM-31 and EM-34 depict a consistent, decreasing trend to the east, interpreted as changes in overburden character.

2.0 GEOPHYSICAL THEORY

2.1 Magnetics

Magnetic exploration is a non-destructive, non-intrusive geophysical technique used to detect localized changes in the Earth's magnetic field caused by buried ferromagnetic objects or materials. A magnetometer is a device employed to record the natural magnetic field of the Earth, which is measured in nanoTeslas (nT). The presence of ferromagnetic materials alters the Earth's natural magnetic field in both magnitude and direction, thus creating magnetic anomalies. The magnitude and extent of these anomalous responses are dependent on several variables including target to magnetic sensor distance, target material, mass, and orientation. A direct relationship between target size, material, depth of burial, and intensity of magnetic anomalies is more comprehensive when integrated with other geophysical methods (e.g., electromagnetics) or physical excavation.

For near-surface (<20 ft) environmental investigations, Berkshire employs a gradiometer system (Figure 1, top). This system consists of two vertically separated proton precession magnetometers that permits an instantaneous determination of the total magnetic field over a known vertical distance. Magnetic gradient data are calculated and recorded in nT/m. One advantage of a gradiometer system is the ability to determine the vertical magnetic field gradient while remaining relatively insensitive to the lateral component thus eliminating the need to reoccupy a base station. Base stations are required for single sensor magnetometers to correct for natural, time-varying (diurnal) magnetic field changes. The effect of diurnal changes are negated by a gradiometer since recorded values are the instantaneous difference between the two sensors. Furthermore, gradiometer systems filter deeper responses, providing a more focused, near-surface investigation. For this survey, Berkshire employed its in-house GEM Overhauser GSM-19 Overhauser gradiometer with a magnetic sensor separation of 0.56 m (1.84 ft).

2.2 Time-Domain Electromagnetic Induction - EM-61

Time-domain electromagnetic induction is a non-intrusive exploration technique that uses an alternating magnetic field to induce eddy currents in buried conductive materials. The decay rate of these eddy currents is monitored after the alternating signal is switched off and this decay rate is slower for metallic objects than in less electrically conductive materials, resulting in higher (voltage) readings over metallic targets. In addition, decay rates in deeper metal objects persist longer than for shallow objects. For this geophysical investigation, Berkshire utilized its in-house Geonics EM-61 high sensitivity metal detector (Figure 1, bottom) which is capable of detecting metal targets to depths of 10 ft, while remaining insensitive to conductivity changes related to soil and dissolved ions.

The EM-61 system provides several advantages for buried metal detection. First, the EM-61 system is designed to induce eddy currents in a near-vertical section. This permits data collection proximal to some surface features which cause magnetic or EM-31 interference. A second advantage of the vertical signal is that buried targets are not sensed once the EM-61 coils (1 m^2) are towed past the vertical plane of sensitivity.

2.3 Frequency-Domain Electromagnetic Induction - EM-31 & EM-34

Frequency-domain electromagnetic induction is used to map electrical conductivity variations and is sensitive to surficial and buried metal and changes in subsurface saturation, soil thickness, and dissolved ion concentration. The method involves the generation of an alternating magnetic field which induces eddy currents to flow in conductive materials. These eddy currents produce a secondary magnetic field which is sensed and measured by the field instrumentation. The subsurface's apparent conductivity

is derived by comparing the primary magnetic field with the measured secondary field and recorded in milliSiemens/meter (mS/m), the inverse of resistivity.

The apparent conductivity represents a composite value for all materials within the zone of exploration. The depth of investigation is dependent on the spacing between the transmitter and receiver coils and their orientation. For near surface imaging, Berkshire utilized its in-house Geonics EM-31 (Figure 2, top), while the EM-34 (Figure 2, bottom) was implemented for deeper exploration. EM-31 data (ground conductivity & in-phase) were collected in the vertical dipole mode which is capable of detecting targets to a maximum depth of 15 ft. In-phase EM-31 data are most sensitive to ferrous and non-ferrous metal objects and are recorded in units of parts per thousand (ppt). EM-34 (ground conductivity) data were collected using a 10 m (32.8 ft) intercoil spacing in both the horizontal and vertical dipole modes. This geometry provides maximum exploration depths of 25 and 50 ft, respectively.

3.0 FIELD DESIGN

The limits of the geophysical survey area were designed to overlap historical disposal areas. AMA and Berkshire designed, surveyed, and flagged a 10 x 10 ft control grid on the 3.1 acre site relative to permanent site features (fences, building, etc.) using non-magnetic PVC-staffed pin flags (Figure 3). Berkshire and AMA cleared vegetation along the treeline to extend data collection toward the stream in overgrown areas and installed oak stakes or steel spikes (paved areas) on 100 ft centers to provide more permanent survey control. The geophysical survey grid was not extended into the southeast portion of the fenced area, since large soil piles, thick vegetation, and storage trailers obstructed the area and precluded data collection.

Magnetic gradient data were collected on a 10 x 10 ft pattern resulting in 1,390 total data points (Figure 4). A total of 5,352 EM-61 and 5,392 EM-31 data points were collected on a 5 x 5 ft grid pattern by bisecting the control grid (Figures 5-6). A tighter grid was used for the EM surveys since the rate of EM data collection was more rapid compared to the gradiometer. In addition, the difference between EM-31 and EM-61 coverage is due to the more portable nature of the EM-31 over non-metallic surface obstructions (trees, etc.). Geophysical data were not collected adjacent to some large surface obstructions which generated interference.

All magnetic gradient, EM-61, and EM-31 data were digitally stored, downloaded to an infield computer, and reviewed for data quality and integrity. Preliminary, color-enhanced contour maps were generated and printed in the field to locate anomalous areas. Due to the pervasive nature of recorded anomalies, no single feature was field-flagged. An analysis of the preliminary contour maps was used to place EM-34 profiles in downgradient positions which were unlikely to encounter interference from surficial and buried materials.

Due to limited available survey areas, 520 ft of EM-34 profiling was conducted at 10 ft intervals along four (4) separate profiles (Figure 6). Both vertical and horizontal dipole data were recorded

at each station using a 10 m (32.8 ft) coil separation.

4.0 INTERPRETATION and RESULTS

All magnetic gradient, EM-61, and EM-31 data were digitally recorded, downloaded to an in-field computer, and reviewed for data QA/QC. Final contour maps were gridded, splined, and contoured using the SURFER (v.6.01) software package. The location of surficial features were recorded in the field notes and correlated with recorded data to isolate responses due to subsurface targets. Based on data point spacing and contouring parameters, the lateral resolution of all interpreted anomalies is estimated at +5.0 ft.

In general, the magnetic gradient and EM-61 maps (Figures 7-9) display high-amplitude, tightly closed (bulls-eye) responses superimposed on relatively calm, background conditions. In contrast, the EM-31 maps (Figures 10-11) exhibit fewer bulls-eye responses and more regional trends. Typically, high-amplitude, laterally abrupt responses are due to surficial and near-surface buried metal objects, while geologic features related to variations in nonmetallic soil/fill, bedrock, and groundwater conditions tend to be of lower magnitude and follow more subtle trends. In addition, negative EM responses depicted as dashed red contours, are a characteristic response from surface, very near-surface, or massive ferrous objects, while similar objects typically produce dipolar responses in magnetic gradient data. At this latitude, the buried target causing a dipolar magnetic anomaly is typically centered between the positive peak and the inflection point of the anomaly (Nettleton, 1971).

4.1 Magnetic Gradient

An examination of the magnetic gradient contour map (Figure 7) reveals numerous high amplitude bulls-eye responses interpreted as probable disposal trenches, separated by background values (±50 nT/m). The pervasive nature of recorded anomalies indicates many interpreted trenches contain ferrous objects. The interpreted anomalies appear concentrated in the northern and southeastern portions of the survey area with only one (1) located between Y-coordinates 520-650. The coordinates of interpreted magnetic anomalies are summarized in Appendix A.

The lateral limits of interpreted trenches (Figure 7) are a function of the extent of ferrous fill and include the peak-to-peak response from dipolar anomalies and high- amplitude bulls-eye responses. Most interpreted trenches appear isolated, however the magnitude and extent of the anomalies between coordinates (470,340) and (620,340) precludes discrimination between target boundaries. Since the gradiometer is sensitive only to ferromagnetic materials, it is possible that trenches devoid of ferrous fill may remain undetected by the magnetic method. Furthermore, the actual lateral limits of some interpreted trenches could be greater if ferrous fill was not placed along trench edges.

Magnetic data encountered interference from several sources at the CE site, including the chain-link fence, culvert, parked trailers, and electrical utilities. High- amplitude responses located near coordinates (390,550), (290,830), (520,620), (340,840), (370,840), and (340,910) are all attributed to cultural features.

4.2 EM-61

Contoured EM-61 data (Figures 8-9) display discrete anomalies within near-zero

background conditions. Since EM-61 data are sensitive strictly to metal objects and are relatively unaffected by features outside the coils' vertical plane of sensitivity (Figure 1, bottom), the strong responses are interpreted as metal fill within the disposal trenches. The distribution of interpreted trenches appears concentrated in the northern and southeastern portions of the survey area. Since the EM-61 possesses a high dynamic range, crisp delineation of buried metal objects is provided by the contoured data. The coordinates of interpreted EM-61 anomalies are summarized in Appendix A.

Since the EM-61 is sensitive only to metallic materials, it is possible that trenches devoid of metal may remain undetected by the EM-61. Similar to the magnetic gradient, if metallic fill is not present at the edges of a disposal trench, the lateral limits would appear less extensive. The EM-61 is less susceptible to external interference than either the gradiometer or the EM-31, however cultural features, such as buried utilities and reinforced concrete encountered within the vertical plane of sensitivity limit EM-61 exploration.

4.3 EM-31

Interpreted ground conductivity (Figure 10) and in-phase (Figure 11) data display less anomalous activity than either the magnetic gradient or EM-61 data. Instead of exhibiting numerous bulls-eye anomalies, ground conductivity data depict generally background trends in conductivity and a single interpreted trench at coordinate (430,770). Although this interpreted trench straddles the fence, which is an identified source of interference, the magnitude and extent of this anomaly, which correlates with magnetic and EM-61 responses, exceeds that which would be expected from the fence alone. Despite interference from the chain-link fence and a utility along the southern boundary, a definite decreasing trend is present to the east. Since EM-31 data are sensitive to surficial and buried objects to a distance of 15 ft, the elevated ground conductivity values and apparent lack of bulls-eye responses suggest recorded values are related to the clay-rich soil and not discrete metallic targets.

In-phase data (Figure 11) show several moderate-to-high amplitude bulls-eye responses in the northern and southeastern portions of the site. The sensitivity of the in-phase mode suggests that these anomalies are due to buried metallic objects. The presence of the fence, reinforced concrete and other sources of interference inside the fenced area make the interpretation of subsurface features in this area less definitive than that in open areas free of surficial obstructions. The coordinates of interpreted EM-31 anomalies are summarized in Appendix A.

4.4 EM-34

A total of four (4) EM-34 profiles were collected in topographically downgradient areas which, based on preliminary interpretation of field-generated contour maps, were devoid of metal-filled disposal trenches. Plotted EM-34 data (Figures 12-15) all display a trend of decreasing conductivity toward the stream which is consistent with EM-31 ground conductivity data (Figure 10). Furthermore, a comparison of the EM-34 plots with Figure 10 shows that EM-34 ground conductivity data (0-50 ft) are all of lower magnitude than corresponding EM-31 (0-15 ft) data indicating decreasing conductivity with depth.

Further examination of Figures 12-15 reveals that the horizontal dipole data are more consistent between survey stations and display less variation. Since horizontal dipole data are more sensitive to near-surface materials (McNeil, 1983) than vertical dipole data, the

consistency of horizontal mode data may indicate consistency in the near-surface clay overburden. The decreasing conductivity to the east could be the result of thinning or deepening clay layers.

Although vertical dipole data follow similar trends to that of the horizontal dipole data, certain variations exist. For example, since vertical dipole data explored depths to a maximum of 50 ft, it is possible that minor variations in vertical dipole data are a result of variable conditions at the bedrock interface. The vertical dipole data exhibit higher amplitude, possibly skewed, peaks at coordinates A-70, B-20, and B-60. A comparison of EM-34 profile locations (Figure 6) to interpreted trench locations (Figures 7-9), suggests that these anomalous points are the result of influence from disposal trenches within the radius of instrument sensitivity. Since inorganic plumes typically increase electrical conductivity due to an abundance of dissolved ions, the relatively consistent values recorded at the CE facility suggest that no inorganic plumes were intersected along these profiles.

4.5 Integrated Interpretations

The objective of integrated interpretations is to develop a better understanding of subsurface conditions by capitalizing on the varied sensitivities of each instrument. Similarities and differences in data permit an evaluation of target material composition, relative depth, and lateral position. A summary of the geophysical methods utilized for this study and their sensitivity is presented in Table 1.

Table 1

Summary of Geophysical Techniques and Sensitivities

Instrument	Mode	Depth (ft)	Sensitivity
Gradiometer		20	ferromagnetic material
EM-61		10	metal objects
EM-31	Quadrature	15	ground conductivity
	In-phase	15	ferrous and non-ferrous metal
EM-34	Vertical dipole	50	ground conductivity
	Horizontal dipole	25	ground conductivity

From Table I, it is apparent that correlation of magnetic gradient with EM-61 or in- phase data can be used to differentiate between buried ferrous (typically iron & steel) materials and other metallic objects. Furthermore, the magnetic gradient and EM-61 data do not respond to geologic changes such as soil moisture, clay content, and overburden thickness. Therefore, ground conductivity variations resulting from these factors are best established from interpreted EM-31 and EM-34 data.

Based on correlation between the magnetic gradient (Figure 7) and EM-61 (Figures 8-9) contour maps, nearly all interpreted disposal trenches were detected due to ferrous materials within the fill. An exception is noted at coordinate (595,850) where EM-61 data

indicate buried metal and magnetic gradient values show no anomaly. The EM- 61 response at coordinate (440,670) may also be due to non-ferrous metal, however a dipolar magnetic response may be masked by the negative response at this location. Similar to EM-61 data, all interpreted in-phase bulls-eyes (Figure 11) correlate to magnetic gradient anomalies.

Based on integrated magnetic gradient, EM-61, and EM-31 interpretations, identified disposal trenches contain primarily ferrous and some non-ferrous metal materials. To meet the third project objective, "determine the lateral extent of trenches for drilling purposes," Berkshire constructed a basemap which combines the outline of all interpreted geophysical anomalies (Figure 16). Highlighted areas on this map were detected via one or more of the near-surface geophysical techniques and should be avoided to reduce the possibility of encountering a disposal trench during any intrusive activities.

Analysis of the EM-31 (Figure 10) and EM-34 (Figures 12-15) ground conductivity data reveals a decreasing trend toward the east and only minor sensitivity to buried metal targets. EM-31 ground conductivity data sensed a portion of the largest interpreted disposal area which straddles the fence near coordinate (430,770), however other disposal trenches do not appear as discrete anomalies. The elevated ground conductivity values in the study area are likely due to documented clay-rich soils, however conductive materials within disposal trenches may provide a regional increase in conductivity.

Although ground conductivity data were less useful in locating disposal trenches than other geophysical techniques at this site, they do provide useful insight into subsurface conditions. Horizontal mode EM-34 values display relatively consistent responses which decrease towards the stream. The consistency of these data suggest that no inorganic groundwater plumes were intersected and that influence from buried conductive materials was not encountered by horizontal mode data. Geologic conditions which might explain the eastward decrease in conductivity include a deepening or thinning of subsurface clay layers.

The geophysical maps also depict areas devoid of anomalous activity. These background conditions may be due to a lack of burial trenches, although it is possible that no discernible physical contrast exists between the soil and fill materials. This would require fill material to be both non-ferrous and non-metallic in nature and also display similar background electrical conductivity as native or fill soils.

5.0 SUMMARY and CONCLUSIONS

AMA contracted with Berkshire to collect magnetic gradient, EM-61, EM-31, and EM-34 data over a 3.1 acre area at the CE Combustion Engineering facility in Hematite, Jefferson County, MO between August 10th and 13th, 1998. The objectives of the geophysical investigation were to: 1) characterize the aerial extent of buried materials; 2) determine the number and location of disposal trenches and characterize their contents; 3) determine the lateral extent of trenches for drilling purposes; and 4) explore for possible inorganic soil or groundwater contamination related to the trenches.

Berkshire collected and digitally recorded a total of 1,390 magnetic gradient datapoints on a 10 x

10 ft pattern in addition to 5,352 EM-61 and 5,392 EM-31 data points on a 5 x 5 ft grid pattern. A total of 520 linear ft of EM-34 profiling was conducted at 10 ft spacings in areas devoid of field interpreted burial trenches. Specific results of the investigation reveal:

- The exact number of disposal trenches was not determined, however numerous disposal trenches were detected and delineated within the study area. The coordinates of interpreted anomalies for each instrument are summarized in Appendix A.

- Magnetic gradient and EM-61 contour maps were most useful in locating and mapping disposal trenches.

- Except for an anomaly at coordinate (595,850), all interpreted disposal trenches are interpreted to contain ferrous materials.

- Areas devoid of anomalous activity could indicate areas with no disposal trenches, or if trenches exist in these areas, they must contain materials which do not provide a discernible contrast to the geophysical techniques employed.

- Based on the strength of the EM-61 responses, a high percentage of buried metal is present within 10 ft of the surface.

- No inorganic plumes were interpreted along the 520 linear ft of EM-34 profiles and consistently decreasing ground conductivity values suggest that clay layers may thin or dip to the east.

6.0 REFERENCES CITED

McNeil, J.D., 1983, EM-34-3 survey interpretation techniques, (technical Note TN-8): Geonics Limited, Mississauga, Ontario, Canada, 7 p.

Nettleton, L.L., 1971, Elementary gravity and magnetics for geologists and seismologists: Tulsa, Oklahoma, Society of Exploration Geophysicists, 121 p.

Papadakis, C.E., 1998, Integrated Geophysical Investigation at CE Combustion Engineering, Hematitle, Jefferson County, Missouri: Berkshire Environmental, Inc., Wyomissing, PA

7.0 CLOSING

The geophysical techniques, data collection geometries, field procedures, and interpretative methodologies used in this project are consistent with standard, recognized practices in similar geophysical investigations. The correlation of geophysical responses with probable subsurface features is based on the past result of similar surveys although it is possible some variation could exist at this site. This warranty is in lieu of all other warranties either implied or expressed.

GEM GSM-19 Overhauser Gradiometer

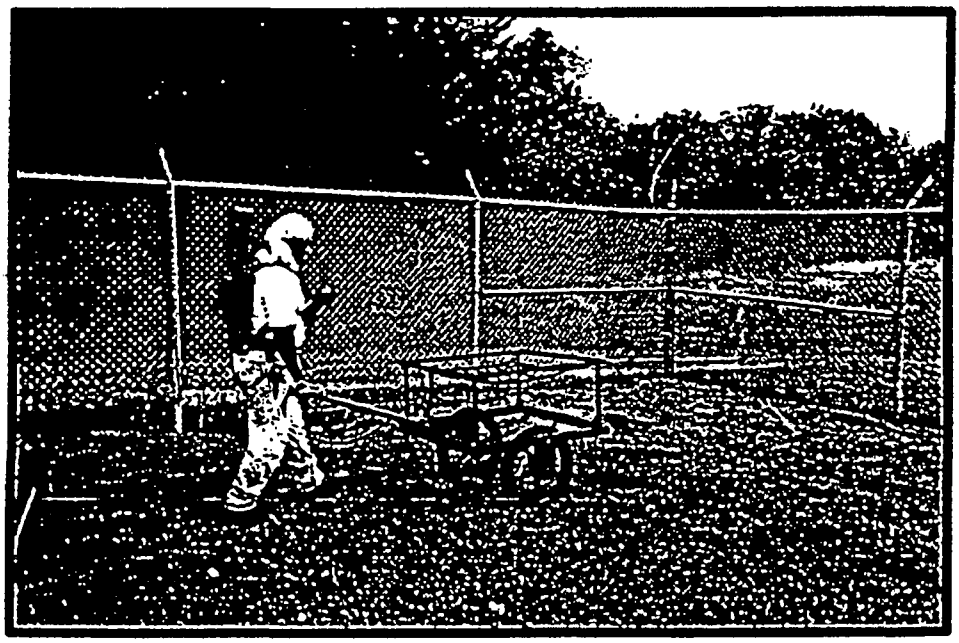

Geonics EM-61

Berkshire
Project # 98-649

Geophysical Instrumentation

Figure 1

Geonics EM-31

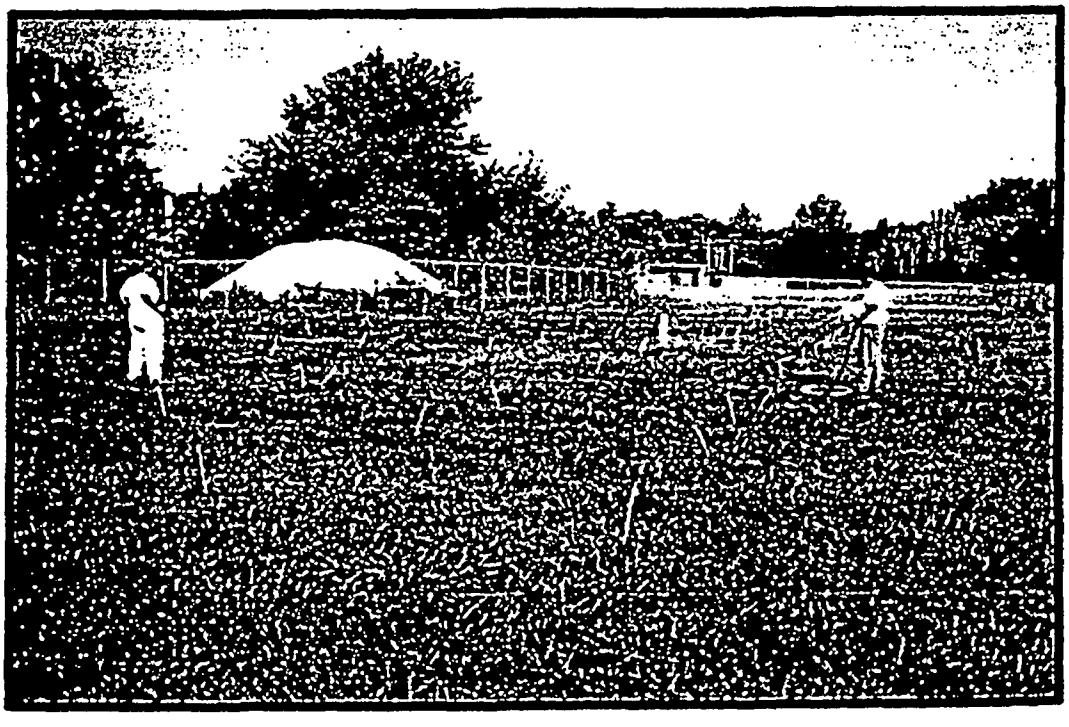

Geonics EM-34-XL

Berkshire
Project # 98-649

Geophysical Instrumentation

Figure 2

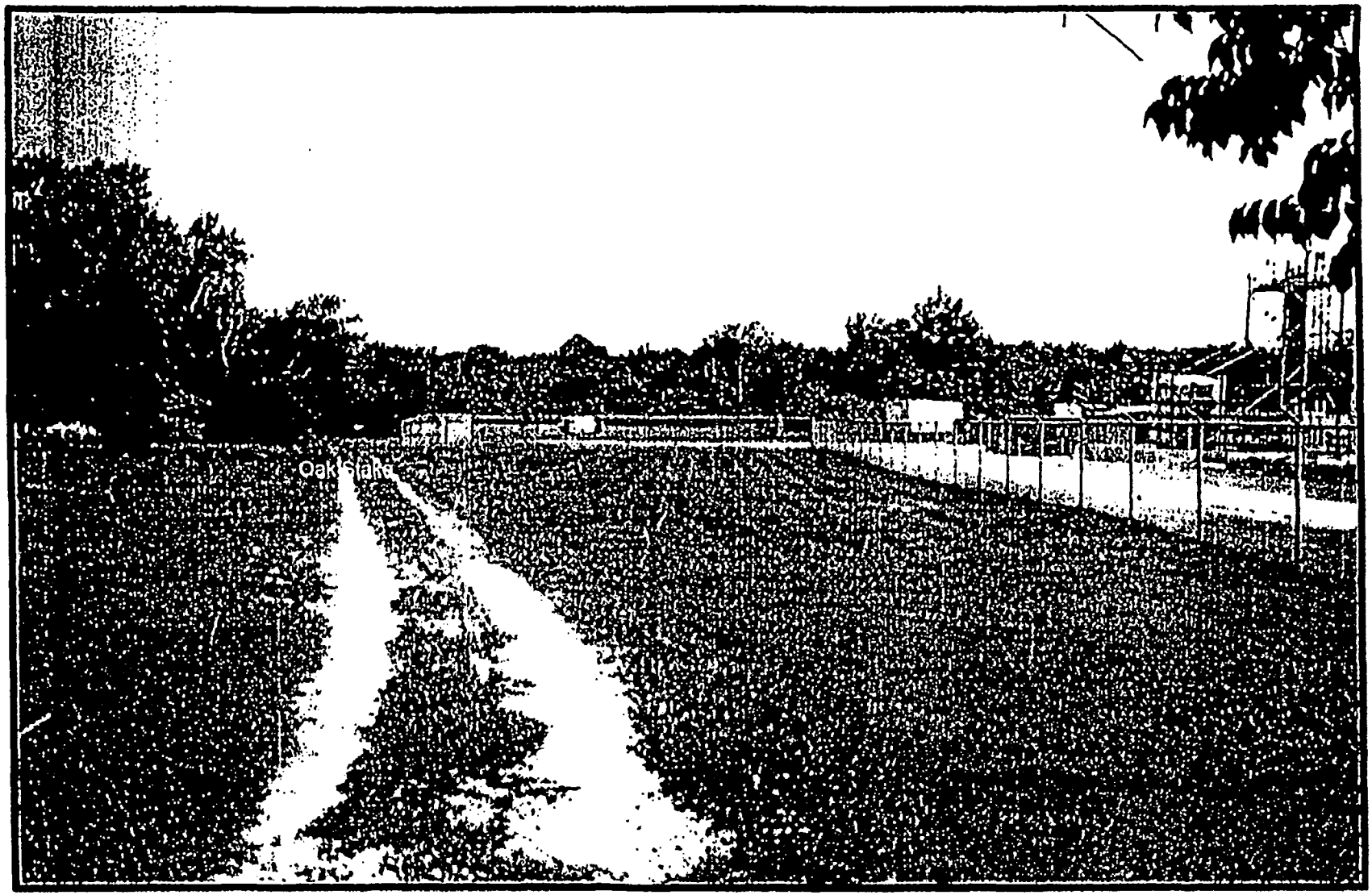

Berkshire
Project # 98-649

Surveyed Control Grid

Figure 3

Combustion Engineering

Hematite, Jefferson County, MO

August 1998

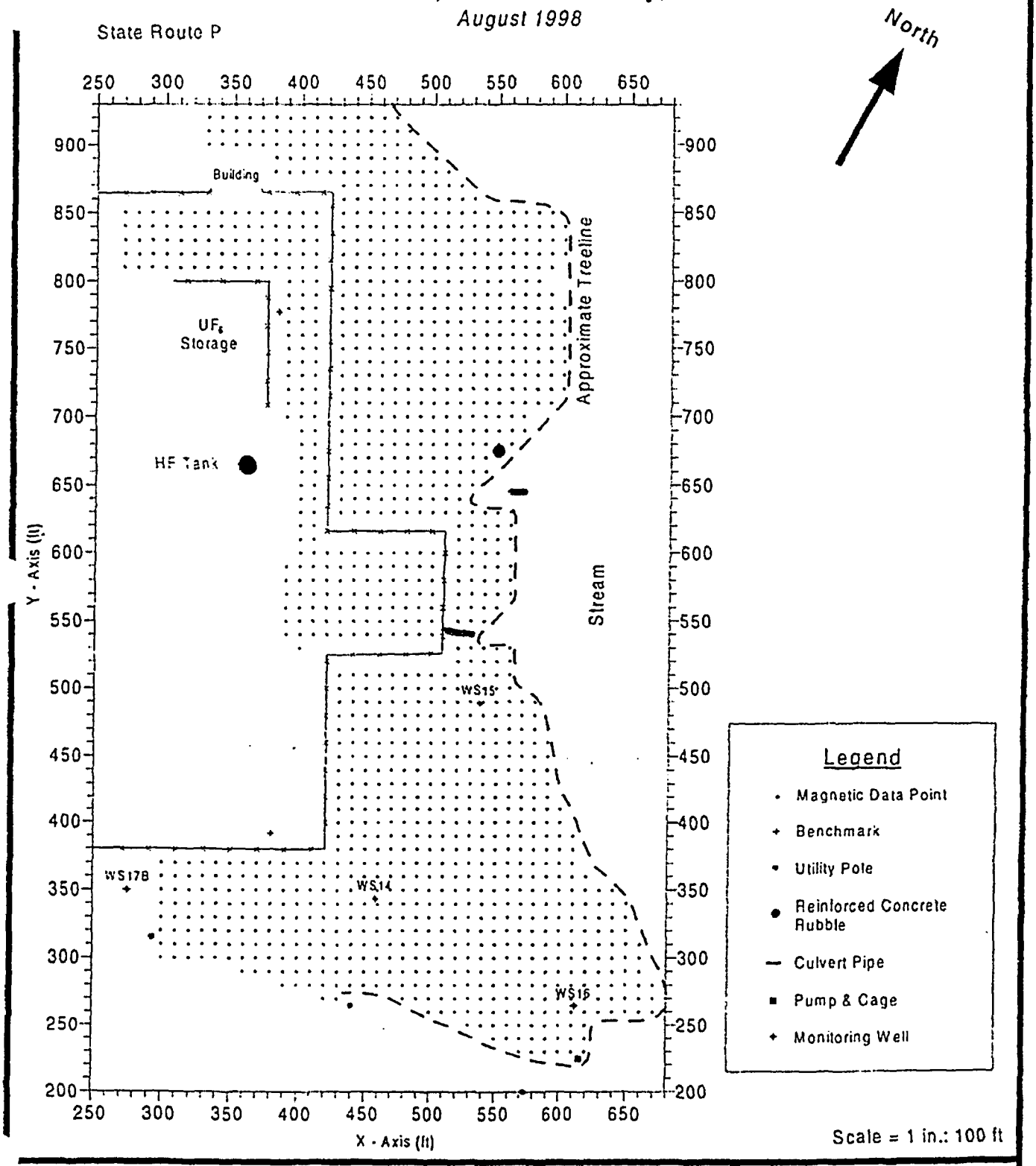

Berkshire
Project # 98-649

Magnetic Data Reference Map

Figure 4

Combustion Engineering

Hematite, Jefferson County, MO

August 1998

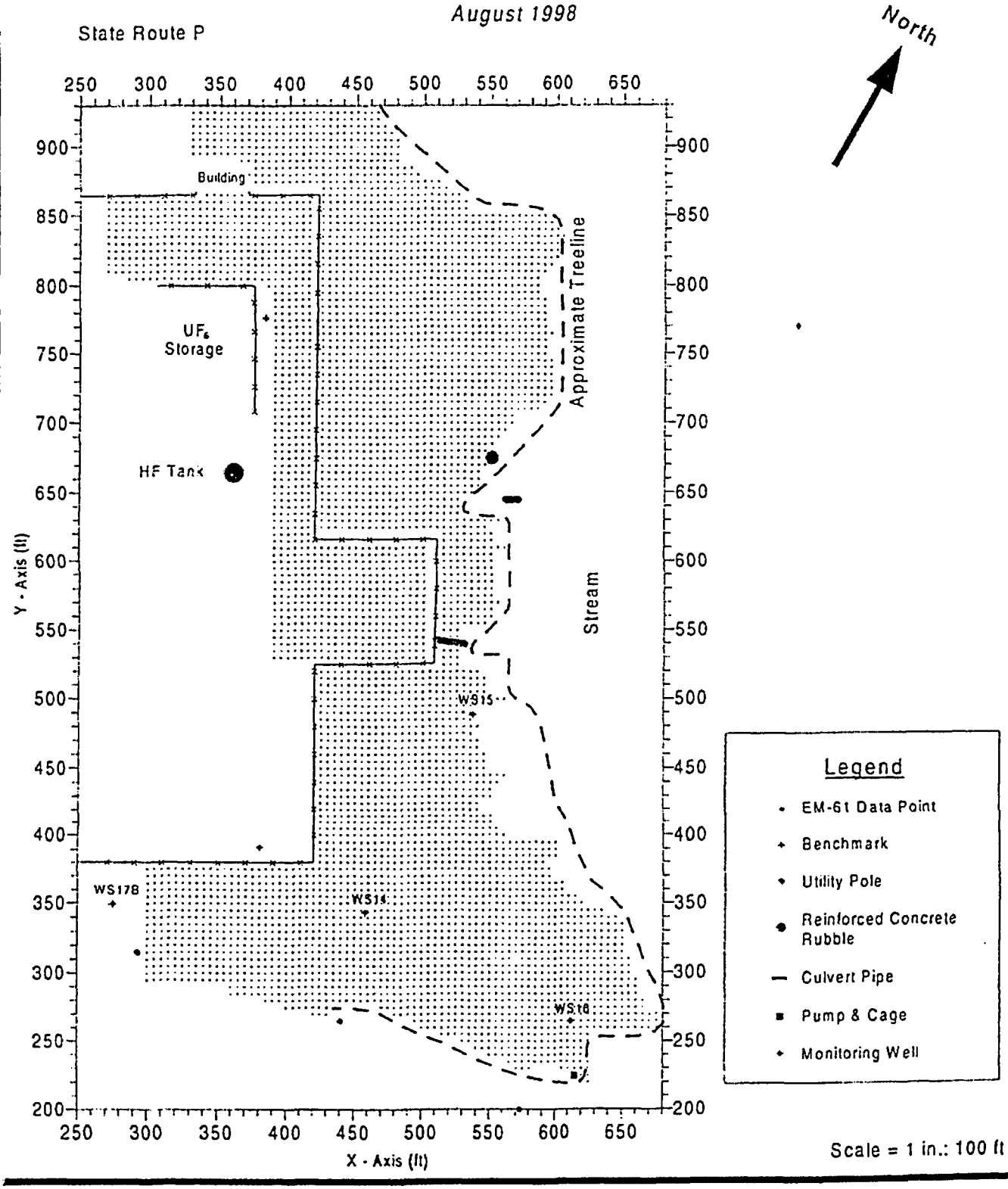

Berkshire
Project # 98-649

EM-61 Data Reference Map

Figure 5

Combustion Engineering

Hematite, Jefferson County, MO

August 1998

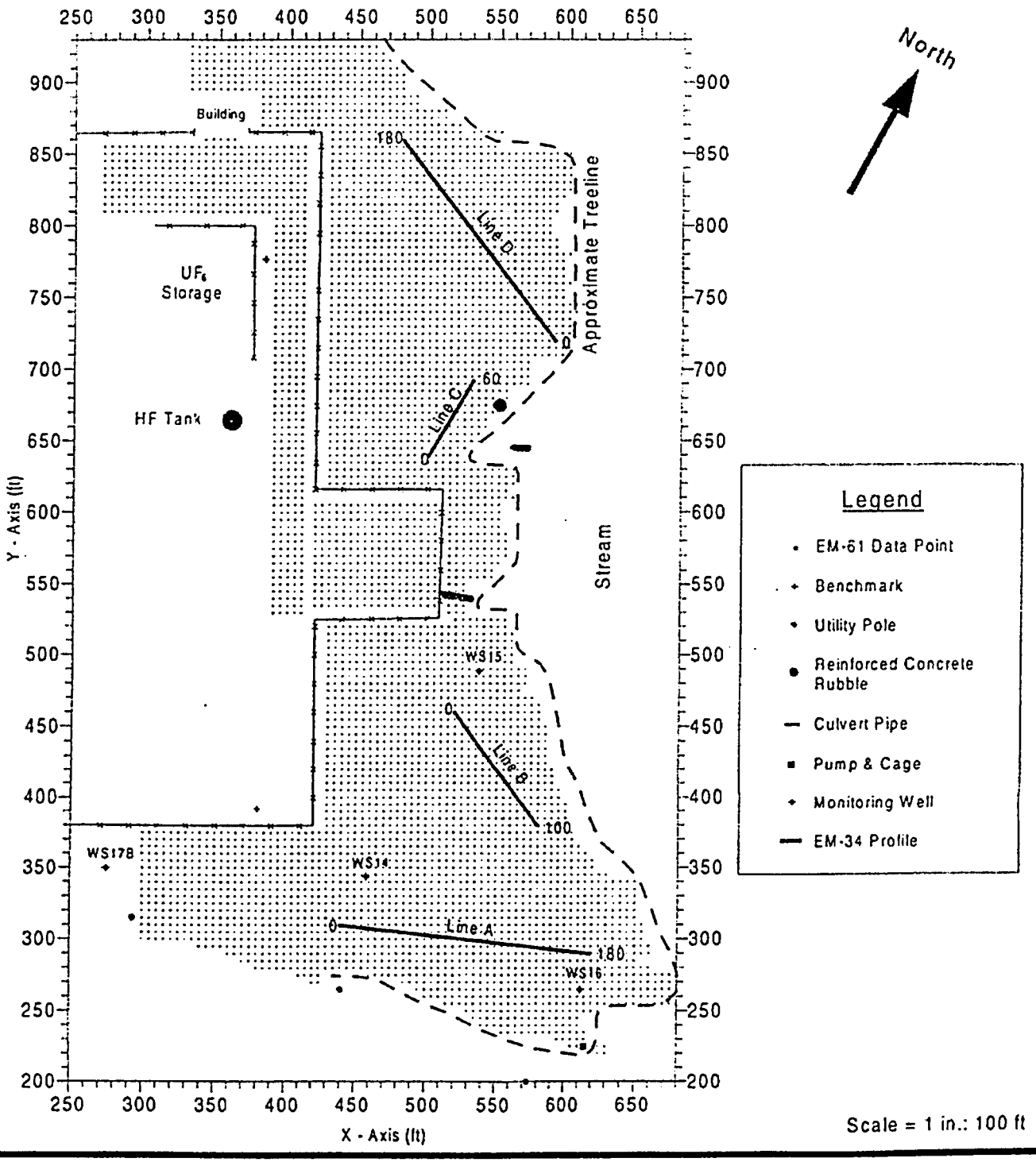

Berkshire
Project # 98-649

EM-31 & EM-34 Data Reference Map

Figure 6

Combustion Engineering

Hematite, Jefferson County, MO

August 1998

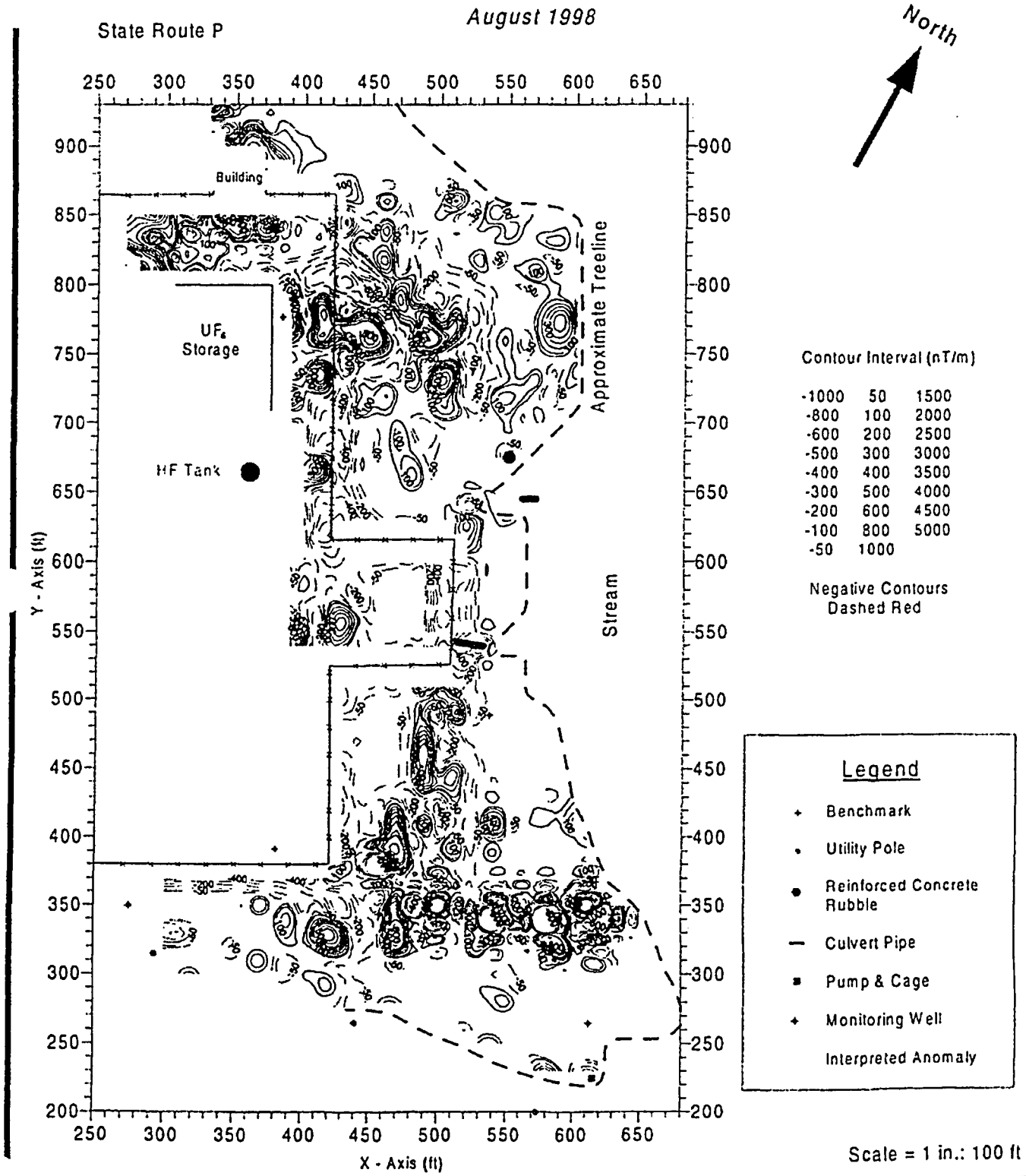

Berkshire
Project # 98-649

Magnetic Gradient Contour Map

Figure 7

Combustion Engineering

Hematite, Jefferson County, MO

August 1998

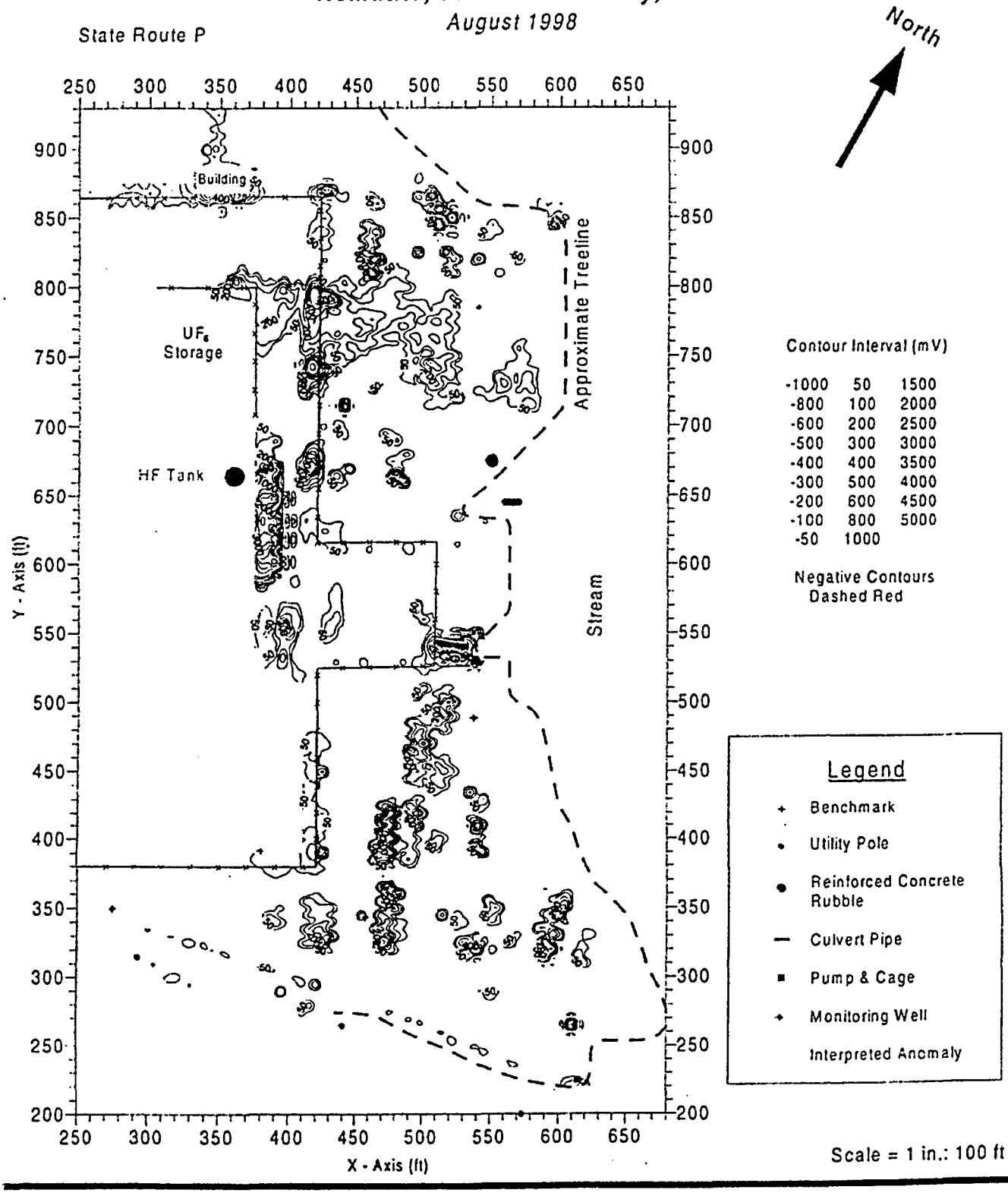

Berkshire
Project # 98-649

EM-61 Lower Coil Contour Map

Figure 8

Combustion Engineering

Hematite, Jefferson County, MO

August 1998

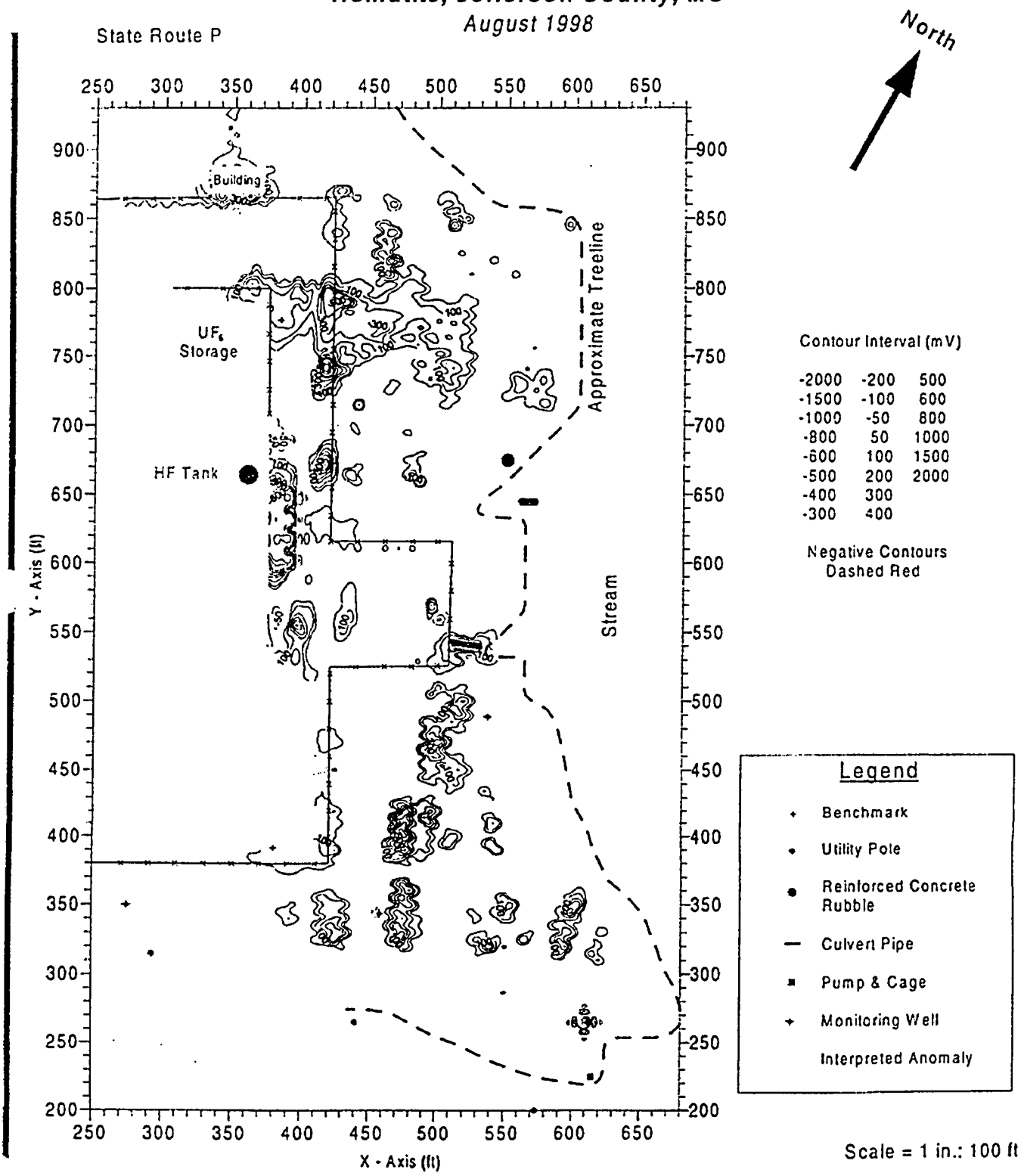

Berkshire
Project # 98-649

EM-61 Differential Contour Map

Figure 9

Combustion Engineering

Hematite, Jefferson County, MO

August 1998

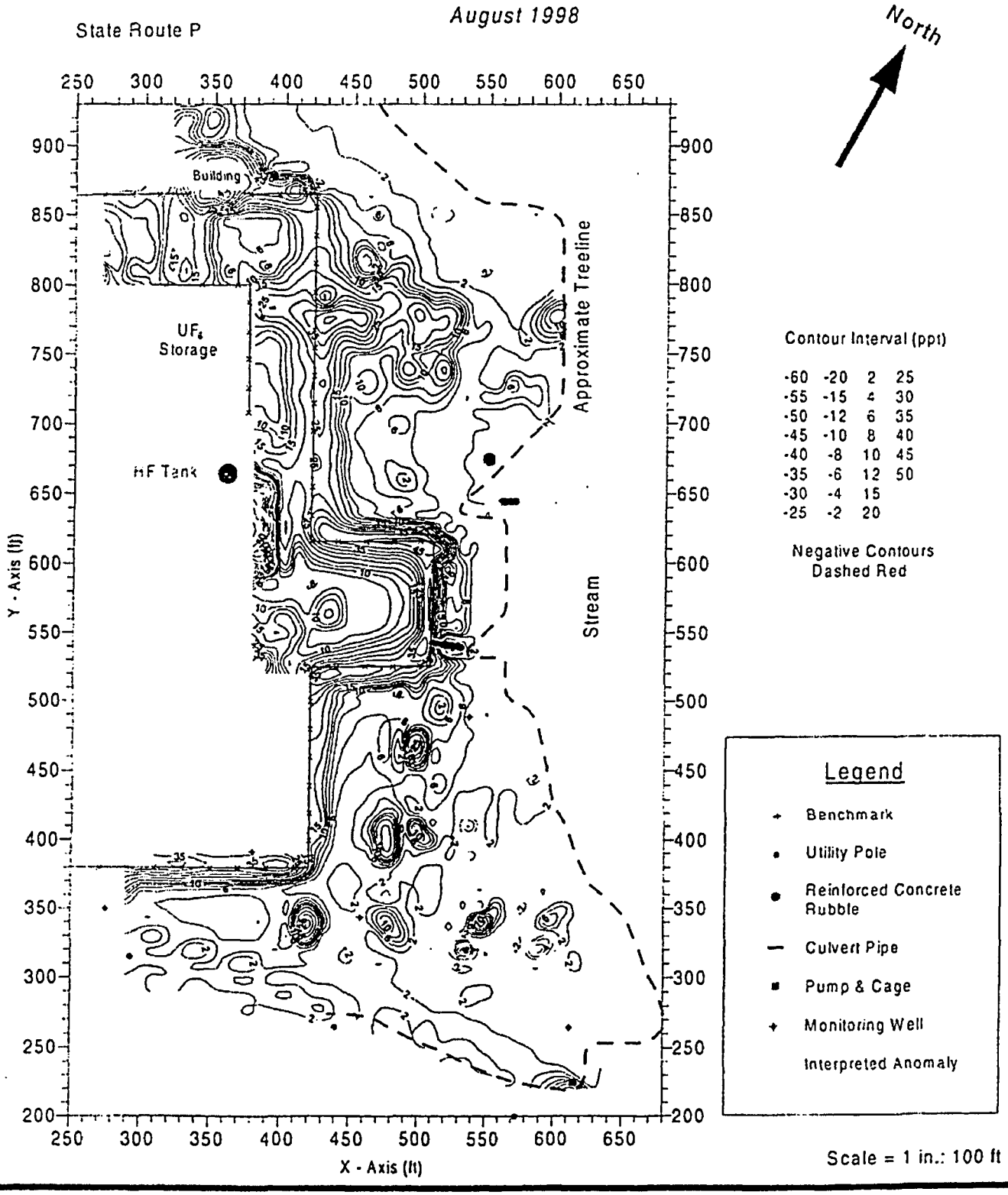

Berkshire
Project # 98-649

In-Phase Contour Map

Figure 11

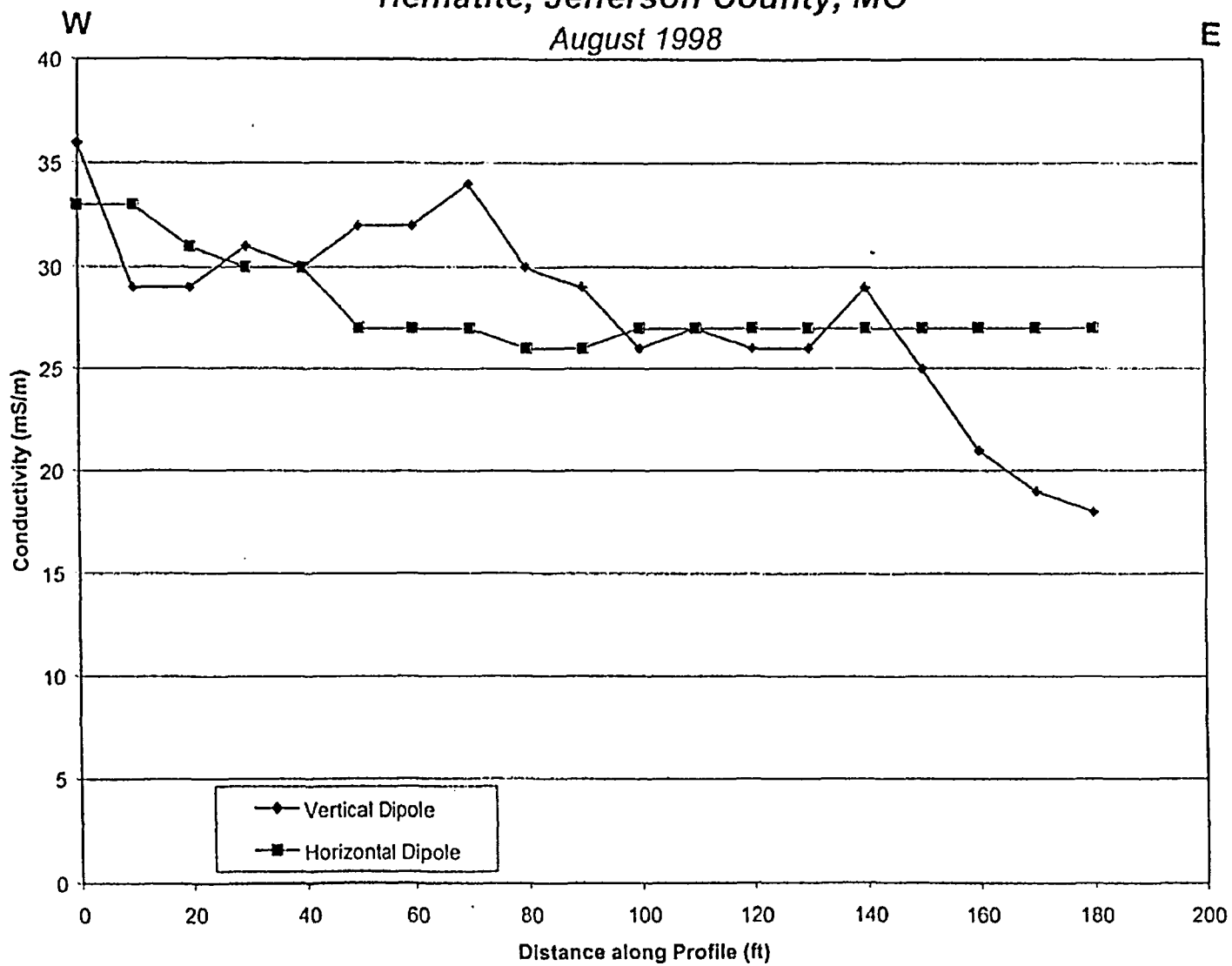

Berkshire
Project # 98-649

EM-34 Profile - Line A

Figure 12

Combustion Engineering

Hematite, Jefferson County, MO

August 1998

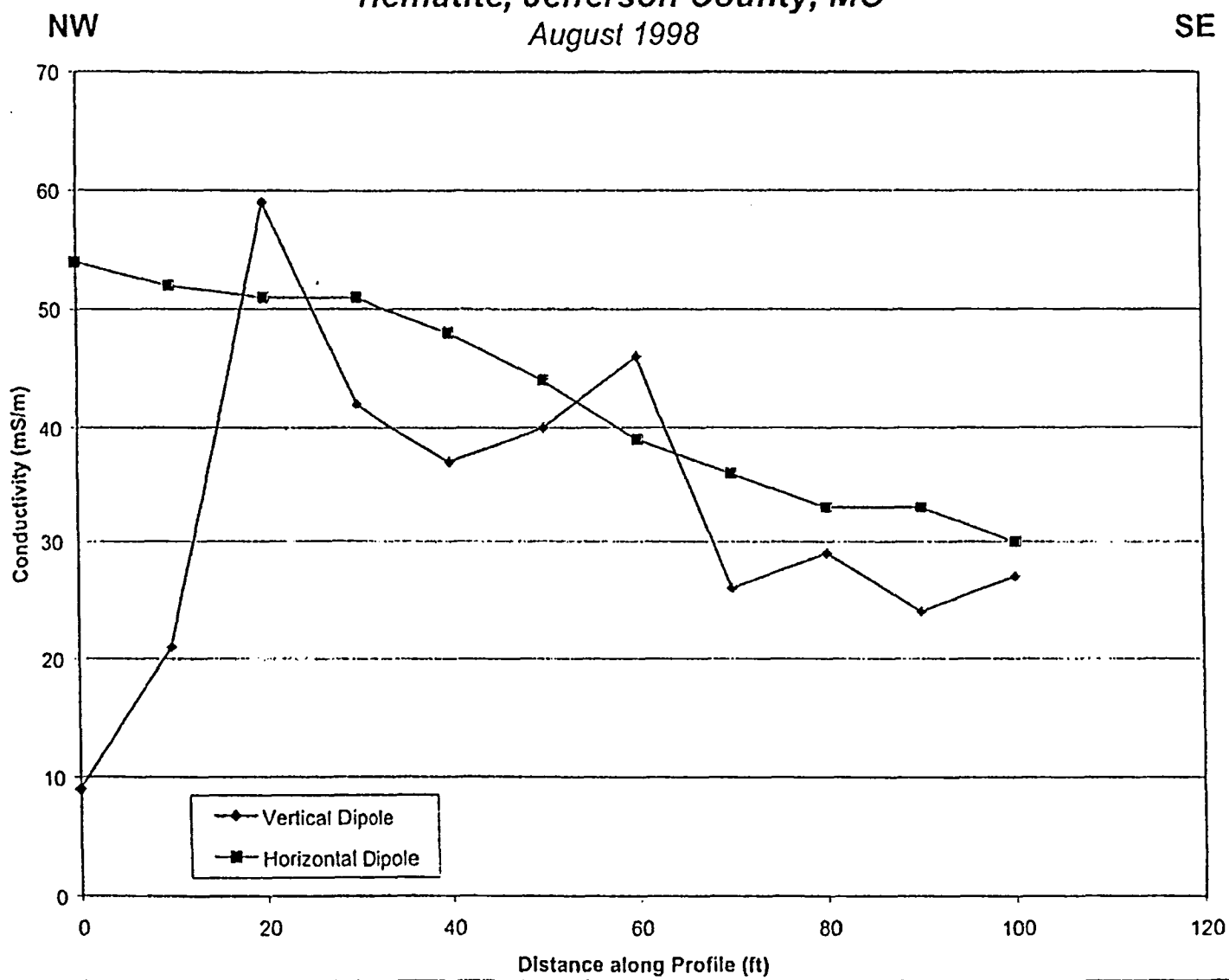

Berkshire
Project # 98-649

EM-34 Profile - Line B

Figure 13

Combustion Engineering

Hematite, Jefferson County, MO

August 1998

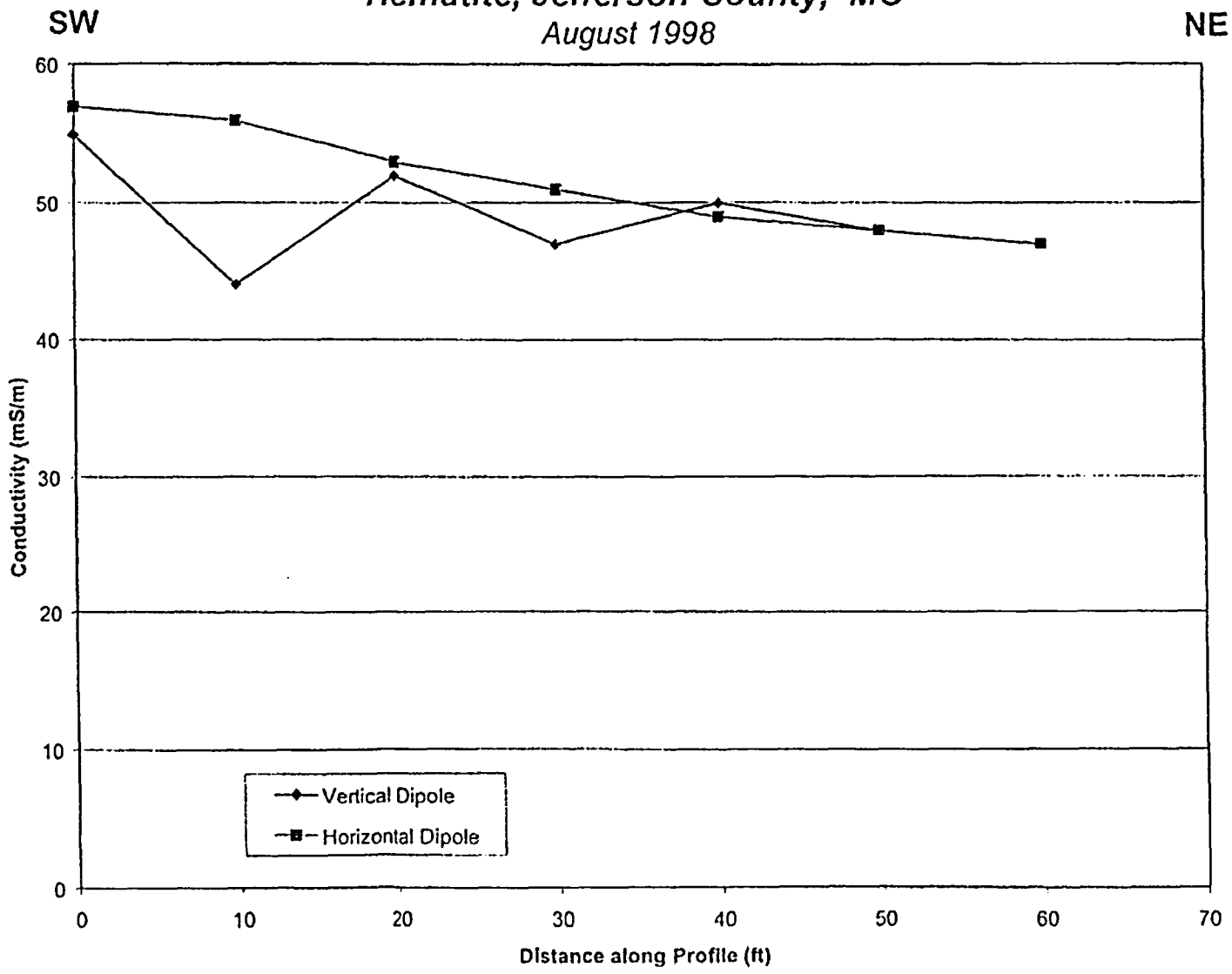

Berkshire
Project # 98-649

EM-34 Profile - Line C

Figure 14

Combustion Engineering

Hematite, Jefferson County, MO

August 1998

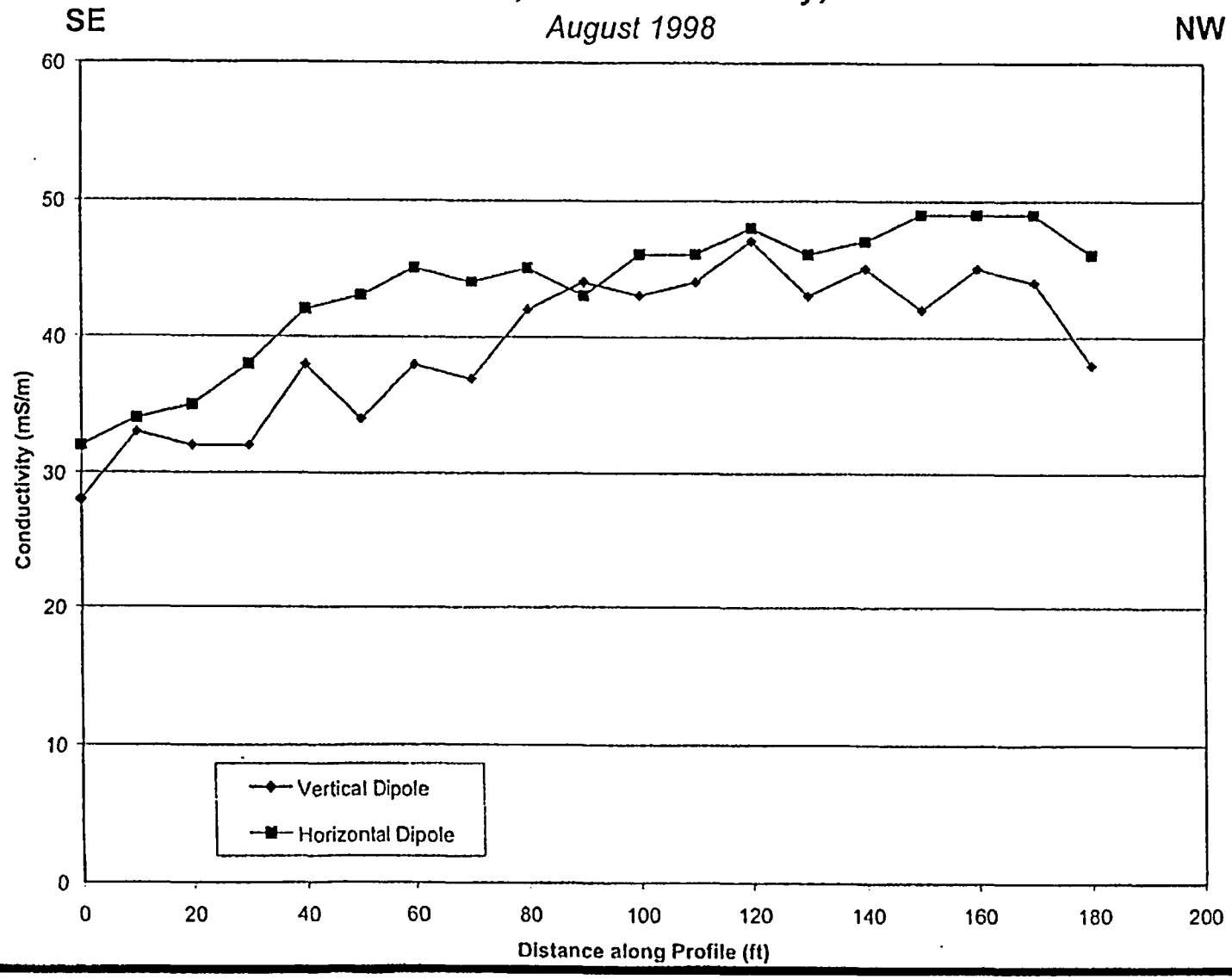

Berkshire
Project # 98-649

EM-34 Profile - Line D

Figure 15

Combustion Engineering

Hematite, Jefferson County, MO

August 1998

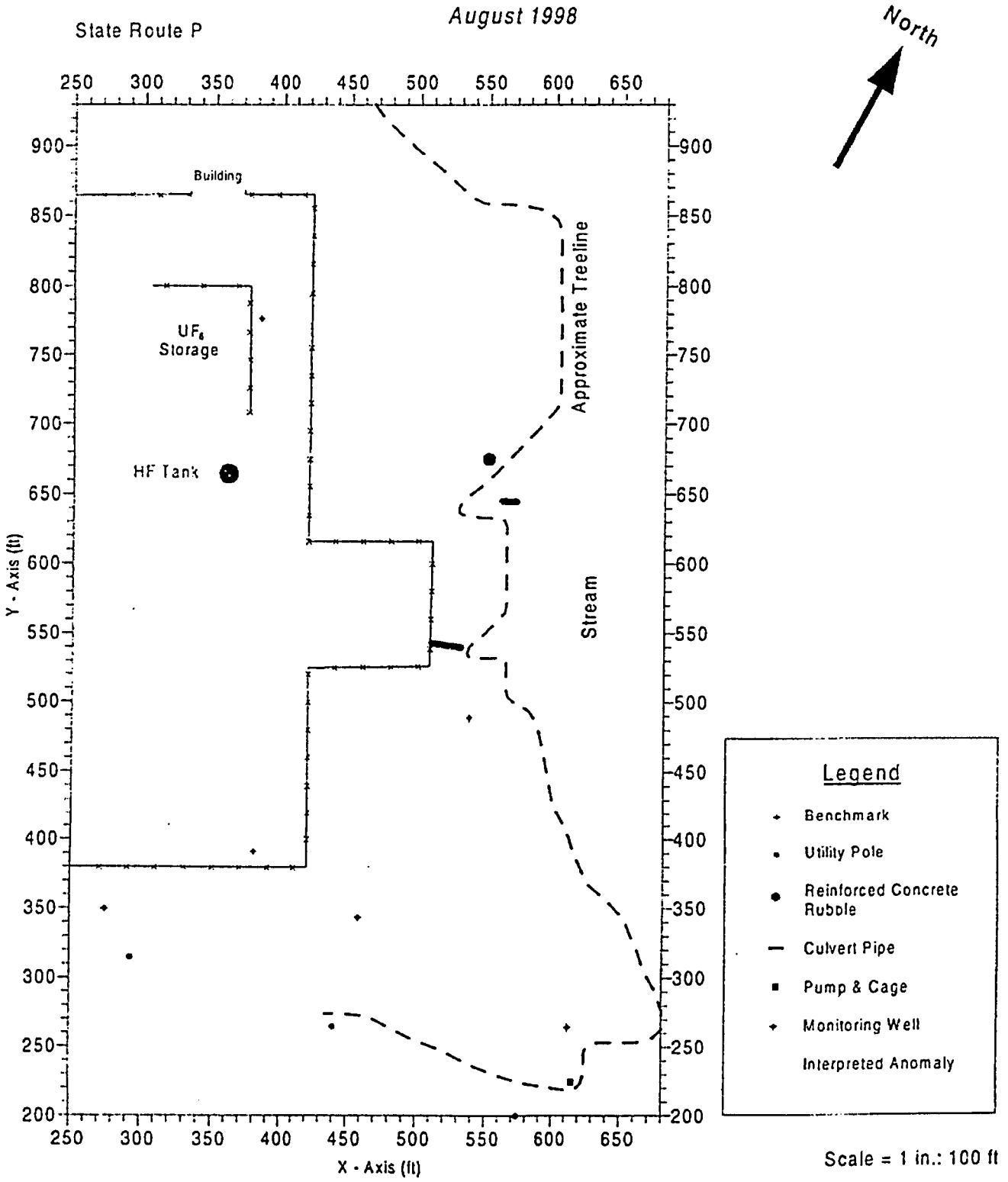

Berkshire
Project # 98-649

Combined Anomaly Map

Figure 16

APPENDIX A

SUMMARY OF INTERPRETED ANOMALY COORDINATES

Interpreted Anomaly Coordinates

Magnetic Gradient
(390,340)
(420,330)
(460,340) to (640,340)
(470,400)
(490,410)
(510,390)
(540,410)
(510,440)
(490,440) to (490,500)
(510,500)
(430,560)
(410,665)
(470,675)
(410,735)
(450,720)
(500,725)
(555,720)
(585,770)
(500,760) to (450,840)
(460,750) to (405,775)
(570,810)
(545,845)
(510,860)
(460,860)
(580,830)
(525,815)
(480,735)

EM-61
(420,320) to (420,360)
(480,320) to (475,370)
(535,325)
(550,350)
(590,310) to (605,360)
(620,315)
(540,395)
(540,410)
(510,400)
(480,380) to (485,430)
(410,670)
(430,565)
(400,530) to (400,575)
(480,670)
(570,730)
(510,440) to (490,485) to (520,500)
(410,725) to (410,805) to (460,805) to
(460,850) to (515,790) to (510,730) to
(480,760) to (410,725)
(510,855)
(515,345)
(535,435)
(425,540) to (435,580)
(440,670)
(475,690)
(435,700)
(440,715)
(540,820)
(520,820)
(495,825)
(550,840)
(595,850)
(505,860)
(460,860)

EM-31
Ground Conductivity
(430,770)

In-phase
(535,320)
(550,340)
(590,330)
(475,405)
(500,405)
(500,470)
(595,775)
(490,730) to (520,785) to
(410,780)
(470,350)
(420,340)
(520,495)
(460,820)
(510,850)